METAL-ORGANIC COMPLEXING IN NATURAL SOIL SYSTEMS

A thesis
submitted in partial fulfilment
of the requirements for the degree
of
Doctor of Philosophy in Chemistry
University of Canterbury

by

J. A. Kennedy

University of Canterbury

1984

ABSTRACT

A series of metal-ligand equilibria have been studied which may be pertinent to the dissolution and transport of sesquioxides in soil systems. In particular the interactions of Al(III) and Fe(III) with polyphenols (1,2-dihydroxybenzenes) in aqueous solution have been investigated.

The complexing reactions between Al(III) and catechol, protocatechuic acid and catechin, and between Fe(III) and protocatechuic acid have been studied quantitatively. The reactions of epicatechin, an epicatechin dimer (designated B2) and an epicatechin polymer (designated B13) with these metal ions were studied semi-quantitatively. It was observed that those ligands with a standard reduction potential < 0.9 V underwent both complexing and redox reactions with Fe(III) at pH $\lesssim 5.6$.

The polyphenols chosen for study are representative of species found in soil solutions. These polyphenols may be important in solubilizing, and hence mobilizing, Fe(III) and Al(III) in soil systems.

This study reports the protonation constants for catechol, protocatechuic acid, catechin and epicatechin derived from both potentiometric and spectrophotometric measurements. By reference to model compounds the protonation sequence for the four phenolate oxygens in catechin and in epicatechin have been assigned. The epimerization of catechin to epicatechin and vice versa was investigated.

The protonation and complexing studies used a glass/calomel electrode system as a probe for hydrogen ion concentrations in the pH range 3.0 - 11.5. A method of electrode calibration using a series of titration-generated o-phthalic acid buffers of known $[H^+]$ was further developed in this work.

Spectrophotometric and visual tests for extractable Fe(II) and Al(III) in the soil have been developed and their possible use in the field investigated.

A computer model was used to rank some of the above polyphenols and a representative series of other ligands in their ability to complex aluminium(III) and to dissolve gibbsite, $Al(OH)_3$.

ACKNOWLEDGEMENTS

I wish to express my thanks to my supervisor Dr. H. K. J. Powell for his advice and encouragement during this work.

Special thanks go to my wife Philippa and my family without whom this thesis could not have been completed.

I am also grateful to Mr. J. McCombs for the assistance in producing the photographs contained in this thesis.

C O N T E N T S

CHAPTER 7 INTERACTIONS OF IRON(II) AND IRON(III) WITH POLYPHENOLS

CHAPTER 1

INTRODUCTION

1.1.1 Soil formation

Soil is the end product of weathering action on the upper and exposed layers of the earth's crust.

The following factors will influence the formation of soils[1]: (i) the nature of the parent material, (ii) climate, (iii) living organisms, (iv) relief, and (v) time.

A mature soil resulting from the prolonged effect of these variables on the parent material will show a developed horizontal layering. A vertical cross section of a layered soil is described as a soil profile.

One soil type and profile which has received much interest is the 'podzol'. The interest in podzols can perhaps be ascribed to the distinctive visual characteristics of these soils, namely a series of horizons that differ both in texture, and in colour.

1.1.2 Podzols

The term Podzol is generally thought to be derived from the Russian preposition 'pod' meaning 'under' and the noun 'zol' meaning 'ashes'[2], although there are other interpretations[3,4].

A well developed or mature podzol has a number of distinctive horizons which are easily recognized; they arise from the translocation of coloured substances such as soil organic matter and iron oxides.

Figure 1.1 shows a podzol formed on glacial moraine, and indicates clearly the podzol horizon sequence. The upper horizon has a high content of organic matter, deriving its dark colour from 'raw' humus. Because podzols generally form in cool-temperate climates slow decomposition of the soil organic matter (SOM) results in a build up of this horizon. This is aided further by the reduced earthworm activity in podzols[5]. This dark grey-black layer is designated the A_1 horizon[6]. The SOM is rich in organic acids[7], thus the pH of this horizon is low, say 3.8 - 4.5[8,9]. This layer, which is a mixture of mineral and organic material, may in an undisturbed forest situation be overlain by, and merge into, a layer of organic litter (mor humus).

The next layer immediately under the top soil is an eluvial horizon designated A_2 or A_e[6]. It is typically ash-coloured (grey or white). The ash-like appearance of this horizon results from the removal of organic matter and of iron oxide coatings from soil particles.

Below the A_2 or eluvial horizon a number of illuvial horizons may exist; these zones of accumulation are designated B horizons[6]. These horizons may be less distinct to the eye but are all enriched in iron, aluminium and soluble organic matter with respect to the A_2 horizon and the parent material (C horizon). Typically they are less acidic than the A horizons (e.g. pH 4 to 6)[8,9].

Within this metal enriched zone three distinct horizons may develop. The dominant feature is the B_s or sesquioxide horizon. This layer has an accumulation of

Figure 1.1 Profile (0-500 mm) of a podzol developed on glacial moraine

sesquioxides (Al_2O_3, Fe_2O_3) and possibly clays. The sesquioxides may occur as amorphous coatings on clay particles, as interstratified layers (Al_2O_3) in clays, as metal-organic complexes or in association with silica in gel-like cementing materials. The distinctive orange-brown colour arises from iron oxides and humic and fulvic acids.

Directly on top of this layer a B_h (humus) horizon may form. It is generally dark in colour and is specifically enriched with SOM. Further in some podzols an iron pan or B_{fe} horizon is observed between the B_s and the B_h horizons. The accumulation of organic material (B_h horizon) above the B_{fe} and B_s horizons could suggest that the organic matter has been arrested in its progress down the profile by virtue of its increased loading with metal ions. Alternatively the enrichment of the B_s horizon with water soluble fulvic acids, relative to A_e and C horizons, may indicate that the trivalent ions have moved through the profile in association with organic matter.

Although podzol formation requires a free draining parent material (e.g. sands, moraine) the ultimate formation of an iron pan (a cemented B_{fe} horizon) will result in restricted vertical drainage; frequent or continual water-logging will result.

1.1.3 The podzolization process

The highly acidic conditions encountered in the upper horizons of podzolized soils arise from acidic organic matter e.g. the litter from beech forests[10]. These conditions led some workers[11] to postulate that acidity alone promotes the dissolution of iron and aluminium. These

elements are then translocated down the soil profile as simple ions or as hydroxide complexes; higher pH in lower horizons causes their precipitation. This theory has been negated by Stobbe et al.[12] on the grounds that the pH in podzols does not get low enough for iron(III) to be mobilized.

Another mechanism proposed for the podzolization process involves the movement of metals and organic matter from the upper soil horizons in a colloidal state. This theory has been used by Mattson and co-workers[13,14] to explain podzolization entirely in terms of the movement of a positively charged iron-oxide (or aluminium-oxide) sol in association with negatively charged humus. Deb[15] considered it more probable that the colloids (Al and Fe) combine with organic matter thus moving as humus-protected sols. However Petersen[16] has suggested that these sol theories do not provide an adequate mechanism for the removal of sesquioxides from the A_e horizon. A currently accepted theory involves the movement of aluminium and iron as soluble organic complexes.

It has been suggested that many organic compounds found in the soil are capable of forming soluble complexes with iron and aluminium[17]. The formation of such complexes will increase the mobility of these elements in the soil. This effect has been demonstrated by Atkinson and Wright[18] for artificial chelating compounds (EDTA) applied to soil columns in the laboratory. Experiments by Bloomfield[19-24] with aqueous extracts of leaf and bark from a series of plant species have shown that the extracted

organic compounds are capable of dissolving iron and maintaining it in solution at pH values where precipitation would normally occur; it was concluded that polyphenols were the active organic compounds. Bloomfield[25] deduced that the initially formed polyphenol ferric complexes were subsequently reduced to the ferrous state under pH conditions encountered in the soil.

Muir et al.[26,27] determined that the iron complexing acids found in pine needles are -hydroxy carboxylic acids; they are capable of maintaining iron in solution from pH 4 to 9.5.

Coulson and workers[10,28] identified two catechin molecules ((3',4'-dihydroxyphenyl)-3,4-dihydro-2H-1-benzo-pyran- 3,5,7-triol[29]) that they isolated from fresh green leaves of a number of tree species. They established that these phenolic compounds could solubilize ferric oxides in much the same way as did Bloomfield's[24] leaf extracts. Davies[17] supported the assumption that polyphenols and carboxylic acids are active iron and aluminium chelating agents but also noted the effectiveness of high molecular weight organic molecules such as fulvic acid in complexing these metal ions.

The fulvate mechanism

The abundance of literature on the formation of soluble metal-organic complexes in soils is an indication that mobilization of metal ions by SOM containing phenolic or carboxyl complexing sites is still a widely accepted mechanism for the podzolization process[16]. However the question as to the type of organic matter that plays the dominant role in mobilizing iron and aluminium is as yet

unresolved. Simple organic molecules such as protocatechuic acid, gallic acid, catechin and citric acid have been shown to dissolve and complex metal ions from precipitated metal hydroxides[10,30,31] and selected clay minerals[32]. Buurman et al.[33] in a recent paper discussing current theories for the podzolization process suggested that low molecular weight organic acids are the dominant transporting agents.

The high molecular weight fraction of SOM consists of humus (insoluble in water), humic acid (insoluble in aqueous acid) and fulvic acid (soluble in water).
Schnitzer et al.[34,35] have reported that fulvic acids, which tend to accumulate in the B_s horizon, are able to form soluble complexes with a range of metal ions including iron and aluminium. They have also shown by selective blocking of carboxyl (COOH) and phenolic groups in fulvic acid samples that these functions are likely to be jointly involved in reactions with aluminium and iron[36], i.e. the salicylic moiety may be an important complexing site.

The precipitation of iron, aluminium and organic matter in the B horizon has received less attention than has their dissolution in the A_2 horizon[37]. One explanation for the subsequent deposition lower in the soil profile involves biological decomposition of the organic chelating molecules[38,39]. When larger molecules such as tannins or fulvic acid are the mobilizing agents, the increasing availability of iron and aluminium with depth would cause them to become saturated with these metals, rendering the 'complex' insoluble[40]. Because of the availability of sesquioxides in the B_s horizon the SOM is maintained in an

insoluble state; there is a continual accumulation of iron, aluminium and organic matter which has moved down from the A horizon.

The silicate mechanism

Farmer et al.[41-43] have recently published a number of papers on an alternative theory for the podzolization process. This 'silicate' mechanism focuses attention on the origin of allophane and imogolite materials (poorly ordered alumino-silicates) found to occur in many B_s horizons. Farmer suggests that these materials do not form in situ in the B_s horizon but are transported as a soluble alumino-silicate precursor. In support of the mechanism Farmer has synthesized a soluble imogolite precursor called 'proto-imogolite'[44] which can be converted to imogolite on heating[45]. Farmer[46] has also produced Al_2O_3-Fe_2O_3-SiO_2-H_2O sols which are reported to be as stable as Al_2O_3-SiO_2-H_2O sols up to a critical Fe/Al ratio of 1.5. He infers that migration of Al and Fe as mixed hydroxide sols can account for the almost constant ratio of (amorphous) Al to Fe in acid oxalate extracts from B_s horizons of some podzols.

This work has not passed without criticism. Inoue and Huang[47] observed that organic ligands such as citric acid at low ligand/Al ratios (0.03) inhibit the formation of imogolite. Buurman et al.[33] have also criticized the 'silicate' theory; they stated that the continuous production of low molecular weight complexing acids such as protocatechuic acid, even if present in small amounts, makes them also potentially important transporting agents.

Polyphenols (in particular 1-2,dihydroxybenzenes) are one group of organic acids that have been characterized in aqueous leaf extracts[19-24] and in the soil[32]. Many workers[48] have claimed that these polyphenols, along with carboxylic acids, are active as complexing and solubilizing agents for iron and aluminium in the soil. For example laboratory experiments have provided evidence for the dissolution of iron from hydrated ferric oxide as soluble metal organic complexes[49].

1.2 SCOPE OF THIS WORK

The aim of this work was to study the interactions of a series of polyphenols with the metal ions iron(III) and aluminium(III) such that their possible role in the podzolization process could be assessed.

The polyphenols studied quantitatively in this work were 1,2-dihydroxybenzene (1), 4-methylbenzene-1,2-diol (2), 3,4-dihydroxybenzoic acid (3), 3',4'-di-O-methylcatechin (4), catechin (5) and epicatechin (6). In addition semiquantitative studies were undertaken on an epicatechin dimer designated B2 (7) and an epicatechin polymer designated B13 (8), which has on average 13 linked (C(4)-C(8))[50] epicatechin units. Figure 1.2 gives the molecular structures for the compounds (1)-(8).

The protonation reactions and metal complexing reactions of the polyphenols were studied by potentiometric and/or spectrophotometric techniques. These techniques and other experimental details are discussed in Chapter 2.

Figure 1.2 Compounds investigated

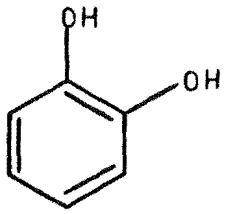

(1)

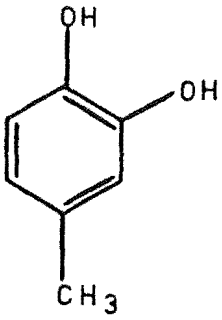

(2)

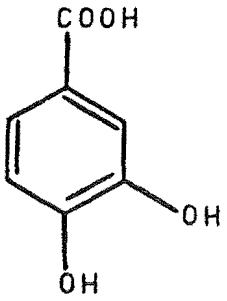

(3)

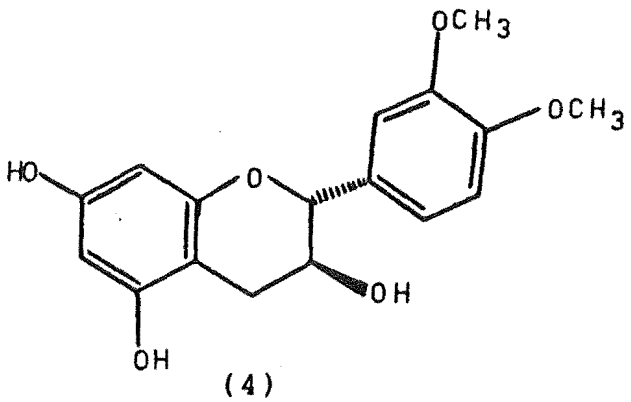

(4)

Figure 1.2 (cont.)

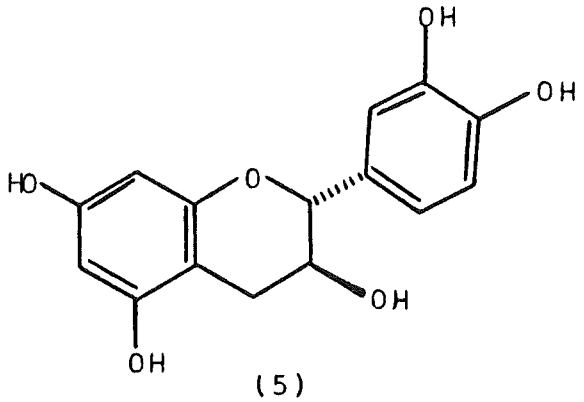

(5)

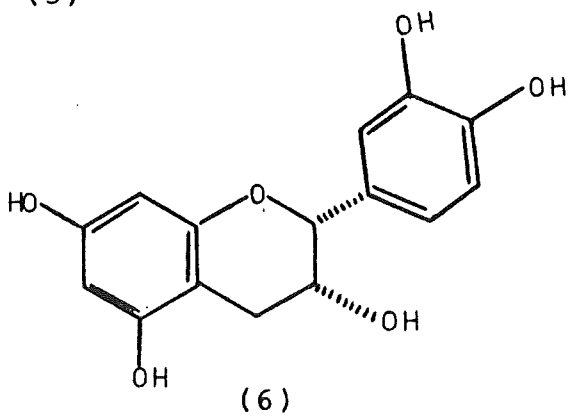

(6)

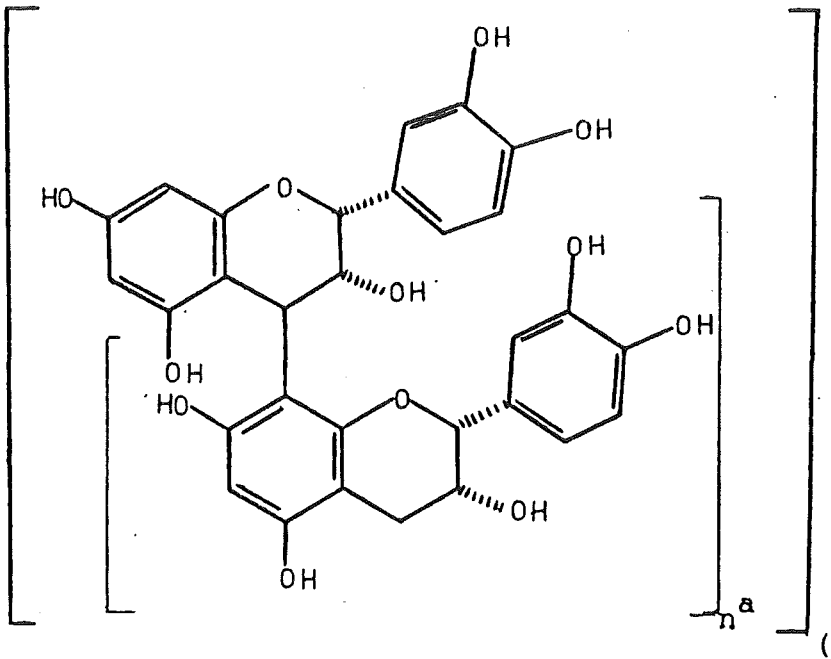

(7)

a n = 13 for B13

To interpret the ligand-proton or ligand-metal equilibria in solution it was necessary to have a probe capable of accurately determining equilibrium hydrogen ion concentrations. In this work a glass-calomel electrode pair was calibrated as a hydrogen ion concentration 'probe' by a method involving titration-generated buffers. The procedures required to standardize and calibrate the electrode pair to measure hydrogen ion concentration are discussed in Chapter 3.

The methods employed to calculate the ligand protonation constants (Chapter 5) and the metal ligand stability constants (Chapters 6 and 7) from spectrophotometric and potentiometric data are explained in Chapter 4.

Examination of protonation equilibria for the model compounds 4-methylbenzene-1,2-diol and 3',4'-di-O-methylcatechin facilitated the assignment of protonation equilibria for catechin and epicatechin to reactions on the A or B rings. These assignments were necessary because the catechins coordinate to metal ions via the phenolate oxygens of the B ring and the quantitative study of metal complexing reactions therefore required this information.

A detailed investigation was made of the redox reaction

$$Fe(III) + \text{polyphenol} \quad Fe(II) + 2H^{+} + \text{quinone} \qquad (1.1)$$

in which a series of polyphenols and high molecular weight species such as fulvic acids were examined. This reaction may be important in mobilizing insoluble Fe(III) oxide

coatings on soil particles, as Fe(II) has a greater solubility. Factors such as pH, time, ligand to metal ratio and absolute reagent concentration were studied; the results are given in Chapter 7.

Chapter 8 describes the development of experimental conditions for two field tests, one for Fe(II) in soil and the other for readily exchangeable Al(III) in soil. Analytical results are given for extractable Fe(II) and Al(III) in a number of soils tested both in the laboratory and in the field situation.

From the stability constants determined for Al(III)-polyphenol complexes it was possible to compare the complexing ability of these ligands with that for other ligands (e.g. citric acid, salicylic acid) at concentration levels found in soils. From a computer simulation described in Chapter 9 ligands were ranked according to their ability to solubilize an aluminium compound (gibbsite).

To complement these calculations the ability of polyphenols to dissolve freshly precipitated $Fe(OH)_3$ was investigated. This work included an assessment of the iron(III) loading necessary to precipitate the high molecular weight epicatechin polymer B13 from solution.

Chapter 10 considers the possible relevance of these results to the proposed mechanisms for podzolization viz. the 'fulvate' and 'silicate' mechanisms.

CHAPTER 2

EXPERIMENTAL

2.1 [H^+] Measurements

2.1.1 pH Meter

Most pH measurements were recorded using a Radiometer PHM64 research pH meter. This meter is a digital high precision instrument which has a resolution of $\pm$ 0.001 pH unit[51].

When necessary a Beckman Research pH meter was used. It is of the null potentiometric type and has a quoted relative accuracy of $\pm$ 0.00099 pH unit[52].

2.1.2 Electrodes

For accurate work the following electrodes were coupled to the Radiometer pH meter;

a) A Beckman E-2 glass electrode with an internal silver-silver chloride element[53]. The response of these electrodes to H^+ activity has been shown to be linear even in concentrated acid and alkaline solutions. They can be recognised by their all blue glass bulbs which are extremely fragile.

b) a Beckman frit junction calomel reference electrode Type 39071 or a Radiometer calomel electrode Type K401. Both electrodes had saturated potassium chloride as the filling electrolyte. A porous frit in each electrode provided the liquid junction between the electrode solution and the test solution. Minimal contamination of the test solution by KCl is a characteristic of these electrodes.

For routine measurements either an Orion or a Radiometer combination electrode was used.

When in regular use the electrodes were kept permanently at 25°C. For stable drift-free readings it was found necessary to thermostat the calomel electrodes at 25°C for at least 12 h before use. To minimize drift associated with variable liquid junctions the calomel electrodes were stored in saturated KCl[54].

2.2 Titration Cell

The ligands studied in this work were extremely oxygen sensitive under alkaline conditions. This required the complete exclusion of molecular oxygen from the titration solution. A titration cell designed by Taylor[55] was employed for accurate pH measurements. The cell assembly is shown in Figure 2.1.

A smaller titration cell was also designed specifically for use with smaller volumes of solution (c. 40 ml, cf. 185 ml for the larger cell). This cell was used for spectrophotometric titrations at high pH (> 12.5). It was of similar design to the larger cell except that it had one fewer electrode port and no water jacket. Although the size of this cell precluded the use of the polarographic oxygen electrode for monitoring the concentration of dissolved oxygen (see Section 2.3) it was known from work with the larger cell that 2.5 h of nitrogen purging was sufficient to remove all oxygen from the system. This small cell was thermostated by placing it inside the larger cell which acted as the water jacket (see Figure 2.1). The lid was sealed to the cell by means of a ground-glass flange.

Figure 2.1 Titration cells

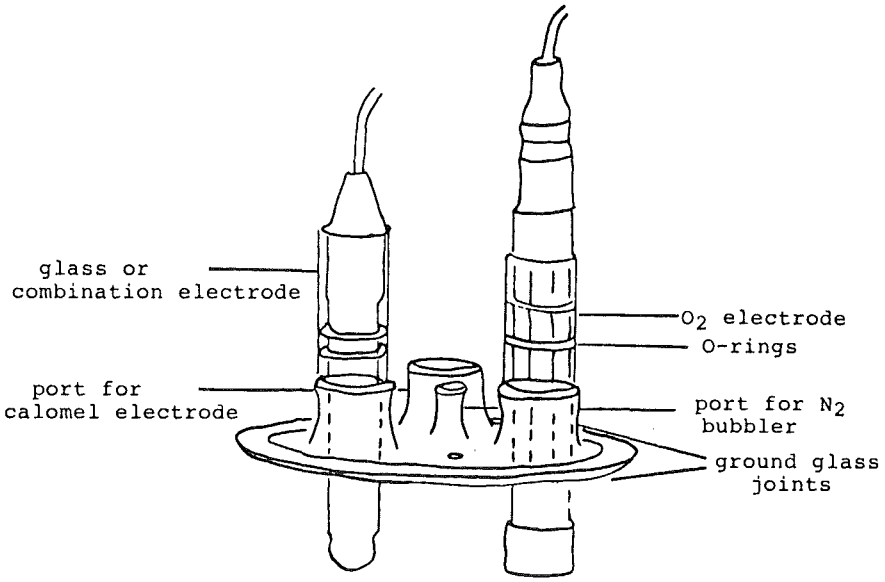

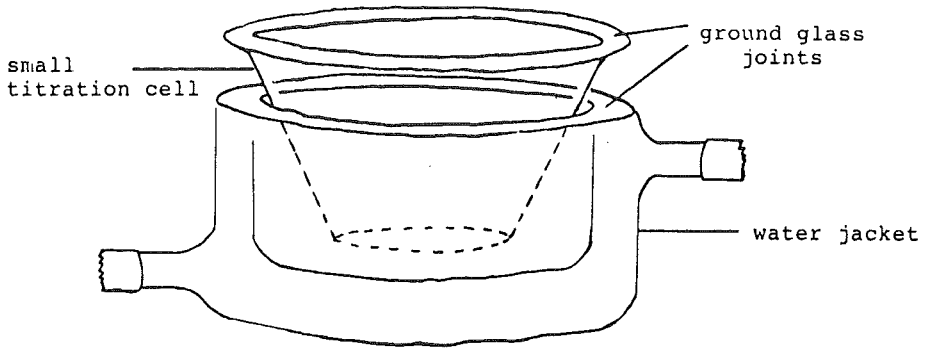

The lid contained two B19 electrode ports and one B7 bubbler port. Electrodes were made air tight inside their glass ports by rubber O-rings. When the ground glass joints were smeared with silicone grease the assembly was air tight. Two small holes in the lid enabled addition or removal of solution via plastic tubing or syringe needles fitted through septum seals or rubber bungs.

2.3 Deoxygenation

2.3.1 Oxygen analyser

Where possible, for titrations on oxygen sensitive ligands, the concentration of dissolved oxygen in a test solution was monitored with a Beckman 100802 Fieldlab oxygen analyser coupled with a Beckman 39550 polarographic oxygen electrode. The oxygen-responsive electrode determines the partial pressure of dissolved oxygen. Oxygen which has passed through a semi-permeable Teflon membrane is reduced at a Rhodium electrode according to the following equation:

$$2H_2O + O_2 + 4e^- \rightleftharpoons 4OH^- \qquad (2.1)$$

The resultant current is proportional to the partial pressure of oxygen in the bulk solution. Kee[56] has shown that the current response is linear with the concentration of dissolved oxygen from 0 ppm to c. 9 ppm (air saturation level).

2.3.2 Deoxygenation procedure

Test solutions that required the removal of oxygen were purged with oxygen-free nitrogen until no measurable oxygen remained in solution. The purified nitrogen was prepared by bubbling commercial nitrogen through a solution of sodium or potassium hydroxide to remove carbon dioxide

and then through an acidic vanadium(II) solution to remove traces of oxygen.

The V^{2+} was produced initially from VO^{2+} and then regenerated *in situ* by Zn/Hg amalgam reduction. The 'purified' nitrogen was then passed through the test solution. The bubbler unit that was used to pass the nitrogen into the titration cell allowed the gas to leave via the same port on the cell lid[57]. This gas stream was then passed through another gas wash bottle before being vented to the atmosphere.

The vanadium/zinc amalgam scrubbers were prepared by reaction of zinc metal with acidified mercuric chloride, as described by Russell[58].

2.4 Volumetric Equipment

(a) All pipettes used in quantitative work were calibrated by weighing the volumes of double distilled water delivered at 25°C. The weight of liquid dispensed was converted to a volume by means of published density data[59].

(b) The errors in total volumes assumed for volumetric flasks (B grade) were those given by Vogel[60].

(c) Micrometer syringes.

For quantitative work additions of standard titrant solutions were made with a Gilmont micrometer syringe (2.5 ml capacity) or an Agla micrometer syringe (0.5 ml capacity) calibrated in 0.001 ml and 0.0001 ml divisions respectively. A calibration of the Agla syringe by Hedwig[61] showed that the delivery was uniform along the syringe and that the volume dispensed was within 0.06% of

the scale reading. A similar calibration of the Gilmont syringe established uniform delivery and an error of -0.22%.

2.5 Preparation of solutions

2.5.1 Buffer solutions

The buffer solutions used to standardize the glass-calomel electrode assembly were potassium hydrogen tartrate (saturated at 25°C), potassium hydrogen phthalate (0.05 m), 1:1 potassium dihydrogen phosphate (0.025 m) : di-sodium hydrogen phosphate (0.025 m), borax (0.01 m), and 1:1 sodium bicarbonate (0.025 m) : sodium carbonate (0.025 m). The assigned pH(S) values are given in Chapter 3 Table 3.1. The buffer solutions were prepared by dissolving the indicated weight of pure dry buffer substance in 1 or 2 litres of double distilled carbon dioxide free water, according to the methods outlined by Bates[62]. o-Phthalic acid solutions used to calibrate the electrode assembly as a hydrogen ion concentration probe (see Chapter 3) were made from the recrystallized[63] acid. Analar grade chemicals were used in the preparation of all other buffer solutions.

2.5.2 Acid, base and electrolyte solutions

a) Potassium hydroxide. Analar KOH pellets (50% excess for the required stoichiometry) were washed quickly with distilled water. The pellets were then dissolved in carbon dioxide free double distilled water (DDW). The washing procedure removed sodium carbonate from the KOH pellets.

KOH solutions were standardized by potentiometric titration against potassium hydrogen phthalate. End points were located by a Gran's[64] analysis on the volume-

potentiometric data. Repeated titrations established concentrations with a precision of > 99.7%.

(b) Analar concentrated hydrochloric acid was diluted with carbon dioxide free DDW to make a solution of c. 1 M. The acid solution was standardized against sodium carbonate (dried at 260°C) and standard potassium hydroxide. These two methods consistently gave results to within ± 0.4%

(c) Potassium chloride. Titrations were performed in KCl solution, ionic strength 0.1 M. Analar potassium chloride, dried at 100°C and stored in a desiccator over $CaCl_2$, was used for the preparation of solutions.

2.5.3 Ligands

(a) Catechol (1,2-dihydroxybenzene) Koch-Light, pure and methyl catechol (4-methylbenzene-1,2-diol) ICN Pharmaceuticals were used without further purification. (Found for catechol: C,65.6; H,5.4; calc for $C_6H_6O_2$: C,65.4; H,5.5%.

Found for 4-methylbenzene-1,2-diol: C,67.9; H,6.2; calc for $C_7H_8O_2$: C,67.7; H,6.5%).

(b) Protocatechuic acid (3,4-dihydroxybenzoic acid) Koch-Light, pure was recrystallized three times from water and dried over P_2O_5. (Found for protocatechuic acid anhydrous: C,54.4; H,4.1; calc for $C_7H_6O_4$: C,54.6; H,3.9%). In contrast, Rodd[65] reported protocatechuic acid as a mono hydrate. Analysis by potentiometric titration with standard alkali confirmed the stated composition.

(c) Catechin (Fluka) and epicatechin (Goel Industries) were purified by Drs. L. J. Porter and L. Yeop Foo[66]. The method and tests for purity have been

described[67]. (Found for catechin: C,62.4; H,4.6; found for epicatechin: C,62.0; H,4.7; calc for $C_{15}H_{14}O_6$: C,62.1; H,4.9%).

(d) 3',4'-Di-O-methylcatechin was prepared by Porter and Yeop Foo[66] following the method of Sweeney and Iacobucci[68].

(e) The dimeric procyanidin B2 [epicatechin - (C(4)-C(8)) epicatechin] and a quince tannin polymer were made by Porter et al.[69,70]. The polymer with composition $(epicatechin)_n$, where n is 12 to 14, is designated B13.

The epicatechin dimer (B2) was dried in Al-foil capsules[50] under vacuum at 100°C. It analysed as anhydrous after a moisture weight loss of 8.85%. (Found for B2: C,62.1; H,4.59; calc for $C_{30}H_{26}O_{12}$: C,62.3%; H,4.5%).

(f) The following ligands were used semi-quantitatively in the study of iron-redox reactions: Tiron (1,2-dihydroxybenzene-3,5-disulphonic acid) BDH, laboratory reagent; tannic acid (Merck), tannic acid (Fluka), gallic acid (3,4,5-trihydroxybenzoic acid) BDH; and fulvic acid (2 samples). Fulvic acid samples were obtained by courtesy of Dr. M. Schnitzer (Agriculture Canada, Ottawa) and Dr. H. Anderson (Macaulay Institute for soil research, Aberdeen).

2.5.4 Ligand solutions

For ligands a, b, c, e and f solutions were prepared by dissolving a calculated weight of solid material in carbon dioxide free DDW. Where necessary solutions were stabilized against atmospheric oxidation by addition of a known volume of standard HCl. For quantitative work

solutions were not kept for more than three days; if stored they were refrigerated. For ligand e no acid was added and solutions were prepared immediately before use because this compound is known to undergo molecular rearrangement in acidic media[71].

3',4'-Di-O-methylcatechin is sparingly soluble in water. For use in pKa studies it was dissolved in dilute KOH to deprotonate and then titrated with HCl.

2.5.5 Metal solutions

(a) Aluminium Chloride. Analar aluminium chloride ($AlCl_3.6H_2O$) was dissolved in carbon dioxide free DDW. Metal hydrolysis was suppressed by the addition of standard HCl ($1.00x10^{-2}$ M). The aluminium ion concentration was determined accurately by gravimetric analysis as the 8-hydroxyquinolate[72].

(b) Ferric Chloride. Analar grade ferric chloride ($FeCl_3.6H_2O$) was dissolved in standard (1 M) HCl solution. The ferric ion concentration was determined by gravimetric analysis of iron as Fe_2O_3 as described by Vogel[73].

(c) Ferrous ion solutions. Ferrous ammonium sulphate, Analar grade, was dissolved in 1 M HCl. The solutions were deoxygenated and the flasks were kept firmly stoppered when not in use. These precautions were taken to suppress the atmospheric oxidation of Fe(II) to Fe(III). Prior to analytical measurements using these solutions, the ferrous and ferric content were checked spectrophotometrically (see Section 2.6.2); solutions were discarded when the Fe(III) content was greater that 5%.

(d) Copper Nitrate. An accurately weighed portion of Analar copper nitrate ($Cu(NO_3)_2.3H_2O$) was dissolved in 0.1 M acid solution to give a stock solution c. 0.1 M.

2.5.6 General Solutions

(a) Ammonium acetate (M&B Analar) was dissolved in double distilled water to give the required concentration, usually 1 M, pH 7.

(b) Anhydrous nitrilotriacetic acid, NTA, (Sigma) was dissolved in double distilled water by adding a calculated amount of base to deprotonate the acid. A small quantity of 2,2'-bipyridyl was added to convert any iron(III) contained in the NTA to iron(II); this lowered the measured blank in polarographic analyses.

(c) 2,2'-Bipyridyl (Baker 'Analysed') was solubilized in double distilled water by protonation with dilute Analar HCl. Typical concentrations ranged from 0.01 - 0.1% w/v.

2.6 Spectrophotometric measurements

Ultraviolet and visible absorption spectra were recorded on a Varian Superscan 3 spectrophotometer.

2.6.1 Ligand species

(a) For solutions that were not sensitive to oxygen, spectra were recorded using 1 mm, 10 mm, or 20 mm spectrophotometer cells.

(b) Spectra were recorded for oxygen sensitive solutions in a specially designed 1 mm flow cell. This cell, which has been described in detail by Taylor[74], allowed test solution to flow from the large (185 ml) or small (40 ml) oxygen proof titration cells to the spectrophotometer cell without being contaminated with

oxygen. Flow under N_2 pressure was aided by suction (water pump). Waste from the spectrophotometer cell was collected in a 5 ml measuring cylinder so that the total volume remaining in the titration cell could be calculated.

2.6.2 Determination of iron

(a) Iron(III). Ferric iron was determined quantitatively by spectrophotometric measurement as the $Fe(NCS)(H_2O)_5^{2+}$ complex.

A sample of the test solution was added to an equal volume of 5 M HCl in either a 10 or 25 ml volumetric flask. The high acidity froze both ferric and ferrous ions in their respective oxidation states. A standard quantity of 2 M ammonium thiocyanate was then added, followed by DDW up to the mark. The absorbance of the coloured iron(III)-thiocyanate complex was measured within 2 min at 480 nm. The absorbance was then compared with a linear calibration curve for the concentration range being investigated (typically $5x10^{-6}$ - $1x10^{-4}$ M).

(b) Iron(II). Ferrous iron was determined quantitatively by spectrophotometric measurement as the Fe(II)(2,2'-bipyridyl)$_3$ complex.

In the presence of 2,2'-bipyridyl (bp) and oxidizable organic matter Fe(III) is reduced to Fe(II), even at a pH of 7. It was therefore necessary to mask Fe(III) with NTA in NH_4COOCH_3 buffer(pH 7). The development of suitable reagent concentrations for this method is discussed in Chapter 7.

In a typical analysis a test solution (1 - 5 ml), having a concentration of 1 - $10x10^{-5}$ M Fe(II) was added to a buffered premixed solution of 2,2'-bipyridyl (2 ml, 0.02%)

and NTA (2 ml, 0.1 M) in a 10 ml volumetric flask and made up to the mark. The intensity of the colour resulting from the quantitative formation of the tris bipyridyl species was measured spectrophotometrically at 525 nm. The test absorbance was compared with a linear calibration curve for the concentration range being investigated (typically $1 - 10 \times 10^{-5}$ M).

2.6.3 Aluminium

The concentration of aluminium ion in solutions was measured by complexing with the colourimetric reagent chrome azurol S, CAS. In a typical test, aluminium solution (2 ml), CAS (0.6 ml 3×10^{-3} M) and hexamine buffer (pH 4.9, 2 ml; 1 M) were mixed in a 10 ml volumetric flask and DDW was then added up to the mark. The absorbance was measured at 544 nm and after a small absorbance correction for uncomplexed CAS, it was compared with a linear calibration curve (0.03 - 0.8 ppm). This test is discussed in more detail in Chapter 8.

2.7 H.P.L.C. measurements

Samples of catechin and epicatechin were checked for epimeric purity and for epimerization or rearrangement during pH titrations by h.p.l.c. measurements. The instrument used was a Varian 5020 h.p.l.c. coupled with an ultraviolet detector operating at 280 nm. Adequate separation of the isomers and rearrangement product were obtained using a C-18 reverse phase column and 1.5 ml min^{-1} of 30% CH_3OH, 0.05% trifluoro-acetic acid 70% (v/v) as eluent.

2.8 Microanalyses

Microanalyses of the ligands and complexes for C and H were performed by the Microanalytical Laboratory, University of Otago, Dunedin.

2.9 Atomic absorption spectroscopy

Atomic absorption analysis employed a Varian.A.A. 1475 instrument. Air/acetylene or N_2O/acetylene flames were used for the detection of iron, copper and calcium, or aluminium respectively.

2.10 Infrared spectroscopy

A Pye Unicom SP3-300 instrument was used to obtain Infrared spectra in the range 200 - 4000 cm^{-1}. Aluminosilicate samples were prepared as KBr discs (1 - 3 mg in 500 mg KBr) and dried at 150°C for 16 h [75].

2.11 Polarography

(a) Polarography was used to study the composition of dilute solutions of ferrous and ferric ions. The polarographic method involved measuring the current at a dropping mercury electrode as a function of applied potential for the reduction of iron(III) to iron(II). Development of a suitable complexing medium for application of this technique is discussed in Chapter 7. Typically a solution containing ferrous and ferric ions was added to a mixed reagent consisting of NTA, 2,2'-bipyridyl, and CH_3COONH_4 (pH 7) in a 10 ml volumetric flask, with final reagent concentrations of 0.25 M, 0.1% and 0.25 M respectively. This solution was then transferred to a polarographic cell and deoxygenated by nitrogen purging. Molecular oxygen must be removed from solution to eliminate

possible interference from its reduction which occurs at a similar voltage to that for reduction of the Fe(III) NTA complex. The nitrogen purge gas was purified by passage through vanadous scrubbers. Between 8 and 12 minutes of purging was required before an oxygen free polarogram could be recorded.

(b) For polarographic measurements a Princeton Applied Research Model 174A Polarographic analyser[76], and Model 303 Static Mercury Drop Electrode[77] were used, coupled to an X-Y recorder.

CHAPTER 3

CALIBRATION OF THE GLASS ELECTRODE AS A HYDROGEN ION CONCENTRATION PROBE

3.1 Introduction

The manner in which the glass electrode is responsive to the activity of hydrogen ions, the ease with which it can be handled, and its reliability have contributed to its widespread use in industry and research. The glass membrane electrode parallels the hydrogen gas electrode, the primary reference for hydrogen ion measurements[78], in that its potential (E_H) changes with hydrogen ion activity in accordance with the Nernst equation.

$$E_H = E^o - (RT/F)\ln a_{H^+} \qquad (3.1)$$

The response of the glass electrode may not be ideal when compared to the hydrogen electrode, i.e. the slope may be non-Nernstian. This response difference is expressed as the "electromotive efficiency", βe,

$$\beta e = (Ex - Es)/(Ex' - Es') \qquad (3.2)$$

where Ex, Es are the E_H values derived from the glass-calomel electrode assembly for solutions X and S respectively, and Ex', Es' are the E_H values for the same solutions when a hydrogen electrode replaces the glass electrode. The quantity βe is usually greater than 0.95[79] for modern glass electrodes. It is possible to apply mathematical corrections that compensate for non-Nernstian response.

3.2 Interpretation of "pH" measurements

The electrochemical cell employed in this work was

glass electrode||Soln.|KCl(satd), Hg_2Cl_2(s); Hg(l) (3.3)

The internal reference electrode within the glass electrode is not shown in this scheme. The emf (E) given by this electrode system is

$$E = E^{o} + Eas + E_{LJ} - (RT/F)\ln a_{H}^{+} \quad (3.4)$$

where Eas is the asymmetry potential of the glass electrode, E_{LJ} is the liquid junction potential across the liquid-liquid boundary and E^{o} is the standard emf for the cell. Equation (3.4) can be expressed

$$E = E^{o'} + E_{LJ} - (RT/F)\ln a_{H}^{+} \quad (3.5)$$

where $E^{o'} = E^{o} - Eas$, assuming that at constant temperature and pressure Eas will not change over short periods of time. Rearrangement allows expression in terms of a_H:

$$paH = (E - (E^{o'} + E_{LJ}))F/2.303RT \quad (3.6)$$

or in terms of mol l^{-1} of hydrogen ions

$$pcH = (E - (E^{o'} + E_{LJ})F/2.303RT + \log f_H \quad (3.7)$$

Examination of equation (3.6) indicates that the emf of the cell provides a measure of the activity of hydrogen ions (paH) in solution only if E_{LJ} is known. Furthermore, to obtain the molar concentration of hydrogen ions in solution (pcH^{a}) it is necessary to estimate the activity coefficient f_H. Neither of these quantities is easy to calculate. f_H is dependent on both the ionic strength, and the composition of solution with respect to each other ion present[80],

---

[a] pcH will from now on be represented as p[H]

as expressed by the Debye-Huckel equation (see equation (3.12)). The liquid junction potential (E_{LJ}) is unable to be computed without a knowledge of the individual ion activities[81]. Although detailed investigations have yielded estimates of liquid junction potentials[82], calculation is impractical for routine pH measurements.

Thus the paH or p[H] defined in equations (3.6) and (3.7) respectively is immeasurable. Therefore it is necessary to define the pH in terms of the operation or method used to measure it.

3.3 The practical pH scale

3.3.1 Standardization of the pH electrode system

The hydrogen ion activity may be derived from the emf of cell (3.3) once a value of $E^{o'} + E_{LJ}$ is selected. However the value of $E^{o'} + E_{LJ}$ for one cell assembly may differ from that for another of apparently identical design; it may also vary considerably with time. A value cannot be obtained from tables and therefore it is necessary to redetermine $E^{o'} + E_{LJ}$ at frequent intervals.

This standardization of the pH assembly is accomplished by the measurement of E(s), the emf of cell (3.3) when it contains a standard buffer solution whose paH is denoted pH(s).

$$E(s) = E^{o'} + E(s)_{LJ} - 2.303RT/F.pH(s) \qquad (3.8)$$

The emf of a test solution of unknown pH (whose paH is denoted pH(t)) can then be measured relative to the standard solution:

$$E(t) = E^{o'} + E(t)_{LJ} + 2.303RT/F.pH(t) \qquad (3.9)$$

The unknown pH(t) is then related to pH(s) by expression (3.10)

$$pH(t) = pH(s) + ((E(s) - E(t)) + (E(t)_{LJ} - E(s)_{LJ}))F/2.303RT \qquad (3.10)$$

which is obtained from equations (3.8) and (3.9). Equation (3.10) is the operational definition of pH which is widely accepted today. Use of this relationship requires reference solutions of known pH(s). The assignment of pH(s) values to the National Bureau of Standards (NBS) primary buffers is discussed in Section 3.4.1.

3.3.2 Limitations of the conventional activity scale

In practical terms determination of pH(t) (paH for the unknown) requires that the residual liquid junction potential $(E(t)_{LJ} - E(s)_{LJ})$ be approximately zero when the NBS standard is replaced by the test solution. In fact the measured pH, pHm, will equal pH(t) only when $E(t)_{LJ} - E(s)_{LJ} = 0$. For cell (3.3) in which the calomel electrode contains saturated KCl, the residual junction potential will be approximately zero for concentrations of test solutions and standard buffers of low ionic strength whose pH is greater than 3 and less than 11[83]; i.e. a linear relationship will be obtained between the measured pH (pH(t)) and the conventional pH(s) value of a series of buffers when referenced to a single primary standard.

It is unlikely that the test solution arising from equilibrium constant measurements will have the same ionic activity as the standard buffer solutions. Further, any residual liquid junction potential is changed at high acidities and high alkalinities because of unequal diffusion

of ions in the two directions across the liquid boundary (viz. at low pH and high pH the highly mobile hydrogen and hydroxyl ions contribute significantly to E_{LJ}). The glass electrode also suffers from alkali metal ion errors at high pH[53].

To calculate p[H] from pHm or pH(t) one requires a value for f_H (equation (3.11).

$$pH(t) = -\log a_H = -\log [H]f_H \qquad (3.11)$$

f_H is the (hypothetical) single ion activity coefficient for H^+. It may be calculated, but only approximately, by use of a relationship such as the Huckel form of the Debye-Huckel equation (3.12):

$$\log f_i = Az_i^2 I^{0.5}/(1 + B.a_o I^{0.5}) + b_i I \qquad (3.12)$$

where I = "ionic strength" = $0.5 \sum m_i z_i^2$

z_i = charge of ionic species i

a_o = "ion size parameter"

m_i = concentration of ionic species i in units mol Kg^{-1}

A,B = constants dependent on temperature and dielectric constant of the solvent

Parameters a_o and b are empirically derived and are dependent on the chemical nature of the ions involved.

It should not be assumed that this empirical equation is reliable for mixed electrolyte solutions as would exist in metal-ligand equilibrium studies.

Calibration of the electrode assembly at the same ionic strength as the test solutions can be achieved by the use of standard solutions S' of known $[H^+]$, including buffer systems of known $[H^+]$. This calibration is made relative to

NBS buffers as pH standards. It eliminates the problems discussed above since $E(t)_{LJ} - E(S')_{LJ} = 0$ and a value for f_H is not required. This calibration procedure is outlined fully in Section 3.5.

3.4 Electrode standardization

3.4.1 NBS standard pH scale

"pH" is defined in terms of the pH(s) values for several selected buffer standards on the NBS conventional paH scale. The NBS multistandard scale has been adopted by the American Society for Testing and Materials[84] and has received the endorsement of the IUPAC[85]. The seven primary standards of the National Bureau of Standards together with their assigned pH(s) values at 25°C[86,87] are listed in Table 3.1.

Table 3.1 Primary Standards of the NBS "pH" scale at 25°C

Primary Buffer Solution	pH(s)	Ref
KHtartrate (satd)	3.557	90
KH_2 citrate (m = 0.05)	3.776	91
KH phthalate (m = 0.05)	4.008	92,93
KH_2PO_4 (m = 0.025), Na_2HPO_4 (m = 0.025)	6.865	94
KH_2PO_4(m = 0.0089695), Na_2PO_4 (m = 0.03043)	7.413	95
$Na_2B_4O_7$ (m = 0.01)	9.180	92
$NaHCO_3$ (m = 0.025), Na_2CO_3 (m = 0.025)	10.012	92

These buffer solutions were selected for their reproducibility and ease of preparation. The pH range from 3.5 to 10 is covered and within this range the liquid junction potential is nearly constant.

The standardization procedure adopted by the NBS to obtain pH(s) values for these and other reference solutions consisted of four steps[88].

1. Measurement of the emf, E for the reference buffer with a hydrogen electrode and Ag, AgCl reference electrode without a liquid junction. Alkali metal chloride was added in small concentration increments. The function $p(a_H\ f_{Cl})$ was obtained from the measured emf and the standard emf of the cell by

$$p(a_H\ f_{Cl}) = (E - E^o)F/2.303RT + \log m_{Cl} \qquad (3.13)$$

2. Extrapolation of $p(a_H\ f_{Cl})$ to $M_{Cl} = 0$, to obtain $p(a_H f_{Cl})^o$.

3. Calculation of pa_H from

$$pa_H = p(a_H\ f_{Cl})^o + \log f_{Cl} \qquad (3.14)$$

by introduction of the "Bates-Guggenheim" convention,

$$\log f_{Cl} = - AI^{0.5}/(1 + 1.5I^{0.5}). \qquad (3.15)$$

4. Identification of this conventional pa_H for selected reference solutions with pH(s) in the operational definition of pH, equation (3.10).

3.4.2 Electrode response to NBS buffers

Standardization of the electrodes used in this work was against three NBS primary standard buffers (viz. 1:1 phosphate, pH(s) 6.865; potassium hydrogen phthalate, pH(s) 4.008; borax, pH(s) 9.180). The emf response was linear from pH(s) 3.557 (KHtartrate) to pH(s) 10.012

(carbonate/bicarbonate). Standardization procedures were carried out with 3 buffers before and after each titration. Hedwig has shown that buffers prepared from Analar chemicals have pH values identical with those prepared from NBS certified chemicals[89]. Once used the buffer solution was discarded; this required regular preparation of fresh buffer solutions.

3.5 Calibration of the glass electrode as an hydrogen ion concentration probe

3.5.1 Introduction

To obtain information on the equilibria involved in acid-base and metal-ligand systems it is necessary to know the equilibrium concentration of the hydrogen ion in solution, $[H^+]$. The glass electrode measures the activity (paH) of the hydrogen ions and it is therefore necessary to convert paH to p[H].

The problems encountered in the determination of $[H^+]$ from measurement in cells with liquid junctions have been discussed in Section 3.3. By calibrating the electrode system against solutions of known $[H^+]$ and at the same ionic strength as for the test solutions one avoids the approximations that otherwise have to be made concerning activity coefficients and liquid junction potentials. Any such electrode calibration is still relative to the NBS buffers. The calibration is therefore valid for all pH measurements when the electrodes are first standardized against the NBS primary buffers.

McBryde[96] has calibrated glass/calomel electrode pairs using solutions of strong acid and strong base in

media of constant ionic strength. Powell and co-workers[97-99] extended the calibration procedure to the intermediate pH range by titration of buffer solutions with standard acid or alkali at constant ionic strength.

In this work cell (3.3) was calibrated against solutions of known hydrogen ion concentration in the pH range 3 - 12 by use of a titration generated series of o-phthalic acid buffers and by use of dilute potassium hydroxide solutions in KCl medium. The hydrogen ion concentrations for the buffer solutions were readily calculated from the solution composition at each datum point and from the published concentration quotients for the buffer. Values for the H^+ concentration in the KOH calibrations were calculated from the analytical concentrations of alkali (assuming complete dissociation) and from Kwc, the ionic activity product of water.

3.5.2 Potassium hydroxide calibration

Calibrations at high pH were obtained by the titration of standard KOH into potassium chloride solution (I = 0.10 M). A total of seven titrations and 250 data points were used to define the p[H] versus pHm relationship in this region. Data were not corrected for liquid junction or potassium ion errors and at pHm > 11.8 the plot of $p[H^+]$ versus pHm was non-linear. Hydrogen ion concentrations were calculated from the known [OH] and Kwc of water.

$$Kwc = a_H.a_{OH} /a_{H_2O} = [H].[OH].(f_H.f_{H_2O} /a_{H_2O}) \quad (3.16)$$

Because the ionic strength varied slightly in the course of a titration (0.095 - 0.105) Kwc was adjusted by an

empirical relation for $(f_H.f_{H_2O}/a_{H_2O})$[100] as described by Taylor[101]. Calculated values of $p[H^+]$ are tabulated against measured pH values, pHm, in Table 3.2.

3.5.3 o-Phthalic acid calibration

Solutions containing weighed amounts of o-phthalic acid and potassium chloride were titrated with standard potassium hydroxide to generate a set of buffer solutions from pHm 2.9 to 5.1. Three titrations were performed, each consisting of at least 43 data points. For each datum point a FORTRAN[102] program was used to calculate p[H] from the volume of alkali titre; it used pHm as a trial value of p[H] in Newton-Raphson iterative calculations. Other input data required by the program were the initial volume, parameters for activity calculations and information relating to solution stoichiometry (e.g. total o-phthalic acid concentration). In addition to these data the program required the concentration quotients for the o-phthalate association equilibria.

$$HPh + H \rightleftharpoons H_2Ph \qquad (3.17)$$

$$Ph + H \rightleftharpoons HPh \qquad (3.18)$$

The concentration quotients for these equilibria are

$$K1 = [H_2Ph]/[H][HPh] \qquad (3.19)$$

$$K2 = [HPh]/[H][Ph] \qquad (3.20)$$

respectively. These quotients, which varied with ionic strength and therefore with solution composition, were calculated from the thermodynamic acid dissociation constants[92,93] by evaluating the activity coefficients from an empirical equation (an extended form of the Debye-Huckel equation).

Table 3.2 p[H] and pHm values from KOH/KCl titrations[a]

titre (ml)[b]	p[H]	pHm
0.250	11.041	11.151
0.300	11.120	11.232
0.350	11.187	11.300
0.400	11.245	11.358
0.450	11.296	11.410
0.500	11.341	11.454
0.600	11.420	11.535
0.700	11.487	11.600
0.800	11.545	11.658
0.900	11.595	11.707
1.000	11.641	11.755
1.200	11.720	11.831
1.400	11.786	11.897
1.600	11.843	11.953
1.800	11.894	12.003
2.000	11.939	12.047
2.200	11.980	12.087
2.400	12.017	12.121

a Initial total volume = 150 ml,

initial ionic strength = 0.095 M

b [KOH] = 1.064 M

The electrode system was first standardized against 1:1 phosphate, phthalate, tartrate and potassium tetroxalate buffers; a linear response was obtained for buffers in the pH range 6.9 - 3.5. At pH < 3.5 deviation from linearity was apparent; the pH value for 0.05 M tetroxalate measured relative to the other buffers was 0.034 pH units lower than its pH(s) value of 1.679. Corrections were applied to all data below a pH of 3.5 based on the assumption that the deviations caused by liquid junction effects are a function of pH and the liquid junction assembly only. This assumption was verified by Taylor[103] from measurements on cells without liquid junctions.

Representative data from the titration of o-phthalic acid solutions with standard potassium hydroxide at an ionic strength of 0.1 M (KCl) are given in Table 3.3. A regression line was calculated from data in Tables 3.2 and 3.3. The results are presented as coefficients of the equation

$$pHm = M \times p[H] + C \qquad (3.21)$$

Two independent calibrations were performed, yielding slopes of 1.000 and intercepts 0.114 and 0.109.

Instead of titration generated buffers, individual calibrant solutions can be prepared, for example by addition of selected volumes of 1.00 M KOH into 100.0 ml of 5×10^{-3} M phthalic acid solution. Table 3.4 lists the volumes of KOH required to generate solutions of known p[H]. Further data for phthalate buffers generated by incremental addition of standard KOH have been published by the author[99].

Table 3.3 Titration[a] of o-phthalic acid[b] with standard KOH at 25°C

titre (ml)[c]	p[H]	pHm
0.010	2.972	3.042
0.020	2.985	3.052
0.030	2.997	3.066
0.050	3.023	3.093
0.070	3.050	3.125
0.090	3.079	3.154
0.110	3.109	3.186
0.130	3.141	3.220
0.150	3.175	3.256
0.180	3.230	3.314
0.200	3.270	3.356
0.220	3.312	3.402
0.240	3.359	3.452
0.260	3.409	3.506
0.280	3.465	3.565
0.300	3.525	3.630
0.320	3.593	3.703
0.340	3.668	3.783
0.360	3.751	3.870
0.380	3.843	3.970
0.390	3.892	4.027
0.400	3.943	4.072
0.410	3.996	4.128
0.440	4.157	4.289
0.450	4.210	4.346
0.460	4.263	4.393
0.470	4.314	4.447
0.480	4.364	4.493
0.490	4.413	4.543
0.500	4.460	4.585
0.510	4.506	4.636
0.520	4.551	4.679
0.530	4.595	4.721
0.540	4.638	4.762
0.550	4.680	4.804
0.560	4.722	4.854
0.570	4.762	4.886
0.580	4.803	4.928
0.590	4.843	4.965
0.600	4.882	5.008

a initial total volume = 150.00 ml

b [o-phthalic acid] = 1.69×10^{-3} M

c [KOH] = 0.612 M, ionic strength ranged from 0.095 to 0.105 M

Table 3.4 p[H] for phthalate buffers[a] generated by titration[b], 25°C

titre (ml)[c]	p[H]	Ionic strength[d]
0.050	2.702	0.097
0.075	2.736	0.097
0.100	2.772	0.097
0.125	2.810	0.097
0.150	2.849	0.098
0.175	2.891	0.098
0.200	2.936	0.098
0.225	2.983	0.098
0.250	3.033	0.098
0.275	3.087	0.098
0.300	3.146	0.098
0.325	3.209	0.098
0.350	3.279	0.099
0.375	3.357	0.099
0.400	3.444	0.099
0.425	3.542	0.099
0.450	3.653	0.099
0.475	3.777	0.100
0.500	3.910	0.100
0.525	4.047	0.100
0.550	4.177	0.100
0.575	4.299	0.101
0.600	4.410	0.101
0.625	4.512	0.102
0.650	4.607	0.102
0.675	4.696	0.103
0.700	4.783	0.103
0.725	4.867	0.104
0.750	4.950	0.104
0.775	5.034	0.105
0.800	5.121	0.105
0.825	5.211	0.105
0.850	5.309	0.106
0.875	5.416	0.106
0.900	5.540	0.106

a [o-phthalic acid] = 5×10^{-3} M

b Initial total volume = 100 ml

c [KOH] = 1.00 M

d Initial ionic strength = 0.094 M

3.6 Discussion

Although the coefficients M and C in equation (3.21) will depend on the particular electrode system used, reasonable agreement is expected between cells of similar design. The slope and intercept obtained in this work were similar to those determined by Taylor[104] for phthalate buffers in 0.1 M KCl (slope, 1.001; intercept, 0.087), by Avdeef and Bucher[105] for mixed acetate, phosphate, boric acid buffer systems in 0.1 M KCl (0.998, 0.10), by McBryde[96] for dilute HCl/NaOH in 0.1 M NaCl (0.994, 0.105) and by Hedwig and Powell[98] for ethylenediamine-ethylenediammonium buffers in 0.1 M NaCl (0.995, 0.088). Buffers generated by the titration technique described may be used to calibrate electrode systems for $[H^+]$ if concentration quotients are known accurately from measurements in cells without liquid junctions.

By use of equation (3.21) it is possible to obtain a direct measurement of the hydrogen ion concentration in solution from the instrumental reading pHm. Electrode calibration against solutions of known $[H^+]$ is done relative to the NBS buffers as primary standards. Regular standardization ensures the validity of the pHm-p[H] relationship.

Two methods for determining $[H^+]$ in solution without reference to standard NBS buffers have been reported by May et al.[106]. The glass electrode-reference electrode pair were directly calibrated against solutions of known $[H^+]$ generated from the titration of (i) a strong acid with a strong base or (ii) a weak acid (glycine) with a strong

base. This second method involved simultaneous determination of the coefficients to equation (3.21) and the protonation constants for the acid from a single titration. However, although these workers referred to the error introduced by calibrating in a pH region where liquid junction potentials vary with $[H^+]$ (viz. < 3.5, and > 10.5) they made no allowance for this effect. Although the calibrations at low pH and high pH may be linear in their respective pH regions , they may not be colinear when extrapolated into the pH range 4 - 9.2 where liquid junction potentials are approximately constant. This has been shown to be the case by Powell and Taylor[107].

The most reliable method for determination of $[H^+]$ is that described in this chapter which (i) employs a titration generated series of buffers for a compound having accurately known protonation constants (determined from measurement in cells without liquid junctions) and (ii) makes allowance for the pH dependence of E_{LJ} at low pH and at high pH.

CHAPTER 4

COMPUTATIONAL METHODS

The interactions of polyphenols (catechol, catechin) with protons and metal ions have been studied by potentiometric and spectrophotometric methods.

At any particular point in a ligand-acid or ligand-metal titration the concentrations of all the species in solution may be described by mass balance equations. The equilibrium concentration of each species may then be expressed as a function of the known or unknown equilibrium constants. It is possible to solve these mass balance equations by computational analysis to yield values for the equilibrium constants. This chapter outlines the derivation of mass balance equations and the method of solving them used in this work. Also considered is the evaluation of equilibrium constants from spectrophotometric data.

4.1 Equilibrium constants

Equilibrium constants are given for both stepwise and cumulative processes. Cumulative constants (β_{pqr}) are defined for the general reaction:

$$pM + qL + rH \rightleftharpoons M_pL_qH_r$$

$$\beta_{pqr} = [M_pL_qH_r]/[M]^p[L]^q[H]^r$$

Stepwise constants are defined as in

$$M + L \rightleftharpoons ML \qquad K_{110} = [ML]/[M][L]$$

$$ML + L \rightleftharpoons ML_2 \qquad K_{120} = [ML_2]/[ML][L]$$

where $K_{120} = \beta_{120}/\beta_{110}$.

Cumulative protonation constants can be represented in a similar way.

e.g. $L + rH \rightleftharpoons LH_r$ $\qquad \beta_{01r} = [LH_r]/[L][H]^r$

4.1.1 Ligand protonation equilibria

Titration of a weak acid such as a polyphenol (LH_r) with a strong base (KOH) generates successively a number of deprotonated species (LH_r, LH_{r-1}, ... L). These species are related by the following equilibria and protonation constants:

$$L + H \rightleftharpoons LH \qquad K_{011} = [LH]/[L][H] \qquad (4.1)$$

$$LH + H \rightleftharpoons LH_2 \qquad K_{012} = [LH_2]/[LH][H] \qquad (4.2)$$

$$LH_{r-1} + H \rightleftharpoons LH_r \qquad K_{01r} = [LH_r]/[LH_{r-1}][H] \qquad (4.3)$$

The charges have been omitted for clarity. The total analytical concentration of the ligand (TL) and of ionizable protons (TH) can be equated to the sum of the equilibrium concentrations of the individual species:

$$TL = [L] + [LH] + [LH_2] + ... + [LH_r] \qquad (4.4)$$

and $$TH = [H] + [LH] + 2[LH_2] + ... + r[LH_r] - [OH] \qquad (4.5)$$

The term [OH], the equilibrium concentration of hydroxide ion, is included because of hydrolysis reactions of the type

$$LH_{r-1} + H_2O \rightleftharpoons LH_r + OH \qquad (4.6)$$

which will be important if LH_{r-1} is a measurably strong base.

TL and TH may be expressed in terms of measurable quantities. They were derived respectively from the initial concentration of ligand, TLI, and from the initial concentration of ionizable protons associated with the ligand. These quantities were adjusted for dilution and for

concentration of added acid [AH], and the concentration and volume of alkali titrant:

$$TL = TLI\ V/(V + v) \qquad (4.7)$$

and $$TH = r\ TL + [AH] - [KOH]\ v/(v + V) \qquad (4.8)$$

V is the initial volume of the titration solution and v is the volume of added KOH.

A secondary concentration variable $\bar{n}H$[108] was used in the evaluation of protonation constants from potentiometric data. This variable defines the degree of protonation of the ligand, L.

$$\bar{n}H = ([LH] + 2[LH_2] + ... + r[LH_r])/TL \qquad (4.9)$$

For example, a ligand such as catechol (1) in an acidic medium has $\bar{n}H$ 2.0; that is the catechol is in its fully protonated form. In contrast at pH 15 the numerator of equation (4.9) is close to zero because virtually all the catechol is doubly deprotonated (i.e. L^{2-}).

Incorporating equation (4.5) into equation (4.9) gives

$$\bar{n}H = (TH - [H] + [OH])/TL \qquad (4.10)$$

which allows $\bar{n}H$ to be calculated from the experimentally measurable quantities TH, [H], [OH] and TL at each datum point in a titration. This affords a value designated $\bar{n}H(obs)$.

On the other hand by use of the equilibrium expressions for the various ligand species (equations (4.1) to (4.3)), substitution in equation (4.9) allows $\bar{n}H$ to be expressed as a function of the protonation constants and the equilibrium hydrogen ion concentration. For example, for catechol (r = 2),

$$\bar{n}H = (K_{011}\,[H] + 2K_{011}\,K_{012}\,[H]^2)/$$
$$(1 + K_{011}\,[H] + K_{011}\,K_{012}\,[H]^2) \quad (4.11)$$

Thus for each point on the generated titration curve $\bar{n}H$ is a function of the equilibrium concentrations of all the species in solution. By assuming values for K_{011} and K_{012}, $\bar{n}H$ can be calculated at each datum point, viz. $\bar{n}H(calc)$. The values of $\bar{n}H$ derived from equation (4.10), $\bar{n}H(obs)$, and from equation (4.11), $\bar{n}H(calc)$, can be used as the basis for a least squares analysis to find the best values of K to fit the experimental data.

4.1.2 Protonation constant determination by least squares analysis

The set of successive protonation constants for a ligand such as catechol can be determined by a number of methods[109-111]. In this work a non-linear least squares[112] process was used to iteratively refine the equilibrium constants to obtain a best fit to the experiment data. The non-linear least squares program altered the trial parameters (protonation constants) to minimize the squares of residuals for the $\bar{n}H$ functions, summed over all the experimental data points:

$$(\bar{n}H(obs) - \bar{n}H(calc)(f\,K_{011}K_{012}\,..\,K_{01r}))^2 \quad (4.12)$$

The FORTRAN programs written to calculate $\bar{n}H(obs)$ and $\bar{n}H(calc)$ are listed in appendices A-C.

For the polyphenols studied data in the pH range 3.5 to 11.2 were used in the calculations although points near inflexions in a titration curve were routinely excluded. Unit weighting was applied to each datum point[113,114]. Above a pH of 11.2 the individual residuals became

unacceptably large (> 5% of $\bar{n}H(obs)$) for accurate refinement of K values. For data at high pH deviation of the residuals from a mean of zero was attributed to (i), the larger uncertainty associated with the pH measurements in strongly alkaline solutions, and (ii) the increasing dependence of $\bar{n}H(obs)$ (equation (4.10)) on the hydrolysis term, [OH].

4.2 Metal ligand stability constants

The association reactions between the metal ion Al^{3+} (M) and the anions of weak acids LH_r (e.g. catechol, LH_2) have been studied potentiometrically by addition of KOH to acidified solutions containing known amounts of ligand and metal.

In such a system, metal-ligand and metal-hydroxide equilibria must be considered in addition to the competing ligand proton interactions (equations (4.1) - (4.3)). The following equilibrium reactions and mass balance equations illustrate this point but are for a simplified metal system in which only mono, bis and tris complexes (ML, ML_2, ML_3) and one metal hydroxide species are considered. Equations (4.13) - (4.16) express the equilibrium relationships between species in solution.

$$M + L \rightleftharpoons ML \qquad K_{110} = [ML]/[M][L] \qquad (4.13)$$

$$ML + L \rightleftharpoons ML_2 \qquad K_{120} = [ML_2]/[ML][L] \qquad (4.14)$$

$$ML_2 + L \rightleftharpoons ML_3 \qquad K_{130} = [ML_3]/[ML_2][L] \qquad (4.15)$$

$$M + H_2O \rightleftharpoons MOH + H \qquad \beta_{10-1} = [MOH][H]/[M] \qquad (4.16)$$

The charges are omitted for convenience. The K_{pqr} values are termed stability constants[111] and the β_{p0r} is the metal hydrolysis constant.

In order to calculate the stability constants from the potentiometric pH titration data it is necessary to define three mass balance equations for the total concentrations of ligand (TL), metal (TM) and ionizable protons (TH):

$$TL = [L'] + [ML] + 2[ML_2] + 3[ML_3] \quad (4.17)$$

$$TM = [M] + [MOH] + [ML] + [ML_2] + [ML_3] \quad (4.18)$$

$$TH = [H] + [LH] + 2[LH_2] - [MOH] - [OH] \quad (4.19)$$

The term [L'] encompasses all the ligand species that are not coordinated to the metal, while [M] is defined as "free" metal viz. $Al(H_2O)_6^{3+}$. These mass balance equations can be expressed in terms of stability constants by substituting (4.13) - (4.16) and (4.1) - (4.2) into equations (4.17) - (4.19).

$$TL = [L'] + [L](K_{110}[M] + 2K_{110}K_{120}[L][M] + 3K_{110}K_{120}K_{130}[M][L]^2) \quad (4.20)$$

$$TM = [M](1 + K_{110}[L] + K_{110}K_{120}[L]^2 + K_{110}K_{120}K_{130}[L]^3 + \beta_{10-1}/[OH] \quad (4.21)$$

$$TH = [H] + K_{011}[L][H] + 2K_{012}K_{011}[L][H]^2 - \beta_{10-1}[M]/[H] - [OH] \quad (4.22)$$

As described in Section 4.1.1 it is possible to express these mass balance equations in terms of the analytical concentrations of the particular reactant:

$$TL(obs) = TLI\ V/(V + v) \quad (4.23)$$

$$TH(obs) = (r\ TL + [AH]) - [KOH]\ v/(V + v)) \quad (4.24)$$

and

$$TM(obs) = TM\ V/(V + v). \quad (4.25)$$

4.2.1 Solution of mass balance equations and determination of stability constants

For each point in the titration curve the mass balance equations (4.20) - (4.22) were solved iteratively using a successive approximation technique[115] and the stability constants were then obtained by the non-linear least squares method described below.

The unknown quantities in the TL, TM and TH expressions were the free metal concentration [M], the free ligand concentration [L] and the stability constants K_{110}, K_{120}, K_{130}. The refinement process began with a trial value for [L] which was estimated from the total ligand concentration, the pH at which complexing occurred and the known protonation constants for the ligand. This enabled equation (4.21), the total metal mass balance to be solved to obtain an approximate value of [M]. The trial values for the stability constants were estimated from the positions of buffer regions in the potentiometric titration curve. TM, the total concentration of metal in solution was known from the initial stoichiometry and the dilution factor (V/V + v) as alkali was added quantitatively to the titration solution. [H], the equilibrium hydrogen ion concentration was measured using the electrode system and the calibration procedure described in Chapter 3.

An improved value of [L] was then found by solving equation (4.20) using a Newton-Raphson[115] iterative method and the value of [M] obtained from equation (4.21). The refined value of [L] was used to recalculate [M] from equation (4.21) which was then compared with the previous

value of [M] for this datum point; if the two values differed by more than a preselected margin (viz. log [M1] - log [M2] $\geqslant$ 0.001) the process of refinement was repeated from the second step. When the two values of [M] were in acceptable agreement the total acid mass balance equation (4.22) was evaluated; the resultant value of TH was designated TH(calc). TH(obs) was calculated from equation (4.24).

The FORTRAN programs written to calculate TH(obs) and TH(calc) are listed in appendices D and E. These programs were subroutines to the least squares program ORGLS[112]. The least squares refinement varied the stability constants (K_{110}, K_{120}, K_{130}) to minimize the function

$$(TH(obs) - TH(calc)(f\ K_{110}\ K_{120}\ K_{130}))^2 \qquad (4.26)$$

over all the data points. The criteria adopted for an acceptable refinement are discussed in Chapter 6.

Highly charged metal ions such as Al(III) form many monomeric and polymeric hydrolysis species (see Chapter 6). When these species were incorporated in equation (4.21) it became non-linear with respect to [M] and was therefore solved iteratively by the Newton-Raphson method. The β_{p0r} values used in this calculation were selected from the literature, as discussed in Chapter 6. For equilibrium species with numerically large constants (e.g. $Al_{13}(OH)_{32}$, $\log \beta_{130-32} = -103.1$) it was necessary to express the equilibrium equation in log units in order to avoid "overflow" on the computer.

By interchanging the roles of equations (4.20) and (4.22) it was possible to refine on TL (equation (4.20));

the values for the derived parameters were the same as those arising from refinement on TH. Further, in the refinement of metal-ligand equilibria using the Prime computer, L^{2-} was replaced with the species H_2L; not only is this species dominant in the pH range encountered for metal ligand equilibria but its use helped to prevent computer "underflow" which can arise in equations with $[L^{2-}]^3$.

4.3 Hardware

The FORTRAN program ORGLS and the subroutines were used on a Burroughs 6700 or a Prime computer.

4.4 Spectrophotometric determination of protonation constants

4.4.1 Spectrophotometric analysis

Ligands such as the polyphenols investigated in this work do not absorb in the visible region of the electromagnetic spectrum, but because of their benzene ring chromophore(s)[116] they absorb ultraviolet radiation. These chromophores obey Beer's law[117]

$$\log Io/I = Ab = alc \qquad (4.27)$$

where the absorbance Ab is equal to the log of the intensity of the incident radiation divided by the intensity of the transmitted radiation; a is the molar absorptivity, often termed ε the molar extinction coefficient, which is characteristic of the absorbing species. The terms l and c are the cell path length (cm) and concentration of absorber (mol l^{-1}) respectively.

In a system where several species absorb at a given wavelength Beer's law can be expressed as a sum of absorbances,

$$Ab = a_1 l c_1 + a_2 l c_2 + ... a_n l c_n \qquad (4.28)$$

where l is the same for each species; that is, absorbance is an additive property.

Protonation of a ligand such as catechol changes the electronic state of the chromophore, creating an independent absorbing species, viz.

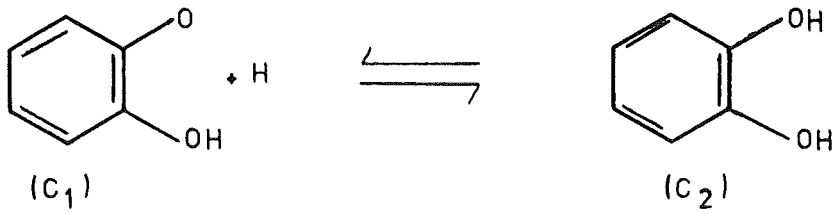

(C_1) (C_2) (4.29)

The concentration c_1 or c_2 can be calculated from the measured absorbance at a given wavelength if the total ligand concentration is known,

$$c_1 + c_2 = TL \qquad (4.29a)$$

and if the absorption coefficients, a_i, are known (equation (4.28)). Evaluation of the equilibrium constant (K_{011}) for reaction (4.29) then requires only the equilibrium hydrogen ion concentration.

$$K_{011} = c_2 / c_1[H] \qquad (4.30)$$

The hydrogen ion concentration can be measured reliably for solutions whose pH is within the range of the calibrant solutions or it can be calculated for solutions of very high pH (see appendix F).

In systems where one extinction coefficient was not known because of overlapping consecutive equilibria, alternative methods were used to calculate equilibrium constants. For equilibria studied at constant ionic strength knowledge of the absorptivity for one species (a_i), the total absorbance Ab at a particular wavelength, the total ligand concentration TL and the equilibrium hydrogen ion concentration permitted the use of Agren's graphical method[118] to determine the equilibrium constant. This method employed equation (4.31).

$$TL/Ab = 1/a_1 + ([H]\ Ab - (a_2\ TL/Ab))\ K_{pqr}/a_1 \qquad (4.31)$$

which is derived from equations (4.28), (4.29a) and (4.30). TL/Ab was plotted against the expression within the brackets. This resulted in a straight line with an intercept of $1/a_1$ and a slope of K_{pqr}/a_1. This method was used to determine the value of K_{014} for catechin; the value of a_{LH_4} was known and the value of a_{LH_3} was obtained from the intercept.

4.4.2 Determination of extinction coefficients

To determine the extinction coefficient for a particular absorbing species the absorbance was measured for a standard solution of the ligand in a pH range where formation of this species was considered to be complete; e.g. for catechol, LH_2 at pH > 5. If spectrophotometric absorption curves at well separated pH values were identical then the assumption of complete formation of a species was justified. For ligands with well separated protonation constants (e.g. catechol 9.2, 13.4) the spectrum for the intermediate species LH^- could also be measured exactly;

calculations for catechol established that in the pH range 11.2 - 11.4, > 99% of the ligand would exist as LH. Families of absorption spectra confirmed constant composition in this pH range.

For catechin the protonation constants were too similar to permit measurement of individual extinction coefficients for pairs of species in equilibrium. The species LH_4 and L were considered to be present in solution at concentrations close to 100% total ligand for pH values < 5 and > 14.5 respectively. However for each of the species in equilibrium with these, viz. LH_3 and LH, a pH range does not exist where the concentration of this species approaches 100% of TL. This is because of the overlapping protonation equilibrium (formation of LH_2). Calculations based on approximate protonation constants established a concentration maximum for LH in the pH range 12.1 - 12.5 (c. 84% of total ligand). Absorption spectra confirmed an approximately constant concentration of all species in this pH range. Thus the extinction coefficient for LH was evaluated approximately from these spectra and corrected for the contributions from small concentrations of LH_2 and L, the other species present in this pH range. This is discussed in Chapter 5.

4.4.3 Evaluation of protonation constants

For solutions with pH values < 11 (i.e. with constant ionic strength) and containing ligands with well separated protonation equilibria it was possible to calculate the protonation constants directly from the measured absorbance and equations (4.28), (4.30) and (4.29a). For the

equilibrium under study a series of spectra were recorded at pH values corresponding to a range of concentrations c_1 and c_2. By use of the known extinction coefficients the concentration of each absorbing species could be calculated at each measured pH. Calculations were performed at two or more wavelengths. From equation (4.30) the protonation constant was calculated for each of the selected wavelengths and for each solution composition. The resulting protonation constants were averaged to find a mean value. The analytical wavelengths at which the extinction coefficients were evaluated were chosen to correspond to the greatest change in absorbance with change in pH. This afforded the greatest accuracy in the determination of the protonation constants.

For the least acidic hydroxyl group of the polyphenols (log K > 13) it was necessary to work at very high pH. This required concentrated solutions of KOH and as a result the ionic strength was significantly greater that 0.1 and varied with pH. For spectrophotometric titrations the pH was varied by incremental dilution of the ligand/KOH solution with an equimolar solution of ligand ($[LH_r]$ 6 - 14x10^{-4} M). Constant ligand concentration allowed observation of isosbestic points which indicated that only two ligand species were in equilibrium. The spectrum of each test solution was recorded using the special spectrophotometric cell described in Chapter 2. The p[H] was calculated from the known volumes of standard alkali added and the Kwc for water at the relevant ionic strength (see appendix F). The ionic strength was different at each datum point. The

protonation constant was calculated at each datum point by the method described at the beginning of this section, i.e. where the two extinction coefficients are known. The protonation constant at an ionic strength of 0.10 was estimated by extrapolation from a plot of log K_{pqr}, against $I^{0.5}/(1 + I^{0.5})$, where I is the ionic strength of the solution. This is discussed in Chapter 5.

CHAPTER 5

POLYPHENOL PROTONATION REACTIONS

Potentiometric and/or spectrophotometric measurements have been employed to study the stepwise protonation reactions of some naturally occurring polyphenols viz.

$$L + H \rightleftharpoons LH \qquad K_{011} = [LH]/[L][H] \qquad (5.1)$$

$$LH + H \rightleftharpoons LH_2 \qquad K_{012} = [LH_2]/[LH][H] \qquad (5.2)$$

$$LH_{r-1} + H \rightleftharpoons LH_r \qquad K_{01r} = [LH_r]/[LH_{r-1}][H] \qquad (5.3)$$

The protonation constants were determined by non-linear least squares analysis of the potentiometric titration data or by one of the spectrophotometric methods described in Chapter 4.

All the ligand solutions were completely deoxygenated (see Chapter 2) prior to data collection because such polyphenols oxidize rapidly in alkaline solutions in the presence of molecular oxygen.

Catechol (1), 4-methylbenzene-1,2,-diol (2), protocatechuic acid (3), and 3',4'-di-O-methylcatechin (4) were used as model compounds for the catechin (5) and epicatechin (6) molecules. The epicatechin dimer B2 (7), was expected to have similar protonation constants for each epicatechin unit; this was not the case and possible reasons are discussed in Section 5.3. The tannin B13 (8) had too many phenolate groups for qualitative or quantitative protonation analysis.

It was established by h.p.l.c. analysis that the amount of epimerization of catechin and epicatechin was

negligible during the course of a potentiometric or spectrophotometric experiment (1.5 h).

5.1 Potentiometric results

The protonation reactions with log K_{01r} values less than 12 were studied potentiometrically in a supporting electrolyte of 0.1 M KCl and at 25°C. The pH-titrant volume data were analysed to calculate the protonation constants by the least squares procedure described (see Chapter 4). R-factors (see Chapter 6) typically ranged from c. 0.07 to 1%.

5.1.1 Catechol

Titration of standard KOH against a deoxygenated solution of catechol (1.2×10^{-3} M) generated volume of titre-pH data which were used to evaluate the protonation constant K_{012}. Only one quantitative titration was performed for catechol because Taylor[119] had thoroughly investigated reaction (5.2). Data are listed in Table 5.1. The titration curve (Figure 5.1) showed an inflexion at approximately pH 6 which resulted from the neutralization of excess acid. This acid was added to prevent the oxidation of catechol which occurs slowly in neutral solutions, and rapidly in the alkaline region[120] in the presence of oxygen. At pH > 7 the titration curve exhibited buffering due to the ligand deprotonation reactions (5.1) and (5.2). However no distinct inflexion (end point) was observed because of the hydrolysis reaction:

$$LH + H_2O \rightleftharpoons LH_2 + OH \qquad (5.4)$$

No attempt was made to determine K_{011} by this method because of large uncertainties associated with pH measurements in

Table 5.1 Data from a titration of catechol with KOH[a]

Titre (ml)[b]	p[H][c]	$\bar{n}H$(obs)[d]	$\bar{n}H$(calc)[e]
0.070	8.314	1.897	1.899
0.075	8.425	1.872	1.873
0.080	8.516	1.847	1.848
0.085	8.595	1.822	1.824
0.090	8.665	1.796	1.799
0.095	8.733	1.771	1.773
0.100	8.795	1.746	1.747
0.105	8.853	1.721	1.720
0.110	8.906	1.697	1.695
0.120	9.004	1.647	1.646
0.125	9.049	1.622	1.621
0.130	9.092	1.598	1.598
0.135	9.133	1.573	1.575
0.140	9.176	1.549	1.551
0.145	9.217	1.525	1.527
0.150	9.258	1.501	1.504
0.155	9.300	1.478	1.480
0.160	9.342	1.454	1.455
0.165	9.384	1.431	1.431
0.170	9.425	1.408	1.408
0.175	9.468	1.386	1.384
0.180	9.509	1.364	1.362
0.185	9.549	1.342	1.341
0.190	9.589	1.320	1.321
0.195	9.632	1.299	1.300
0.200	9.677	1.280	1.278
0.210	9.767	1.242	1.239
0.215	9.814	1.225	1.219
0.225	9.898	1.191	1.188
0.230	9.937	1.175	1.174
0.240	10.021	1.148	1.148
0.250	10.107	1.126	1.124

a Ionic strength 0.1 M KCl; T 25°C; [catechol] = 1.215×10^{-3} M; total volume = 150.00 ml

b Cumulative volume of 0.9151 M KOH added

c Hydrogen ion concentration obtained from calibration equation (see Chapter 3)

d $\bar{n}H$(obs) as defined in Chapter 4, equation (4.10)

e $\bar{n}H$(calc) as defined in Chapter 4, equation (4.11)

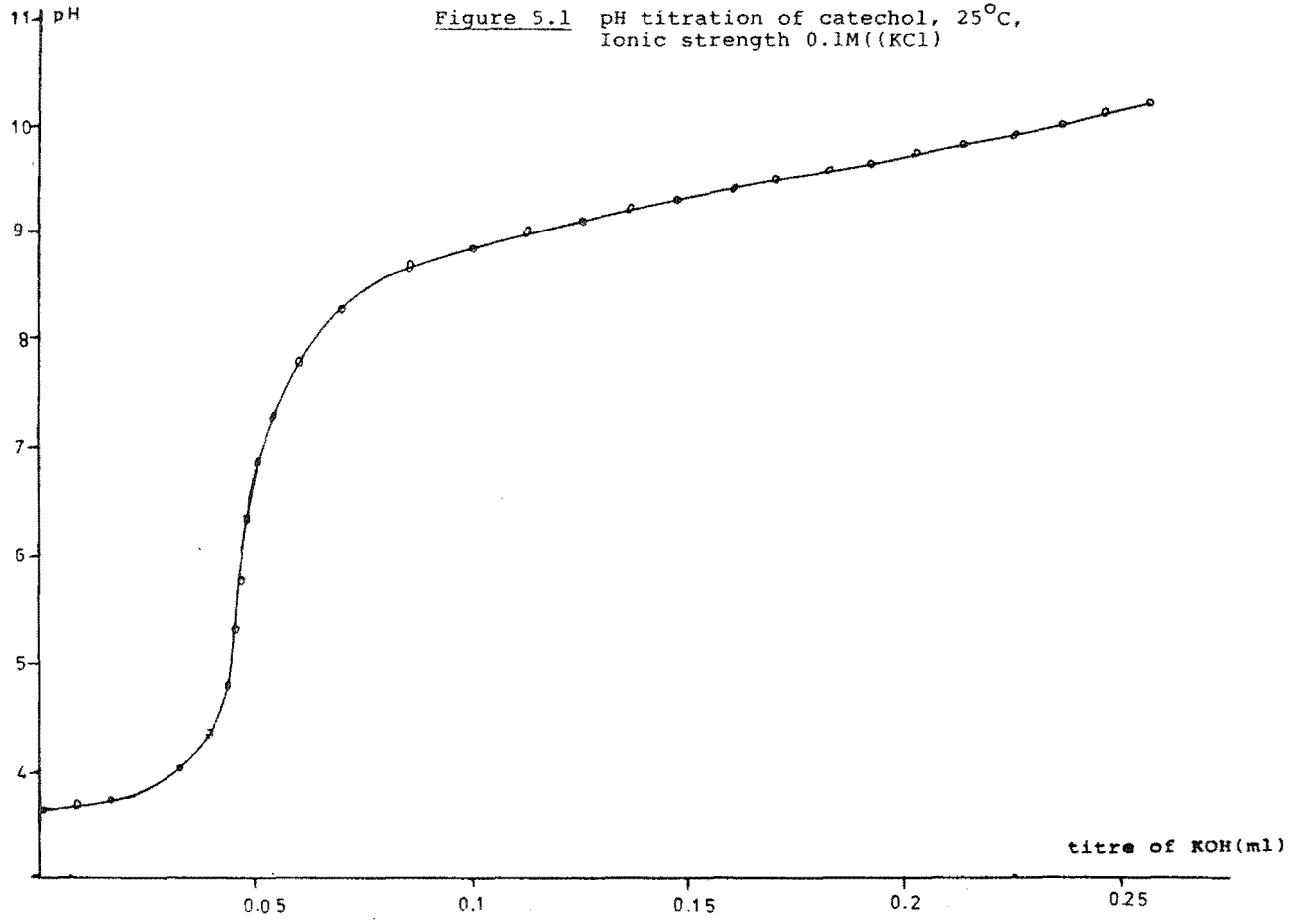

Figure 5.1 pH titration of catechol, 25°C, Ionic strength 0.1M((KCl)

strongly alkaline solutions and the increasing importance of hydrolysis reactions above pH c. 10.8. Listed in Table 5.2 is the protonation constant (K_{012}) determined for this ligand from a least squares analysis of one titration consisting of 32 pH-volume of titre points over the pH range 8.4 - 10.2. The R-factor was 0.12%. Table 5.2 also presents values of log K_{012} obtained by other workers.

5.1.2 4-Methylbenzene-1,2— diol

Data from a titration of standard KOH against a solution of 4-methylbenzene-1,2— diol (6.7×10^{-3} M) are listed in appendix G. These data are presented graphically in the form of a pH-titre curve in Figure 5.2. Only one quantitative titration was performed because this compound was used only as a model for the B rings of catechin and epicatechin and not in metal complexation studies. The titration curve has the same form as that for catechol; this was expected because of the similarity of the two polyphenols. The value for K_{012} only was computed, for reasons already discussed (Section 5.1.1). Listed in Table 5.2 is the protonation constant determined for this ligand from a least squares analysis of one titration consisting of 27 data points over the pH range 8.9 - 10.6. The R-factor was 0.29%. log K_{012} values reported by other workers are also listed in Table 5.2.

5.1.3 Protocatechuic acid

Four titrations of standard KOH against solutions of protocatechuic acid ($1 - 5 \times 10^{-3}$ M) were performed. Data from one titration are listed in appendix H. The pH-titre curve (Figure 5.3) exhibits an end point at pH c. 6

Table 5.2 Protonation constants for polyphenols

polyphenol	log K_{014} $LH_3 + H \rightleftharpoons LH_4$	log K_{013} $LH_2 + H \rightleftharpoons LH_3$	log K_{012} $LH + H \rightleftharpoons LH_2$	log K_{011} $L + H \rightleftharpoons LH$	electrolyte (T°C)	reference
catechol			9.26 ± 0.02[a]	13.43 ± 0.06[b,c]	KCL 0.1 M (25)	this work
			9.23	13.05	KNO_3 0.1 M (25)	138
			9.22	13.0	<0.1 M (27)	138
			9.37	13.7	KNO_3 0.1 M (20)	139
			9.45	12.82	KNO_3 0.2 M (25)	140
			9.28 ± 0.02		KCl 0.1 M (2)	141
			9.20		NaCl 0.6 M (25)	142
4-methylbenzene			9.43 ± 0.02	13.8 ± 0.1[c]	KCl 0.1 M (25)	this work
1,2-diol			9.42 ± 0.02[c]		KCl 0.1 M (25)	this work
			9.44			143
			9.67	12.77		144
			9.56	14.00	KCl 0.1 M (20)	128
protocatechuic		4.26 ± 0.02[d]	8.81 ± 0.01	13.02 ± 0.06[c]	KCl 0.1 M (25)	this work
acid			8.64	14.00	KCl 0.1 M (20)	128
			8.64	13.12	L_iClO_4 0.25 M (25)	145
3',4'-Di-O-methylcatechin			(8.84 ± 0.04)[e]	(10.92 ± 0.04)	KCl 0.1 M (25)	this work
catechin	(8.64 ± 0.01)	9.41 ± 0.02	(11.26 ± 0.06)	13.26 ± 0.05[c]	KCl 0.1 M (25)	this work
	(8.79)	9.44	(11.18)	13.25	KCl 0.1 M (20)	128
epicatechin	(8.72 ± 0.01)	9.49 ± 0.02	(11.26 ± 0.06)	13.40 ± 0.05[c]	KCl 0.1 M (25)	this work

(a) Error reported by Taylor[141]

(b) Error ± 1 standard deviation

(c) Spectrophotometrically determined

(d) Carboxylate protonation

(e) Values in parenthese refer to A ring

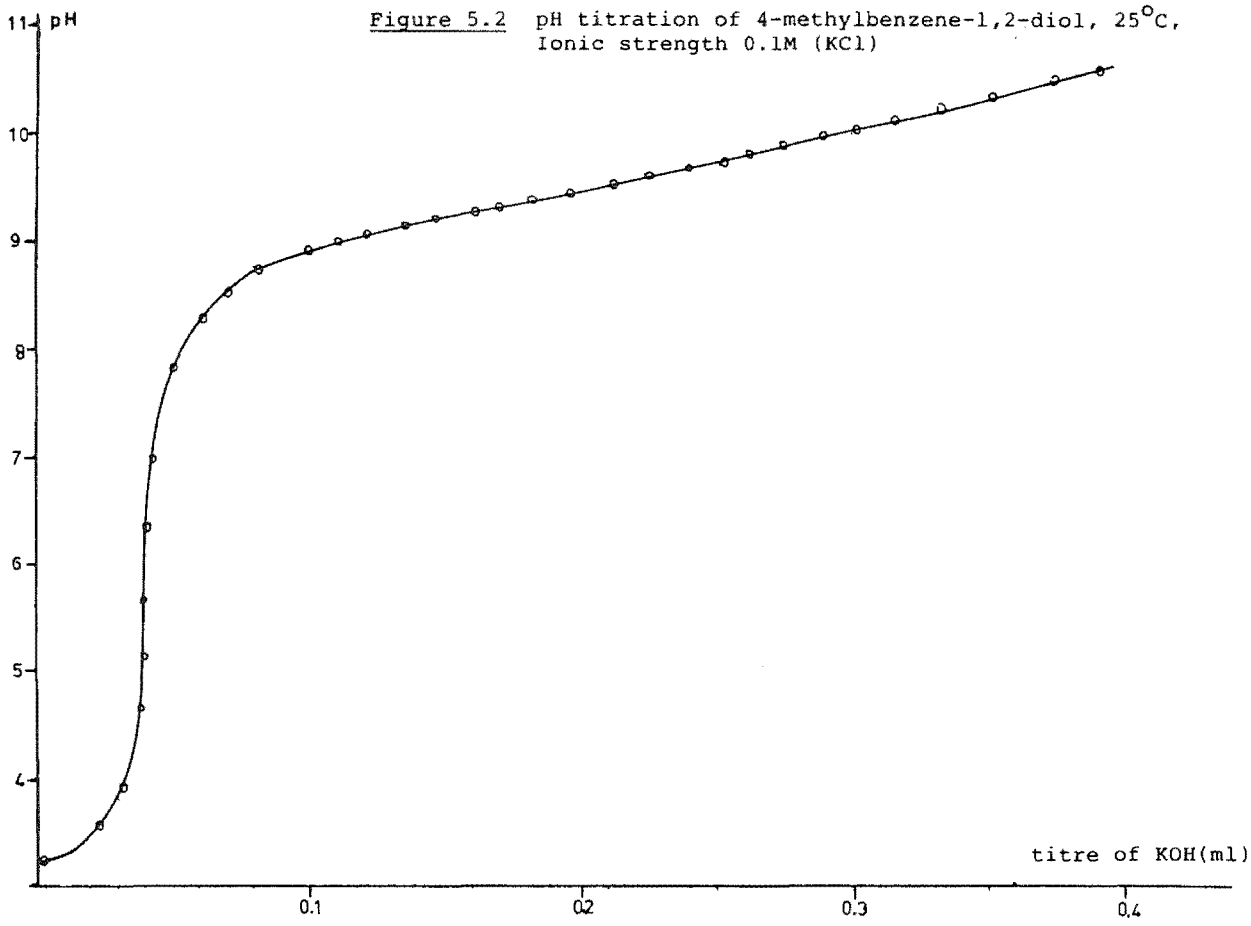

Figure 5.2 pH titration of 4-methylbenzene-1,2-diol, 25°C, Ionic strength 0.1M (KCl)

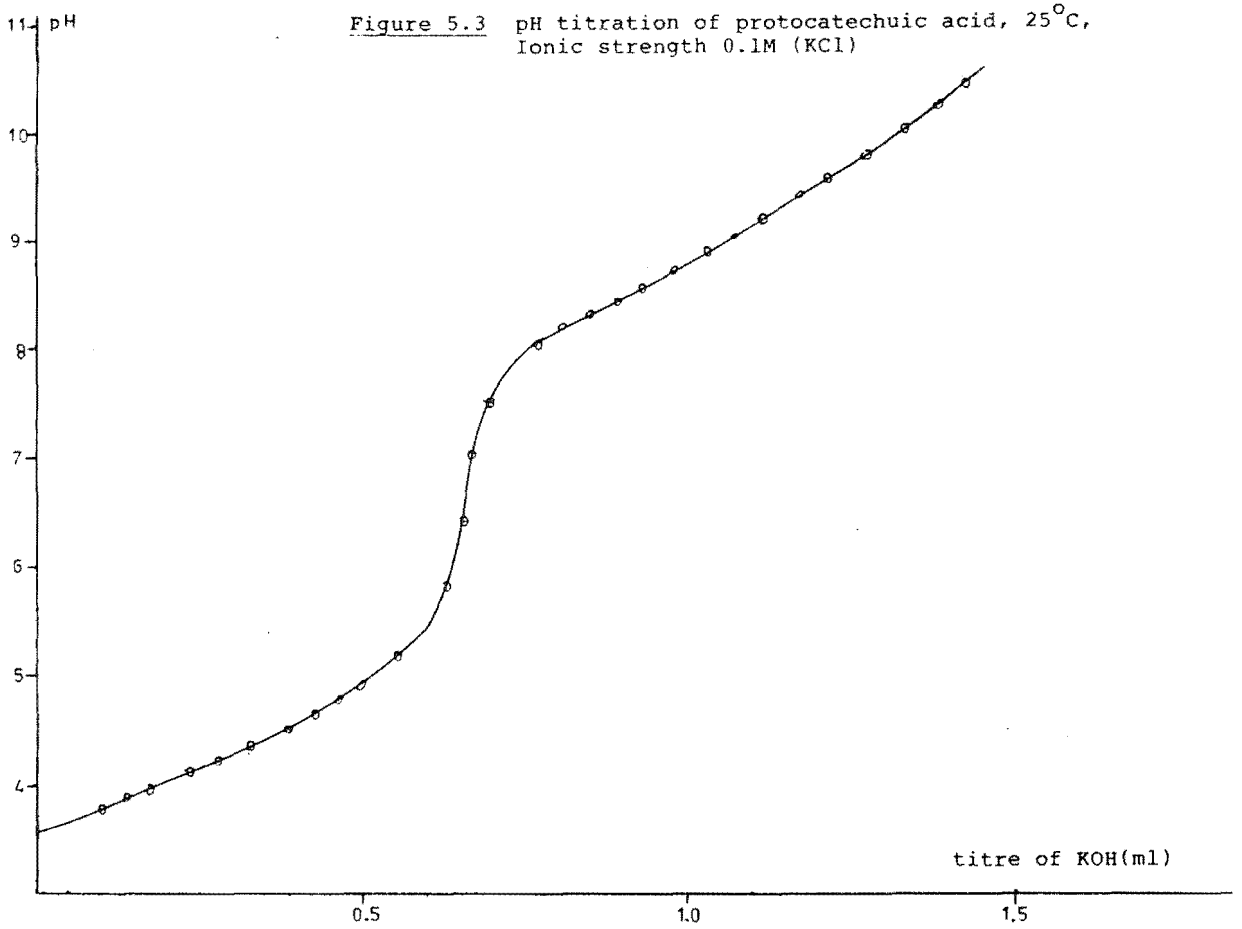

Figure 5.3 pH titration of protocatechuic acid, 25°C, Ionic strength 0.1M (KCl)

corresponding to complete removal of the proton from the carboxylic acid functional group. Exact location of this end point by Gran's analysis confirmed the microanalysis result (Chapter 2 Section 2.5.3) which indicated that protocatechuic acid is anhydrous; this contrasts with the reported composition of one mole of water of crystallization[65]. At pH values greater than 7 the titration curve exhibited buffering due to phenolic deprotonation, however hydrolysis reactions of the type (5.4) masked any distinct inflexions.

From the potentiometric data (four titrations consisting of 20 - 40 data points each) the least squares procedure was used to evaluate protonation constants for the carboxylate group (K_{013}) and for the second proton addition to a phenolate group (K_{012}). The pH range investigated was c. 3.5 - 10.5; data from pH 6 to 7.5 were excluded from the computational procedure because this range was not in a buffer region. Table 5.2 lists the log K values obtained from this work and values reported by other workers. The R-factors for the least squares refinement ranged from 0.23 to 0.47%.

5.1.4 3',4'-Di-O-methylcatechin

3',4'-Di-O-methylcatechin is sparingly soluble in water (1 - 1.4×10^{-3} M) and complete dissolution of the material was difficult to ascertain. Therefore the compound was dissolved in oxygen free standard KOH (dilute) and back titrated with HCl. The titration proceeded until drifting readings indicated precipitation (c. pH 8.2). Three titrations were performed on this compound and one set of

pH-titre data is listed in appendix I. No distinct end points were apparent in the ligand titration curve (Figure 5.4). This compound was used as a protonation model for the A rings of catechin and epicatechin, thus two equilibria were considered. They were the protonation of the phenolate groups at positions 5 and 7 in the A ring (see Chapter 1). Listed in Table 5.2 are the average protonation constants determined for this ligand from a least squares analysis of three titrations consisting of 40 - 58 data points each in the pH range 8.4 - 10.7. R-factors ranged from 0.5 to 0.8%; they were slightly higher for this compound because it was more difficult to know when the ligand began to precipitate from solution. Drifting pH readings were the only probe available to detect this phenomenon.

5.1.5 Catechin and epicatechin

Catechin differs from epicatechin only in the configuration of the heterocyclic ring[29]. The titration method, addition of standard KOH into deoxygenated solutions of catechin (7 - 11x10^{-4} M) or epicatechin (1.5 - 2x10^{-3} M), was the same for each epimer. Listings of representative potentiometric titration data for catechin and epicatechin are presented in Tables 5.3 and 5.4 respectively. The titration curves for catechin and epicatechin (Figures 5.5 and 5.6 respectively) showed an inflexion at approximately pH 6 which resulted from the neutralization of excess acid. This acid was added to prevent oxidation of these ligands (see Section 5.1.1). At higher pH (> 7) the titration curves exhibited buffering due to the ligand deprotonation reactions (5.3), where r = 4, 3 and 2. No attempt was made

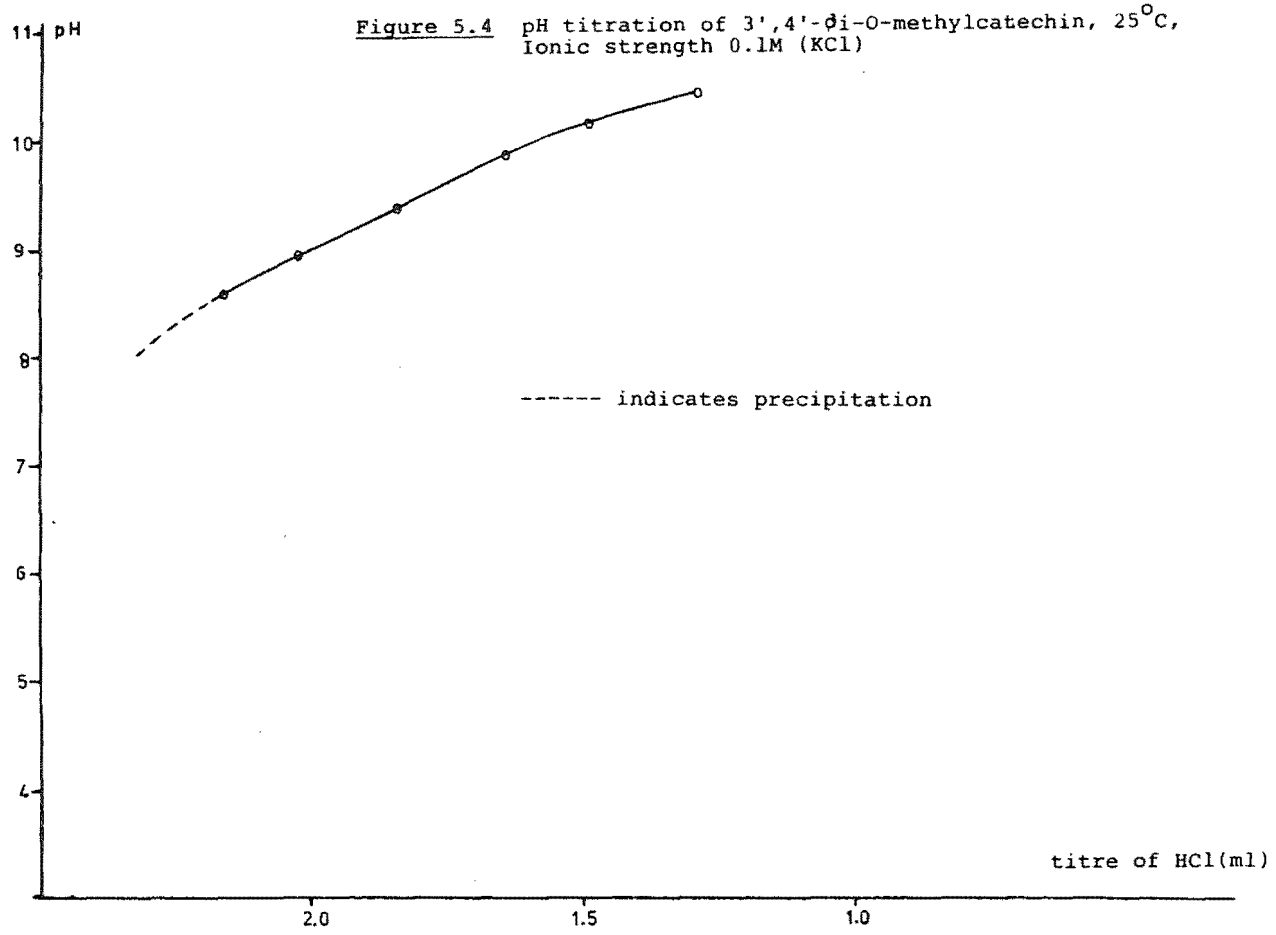

Figure 5.4 pH titration of 3',4'-di-O-methylcatechin, 25°C, Ionic strength 0.1M (KCl)

Table 5.3 Data from a titration of catechin with KOH[a]

Titre (ml)[b]	p[H][c]	$\bar{n}H$(obs)[d]	$\bar{n}H$(calc)[e]
0.140	8.264	3.688	3.373
0.145	8.321	3.651	3.638
0.150	8.368	3.614	3.606
0.155	8.421	3.577	3.569
0.160	8.468	3.540	3.533
0.165	8.513	3.504	3.498
0.170	8.556	3.467	3.462
0.175	8.599	3.430	3.426
0.180	8.639	3.394	3.390
0.185	8.677	3.357	3.356
0.190	8.714	3.320	3.321
0.195	8.751	3.284	3.286
0.200	8.787	3.247	3.250
0.205	8.822	3.211	3.211
0.210	8.858	3.175	3.179
0.215	8.894	3.138	3.143
0.220	8.930	3.102	3.102
0.225	8.962	3.066	3.073
0.230	8.997	3.030	3.037
0.235	9.030	2.994	3.002
0.240	9.065	2.958	2.965
0.245	9.098	2.922	2.930
0.250	9.134	2.887	2.893
0.255	9.167	2.851	2.858
0.260	9.203	2.816	2.822
0.270	9.273	2.745	2.750
0.285	9.379	2.641	2.646
0.290	9.417	2.607	2.610
0.295	9.454	2.574	2.575
0.300	9.490	2.540	2.543
0.305	9.529	2.507	2.509
0.310	9.569	2.475	2.475
0.315	9.611	2.443	2.441
0.320	9.652	2.412	2.407
0.330	9.734	2.351	2.346
0.340	9.822	2.295	2.285
0.345	9.862	2.267	2.259
0.350	9.904	2.242	2.233
0.355	9.946	2.216	2.208
0.360	9.988	2.192	2.184
0.365	10.031	2.170	2.160
0.370	10.069	2.147	2.140
0.375	10.111	2.128	2.118
0.380	10.149	2.108	2.099
0.385	10.185	2.089	2.081
0.400	10.286	2.037	2.034
0.410	10.348	2.007	2.005

Table 5.3 (continued)

0.420	10.405	1.979	1.980
0.440	10.506	1.929	1.934
0.500	10.733	1.810	1.824
0.540	10.846	1.752	1.764
0.600	10.980	1.685	1.688
0.650	11.069	1.641	1.634

a Ionic strength 0.1 M KCl; T 25°C; [catechin] = 1.09×10^{-3} M; total volume = 150.00 ml

b Cumulative volume of 1.224 M KOH added

c Hydrogen ion concentration obtained from calibration equation (see Chapter 3)

d $\bar{n}H$(obs) as defined in Chapter 4, equation (4.10)

e $\bar{n}H$(calc) as defined in Chapter 4, equation (4.11)

Table 5.4 Data from a titration of epicatechin with KOH[a]

Titre (ml)[b]	p[H][c]	ñH(obs)[d]	ñH(calc)[e]
0.044	8.327	3.677	3.674
0.047	8.392	3.637	3.633
0.050	8.448	3.597	3.595
0.053	8.504	3.558	3.554
0.056	8.553	3.518	3.516
0.059	8.602	3.479	3.477
0.062	8.649	3.439	3.437
0.065	8.692	3.400	3.399
0.068	8.733	3.361	3.362
0.071	8.776	3.321	3.321
0.074	8.817	3.282	3.281
0.077	8.854	3.243	3.244
0.080	8.893	3.203	3.206
0.083	8.933	3.164	3.164
0.086	8.970	3.125	3.127
0.089	9.008	3.086	3.086
0.092	9.044	3.047	3.049
0.095	9.078	3.008	3.012
0.098	9.117	2.969	2.972
0.101	9.152	2.931	2.934
0.110	9.262	2.815	2.818
0.114	9.311	2.764	2.767
0.118	9.362	2.714	2.715
0.122	9.414	2.663	2.663
0.126	9.463	2.613	2.616
0.130	9.513	2.564	2.569
0.134	9.568	2.515	2.518
0.138	9.625	2.468	2.468
0.142	9.685	2.421	2.417
0.146	9.739	2.375	2.374
0.150	9.800	2.330	2.327
0.154	9.861	2.287	2.283
0.158	9.923	2.246	2.241
0.162	9.985	2.206	2.201
0.166	10.043	2.167	2.165
0.170	10.104	2.132	2.129
0.174	10.164	2.099	2.095
0.178	10.219	2.067	2.065
0.182	10.275	2.037	2.035
0.190	10.376	1.984	1.982
0.195	10.436	1.955	1.951
0.200	10.489	1.926	1.923

Table 5.4 (continued)

0.205	10.537	1.897	1.898
0.210	10.583	1.872	1.873
0.215	10.627	1.849	1.849
0.220	10.666	1.825	1.827
0.225	10.705	1.805	1.806
0.230	10.738	1.782	1.787
0.240	10.804	1.774	1.778

a Ionic strength 0.1 M KCl; T 25°C; [epicatechin] = 1.53×10^{-3} M; total volume = 60.00 ml

b Cumulative volume of 1.224 M KOH added

c Hydrogen ion concentration obtained from calibration equation (see Chapter 3)

d $\bar{n}H(obs)$ as defined in Chapter 4, equation (4.10)

e $\bar{n}H(calc)$ as defined in Chapter 4, equation (4.11)

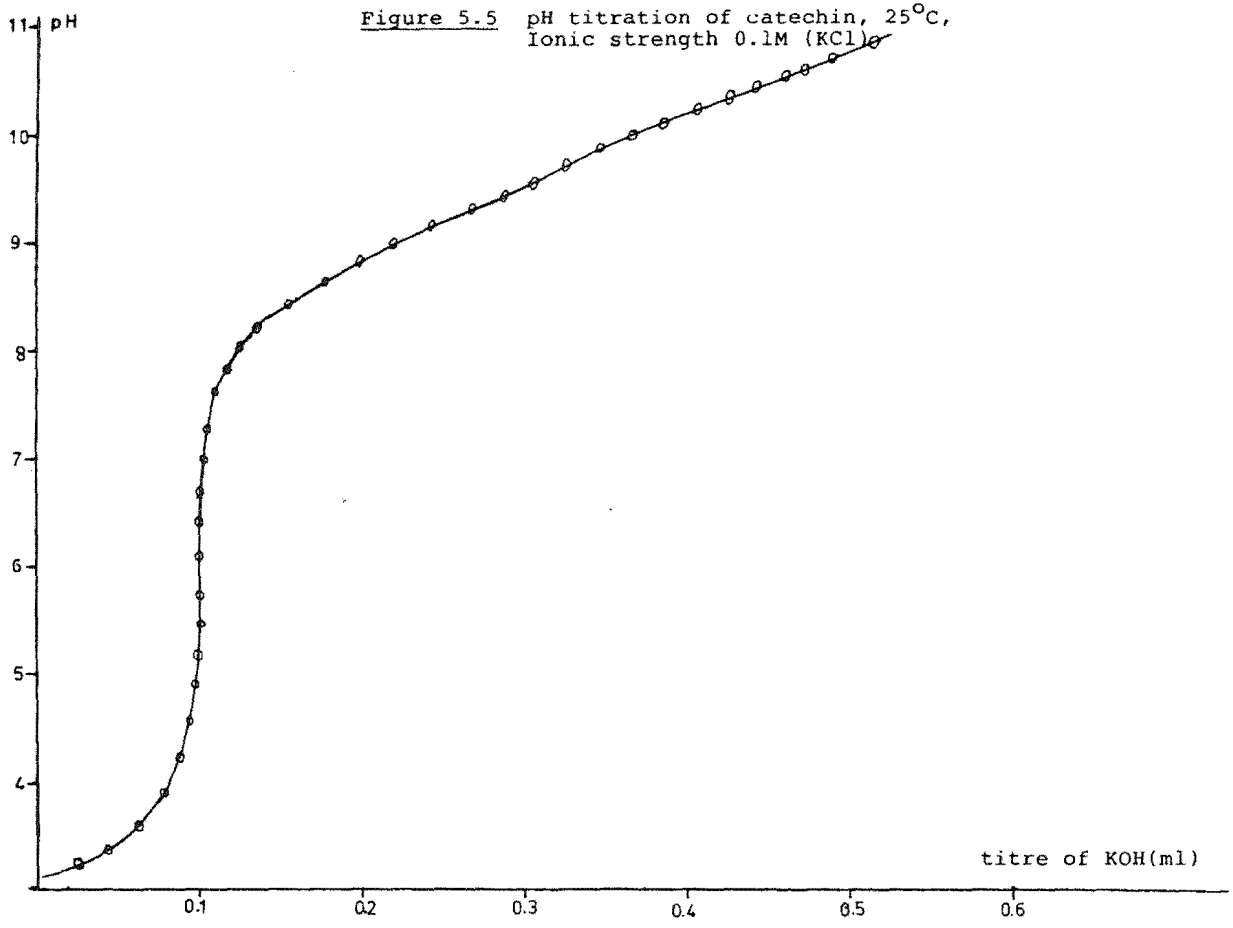

Figure 5.5 pH titration of catechin, 25°C, Ionic strength 0.1M (KCl)

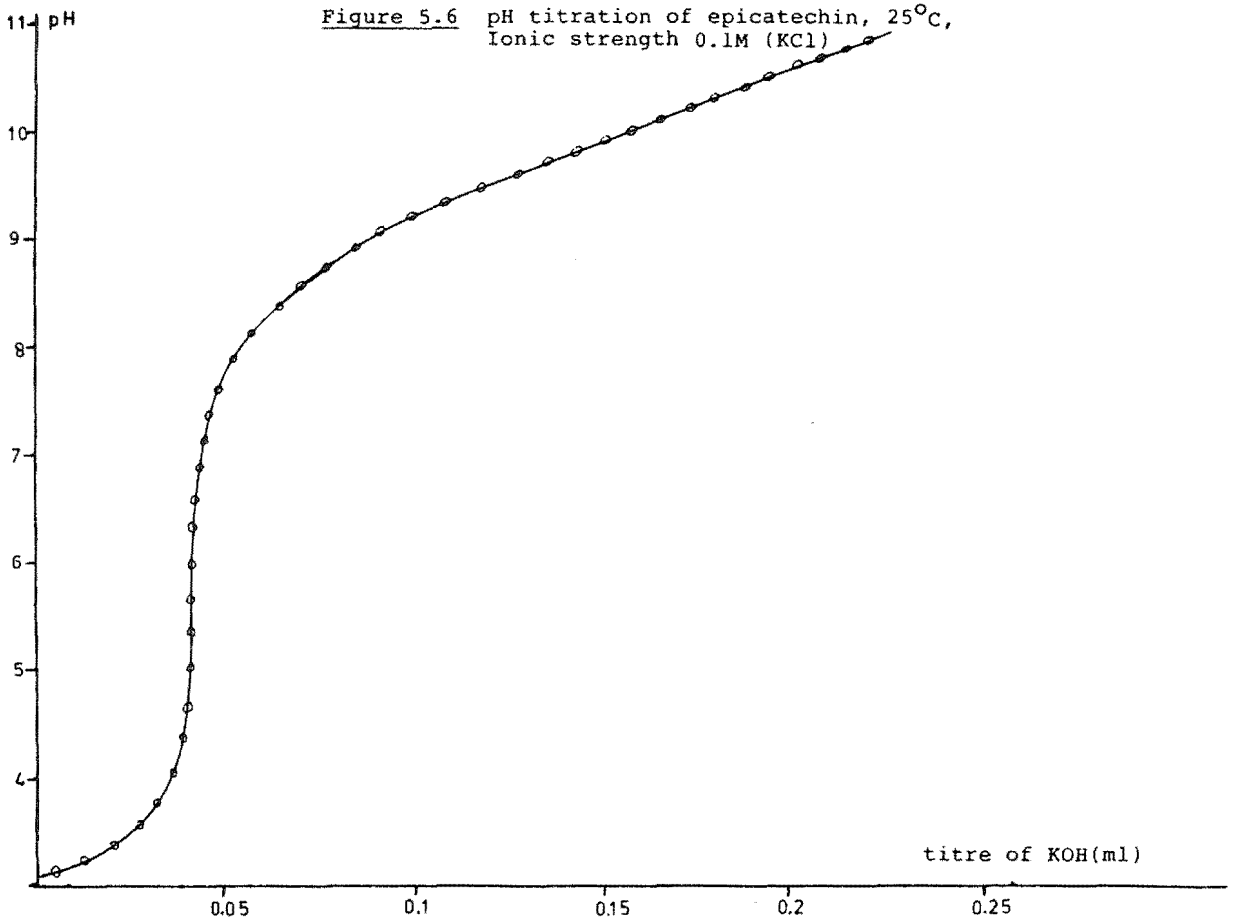

Figure 5.6 pH titration of epicatechin, 25°C, Ionic strength 0.1M (KCl)

to determine K_{011}. However analysis of the titration curves indicated that three phenolic functional groups undergo proton dissociation in the pH range 7 - 11 therefore permitting potentiometric data to be used in the evaluation of protonation constants for their conjugate bases. By comparison with catechol and 4-methylbenzene-1,2-diol it was inferred that only one proton is lost from the B ring in this pH range (log K 9.4), while from the protonation constants for 3',4'-di-O-methylcatechin it was inferred that two protons are lost from the A ring (log K 8.84 and 11.26). Because of the small difference in magnitude of the protonation constants for these equilibrium reactions, no inflexions were observed above pH 7 in the titration curves for catechin or epicatechin. Listed in Table 5.2 are the protonation constants calculated by a least squares analysis on the pH-volume data for three catechin and four epicatechin titrations in the pH range 8.2 - 11.2 (42 - 75 data points each titration). The R-factors varied from 0.07 to 0.34%.

5.1.6 B2 (epicatechin dimer)

In acid solution (pH < 4) the dimer B2 is known to undergo a slow rearrangement (days)[71]. Titrations of standard KOH against solutions of B2 (5×10^{-4} M) prepared from the same acidified stock solution yielded distinctly different titration curves for solutions of different age (viz. 3 h and 5 days). Therefore B2 stock solutions were prepared in oxygen free electrolyte containing no acid. Titrations performed within 8 hours on solutions prepared in this way gave identical pH-titre curves (Figure 5.7).

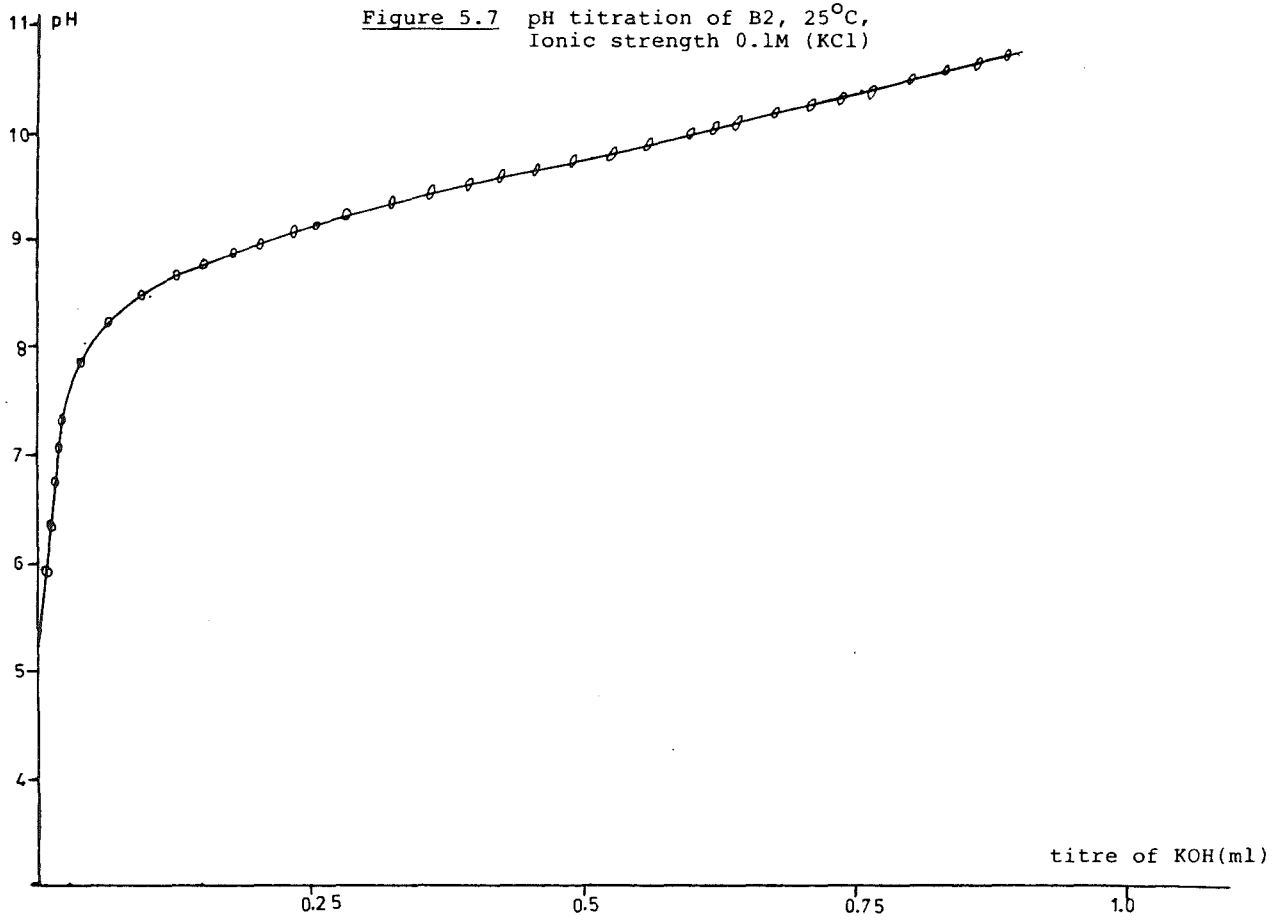

Figure 5.7 pH titration of B2, 25°C, Ionic strength 0.1M (KCl)

Representative pH-titre data from a B2 titration are listed in appendix J. No inflexions were observed in the B2 titration curve above a pH of 7 for the reasons outlined in Section 5.1.5 (cf. epicatechin).

B2 consists of two epicatechin units linked between the C(8) atom of one A ring and the C(4) atom of the hetero ring of a second unit. Thus it was expected that there would be no significant difference in the protonation constants for the B ring phenolate groups and only a small difference in the constants for the A ring. However the difference between the buffer regions of the titration curves for the dimer and monomer indicate that the protonation constants for the same equilibria must be distinctly different; i.e. the epicatechin units are in distinctly different chemical environments in the B2 dimer. From three titrations consisting of 72 - 117 pH-titre data points, three protonation constants were calculated and are listed in Table 5.5. These constants are for the addition of the 6th, 7th and 8th protons to the ligand anion.

Table 5.5 Protonation constants obtained for epicatechin dimer B2 in 0.1 M KCl, 25°C.

$\log K_{016}$	$\log K_{017}$	$\log K_{018}$
9.61±0.06	9.52±0.08	8.59±0.05

The R-factors ranged from 0.35 to 0.75%. Factors which may have caused the difference in these protonation constants are discussed in Section 5.3.

5.2 Spectrophotometric results

The phenolic acids under study have ultraviolet absorption spectra which differ distinctly from those exhibited by their anionic forms[116]. This difference made it possible to determine some of their protonation constants. In particular it permitted the calculation of K_{011} which was not able to be calculated from potentiometric data (Section 5.1).

If extinction coefficients (Chapter 4) could be obtained for both of the species in an equilibrium mixture then the calculation of the equilibrium constant required only the total absorbance, total ligand concentration and the equilibrium hydrogen ion concentration, all of which are known or measurable quantities. For equilibria measured at pH < 12 the [H] was measured potentiometrically, while for equilibria studied at pH> 12, (viz. K_{011} for catechol, 4-methylbenzene-1,2-diol, protocatechuic acid, catechin and epicatechin) [H] was determined from the calculated concentration of KOH and the Kwc of water (see appendix F). The calculations that were used in protonation constant evaluation are described fully in Chapter 4.

5.2.1 Catechol

The protonation constant K_{011}, defined by equilibrium (5.1), was determined from the hydrogen ion concentration and spectrophotometric data because the pH region in which significant concentrations of the species L and LH exist is

above the pH range in which reliable potentiometric measurements can be made.

A spectrophotometric titration on catechol was accomplished by firstly deoxygenating a known volume (typically 20 ml) of standard KOH (c. 1 M) in the small airtight titration cell described in Chapter 2. An accurately known volume of deoxygenated concentrated ligand solution ($1x10^{-2}$ M, 2 ml) was added via a micrometer syringe to the KOH in the titration cell. By use of a specially designed spectrophotometric flow cell (see Chapter 2 Section 2.6.1) a measured volume of the extremely oxygen sensitive ligand solution from the titration vessel was bled into the spectrophotometer cell (1 mm) and its ultraviolet spectrum recorded. The pH of the ligand solution in the titration cell was then lowered by incremental dilution with an equimolar ligand solution ($9x10^{-4}$ M), maintaining a constant total ligand concentration and producing a pH range from c. 13.5 to 13.0. At each pH (typically 4 - 8 increments in the pH range mentioned) the ultraviolet spectrum was recorded as described above. The ionic strength varied from c. 0.75 to 0.2 in the course of the spectrophotometric titration. Well defined isosbestic points were observed in the spectra (Figure 5.8) indicating only two species in equilibrium. Absence of an absorption peak at c. 400 nm indicated that there was no measurable oxidation of the catecholate species to quinone in the time scale of the experiment.

To evaluate ε_L and ε_{LH} spectra were recorded at pH values of 14.8 and 11.3 respectively. Computations using

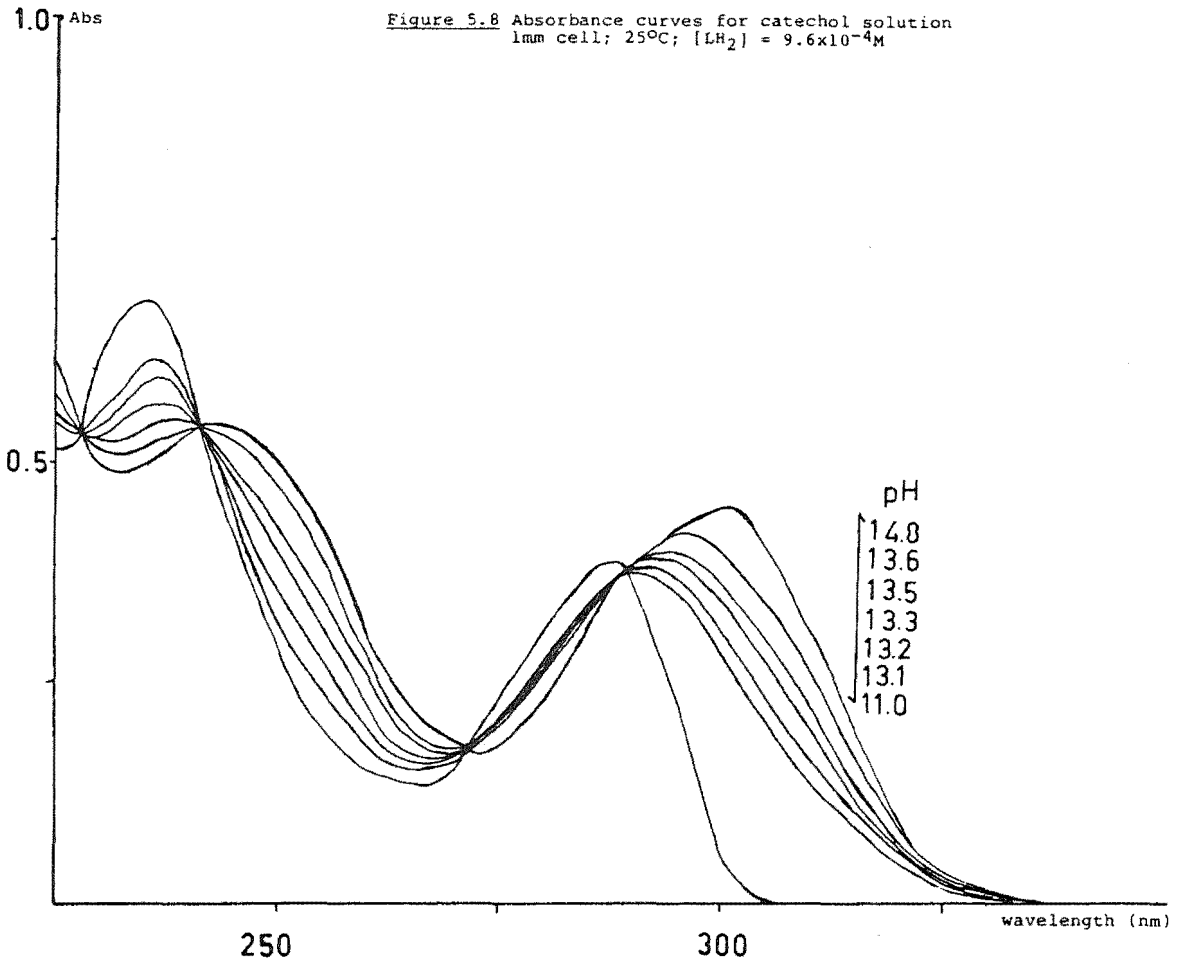

Figure 5.8 Absorbance curves for catechol solution 1mm cell; 25°C; $[LH_2] = 9.6 \times 10^{-4} M$

K_{012} (evaluated potentiometrically) and an estimated value of K_{011} (from the literature) indicated that the concentrations of L and LH were greater than 99% of the total ligand concentration at these pH values. The analytical wavelengths at which ε_L and ε_{LH} were calculated (according to the criteria discussed in Chapter 4) are listed in Table 5.6. Ultraviolet spectrophotometric parameters for the catecholate species are listed in Table 5.7.

The K_{011} value was calculated for individual data points (10 - 20 pH-absorbance points per titration) from duplicate titrations using equations (5.1), (5.5) and (5.6),

$$[TL] = [LH_r] + [LH_{r-1}] \qquad (5.5)$$

$$[LH_{r-1}] = (Ab - \varepsilon_{LH_r}[TL])/(\varepsilon_{LH_{r-1}} - \varepsilon_{LH_r}) \qquad (5.6)$$

where r = 1, Ab (1 cm cell) is the measured absorbance (two analytical wavelengths per spectrum recorded) and [TL] is the total concentration of ligand. Table 5.6 lists the log K values calculated at each pH (ionic strength). From these results a plot of log K_{011} versus $I^{0.5}/(1 + I^{0.5})$ was constructed (Figure 5.9). This plot is linear as required by theory. The quantities log K_{011} and log K^o_{011} (at zero ionic strength) are related by the expression.

$$\log K^o_{011} = \log K_{011} + \log (f_{HL}/f_H f_L) \qquad (5.7)$$

The activity coefficient term in (5.7) may be substituted by an equation for the hypothetical single ion activity coefficients[121] yielding the expression

$$\log K_{011} = \log K^o_{011} + (\Sigma z^2)AI^{0.5}/(1 + I^{0.5}) \qquad (5.8)$$

where I is the ionic strength and z^2 is $((r-1)^2-1^2-r^2)$ for the equilibrium reaction (5.9),

Table 5.6 Representative spectrophotometric data used for log K evaluation for catechol

absorbance	p[H]	ionic strength	$I^{0.5}/(1+I^{0.5})$	log K
0.492[a]	13.587	0.705	0.456	13.172
0.465	13.494	0.579	0.432	13.208
0.436	13.409	0.479	0.409	13.249
0.410	13.331	0.399	0.387	13.278
0.388	13.258	0.335	0.367	13.294
0.367	13.190	0.283	0.347	13.312
0.345	13.124	0.240	0.329	13.339
0.329	13.063	0.205	0.312	13.348
0.402[b]	13.587	0.705	0.456	13.209
0.384	13.494	0.579	0.432	13.220
0.362	13.409	0.479	0.409	13.253
0.344	13.331	0.399	0.387	13.267
0.325	13.258	0.335	0.367	13.290
0.310	13.190	0.283	0.347	13.298
0.295	13.124	0.240	0.329	13.310
0.280	13.063	0.205	0.312	13.330

a wavelength 250.0 nm, ε_L 6350, ε_{LH} 1909

b wavelength 300.0 nm, ε_L 4989, ε_{LH} 650

Table 5.7 Spectrophotometric data[a] (wavelength in nm, ε in cm^{-1} l mol^{-1})

compound	ligand species	pH	absorption maxima		isosbestic points	
			λmax^b	εmax	λiso^b	εiso
catechin	L	14.8	305	7060±100		
	L/LH	13.6-13.0			281	5300±200
					292	6850±200
	LH	12.3-12.0	290	7330±200[c]		
	LH_3 /LH_4	8.0-6.2			266-267[d]	2400-3800
	LH_4	3.7	278	3920±50		
epicatechin	L	14.9	305	7140±100		
	L/LH	13.7-13.1			281	4800±200
					292	6800±200
	LH	12.5-12.3	291	6950±100		
4-methylbenzene-1,2-diol	L	14.7	307	5410±100		
			251	5600±100		
	L/LH	14.4-13.5			297	4350±200
					273	2050±100
					246	5450±200
	LH	11.6	293	4050±100		
			237	6300±100		
	LH/LH_2	11.3-7.6			281	2550±100
					265	1020±50
	LH_2	7.2	280	2570±50		
protocatechuic acid	L	14.8	325	10600±100		
			288	6650±100		
	L/LH	13.6-13.2			311	7880±100
					258	4870±100
	LH	10.68	300	11050±200		
			277	9450±200		
catechol	L	14.8	310	5200±100		
			250	6350±100		
	L/LH	13.6-13.0			288	3800±200
					272	1800±150
					242	5600±200
					228	5700±200
	LH		236	7100±200		
			288	3700±200		

a 25°C

b λvalues ± 1 nm

c corrected for contributions from L and LH; see Section 5.2.5

d the range for which curves were coincident

Figure 5.9 Plot of log K versus $I^{0.5}/(1+I^{0.5})$ for catechol

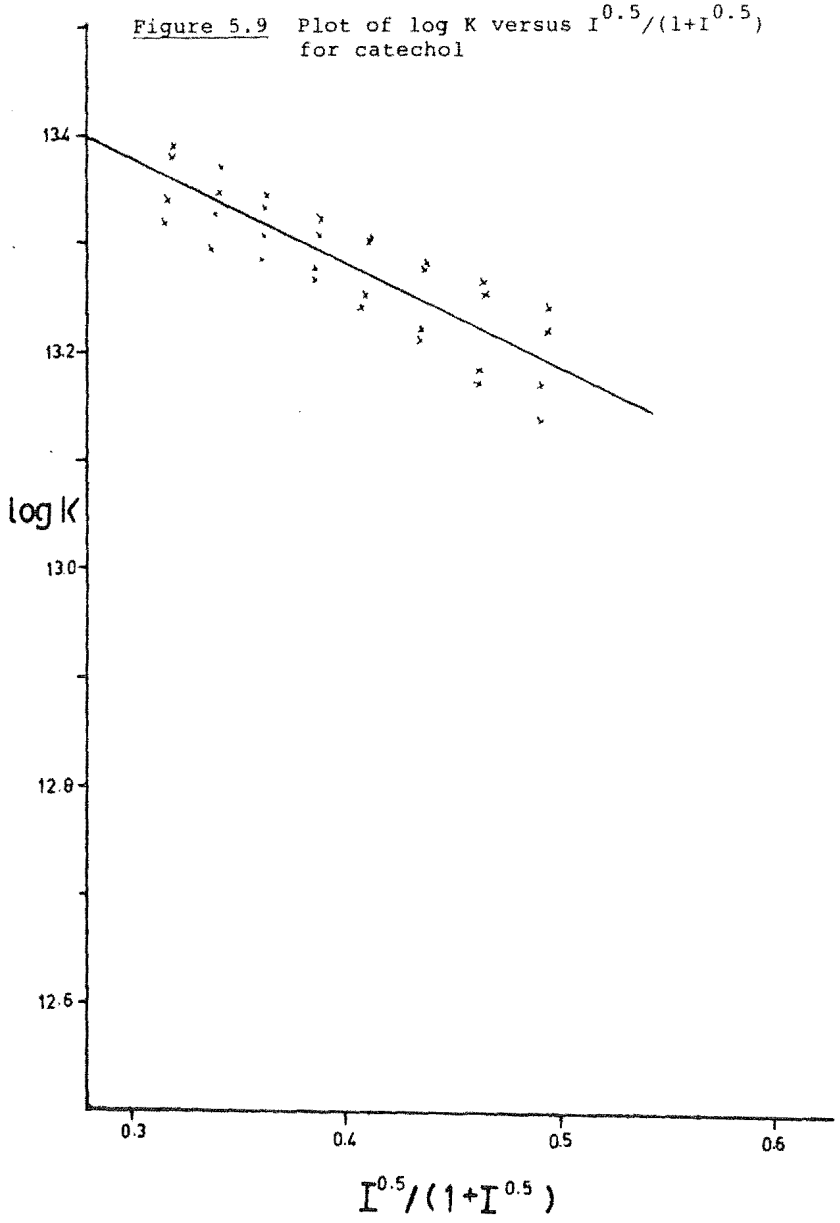

$$L^{r-} + H^{+} \quad LH^{(r-1)-} \qquad (5.9)$$

The slope for equation (5.8) where (Σz^2) for catechol is -4 and A is 0.51 is calculated as -2.0; the observed slope was -1.0.

The log K_{011} value at I 0.1 M was estimated by extrapolation of log K_{011} values against $I^{0.5}/(1 + I^{0.5})$. Table 5.2 lists the log K_{011} value obtained and log K_{011} values reported by other workers.

5.2.2 4-Methylbenzene-1,2-diol

The stepwise protonation equilibria for 4-methylbenzene-1,2-diol, a model compound for the catechin B ring, had protonation constants that were sufficiently different in magnitude to allow extinction coefficients for all the equilibrium species (LH_2, LH, L) to be determined. Spectrophotometric analysis therefore permitted the calculation of both the protonation constants (K_{011} and K_{012}). For the evaluation of K_{012} from the ultraviolet spectra 9 spectra were recorded in the pH range 7.2 to 11.9. Figure 5.10 presents the spectra recorded; these show well defined isosbestic points (265, 281 nm) indicating that only two species were in equilibrium. The protonation constant was calculated as described in Chapter 4. Table 5.2 lists the log K_{012} value obtained from this work and those reported by other workers.

log K_{011} was calculated in the same manner as for catechol, from duplicate spectrophotometric titrations which each provided 4 - 6 pH-absorbance measurements (at two selected wavelengths) in the pH range 13.5 - 14.4 (I = 0.6 - 2.7). Figure 5.11 presents a set of recorded spectra which

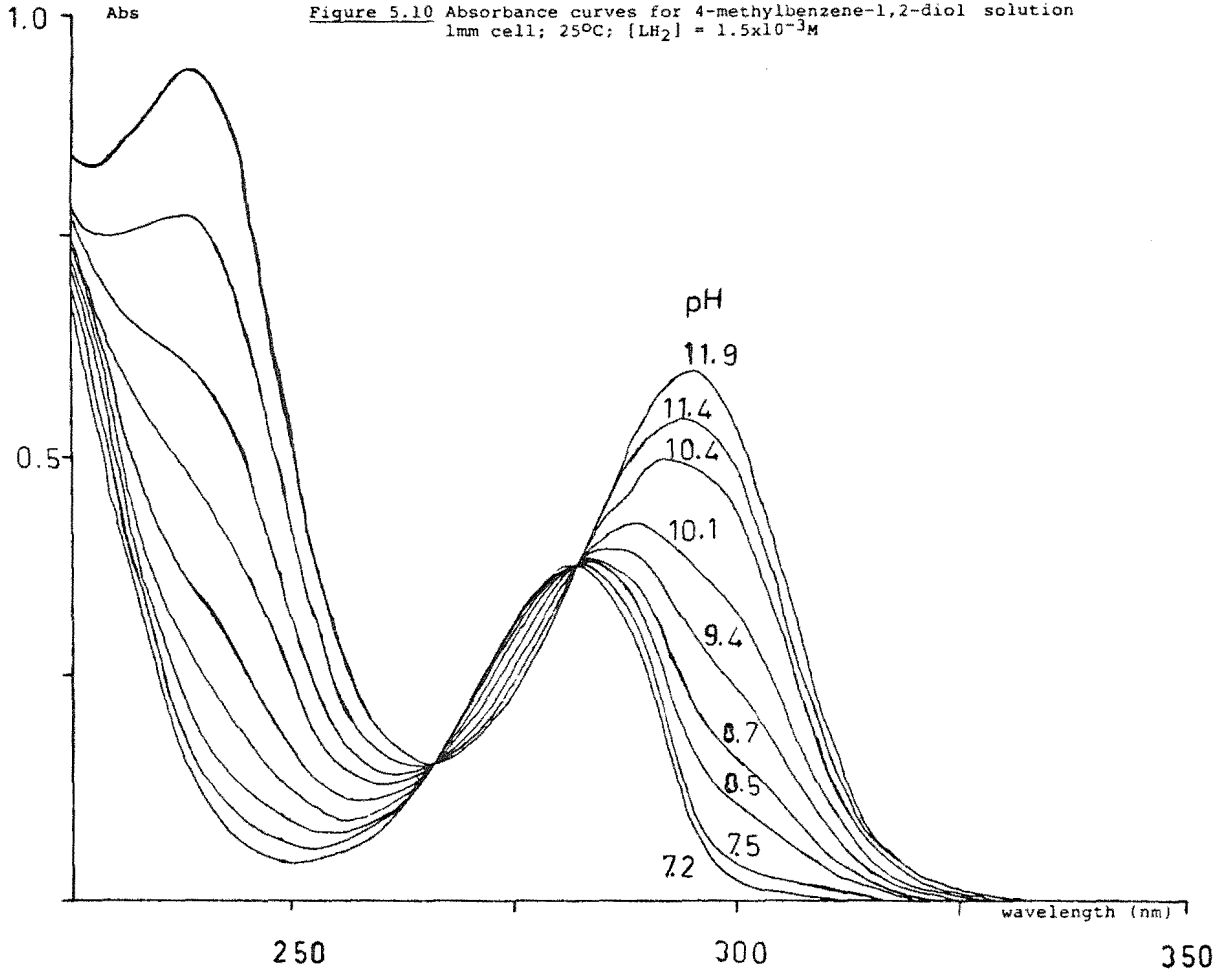

Figure 5.10 Absorbance curves for 4-methylbenzene-1,2-diol solution 1mm cell; 25°C; $[LH_2] = 1.5 \times 10^{-3}$M

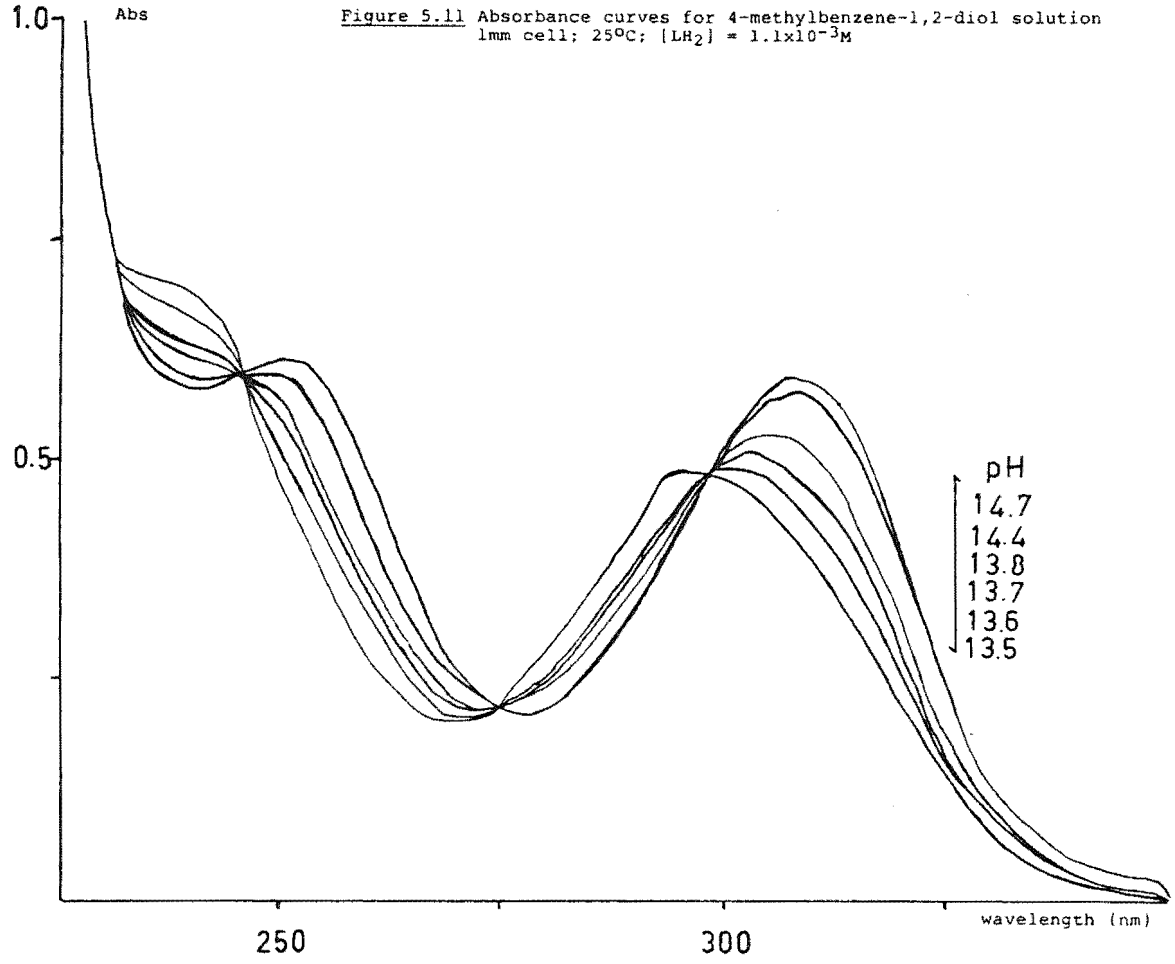

Figure 5.11 Absorbance curves for 4-methylbenzene-1,2-diol solution
1mm cell; 25°C; $[LH_2] = 1.1 \times 10^{-3}M$

show well defined isosbestic points (273 and 292 nm) indicating only two species in equilibrium in solution. The extrapolated value for log K_{011} (I = 0.1 M) is listed in Table 5.2 along with reported log K_{011} values from other workers. Calculated values of log K_{011} at each pH and ionic strength are given in appendix K. Spectral parameters are summarized in Table 5.7.

5.2.3 Protocatechuic acid

For protocatechuic acid K_{011} was calculated in the same manner as for catechol from the calculated [H] and ultraviolet spectrophotometric measurements. The spectrophotometric data consisted of 6 spectra in the pH range 13.0 - 13.5 (I = 0.4 - 0.2). Figure 5.12 presents a set of recorded spectra which show well defined isosbestic points (258 and 311 nm) indicating only two species in equilibrium in solution. Table 5.7 summarizes the the ultraviolet spectral data in Figure 5.12. The extrapolated value for log K_{011} (I = 0.1 M) is listed in Table 5.2 along with reported values. Calculated values of log K_{011} at each pH and ionic strength are given in appendix L.

5.2.4 3',4'-Di-O-methylcatechin

For this model compound only small changes in the ultraviolet spectrum occurred for significant changes in pH. Therefore it was not possible to determine the protonation constants by spectrophotometric measurements. Spectra at five different pH values are shown in Figure 5.13. Both K_{011} and K_{012} were obtained potentiometrically.

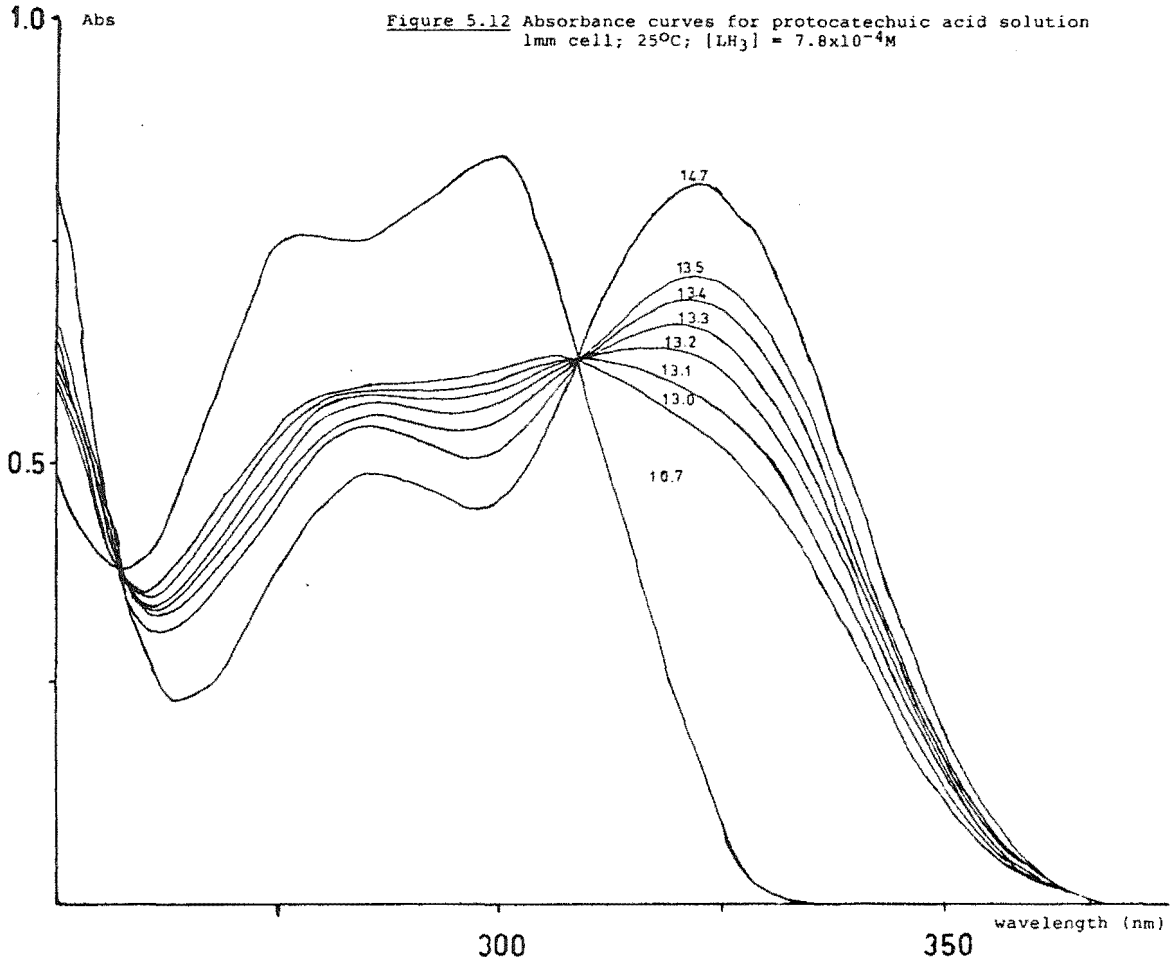

Figure 5.12 Absorbance curves for protocatechuic acid solution
1mm cell; 25°C; $[LH_3] = 7.8 \times 10^{-4}$M

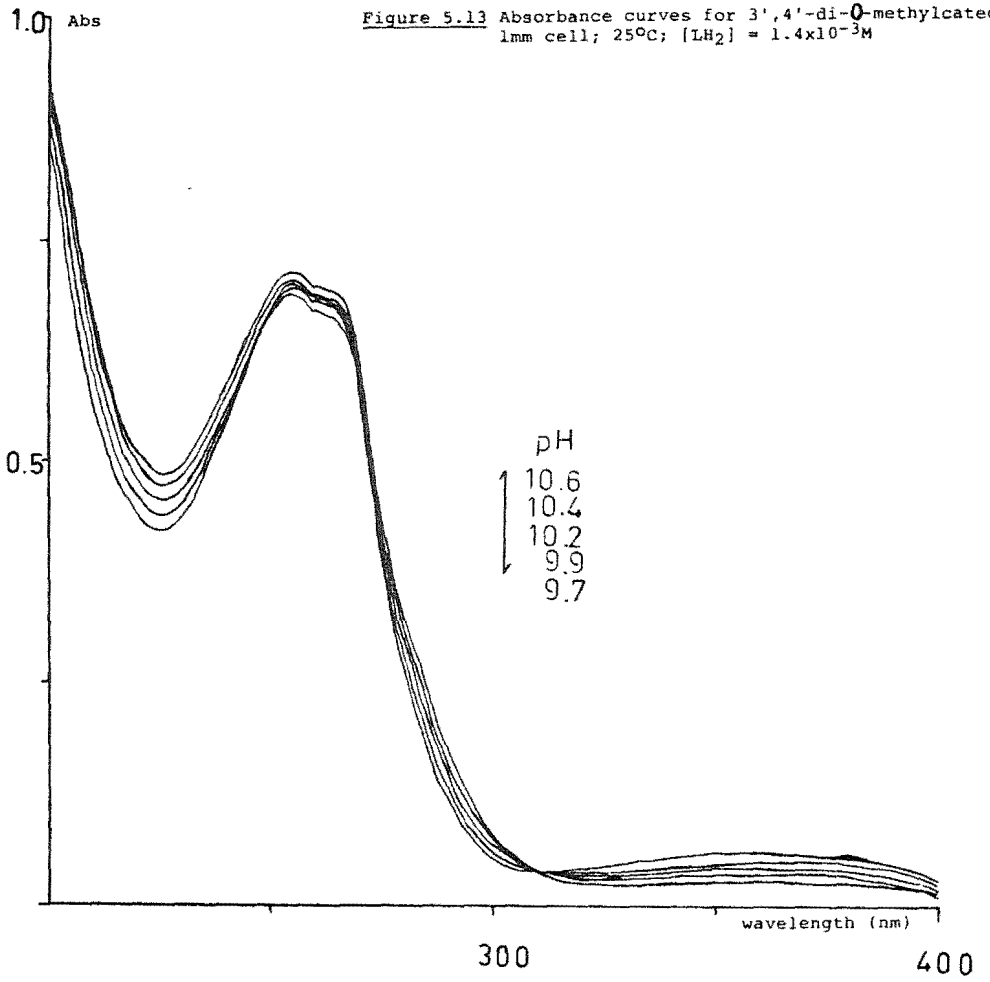

Figure 5.13 Absorbance curves for 3',4'-di-O-methylcatechin solution 1mm cell; 25°C; $[LH_2] = 1.4 \times 10^{-3}M$

5.2.5 Catechin and epicatechin

For both epimers K_{011} was evaluated from the calculated [H] and spectrophotometric measurements. Representative ultraviolet spectrophotometric data recorded for catechin and epicatechin as a function of pH are presented in Figures 5.14 and 5.15 respectively.

For both epimers the extinction coefficients for L and LH were obtained from spectra measured at pH c. 14.7 and 12.3 respectively. Calculations using the potentiometrically determined protonation constants K_{013} and K_{012} and an estimated value for K_{011} indicated that at pH 12.3 the concentration of LH was only 84% of the total concentration of ligand ([L]/[TL] = 0.065 and $[LH_2]$/[TL] = 0.095). It was therefore necessary to apply corrections for small absorbance contributions from LH_2 and L. This was done by subtracting the absorbances at a particular wavelength for L and LH_2 and normalizing ε_{LH} to 100% of total ligand, [TL], using the expression (5.10),

$$\varepsilon_{LH} = (Ab/[TL] - 0.065\,\varepsilon_{L} - 0.095\,\varepsilon_{LH_2})/0.84 \qquad (5.10)$$

ε_{L} was calculated from spectra recorded at pH 14.7 and ε_{LH_2} was estimated from spectra at pH of 10.4. The errors introduced by uncertainties in the value of ε_{LH_2} or from uncertainties in the estimated K_{011} value were assessed by varying these parameters by 10%; they were found to be minimal (< 2%).

Log K_{011} for each epimer was calculated in the same manner as for catechol, that is from duplicate spectrophotometric titrations which each provided 5 - 8 pH-absorbance measurements (at two selected wavelengths) in

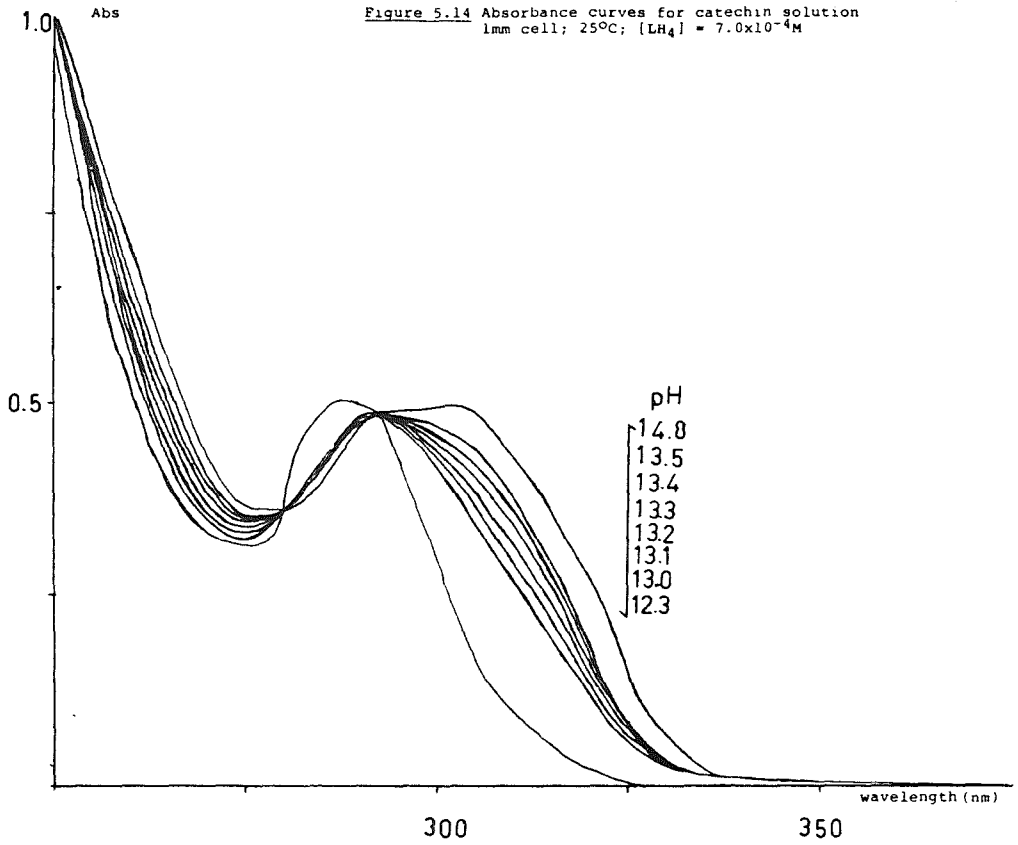

Figure 5.14 Absorbance curves for catechin solution
1mm cell; 25°C; $[LH_4] = 7.0 \times 10^{-4} M$

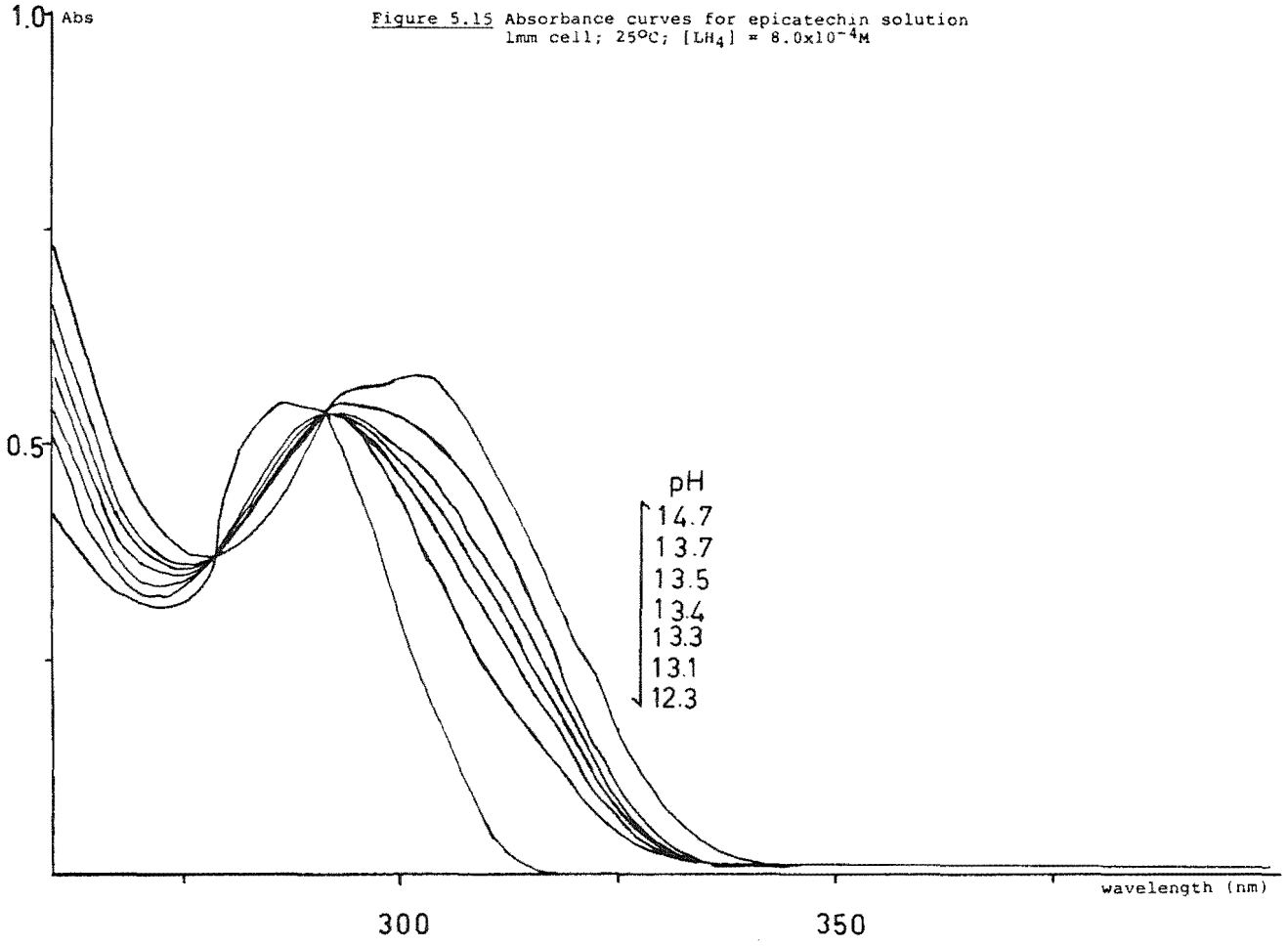

Figure 5.15 Absorbance curves for epicatechin solution
1mm cell; 25°C; $[LH_4] = 8.0 \times 10^{-4}M$

the pH range 13.0 - 13.7 (I = 0.2 - 0.9). Isosbestic points were observed for catechin and epicatechin which indicated only two species were in equilibrium and that no degradation reactions to quinone or catechinic acid had occurred. Table 5.7 lists the ultraviolet spectral parameters for both epimers. log K_{011} values were calculated at each pH; these are plotted against $I^{0.5}/(1 + I^{0.5})$ in Figure 5.16. The slopes obtained (equation (5.8)) were -2.1 for catechin and -1.4 for epicatechin (cf. theoretical value -2.0, assuming Z = 2). Log K_{011} values calculated at each ionic strength are tabulated in Table 5.8 and 5.9. The extrapolated values for log K_{011} (I 0.1 M) are listed in Table 5.2 for both epimers.

The protonation constant for the equilibrium reaction

$$H + LH_3 \rightleftharpoons LH_4 \qquad K_{014} = [LH_4]/[LH_3][H] \qquad (5.11)$$

was evaluated from an experimental value of ε_{LH_4}, potentiometrically measured hydrogen ion concentrations and measured absorbance values using Agrens[118] method (see Chapter 4). The K_{014} value was calculated as a check on the potentiometrically determined value (8.64±0.01) ; the value obtained was 8.65±0.03.

5.2.6 Epimerization studies

It has been reported that in alkaline solutions catechin and epicatechin epimerize; further at pH> 8 the epimerization is accompanied by irreversible rearrangement to catechinic acid[122]. The rate of these reactions has been reported to increase with pH and temperature[123]. Therefore in this work it was essential to establish that the amount

Figure 5.16 Plot of log K versus $I^{0.5}/(1+I^{0.5})$ for catechin and epicatechin

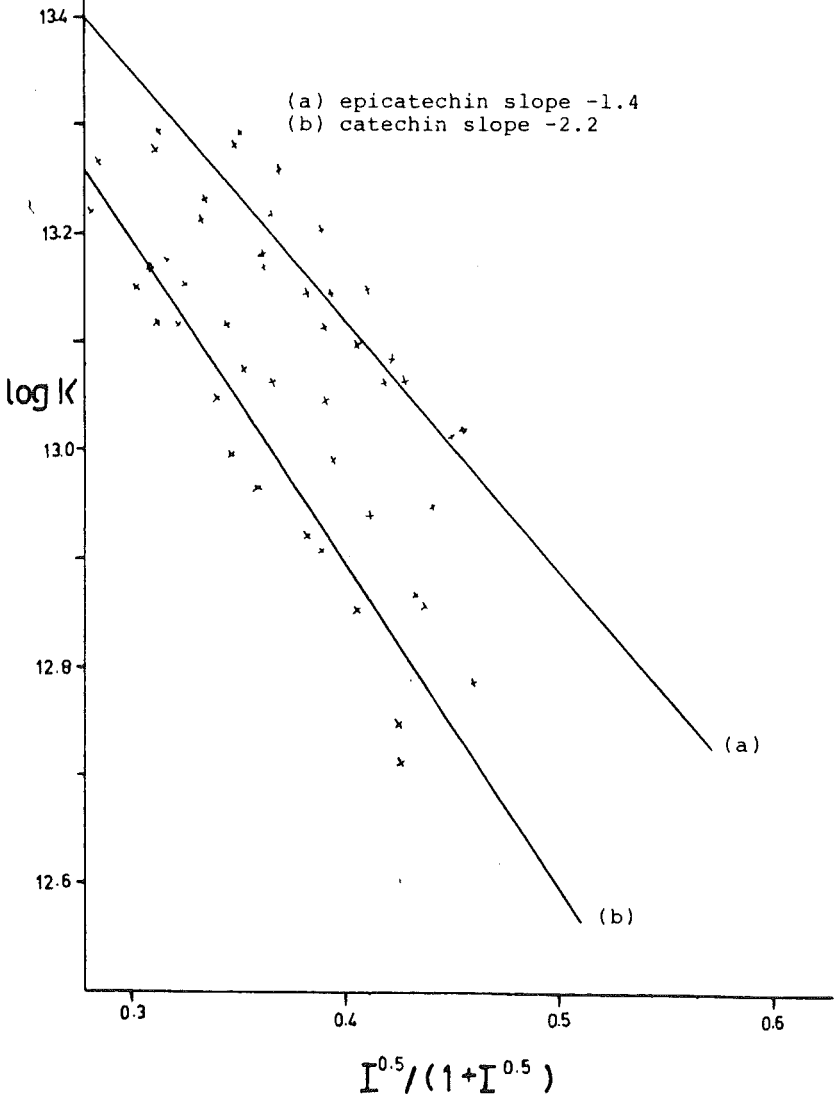

Table 5.8 Representative spectrophotometric data used for log K evaluation for catechin

absorbance	p[H]	ionic strength	$I^{0.5}/(1+I^{0.5})$	log K
0.400[a]	13.588	0.707	0.457	12.881
0.384	13.496	0.581	0.433	12.903
0.362	13.411	0.480	0.409	12.951
0.342	13.332	0.400	0.387	12.978
0.319	13.259	0.336	0.367	13.016
0.296	13.190	0.283	0.347	13.050
0.276	13.125	0.240	0.329	13.072
0.250	13.063	0.205	0.312	13.121
0.559[b]	13.508	0.596	0.436	12.748
0.516	13.354	0.421	0.394	12.885
0.479	13.218	0.304	0.355	12.939
0.426	13.097	0.224	0.321	13.054
0.376	12.986	0.168	0.291	13.159

a wavelength 310.0 nm, ε_L 6679, ε_{LH} 865

b wavelength 305.0 nm, ε_L 7058, ε_{LH} 2420

Table 5.9 Representative spectrophotometric data used for log K evaluation for epicatechin

absorbance	p[H]	ionic strength	$I^{0.5}/(1+I^{0.5})$	log K
0.550[a]	13.689	0.865	0.482	13.047
0.478	13.567	0.677	0.451	13.080
0.447	13.464	0.536	0.423	13.157
0.420	13.359	0.427	0.395	13.190
0.393	13.266	0.341	0.369	13.228
0.367	13.177	0.274	0.344	13.262
0.340	13.093	0.222	0.320	13.331
0.499[b]	13.587	0.705	0.456	13.144
0.469	13.494	0.579	0.432	13.162
0.444	13.409	0.479	0.409	13.162
0.414	13.331	0.399	0.387	13.181
0.375	12.258	0.335	0.367	13.228
0.344	13.190	0.283	0.347	13.255

a wavelength 305.0 nm, ε_L 7137, ε_{LH} 2538

b wavelength 310.0 nm, ε_L 6833, ε_{LH} 848

of epimerization and rearrangement was minor during the course of a potentiometric or spectrophotometric titration.

At high pH (14.7) catechin and epicatechin spectra were stable for hours which indicated that no rearrangement to the common product catechinic acid had occurred; catechinic acid has an extinction coefficient of c. 18600 at 285 nm[122] and its formation would have caused a significant increase in the absorbance at this wavelength (cf. catechins have ε_{6000} at 285 nm).

The h.p.l.c. method described in Chapter 2 was used to study these reactions, in particular the epimerization of catechin to epicatechin or vice versa, at a pH of 13.3. Aliquots (0.4 ml) of the reaction mixture taken at 0 - 100 min were quenched by withdrawal (through a septum seal) into a micrometer syringe primed with 0.4 ml of 2 M HCl. A 10-μl sample of the quenched mixture was then analysed by h.p.l.c. A typical trace for a synthetic mixture of catechin, epicatechin and catechinic acid is shown in Figure 5.17.

Figure 5.17 Typical h.p.l.c trace for a synthetic mixture of catechinic acid, catechin and epicatechin

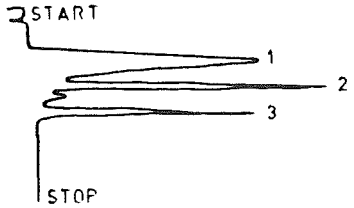

1 catechinic acid 1.81 min
2 catechin 2.66 min
3 epicatechin 3.61 min

Figure 5.18 presents the results obtained; after 1.5 h only 4% of catechin and 15% of epicatechin was epimerized (a typical time for a spectrophotometric titration was c. 60 min). It was noted that the formation of catechinic acid occurred rapidly on the admission of oxygen. As the spectrophotometric titration technique for $\log K_{011}$ determination involved incremental dilution of an alkaline polyphenol solution with a neutral polyphenol solution (in which there would be no epimerization) the percentage epimerization at 1.5 h would be less than determined by the h.p.l.c. analysis.

5.2.7 Epicatechin dimer, B2

It was expected that B2 would undergo B ring deprotonation as for epicatechin. Spectrophotometric analysis of the B2 dimer at high pH (14.7 - 13.7) revealed that the shape of the absorption spectrum for B2 differed slightly from those recorded for the monomers catechin and epicatechin (see Figure 5.19). Further in the pH range 14.7 - 13.7 changes in the ultraviolet absorption spectrum were too small to allow calculation of equilibrium constants, and no isosbestic points were observed. This can be compared with the changes that are observed in the spectrum of catechin for a similar pH range. These differences could imply non-equivalence of the B rings in B2. No attempt was made to evaluate protonation constants from spectrophotometric data.

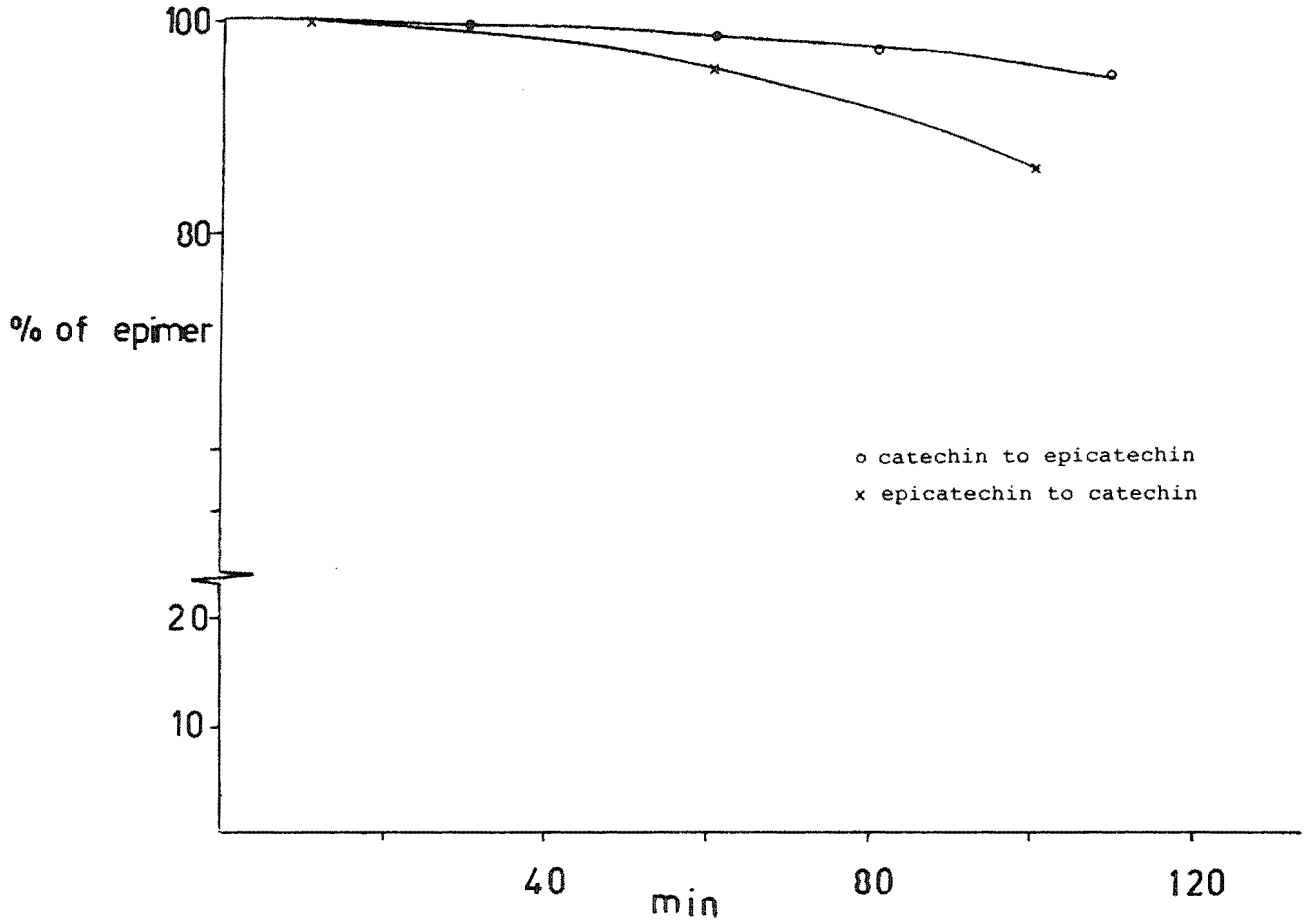

Figure 5.18 Epimerization study of epicatechin and catechin ; (25°C; pH 13.3)

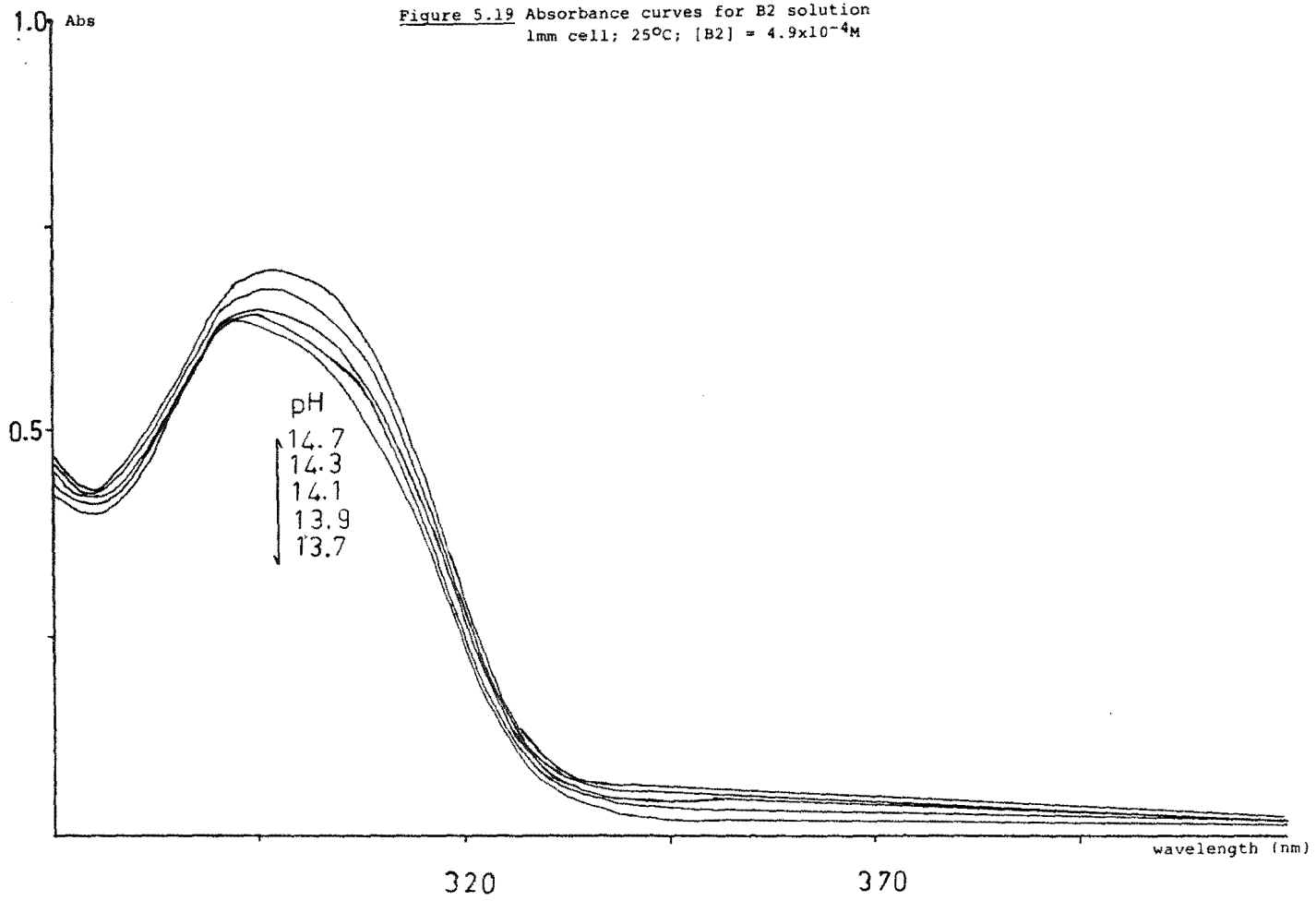

Figure 5.19 Absorbance curves for B2 solution
1mm cell; 25°C; [B2] = 4.9×10^{-4}M

5.3 Discussion

Protonation constants for the plant phenolics[10] catechin and epicatechin have been determined and assigned to reactions on the A and B rings by reference to the log K values of model compounds (viz. 4-methylbenzene-1,2-diol and 3',4'-di-O-methylcatechin). An understanding of the sites of protonation reactions of these naturally occurring hydroxybenzenes permits their interactions with metal ions to be examined. The protonation sites were required because metal complexing occurs only with the B ring. Table 5.2 summarizes the protonation constants obtained in this work and compares them with values reported by other workers.

The polyphenols catechin and epicatechin contain four ionizable hydroxyl groups. The 3-hydroxy (alcoholic) group in the hetero ring has a log K c. 15.5[124]; therefore its deprotonation was not considered. The epimers differ only in the configuration of the heterocyclic ring. Both diastereoisomers have the 2-aryl (B) rings in a pseudo-equatorial conformation[125,126]. Figure 5.20 was generated from calculations[127] based on X-ray crystal data[126] and indicates the general planarity for the A ring and the hetero ring of catechin. The A ring protonation sites are well separated from those on the B ring and in the crystalline state the 3-hydroxy group is some 540 pm from the nearest (3'-) phenolic group[126]. H nmr studies on flavan-4-phloroglucinol adducts[71] have shown that the hetero ring conformation remains unchanged in the temperature range from -10 to +80°C, indicating that this ring is not

Figure 5.20 Molecular structure of 8-bromo-tetra-o-methyl-(+)-catechin

flexible. Thus, on the basis of conformation, any differences in protonation constants for the two epimers were expected to be minor.

The A and B rings of catechin and epicatechin are separated by the pyran ring and are not conjugated; therefore ionization of phenolic groups on one ring should be independent of OH groups on the other. Thus, the protonation reactions of 3',4'-di-O-methylcatechin and 4-methylbenzene-1,2-diol can be used to infer the approximate log K_{01r} values for the protonation of the phenolate groups on the A and B rings respectively. From Table 5.2 log K values inferred for the A ring are c. 10.9 and 8.8, and for the B ring c. 13.6 and 9.3. The log K_{01r} values noted in the Table are numerically similar to those for the model compounds; therefore the ring sequence for the protonation steps for catechin and epicatechin is B, A, B, A. The constants determined for catechin are similar in magnitude to those reported by Slabbert[128] (see Table 5.2). However the sequence B, A, A, B deduced by reference to flavanoids[128] is different from that deduced in this work.

By extrapolation from Figure 5.16 the log K_{011} values at zero ionic strength may be obtained; the values for catechin and epicatechin agree within experimental error (13.78 and 13.73 respectively) but differ at I 0.10 M (see Table 5.2). This difference in log K_{011} values was ascribed either to specific solvation effects or to ion association between the ligand anion and K^+.

Each protonation step on the B ring will involve an equilibrium distribution between the 3'- and 4'- positions; this is inferred from the similar values of log K for m-cresol (c. 10.05) and p-cresol(c. 10.20)[129].

The protonation constants for both catechin and epicatechin were evaluated because it was reported that catechin epimerizes 2 - 3 times more slowly than does epicatechin in alkaline solution[123]. The proposed ionic mechanism[122,130] involving a common quinone methide intermediate (9) requires opening of the hetero ring after deprotonation of the 4'- hydroxy group (see scheme 1). Hence a difference in the numerical values of log K for the B ring deprotonation would support the ionic mechanism; i.e. if log K_{011} and log K_{013} values for epicatechin were lower than those for the catechin B ring.

From this work it was found (see Table 5.2) that the B ring protonation constants for epicatechin were greater than those for catechin; thus as the pH is increased a higher % of catechin would be deprotonated. These results do not support the ionic mechanism.

Under alkaline and rigorously oxygen free conditions it was established by h.p.l.c. and ultraviolet spectrophotometric measurements that negligible epimerization or rearrangement occurred (c. 1.5 h). Therefore the high pH (> 13) equilibrium measurements were made on epimerically pure substances. The dilution technique used in the spectrophotometric analysis added increments of neutral ligand solution (epimerically pure) to an alkaline solution which was then sampled for

Scheme 1

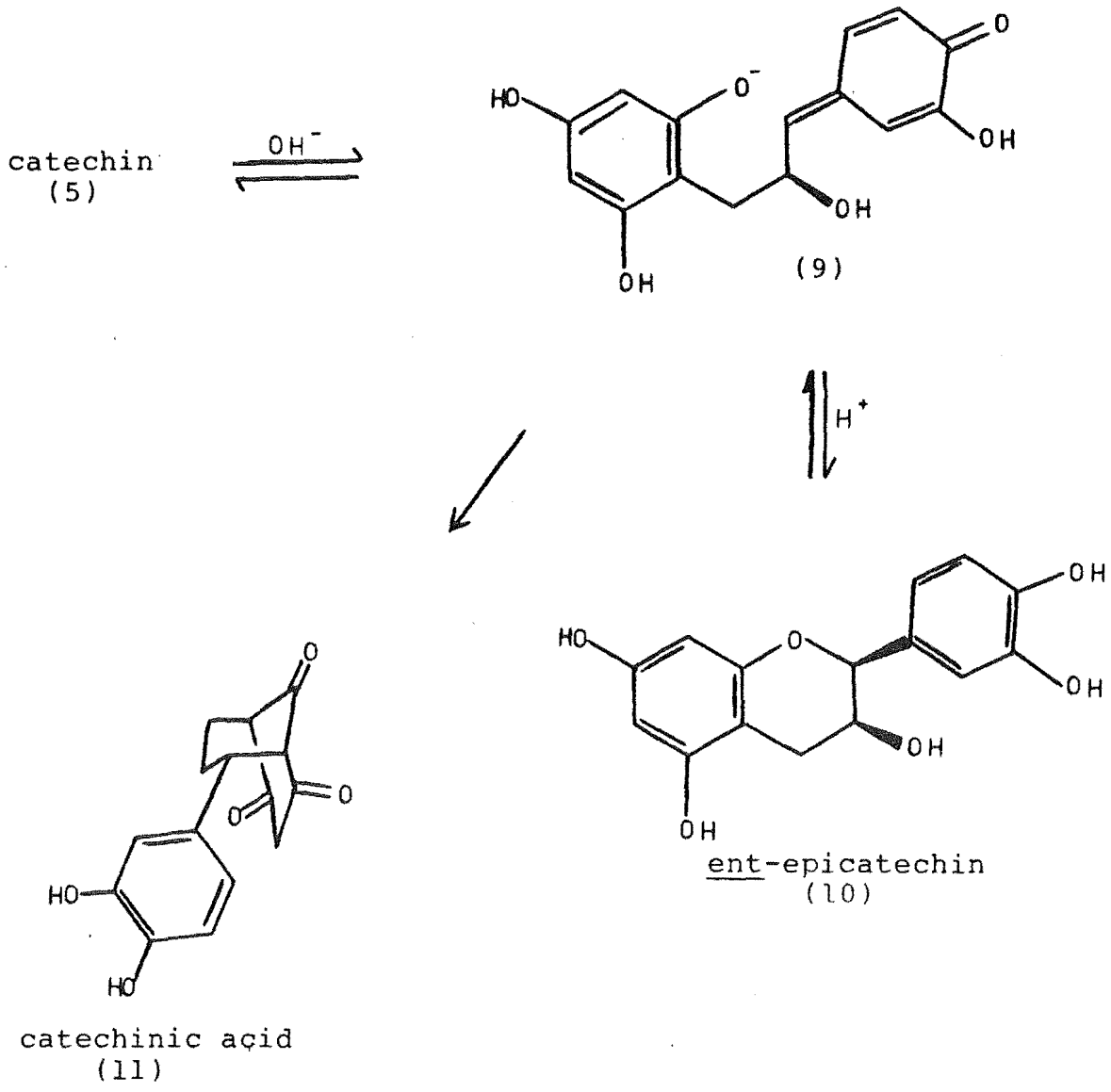
catechin
(5)
OH⁻
HO
O⁻
OH
OH
O
OH
(9)
H⁺
HO
O
OH
OH
OH
ent-epicatechin
(10)
O
O
O
HO
HO
catechinic acid
(11)

spectrophotometric analysis; the final ratio of alkaline ligand solution to neutral ligand solution was c. 1/1.4 and hence the percentage epimerization at 1.5 h would be less than determined by the h.p.l.c. experiment (Figure 5.18). The observed rates of epimerization were much lower than indicated by Kiatgrajai et al.[123] who reported > 20% epimerization at pH 10 at 25°C (only 4% of catechin and 15% of epicatechin were epimerized in 1.5 h in this work, see Figure 5.18). Admission of oxygen produced increased amounts of epimerization products and of catechinic acid.

The formation of catechinic acid from catechin and epicatechin was followed by ultraviolet spectrophotometry at 25°C and under rigorously oxygen free conditions. No catechinic acid was detected in 1.5 h at pH 13.5 nor in 45 min at pH 14.8. However admission of oxygen to these solutions produced an immediate yellowing and rapid absorption increases (within minutes) at c. 400 nm (quinone formation[132]) and 285 nm (catechinic acid). At 47°C and pH 11, a 20% conversion of catechin into catechinic acid was reported[123]; in contrast for this temperature and time, but at pH 14, only 9% conversion was observed in the present study.

The results obtained indicated that both the epimerization reaction and catechinic acid formation were oxygen catalyzed. In this work stringent precautions were taken to exclude oxygen. However Kiatgrajai et al.[123], although performing their kinetic analyses under nitrogen, would still have had traces of oxygen present; hence they

observed much more rapid epimerization and catechinic acid formation.

It has been reported that phenolate anions readily form radicals in the presence of oxygen[133] and that a radical anion forms on the B ring of catechin and epicatechin in the presence of sodium hydroxide[134,135]. Porter et al.[67] suggested therefore that the formation of epimerization and rearrangement products in alkali may proceed through a radical mechanism (see scheme 2) that is catalyzed by the presence of molecular oxygen, rather than by the ionic mechanism (see scheme 1).

The protonation constants for the epicatechin dimer, B2 were expected to be similar to those for catechin and epicatechin, but spectrophotometric and potentiometric measurements indicated significant differences. This may arise from a non equivalence of A and B rings in the upper and lower epicatechin units (see Figure 5.21). Fletcher et al.[71] have concluded from nmr experiments that the rotational energy barriers for a series of catechin-epicatechin dimers including B2 were too small to permit isolation of different conformers; however an examination of molecular models allowed these workers to predict energetically preferred conformations. Figure 5.21 presents schematic models reported for C(4)-C(8) linked 4R dimers (e.g. B2) in phenolic and derivatized forms[71].

For the epicatechin dimer, B2 the possible interactions of the upper and lower ring systems with each other (A....B') and the different extent of solvation of these rings in the monomer and dimer make it extremely

Scheme 2

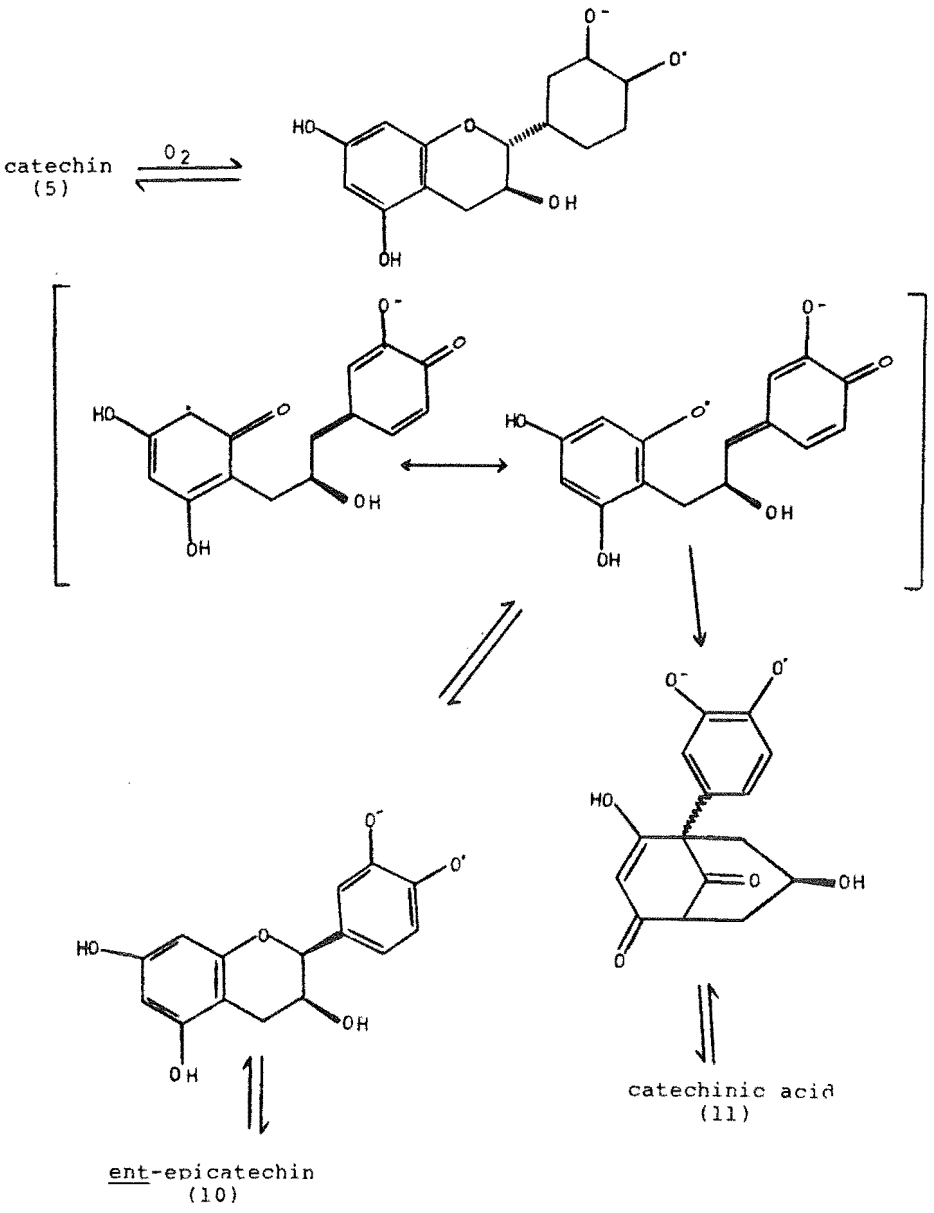

Figure 5.21

Suggested conformations of the epicatechin dimer B2

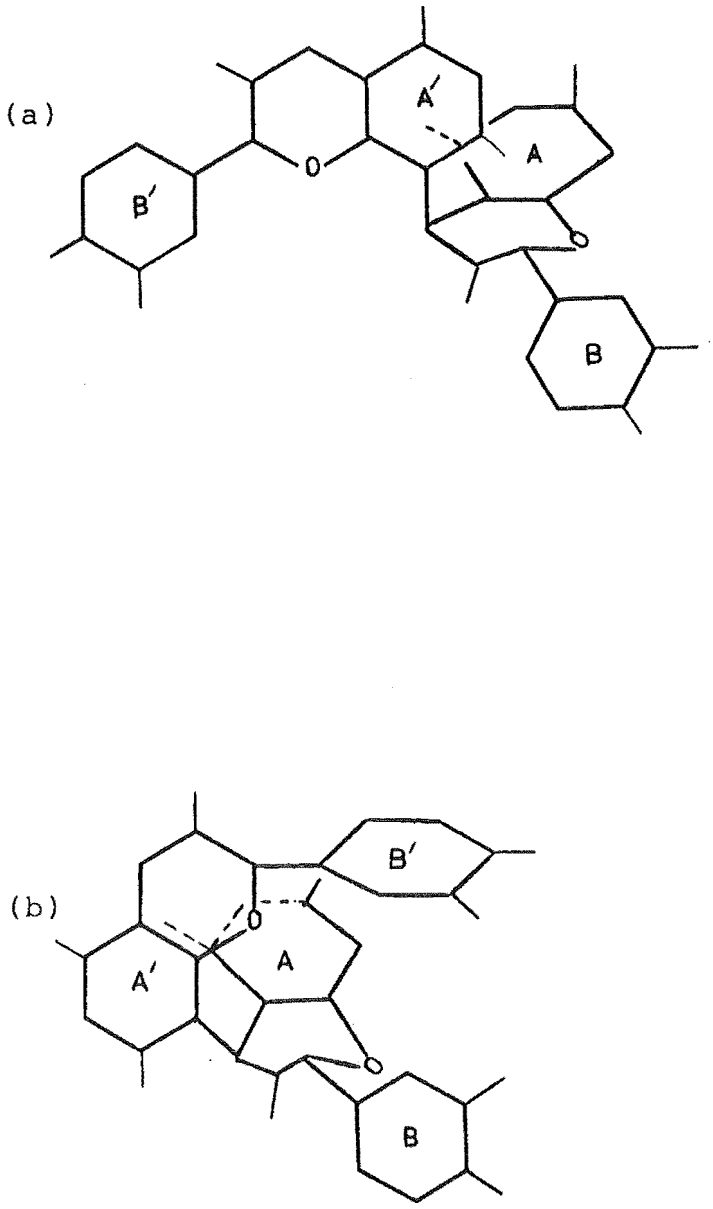

A',B' indicate upper epicatechin unit consisting of A and B rings

position of OR groups indicated by — for substituent

(a) energetically preferred conformation for B2 (R=H)

(b) energetically preferred conformation for derivatised B2 ($R=OOCCH_3$)

difficult to (i) assign sites to the stepwise protonation of B2 and (ii) ascribe the subtle changes observed in the protonation constants to particular thermodynamic or electrostatic phenomena. It has been stated[136] that one must be cautious in attaching significance to specific effects for small changes in protonation constants. It is likely however that solution effects (non ionic and anionic groupings), hydrogen bonding effects (intermolecular and with solvent), and inductive effects (substitution at C(8)) all contribute to the protonation differences observed epicatechin and B2. The difference in K's indicate that one or more of these effects is quite marked.

CHAPTER 6

ALUMINIUM-POLYPHENOL INTERACTIONS

Aluminium polyphenol equilibria were investigated by a potentiometric method; standard KOH was titrated into metal-ligand solutions of known concentrations. From the stoichiometry of the system, the measured hydrogen ion concentration and the volume of titre, it was possible to compute stability constants for postulated equilibrium systems (see Chapter 4). The "goodness of fit" for a particular model was assessed by statistical parameters generated by the least squares computer program. Knowledge of the stability constants for these systems will allow calculations on the role that these naturally occurring ligands may play in soil processes (e.g. podzolization) by virtue of their complexing reactions.

6.1 Aluminium ion hydrolysis

6.1.1 Aluminium hydroxy species

The hydrolysis of aluminium ion has been the subject of extensive investigations and the reported species range from monomeric to polymeric[124,146]. The principal reasons for the lack of a universally accepted hydrolysis scheme for Al(III) are (i) the slow rate of hydrolysis for polymeric species, (ii) the metastable nature of partly neutralized Al(III) solutions, and, (iii) the dependence on the precise conditions used in the hydrolysis experiment.

The aluminium-hydroxy species postulated by Mesmer and Baes[147] were used in this work. The equilibrium expressions

for the species were included in the mass balance equations used to model all Al(III) polyphenol systems.

The equilibrium reactions and the hydrolysis constants for these species are:

$$Al + H_2O \rightleftharpoons AlOH + H$$

$$\beta 10\text{-}1 = [AlOH][H]/[Al] \qquad (6.1)$$

$$Al + 2H_2O \rightleftharpoons Al(OH)_2 + 2H$$

$$\beta 10\text{-}2 = [Al(OH)_2][H]^2/[Al] \qquad (6.2)$$

$$Al + 3H_2O \rightleftharpoons Al(OH)_3 + 3H$$

$$\beta 10\text{-}3 = [Al(OH)]_3[H]^3/[Al] \qquad (6.3)$$

$$Al + 4H_2O \rightleftharpoons Al(OH)_4 + 4H$$

$$\beta 10\text{-}4 = [Al(OH)_4][H]^4/[Al] \qquad (6.4)$$

$$2Al + 2H_2O \rightleftharpoons Al_2(OH)_2 + 2H$$

$$\beta 20\text{-}2 = [Al_2(OH)_2][H]^2/[Al]^2 \qquad (6.5)$$

$$3Al + 4H_2O \rightleftharpoons Al_3(OH)_4 + 4H$$

$$\beta 30\text{-}4 = [Al_3(OH)_4][H]^4/[Al]^3 \qquad (6.6)$$

$$13Al + 32H_2O \rightleftharpoons Al_{13}(OH)_{32} + 32H$$

$$\beta 130\text{-}32 = [Al_{13}(OH)_{32}][H]^{32}/[Al]^{13} \qquad (6.7)$$

The values for the constants β_{pqr} are listed in Table 6.1. The tabulated values were calculated for I = 0.1 M, T = 25°C from values reported by Mesmer and Baes[147]. Recent work by Ohman et al.[148] supports equilibria (6.1), (6.6) and (6.7) proposed by Mesmer et al.[147] but suggests slightly different magnitudes for the hydrolysis constants (Table 6.1).

Concentrations of aluminium hydroxy species were found to be negligible in all the Al ligand systems studied in this work when either Mesmer's or Ohman's hydrolysis schemes were included in the equilibrium model, i.e. the selected

ligand/metal ratios (4-7) were sufficiently high to suppress hydrolysis. At lower ratios hydrolysis was indicated by severe drifting of pH.

Table 6.1 Al(III) hydrolysis constants[a]

species	$\log \beta_{p0r}$	
AlOH	-5.461[b]	-5.418[c]
$Al(OH)_2$	-10.036	
$Al(OH)_3$	-13.694	
$Al(OH)_4$	-23.491	
$Al_2(OH)_2$	-7.7	
$Al_3(OH)_4$	-15.737	-15.454
$Al_{13}(OH)_{32}$	-103.149	-105.422

a I = 0.1 M, T = 25°C

b Calcuated from data of Mesmer et al.[147]

c Calcuated from data of Ohman et al.[148]

6.1.2 Solubility product of Al(III)

Many different values have been reported for the solubility product of $Al(OH)_3$. Chen[149] has reported that the thermodynamic solubility product is different in solutions containing different counter cations, while Singh[150] found that fast titrations of dilute aluminium ion solutions resulted in a Ksp that varied inversely with Al(III) concentration.

The solubility of an amorphous precipitate is greater than that of an aged precipitate of crystalline $Al(OH)_3$.

The time scale (2 - 3 h) of the Al-polyphenol titrations required that a Ksp value for amorphous $Al(OH)_3$ be chosen. Frink et al.[151] have quoted an activity solubility product pKsp = 31.8 which is similar to values quoted by Chen[149] (30.0 - 31.0) and by Singh[150] (32.1). This value was obtained from fast titrations of CO_2 free Al(III) solutions with NaOH. In the present study values of the single ion activity coefficients for Al(III), f_{Al} and OH, f_{OH} were calculated from the Davies' equation[152]; they were used to convert Frink's activity product to a concentration product,

viz. $[Al(III)][OH]^3 = Ksp/f_{Al(III)} \cdot f_{OH}^3 = 10^{-30.4}$.

The product $[Al(III)][OH]^3$ was calculated for each datum point in the computer analysis of Al(III)-ligand titrations and compared with the value derived from Frink's data to check for $Al(OH)_3$ precipitation.

6.2 Choice of a model equilibrium system

The definitive end points in a metal ligand titration were attributed to the quantitative formation of a complex species in solution; from the stoichiometry at each end point the nature of the species was inferred. For example the titration of an Al-catechol solution yields an inflexion (pH 4.8 - 5.2) whose KOH titre volume corresponds to two moles of protons per mole of metal ions, i.e. to the number of protons lost from the ligand for the following reaction:

$$Al + LH_2 \rightleftharpoons AlL + 2H \qquad (6.8)$$

Other definitive end points implied quantitative formation of further ligand metal species (see Section 6.4).

Data from analogous systems can be used to support a particular equilibrium model. For example in the interaction of Fe(III) with polyphenols[153,154] (such as protocatechuic acid, catechol) the visible absorption spectra indicate that three species are formed in the pH range in which Al(III) is found to complex with these ligands. These entities are mono, bis and tris (ML, ML_2, ML_3) species which are coloured green, blue and red respectively; stoichiometries have been determined from analytical plots (e.g. Job variation[155], isomolar[156]) based on their visible absorption spectra.

The end points for the Al-polyphenol titrations indicated the formation of AlL and AlL_2 but not AlL_3 (i.e. no definitive inflexions were observed past the second end point). However AlL_3 is a probable complex species because of the complex FeL_3 in the iron system. So that AlL_3 could be confidently incorporated in the equilibrium model (rather than $AlL_2(OH)_2$ which has the same proton count) evidence for the existence of this species was sought from the changes in the ultraviolet spectrum of catechol when increasing amounts of Al(III) were added incrementally. The pH of the ligand solution (9.1) was held constant and accurate amounts of Al(III) were added. The observed change in the wavelength maximum for the ligand was consistent with ligand deprotonation, confirming a ligand-metal interaction. Figure 6.1 shows the increasing absorbance observed for addition of Al(III) to a catechol solution; for M/L ratios greater than 1 mole of Al to 3 moles of ligand no further increase in absorbance occurred. A plot of moles of Al(III)

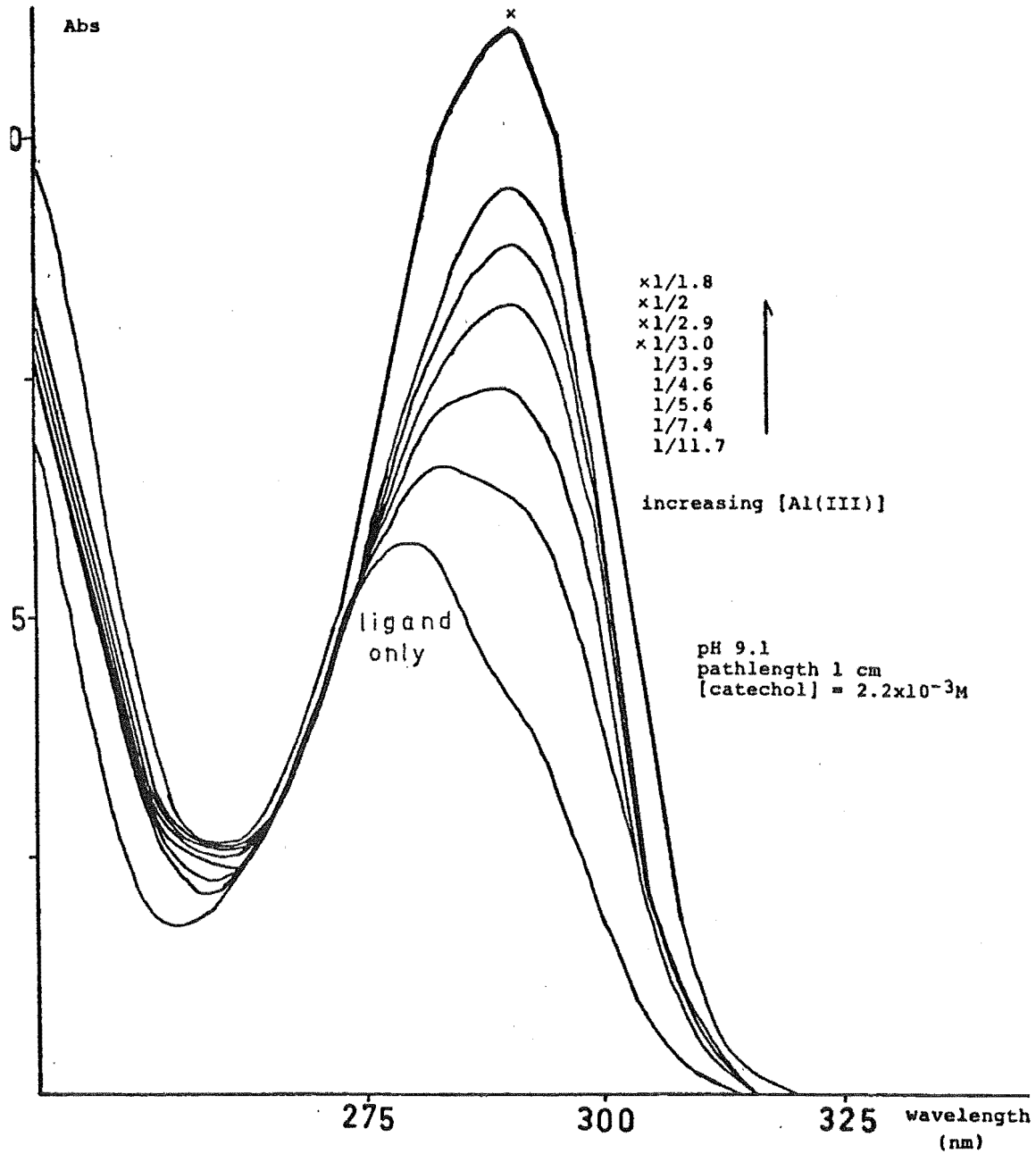

Figure 6.1 Absorbance curves for catechol-Al(III) solutions

added versus absorbance at 290 nm (corrected for the contribution from uncoordinated ligand) confirmed the existence of the tris species AlL_3 (Figure 6.2). The established equilibrium model was then tested by non-linear least squares analysis as described in Chapter 4.

6.3 Model assessment

For each iterative cycle the non-linear least squares computer program printed the residuals (TH(obs)-TH(calc)) for the mass balance equation used in the refinement and printed the estimated standard deviation of the residuals, s,

$$s = [\sum (TH(obs) - TH(calc))^2/(NO - NV)]^{0.5} \quad (6.9)$$

where NO is the number of observations and NV is the number of variables being determined. The crystallographic R-factor[157]

$$R = \frac{\sum_i (TH(obs)_i - TH(calc)_i)^2}{(\sum_i TH(obs)_i^2)} \quad (6.10)$$

was also calculated and gave an overall estimation of the "goodness" of fit. The lower the value of R the better the fit between the calculated data and the experimental data.

By examining the residuals individually it is possible to locate any areas of "bad" fit. These areas were defined as data points whose residuals deviated from the arithmetic mean of zero by more than the mean deviation of 0.8 s[158] (where s is the standard deviation). If a region of "bad" fit was removed on the addition of a trial complex species, if the R-factor was improved and if the magnitude of this species' equilibrium constant was realistic the species was accepted in the equilibrium model. For example

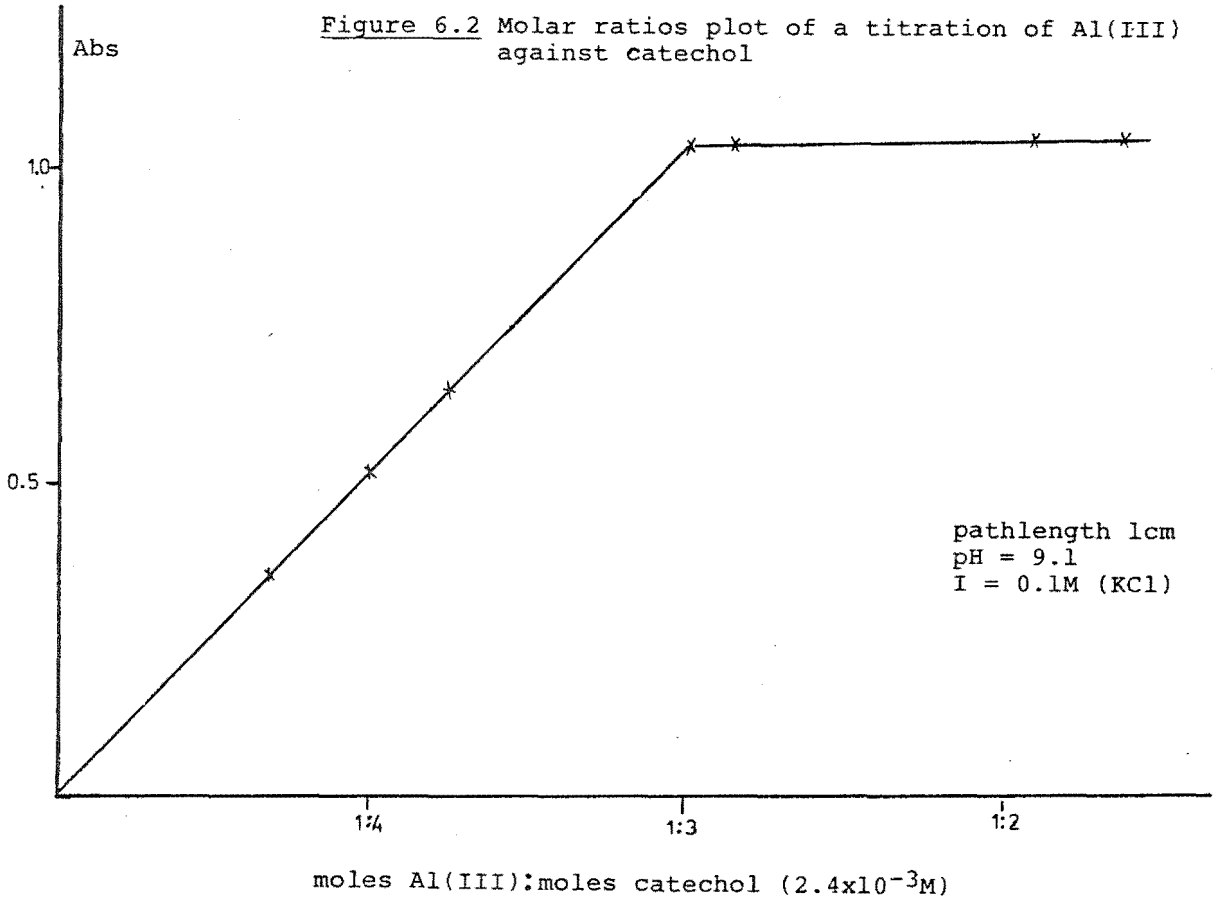

Figure 6.2 Molar ratios plot of a titration of Al(III) against catechol

when modelling the Al-protocatechuic acid (LH_2^-) system large residuals were found in the pH range 4 - 6. In addition to AlL, AlLH and AlL_2 a carboxyl protonated species AlL(LH) was included in the model. The result was a lowering of the R-factor and a slight reduction of the residuals in the region of bad fit. However the magnitude of the derived constant for the deprotonation reaction ($AlL(LH) \rightleftharpoons AlL_2 + H$) was not realistic (i.e. the carboxyl group in the AlLLH species was ascribed a pK > 5.5, whereas for the uncoordinated ligand the value was 4.26). Therefore this species was rejected. In this instance inclusion of a hydroxy species with stoichiometry AlL(OH) was found to improve the fit.

6.4 Results

6.4.1 Al(III)-catechol (LH_2, r = 2)

Data from one of four potentiometric titrations of KOH against oxygen-free solutions of Al(III) (6 - 9×10^{-4} M) and ligand (3 - 5×10^{-3} M) are listed in Table 6.2. There were typically 59 - 123 pH-volume of titre data points per titration. Figure 6.3 is the titration curve generated from the data in Table 6.2. Stoichiometric end points were observed at c. pH 5 and 7 when an excess of ligand was present (L/M > 5). These inflexions corresponded to the completion of the following reactions:

$$Al + LH_r \rightleftharpoons AlLH_{r-2} + 2H$$

$$'K_{11(r-2)} = [AlLH_{r-2}][H]^2/[Al][LH_r] \qquad (6.11)$$

$$AlLH_{r-2} + LH_r \rightleftharpoons Al(LH_{r-2})_2 + 2H$$

$$'K_{12(2r-4)} = [Al(LH_{r-2})_2][H]^2/[Al(LH_{r-2})][LH_r] \qquad (6.12)$$

Table 6.2 Representative data from a titration of a catechol-aluminium solution with standard KOH[a]

titre (ml)[b]	p[H][c]	TH(obs)x10^2	TH(calc)x10^2
0.270	3.855	0.8565	0.8581
0.275	3.883	0.8532	0.8544
0.280	3.910	0.8498	0.8507
0.285	3.934	0.8465	0.8473
0.290	3.959	0.8431	0.8436
0.300	4.005	0.8364	0.8367
0.310	4.049	0.8297	0.8299
0.315	4.072	0.8264	0.8264
0.320	4.093	0.8231	0.8232
0.325	4.116	0.8197	0.8196
0.335	4.162	0.8130	0.8124
0.340	4.184	0.8097	0.8091
0.350	4.229	0.8030	0.8023
0.360	4.275	0.7963	0.7957
0.370	4.327	0.7896	0.7888
0.380	4.381	0.7829	0.7823
0.390	4.442	0.7763	0.7757
0.400	4.508	0.7696	0.7695
0.405	4.552	0.7662	0.7659
0.410	4.595	0.7629	0.7628
0.420	4.706	0.7562	0.7563
0.425	4.786	0.7529	0.7526
0.430	4.864	0.7495	0.7495
0.436	4.980	0.7455	0.7454
0.440	5.050	0.7429	0.7430
0.445	5.134	0.7395	0.7395
0.450	5.210	0.7362	0.7361
0.455	5.274	0.7328	0.7327
0.460	5.328	0.7295	0.7295
0.465	5.377	0.7262	0.7263
0.470	5.423	0.7228	0.7229
0.480	5.499	0.7162	0.7166
0.485	5.537	0.7128	0.7131
0.495	5.604	0.7061	0.7065
0.500	5.634	0.7028	0.7032
0.510	5.697	0.6961	0.6964
0.520	5.776	0.6895	0.6893
0.530	5.817	0.6828	0.6822
0.535	5.845	0.6795	0.6790
0.540	5.875	0.6761	0.6756
0.545	5.906	0.6728	0.6721
0.550	5.938	0.6695	0.6687
0.555	5.970	0.6661	0.6653

Table 6.2 (continued)

0.560	6.003	0.6628	0.6619
0.570	6.072	0.6561	0.6553
0.575	6.108	0.6528	0.6523
0.580	6.147	0.6494	0.6489
0.585	6.189	0.6461	0.6461
0.590	6.236	0.6428	0.6426
0.595	6.284	0.6394	0.6397
0.600	6.341	0.6361	0.6367
0.610	6.489	0.6295	0.6308
0.615	6.579	0.6261	0.6278
0.620	6.704	0.6228	0.6246
0.625	6.844	0.6195	0.6215
0.630	7.010	0.6161	0.6179
0.635	7.143	0.6128	0.6146
0.640	7.267	0.6095	0.6109
0.645	7.368	0.6062	0.6073
0.655	7.521	0.5995	0.6004
0.660	7.590	0.5962	0.5963
0.670	7.699	0.5896	0.5889
0.680	7.785	0.5829	0.5820
0.685	7.824	0.5796	0.5787
0.690	7.859	0.5763	0.5754
0.700	7.926	0.5696	0.5688
0.710	7.989	0.5630	0.5622
0.720	8.044	0.5564	0.5560
0.730	8.102	0.5497	0.5493
0.740	8.155	0.5431	0.5426
0.750	8.206	0.5365	0.5363
0.760	8.256	0.5299	0.5299
0.780	8.353	0.5166	0.5173
0.800	8.449	0.5034	0.5043
0.820	8.546	0.4903	0.4912

---

a Ionic strength = 0.1 M, T 25°C, moles H^+ added = 2.459×10^{-4}, [TL] = 4.236×10^{-3} M, [TM] = 8.072×10^{-4} M, Total vol = 136.000 ml

b Cumulative volume of 1.064 M KOH added

c Hydrogen ion concentration obtained from calibration equation (see Chapter 3)

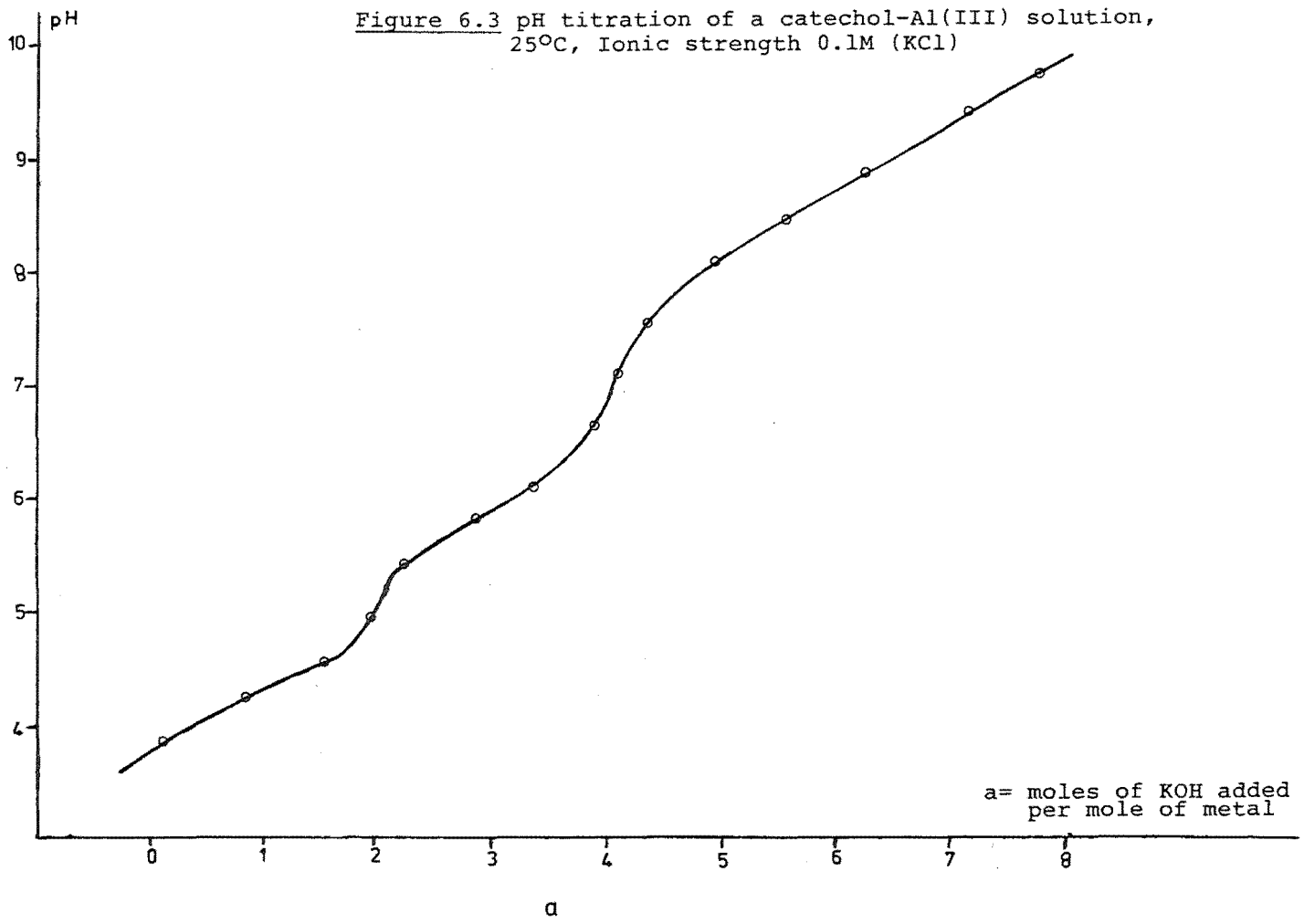

Figure 6.3 pH titration of a catechol-Al(III) solution, 25°C, Ionic strength 0.1M (KCl)

No distinct end point was observed above a pH of 7.5 because of the buffering effect of the excess ligand (log K_{012} 9.2). However spectrophotometric measurements confirmed the formation of AlL_3,

$$Al(LH_{r-2})_2 + LH_r \rightleftharpoons Al(LH_{r-2})_3 + 2H$$

$$'K_{13(3r-6)} = [Al(LH_{r-2})_3][H]^2 / [Al(LH_{r-2})_2][LH_r] \qquad (6.13)$$

Use of equations (6.11) to (6.13) for the equilibrium model resulted in the least squares refinement giving a "poor" fit in the second buffer region (pH c. 5.5 - 6.5) and in the third buffer region (pH > 7.5); i.e. large residuals were observed. The inclusion of reaction (6.14)

$$Al(LH_{r-2}) + H_2O \rightleftharpoons Al(LH_{r-2})OH + H$$

$$'K_{11(r-3)} = [Al(LH_{r-2})OH][H]/[Al(LH_{r-2})] \qquad (6.14)$$

and reaction (6.15)

$$Al(LH_{r-2})_2 + H_2O \rightleftharpoons Al(LH_{r-2})_2OH + H$$

$$'K_{12(2r-5)} = [Al(LH_{r-2})_2OH][H] / [Al(LH_{r-2})_2] \qquad (6.15)$$

reduced the magnitude of the residuals to an acceptable value. The computer output for TH(obs) and TH(calc) is listed in Table 6.2. The R-factors for the least squares refinement on data sets of varying L/M ratios (5.4 - 7) ranged from 0.17 to 0.30; the resultant stability constants are presented in Table 6.3. Figure 6.4 represents the distribution of the Al(III)-ligand species as a function of pH (calculated from the stability constants in Table 6.3).

Al hydrolysis species included in the equilibrium model were those of Mesmer and Baes[147] (see Section 6.1.1). The Al(III) hydroxo species that contributed to the solution

Table 6.3 Stability constants for the formation of Al(III)-polyphenol Complexes

Reaction	Constant	Catechol (LH_2)	Protocatechuic acid (LH_2^-)	Catechin (LH_4)
$Al(III) + LH_{r-2} \leftrightharpoons AlLH_{r-2}$	$\log K_{11r-2}$	16.89 ± 0.03[a]	16.87 ± 0.02	17.10 ± 0.04
$AlLH_{r-2} + LH_{r-2} \leftrightharpoons Al(LH_{r-2})_2$	$\log K_{12(2_{r-4})}$	13.66 ± 0.01	13.01 ± 0.05	13.89 ± 0.02
$Al(LH_{r-2})_2 + LH_{r-2} \rightleftharpoons Al(LH_{r-2})_3$	$\log K_{13(3_{r-6})}$	8.98 ± 0.08	8.76 ± 0.05	9.93 ± 0.07
$Al(LH_{r-2}) + H_2O \rightleftharpoons Al(LH_{r-2})OH + H$	$\log {}'K_{11r-3}$	-6.07 ± 0.09	-5.77 ± 0.07	-5.98 ± 0.09
$Al(LH_{r-2})_{2+} H_2O \rightleftharpoons Al(LH_{r-2})_2OH + H$	$\log {}'K_{12(2_{r-5})}$	-8.10 ± 0.01	-8.39 ± 0.03	-8.22 ± 0.06
$Al(III) + LH_r \rightleftharpoons AlLH_r$	$\log {}'K_{11r}$		2.85 ± 0.15	
$AlLH_{r-2} + H \rightleftharpoons AlLH_{r-1}$	$\log {}'K_{1r-1}$		4.66 ± 0.10	

a mean ± standard deviation for at least 3 titrations.

Figure 6.4 Distribution of Al(III)-hydroxy and Al(III)-ligand complexes for Al(III)-polyphenol solutions

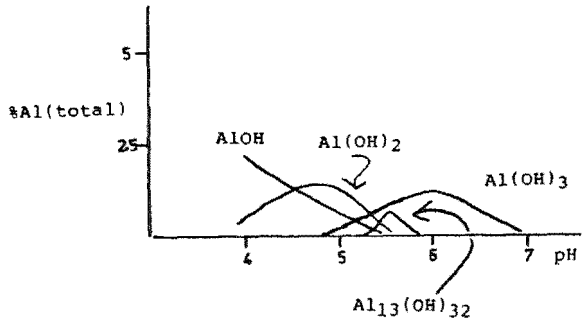

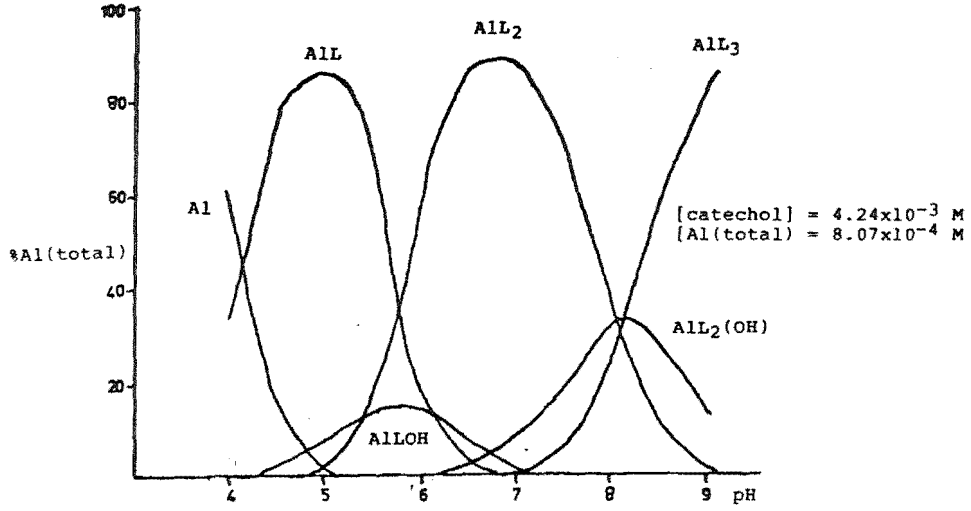

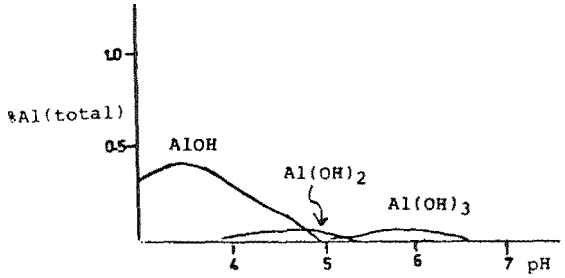

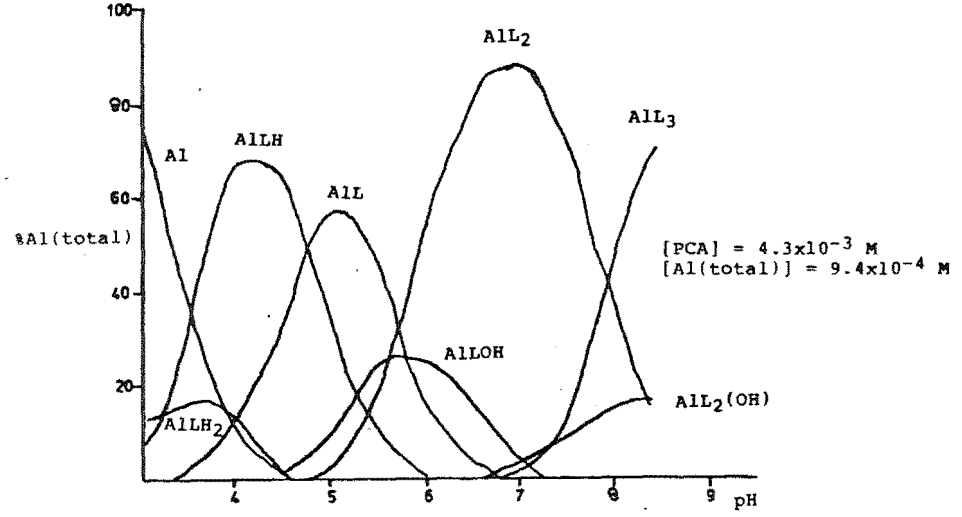

Figure 6.4 cont.

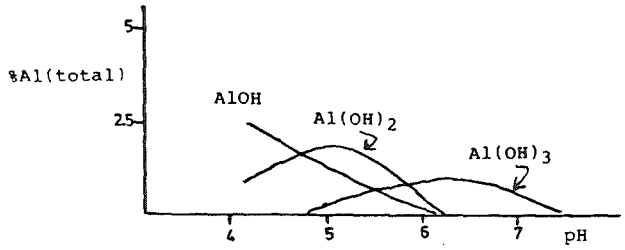

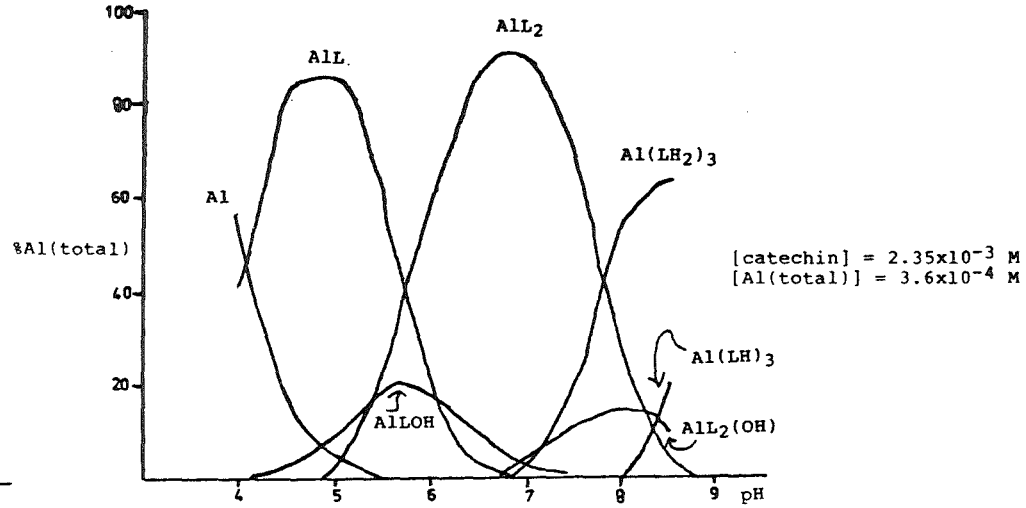

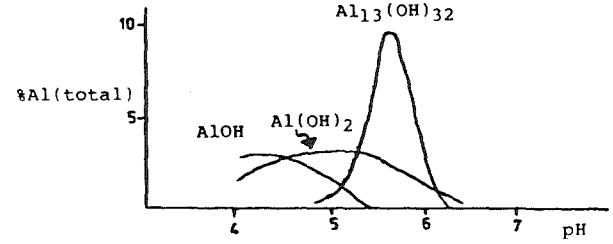

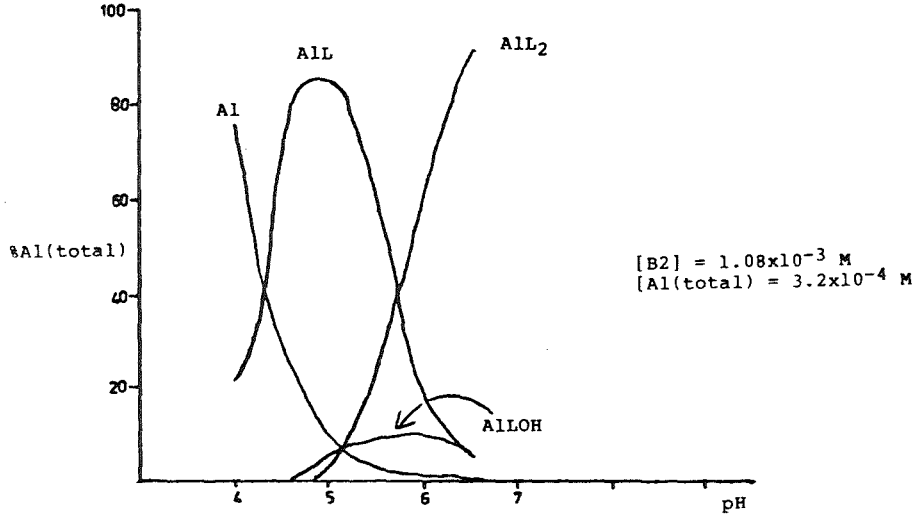

stoichiometry were AlOH, $Al(OH)_2$, $Al(OH)_3(aq)$ and $Al_{13}(OH)_{32}$. Figure 6.4 presents graphically the pH dependent concentrations of these hydroxy species as a percentage of total metal ion in a solution having L/M = 5. For each titration point the product -log $[Al(III)][OH]^3$ was calculated, the minimum numerical value was 30.9 at a pH of 5.8±0.4. A value of 30.4 is claculated for amorphous $Al(OH)_3$ at 25°C[151]. Hence it was inferred that no precipitation of aluminium occurred in the titrations performed.

Uncertainties in the standard solution stoichiometries ([KOH], [ligand], [Al(III)]), pH and titre measurements were applied to the respective input data for the least squares analysis. The resultant cumulative error in all log K values was c. ±0.08. The possible formation of polymeric Al(III)-ligand complexes with the same metal to ligand ratio as the monomeric species in reactions (6.11) and (6.12) was investigated by comparing titrations at different absolute concentrations but the same L/M ratio (TL = 4.0×10^{-3}, 8×10^{-4} M). The refined values of log K differed only by 0.03 and 0.02 for q = 1 and 2. If a di- or polymer species were forming (e.g. Al_2L_4) a doubling of the absolute concentration would favour complexing

$$2Al + 4L \rightleftharpoons Al_2L_4 \qquad (6.16)$$

and increase the apparent stability constant. Hence it was concluded that di- or polynuclear Al_nL_n complexes were not important.

Also the possible formation of di- and trimeric ternary species ($Al_2L_2(OH)_2$ and $Al_3L_3OH_3$) was investigated by

including these species in the equilibrium model. These polymeric species were however rejected in favour of the monomer AlLOH, described in reaction (6.14). This was because the latter species yielded a much better least squares fit.

6.4.2 Al(III)-protocatechuic acid (LH_2^-, r = 2)

Three titrations of KOH against oxygen free solutions of Al(III) (0.7 - 1.4x10^{-3} M) and ligand (3 - 7x10^{-3} M) were performed at varying L/M ratios (L/M > 4.3). These gave stable pH readings in well defined buffer regions; 56 - 122 pH-volume of titre data points were collected per titration. One titration curve is presented in Figure 6.5 and was generated from data listed in Table 6.4. The titration curve showed a single inflexion at pH 6 - 7 corresponding to completion of reactions (6.11) and (6.12) as well as deprotonation of the carboxyl group on coordinated and excess ligand. The deprotonation of the carboxyl group on excess ligand (pKa = 4.26) masked the end point corresponding to the completion of reaction (6.11). A shallow inflexion was noted at pH c. 9.3 for a non-integral value of a. This was ascribed to the completion of reaction (6.13) and to partial deprotonation from the phenolic functional groups on excess protocatechuic acid (reaction (5.2)). Hence this end point could not be assigned definitively to the completion of the above reactions.

The best least square fit was obtained for the equilibrium model described for catechol, plus reaction (6.17) for the protonation of the aluminium ligand mono complex

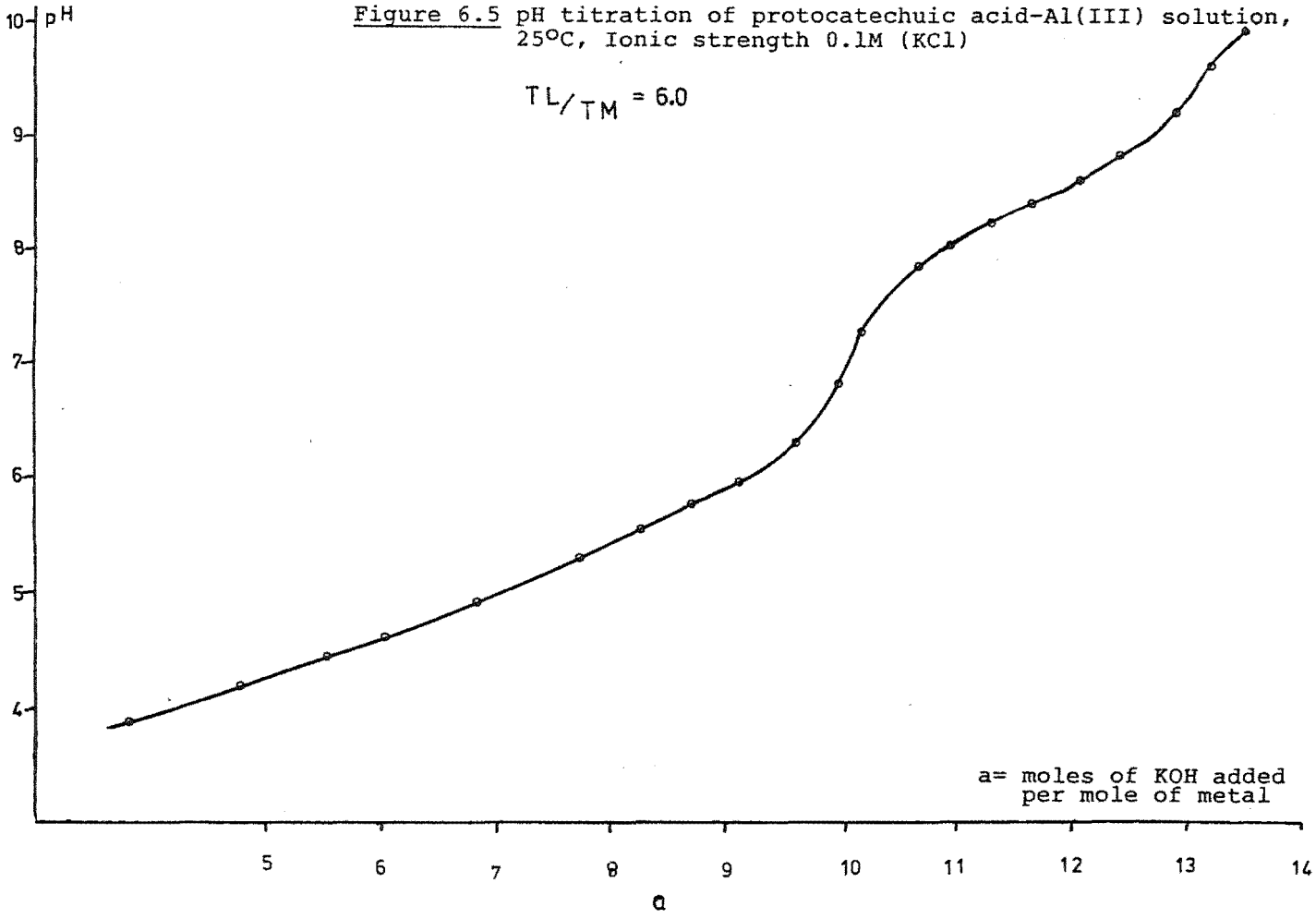

Figure 6.5 pH titration of protocatechuic acid-Al(III) solution, 25°C, Ionic strength 0.1M (KCl)

$TL/_{TM} = 6.0$

Table 6.4 Representative data from a titration of a protocatechuic acid-aluminium solution with standard KOH[a]

titre (ml)[b]	pH[c]	TH(obs)x10^2	TH(calc)x10^2
0.060	3.030	0.1326	0.1330
0.070	3.058	0.1317	0.1320
0.080	3.115	0.1299	0.1300
0.090	3.143	0.1290	0.1290
0.110	3.172	0.1281	0.1280
0.120	3.229	0.1263	0.1261
0.130	3.256	0.1254	0.1252
0.150	3.309	0.1236	0.1233
0.160	3.335	0.1227	0.1225
0.180	3.361	0.1218	0.1216
0.190	3.413	0.1200	0.1198
0.200	3.466	0.1183	0.1180
0.220	3.516	0.1165	0.1163
0.240	3.565	0.1147	0.1146
0.260	3.615	0.1129	0.1127
0.280	3.667	0.1111	0.1111
0.300	3.717	0.1093	0.1094
0.320	3.768	0.1075	0.1077
0.340	3.821	0.1057	0.1059
0.360	3.875	0.1040	0.1042
0.380	3.930	0.1022	0.1024
0.400	3.987	0.1004	0.1006
0.420	4.054	0.9861	0.9883
0.460	4.104	0.9683	0.9701
0.480	4.164	0.9505	0.9519
0.500	4.224	0.9327	0.9340
0.520	4.287	0.9149	0.9158
0.540	4.351	0.8971	0.8969
0.560	4.414	0.8793	0.8790
0.580	4.482	0.8615	0.8601
0.600	4.549	0.8437	0.8421
0.620	4.617	0.8259	0.8244
0.640	4.689	0.8081	0.8062
0.660	4.762	0.7903	0.7886
0.680	4.839	0.7726	0.7708
0.700	4.917	0.7548	0.7535
0.720	4.998	0.7371	0.7361
0.740	5.065	0.7193	0.7222
0.760	5.165	0.7016	0.7017
0.780	5.250	0.6838	0.6844
0.800	5.335	0.6661	0.6668
0.820	5.420	0.6484	0.6491
0.840	5.508	0.6306	0.6316
0.860	5.594	0.6129	0.6139
0.880	5.686	0.5952	0.5951
0.900	5.781	0.5775	0.5773

Table 6.4 (continued)

0.920	5.885	0.5598	0.5591
0.940	5.941	0.5509	0.5505
0.950	6.001	0.5421	0.5420
0.960	6.068	0.5332	0.5330
0.970	6.148	0.5244	0.5240
0.980	6.236	0.5155	0.5155
0.990	6.348	0.5067	0.5063
1.000	6.476	0.4978	0.4983
1.010	6.666	0.4890	0.4892
1.020	6.891	0.4802	0.4802
1.030	7.082	0.4713	0.4717
1.040	7.231	0.4625	0.4625
1.050	7.340	0.4537	0.4538
1.060	7.432	0.4448	0.4447
1.070	7.508	0.4360	0.4356
1.080	7.571	0.4272	0.4270
1.090	7.630	0.4184	0.4180
1.100	7.682	0.4095	0.4092
1.110	7.732	0.4007	0.4004
1.120	7.779	0.3919	0.3918
1.130	7.847	0.3787	0.3789
1.145	7.913	0.3655	0.3657
1.160	7.959	0.3567	0.3568
1.170	8.026	0.3434	0.3436
1.185	8.049	0.3390	0.3392
1.190	8.072	0.3346	0.3348
1.195	8.094	0.3302	0.3307
1.200	8.118	0.3258	0.3261
1.210	8.142	0.3214	0.3217

a Ionic strength = 0.1 M, T 25°C, moles H^+ added = 1.012×10^{-4}, [TL] = 4.982×10^{-3} M, [TM] = 8.295×10^{-4} M, Total vol = 138.000 ml

b Cumulative volume of 1.224 M KOH added

c Hydrogen ion concentration obtained from calibration equation (see Chapter 3)

$$AlLH_{r-2} + H \rightleftharpoons AlLH_{r-1}$$

$$'K_{11r-1} = [Al(LH_{r-1})]/[AlLH_{r-2}][H] \qquad (6.17)$$

and reaction (6.18) the formation of a carboxylate complex.

$$Al + LH_r \rightleftharpoons Al(LH_r)$$

$$'K_{11r} = [Al(LH_r)]/[Al][LH_r] \qquad (6.18)$$

This latter reaction was important at pH values less than 4. The stability constants obtained for this scheme from least squares analysis of potentiometric data are presented in Table 6.3. Figure 6.4 represents the distribution of the Al(III)-ligand species as a function of pH (calculated from the stability constants in Table 6.3). The R-factors for the least squares refinement ranged from 0.18 - 0.26%. The major Al(III) hydroxo species were $Al(OH)_2$ and $Al(OH)_3(aq)$ (see Figure 6.4).

For each titration point the product $-\log [Al(III)][OH]^3$ was calculated; the minimum numerical value was 31.4 at pH c. 5.7.

6.4.3 Al(III)-catechin (LH_4, r = 4)

Three titrations of KOH against oxygen free solutions of Al(III) ($3 - 4 \times 10^{-4}$ M) and ligand ($2 - 3 \times 10^{-3}$ M) were performed at varying L/M ratios. These gave stable pH readings in well defined buffer regions; 92 - 95 pH-volume of titre points were collected per titration. One such titration is presented in Figure 6.6 and was generated from the data listed in Table 6.5. Stoichiometric end points were observed for catechin at pH 5 and 7 (see Figure 6.6). These inflexions corresponded to the completion of reactions (6.11) and (6.12) respectively.

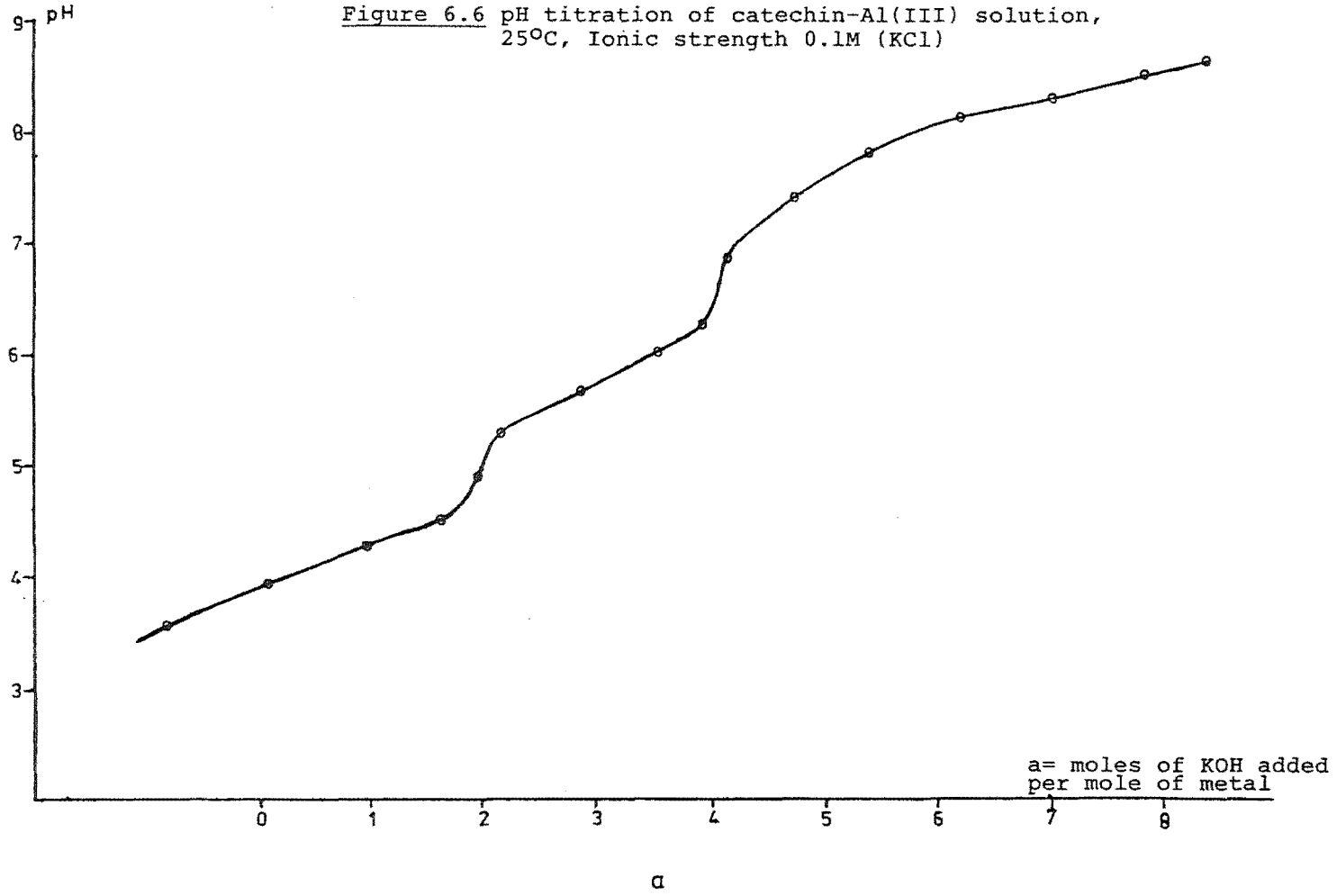

Figure 6.6 pH titration of catechin-Al(III) solution, 25°C, Ionic strength 0.1M (KCl)

Table 6.5 Representative data from a titration of a catechin-aluminium solution with standard KOH[a]

titre (ml)[b]	pH[c]	TH(obs)x10^2	TH(calc)x10^2
1.380	4.046	0.914	0.915
1.400	4.102	0.908	0.909
1.410	4.133	0.906	0.906
1.420	4.162	0.903	0.903
1.430	4.189	0.900	0.900
1.440	4.218	0.897	0.898
1.450	4.248	0.895	0.895
1.460	4.282	0.892	0.892
1.470	4.316	0.889	0.889
1.480	4.355	0.886	0.886
1.490	4.394	0.884	0.883
1.500	4.438	0.881	0.880
1.510	4.491	0.878	0.877
1.520	4.548	0.875	0.874
1.530	4.612	0.873	0.872
1.540	4.688	0.870	0.869
1.550	4.776	0.867	0.866
1.560	4.881	0.864	0.863
1.565	4.935	0.863	0.862
1.570	4.987	0.862	0.861
1.575	5.034	0.860	0.860
1.580	5.078	0.859	0.858
1.585	5.121	0.858	0.857
1.590	5.157	0.856	0.856
1.595	5.193	0.855	0.856
1.600	5.226	0.853	0.855
1.605	5.253	0.852	0.854
1.610	5.286	0.851	0.851
1.620	5.337	0.848	0.849
1.630	5.383	0.845	0.846
1.640	5.426	0.843	0.844
1.650	5.466	0.840	0.842
1.660	5.505	0.837	0.841
1.670	5.543	0.834	0.839
1.680	5.580	0.832	0.837
1.690	5.618	0.829	0.834
1.700	5.655	0.826	0.832
1.710	5.693	0.823	0.830
1.720	5.729	0.821	0.827
1.730	5.766	0.818	0.825
1.740	5.806	0.815	0.823
1.760	5.890	0.810	0.817
1.770	5.937	0.807	0.814
1.780	5.987	0.804	0.812
1.790	6.043	0.802	0.808

Table 6.5 (continued)

1.800	6.109	0.799	0.804
1.810	6.190	0.796	0.800
1.815	6.237	0.795	0.798
1.820	6.287	0.793	0.796
1.825	6.344	0.792	0.794
1.830	6.409	0.791	0.792
1.840	6.568	0.788	0.789
1.845	6.661	0.787	0.787
1.850	6.751	0.785	0.786
1.855	6.841	0.784	0.785
1.860	6.910	0.783	0.784
1.865	6.973	0.781	0.782
1.870	7.034	0.780	0.781
1.875	7.084	0.779	0.780
1.880	7.129	0.777	0.778
1.890	7.208	0.774	0.776
1.900	7.276	0.772	0.773
1.910	7.336	0.769	0.770
1.920	7.386	0.766	0.768
1.930	7.431	0.764	0.766
1.940	7.472	0.761	0.762
1.950	7.509	0.758	0.759
1.960	7.546	0.756	0.756
1.970	7.578	0.753	0.753
1.980	7.609	0.750	0.751
1.990	7.640	0.747	0.749
2.000	7.669	0.745	0.747
2.010	7.697	0.742	0.744
2.020	7.724	0.739	0.741
2.040	7.773	0.734	0.736
2.060	7.821	0.729	0.731
2.080	7.867	0.723	0.724
2.100	7.911	0.718	0.721
2.120	7.955	0.713	0.717
2.140	7.995	0.707	0.712
2.160	8.035	0.702	0.708
2.180	8.075	0.696	0.703
2.200	8.114	0.691	0.698
2.220	8.153	0.686	0.695
2.240	8.190	0.680	0.688
2.260	8.227	0.675	0.682
2.280	8.263	0.670	0.677
2.300	8.299	0.665	0.671
2.320	8.335	0.659	0.666

Table 6.5 (continued)

2.370	8.421	0.646	0.650
2.400	8.469	0.638	0.639

a Ionic strength = 0.1 M, T 25°C, moles H^+ added = 1.773×10^{-4}, [TL] = 2.347×10^{-3} M, [TM] = 3.592×10^{-4} M, Total vol = 51.900 ml

b Cumulative volume of 0.1384 M KOH added

c Hydrogen ion concentration obtained from calibration equation (see Chapter 3)

The best least squares fit was obtained for the equilibrium model described for catechol plus equilibria (6.19) and (6.20) which modelled the deprotonation of catechin's A ring (pKa = 8.6, Chapter 5) above a pH of c. 7.5.

$$Al(LH_2)_2 \rightleftharpoons Al(LH)_2 + 2H$$

$$'K_{122} = [Al(LH)_2][H]^2/[Al(LH_2)_2] \qquad (6.19)$$

$$Al(LH_2)_3 \rightleftharpoons Al(LH)_3 + 3H$$

$$'K_{133} = [Al(LH)_3][H]^3/[Al(LH_2)_3] \qquad (6.20)$$

The pKa value for the free ligand (8.6) was assumed to be valid for proton dissociation from the coordinated ligand. The complex species $Al(LH)_2$ formed in negligible concentration (< 1%) whereas $Al(LH)_3$ was the dominant complex at pH > 8.6.

The stability constants obtained are listed in Table 6.3. Figure 6.4 represents the distribution of the Al(III)-ligand species as a function of pH (calculated from the stability constants in Table 6.3). The R-factors for the least squares refinement ranged from 0.33 to 0.41%. The major Al(III)-hydroxo species were Al(OH), $Al(OH)_2$ and $Al(OH)_3$(aq) (see Figure 6.4).

For each titration point the product $-\log [Al(III)][OH]^3$ was calculated; the minimum numerical value was 31.0 at pH c. 5.7.

6.4.4 Al(III)-B2 (epicatechin dimer, $(LH_4)_2$)

Data from a potentiometric titration of KOH against an oxygen free solution of Al(III) ($1x10^{-3}$ M) and B2 ($3.2x10^{-3}$ M) are listed in Table 6.6 (55 pH-volume of titre data points, pH range 3.5 - 6.5). The titration curve

Table 6.6 Representative data from a titration of a B2-aluminium solution with standard KOH[a]

titre (ml)[b]	p[H][c]	TH(obs)x10^2	TH(calc)x10^2
0.000	3.373	0.4726	0.4728
0.050	3.528	0.4533	0.4583
0.100	3.739	0.4396	0.4430
0.130	3.877	0.4314	0.4336
0.140	3.919	0.4286	0.4307
0.150	3.962	0.4259	0.4276
0.160	4.005	0.4232	0.4245
0.170	4.046	0.4205	0.4213
0.180	4.085	0.4177	0.4182
0.190	4.124	0.4150	0.4151
0.200	4.160	0.4123	0.4122
0.210	4.195	0.4095	0.4093
0.220	4.232	0.4068	0.4062
0.230	4.264	0.4041	0.4036
0.240	4.296	0.4014	0.4009
0.250	4.330	0.3986	0.3982
0.260	4.366	0.3959	0.3953
0.270	4.403	0.3932	0.3925
0.280	4.441	0.3905	0.3897
0.290	4.476	0.3878	0.3871
0.300	4.518	0.3850	0.3844
0.310	4.561	0.3823	0.3818
0.320	4.606	0.3796	0.3792
0.330	4.654	0.3769	0.3767
0.340	4.705	0.3742	0.3742
0.350	4.764	0.3715	0.3718
0.355	4.799	0.3701	0.3703
0.360	4.837	0.3688	0.3690
0.365	4.875	0.3674	0.3677
0.370	4.913	0.3661	0.3664
0.375	4.955	0.3647	0.3651
0.380	4.993	0.3633	0.3640
0.385	5.032	0.3620	0.3628
0.390	5.072	0.3606	0.3616
0.395	5.110	0.3593	0.3605
0.400	5.145	0.3579	0.3594
0.410	5.211	0.3552	0.3570
0.420	5.262	0.3525	0.3553
0.430	5.315	0.3498	0.3533
0.440	5.373	0.3471	0.3507
0.450	5.427	0.3444	0.3483
0.460	5.488	0.3417	0.3454
0.470	5.549	0.3390	0.3424
0.480	5.608	0.3363	0.3392
0.490	5.668	0.3332	0.3339

Table 6.6 (continued)

0.500	5.739	0.3309	0.3316
0.510	5.810	0.3282	0.3273
0.520	5.884	0.3255	0.3230
0.530	5.960	0.3228	0.3185
0.540	6.043	0.3201	0.3134
0.550	6.134	0.3175	0.3095
0.560	6.232	0.3148	0.3063
0.570	6.355	0.3121	0.3034
0.580	6.496	0.3094	0.3013
0.585	6.565	0.3081	0.3008

a Ionic strength = 0.1 M, T 25°C, moles H^+ added = 1.830×10^{-5}, [TL] = 1.079×10^{-3} M, [TM] = 3.221×10^{-4} M, Total vol = 51.664 ml

b Cumulative volume of 0.1384 M KOH added

c Hydrogen ion concentration obtained from calibration equation (see Chapter 3)

(Figure 6.7), generated from the data in Table 6.6, showed a slight inflexion at pH 5 and a distinct inflexion at pH 7 corresponding to the quantitative formation of $Al(LH_2)$ (reaction (6.11)) and $Al(LH_2)_2$ (reaction (6.12)).

Curve (b) in Figure 6.7 represents a titration of KOH against an Al(III)-catechin solution of similar B ring/Al(III) ratio. By comparing the buffer regions of these two titration curves it was inferred that the mono and bis species of B2 and catechin were of similar stability (assuming the pKas for deprotonation of both ligands are similar). The third buffer regions for B2 and catechin at pH > 7.4 were separated by 0.5 pH units at a = 6, which indicated that the tris complexes with these ligands are of different stability.

The similar shape of the B2 and catechin titration curves and the similar pH regions in which the mono and bis species form imply that the B2 ligand maybe acting as a monofunctional bidentate donor towards Al(III) below a pH of 7.

The most acidic phenol group on the B2 molecule has a pKa of 8.65 (Chapter 5); therefore, to a first approximation below pH of 6.5 the free ligand (B2) will not be deprotonated. Therefore it was possible to analyse the potentiometric data listed in Table 6.6 by a non-linear least squares calculation with subroutines written containing proton dependent variable parameters for formation of AlL, AlLOH and AlL_2 (viz. reactions (6.11), (6.14) and (6.12). These calculations do not require a knowledge of the protonation constants for a particular

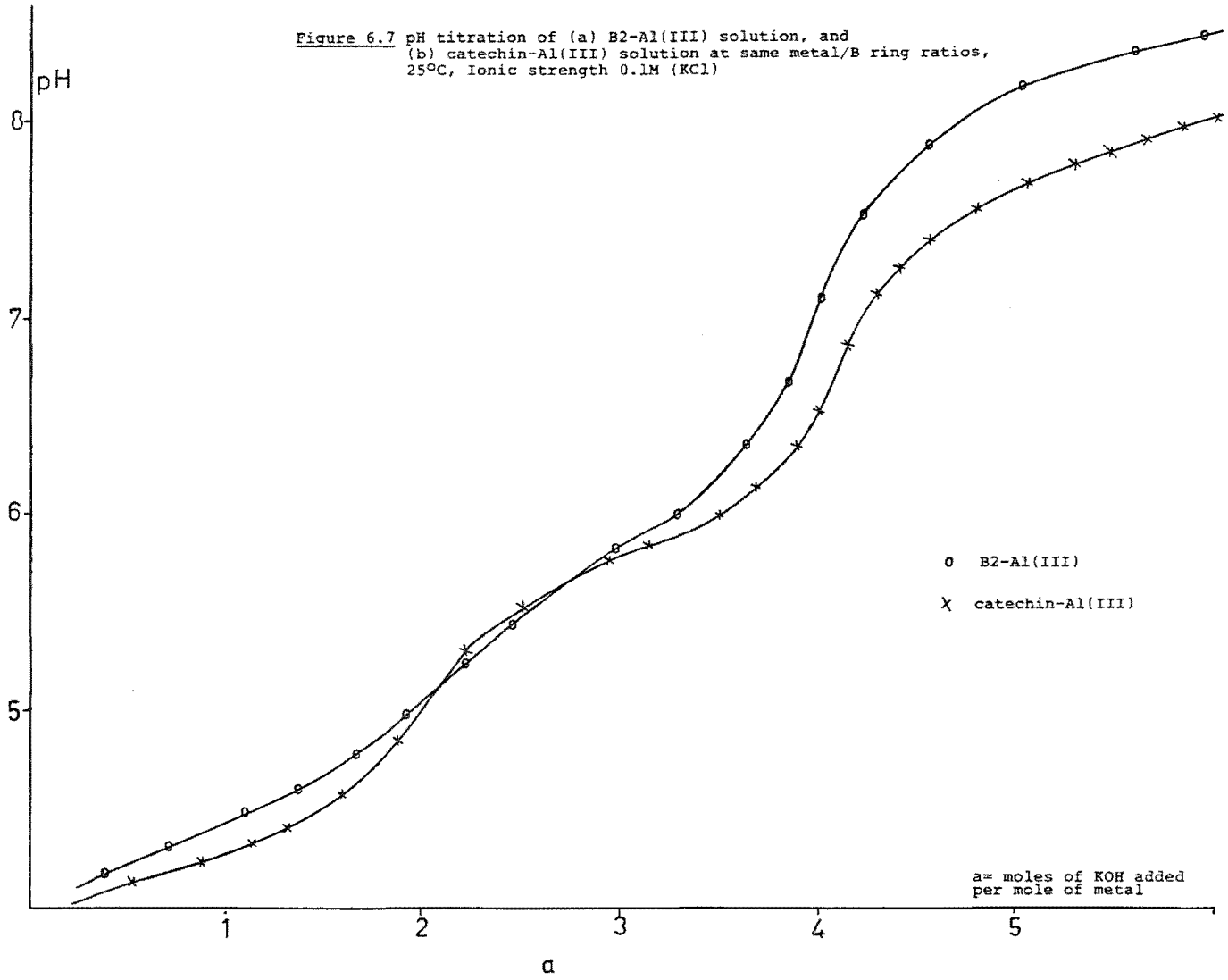

Figure 6.7 pH titration of (a) B2-Al(III) solution, and (b) catechin-Al(III) solution at same metal/B ring ratios, 25°C, Ionic strength 0.1M (KCl)

ligand. The value of the refined parameters for B2-Al complexing are compared with those for catechin in Table 6.7. Figure 6.4 represents the distribution of the Al(III)-ligand species as a function of pH (calculated from the stability constants in Table 6.7). The R-factor for this refinement was 0.86%.

The major Al(III) hydroxo species were AlOH, $Al(OH)_2$ and $Al_{13}(OH)_{32}$ (see Figure 6.4).

For each titration point the product $-\log [AL(III)][OH]^3$ was calculated; the minimum numerical value was 30.65 at pH c. 6.0.

6.5 Discussion

a) Reported stability constants.

Stability constants obtained in this work may be compared with the values reported by other workers, as given in Table 6.8. Only the most recent study by Ohman[142,159-162] considers the hydrolysis reactions of the hydrated aluminium ion and the possible formation of ternary metal ligand hydroxy complexes e.g. AlLOH.

Havelkova et al.[139] employed a catechol/Al(III) ratio greater than 50 which is considered too large to permit accurate calculation of metal complex concentrations in the ligand proton buffer region.

Goina et al.[163] used moderately high L/M ratios of 10 and 15 and collected insufficient data above pH 7 to permit accurate determination of the stability constant for Al(III) tris catecholate species.

Table 6.7 Proton dependent stability constants for the formation of Al(III)-polyphenol complexes

Reaction	constant	Catechol (LH_2)	Catechin (LH_4)	B_2[a] (LH_4)$_2$
$Al(III) + LH_r \rightleftharpoons AlLH_{r-2} + 2H$	log $'K_{1\,r-2}$	-5.80 ± .03[b]	-5.58 ± 0.04[b]	-5.54 ± 0.03[c]
$AlLH_{r-2} + LH_r \rightleftharpoons Al(LH_{r-2})_2 + 2H$	log $'K_{12(2_{r-4})}$	-9.03 ± 0.01	-8.79 ± 0.02	-8.40 ± 0.02
$AlLH_{r-2} + H_2O \rightleftharpoons Al(LH_{r-2})OH + H$	log $'K_{11r-3}$	-6.07 ± 0.09	-5.98 ± 0.09	-6.13 ± 0.08

a assuming only one B ring is involved in complexing.

b mean ± standard deviation for at least 3 titrations.

c mean ± standard deviation calculated in non-linear least squares refinement.

Table 6.8 Reported stability constants for Al(III)-polyphenol complexes

Ligand	log K_{11r-2}	log $K_{12(2_{r-2})}$	log $K_{13(3_{r-6})}$	log $'K_{33(3_{r-3})}$	log $'K_{12(2_{r-5})}$	Electrolyte(T°C)	Ref.
Catechol	16.9	13.6	8.9	-	-	0.1M KNO_3 (20°)	139
	15.30	11.63	-	-	-	- (30°)	164
	16.3	13.5	9.0	-	-	0.2M KCl (-)	163
	16.56	15.6	13.65	-	-	0.2M KNO_3 (25°)	140
	16.36[a]	13.59	9.51	-29.91[b]	-8.01	0.6M NaCl (25)	142
	16.89	13.66	8.98	-	-8.10	0.1M KCl (25)	this work
Protocatechuic acid	17.8	12.35	-	-	-	- (30)	164
	16.87	13.01	8.76	-	-8.39	0.1M KCl (25)	this work

a using protonation constants from this work.

b written as $3Al + 3H_2L \leftrightharpoons Al_3L_3OH_3 + 9H$

Dubey and Mehrotra[140] have reported values of log K_{130} which bear no relationship to their published titration curves for catechol Al(III) titrations.

Jejurkar et al.[164] studied protocatechuic acid complexes but reported no titration curves and an accuracy of ± 0.05 for all pH measurements which must cast suspicion on the accuracy of their constants for the formation of mono and bis complexes.

Havelkova[139], Goina[163] and Jejurkar[164] employed graphical techniques in the determination of Al-ligand stability constants; these are considered inferior to the least squares method of analysis.

Furthermore, procedures for the rigorous exclusion of oxygen have not been mentioned by any of these workers and each group has used different protonation constants in the evaluation of the ligand metal stability constants.

b) Ternary complexes.

In the present study the ternary complexes $Al(LH_{r-2})OH$ and $Al(LH_{r-2})_2OH$ were included in the equilibrium model for all ligand-metal titrations because their presence reduced the large residuals in the second and third buffer regions to an acceptable magnitude. The R-factors for all titrations were then reduced, indicating a better overall fit of calculated data to observed data. The refined constant for the hydrolysis of the AlL species (log $'K_{11r-1}$) has a sensible value for all three ligands; that is in weakly acid solution the mono complex is not as extensively hydrolyzed as the more highly charged hexaquo Al(III) ion (log $'K_{11r-1} > \log \beta_{10-1}$). Further, AlL_2 formation occurs in

the pH range for hydrolysis of Al(OH) (reaction (6.2)). On this basis also AlLOH is a likely species.

However until recently, and at the time when the present calculations were completed, these ternary aluminium-ligand-hydroxy species had only been postulated for ligands such as citrate[165] and NTA[124].

Ohman et al.[142,159,161] reported recently that inclusion of monomeric and polymeric ternary species reduced the magnitude of the residuals obtained in certain pH ranges for a series of Al(III)-ligand systems (L = catechol, 1,2-dihydroxynaphthalene-4-sulfonate and gallic acid). In the study of Aluminium- 1,2-dihydroxynaphthalene-4-sulfonate complexes the inclusion of AlLOH and AlL_2OH species was considered to give the best fit of calculated data to observed data (along with mono, bis and tris species). In contrast, for the Al(III) catechol system, $Al_3L_3OH_3$ and AlL_2OH were considered to best represent the ternary species formed during a titration. Data obtained in the present study do not support the inclusion of di- or trimeric ternary species. When $Al_nL_n(OH)_n$ (n = 2, 3) was included in the equilibrium model for Al(III)-ligand interactions the bad regions of fit removed by inclusion of AlLOH returned, indicating that the monomeric ternary complex was the most appropriate species.

In contrast to the above, in a study of the Al(III)-gallic acid system Ohman et al.[159] postulated a polymeric complex $Al_3(OH)_4(H_2L)$ involving carboxylate coordination rather than species $Al_nL_nOH_n$ or AlL_2OH. Protocatechuic acid also contains a carboxylate group;

however it was found in the present study that potentiometric data were adequately explained by the equilibrium model derived for catechol with the inclusion of monomeric complexes associated with the carboxylate group (see Section 6.4.2). The program rejected polymeric species $Al_nL_n(OH)_n$.

c)Equilibrium models.

The assignment of stoichiometries for $AlLH_{r-2}$ and $Al(LH_{r-2})_2$ for different ligands was consistent with sharp end points in the titration curves at a = 2 and a = 4. For protocatechuic acid a shallow inflexion was noted past the second end point; it was ascribed to the formation of $Al(LH_{r-2})_3$ although partial deprotonation of the excess ligand prevented the assignment of an exact stoichiometry at this end point. For catechin and catechol an end point for the formation of $Al(LH_{r-2})_3$ was not observed because of the buffering action of excess ligand in the pH range where the tris end point occurred; viz. log K_{012} for protocatechuic acid is 8.6 whereas log K_{012} for catechol is 9.2 and log K_{014} and log K_{013} for catechin are 8.6 and 9.2 respectively.

It was considered necessary to establish that the third buffer zone (pH > 7) arose from the formation of AlL_3 and not from an hydroxy species of the same proton count (e.g. $AlL_2(OH)_2$). The existence of $Al(LH_{r-2})_3$ was inferred from the known formation of the analogous iron(III) complexes (see Section 6.2). Direct evidence for the formation of $Al(LH_{r-2})_3$ was obtained from the changes in the ultraviolet spectrum of catechol on the addition of Al(III)

at constant pH (9.1). The absorption maximum shifted from 280 to 290 nm and increased in intensity. This was consistent with ligand deprotonation (see Chapter 5) and therefore coordination. A molar ratio[166] plot confirmed the formation of $Al(LH_{r-2})_3$.

The possible formation of binary polynuclear complexes (e.g. $Al_2(LH_{r-2})_2$) was examined by comparison of catechol-Al(III) titrations at the same ligand/metal ratio but at increased absolute concentrations (see Section 6.4.1). The log K values obtained from a least squares analysis on the pH-volume of titre data differed by less than the error on the respective parameters. Therefore polynuclear binary species were considered to be unimportant for the catechol system and it was inferred that this was the case for the other ligands studied.

Protocatechuic acid differed from the other ligands because of its carboxylate function. The complex AlL formed in a pH range (< 5) where the carboxyl group is only partially deprotonated; therefore it was necessary to include a protonated complex species in the equilibrium models (viz. AlLH). The log $'K_{111}$ value derived for the protonation of AlL (4.65) is greater than that for carboxylate protonation of the free ligand, log K_{013} = 4.26. This can be explained in terms of the electron donating properties of the two O^- groups attached to the aromatic ring. The attachment of an $Al(H_2O)_4^{3+}$ unit via complexing leaves these groups more electron donating than two phenolic OH groups (i.e. log $'K_{111}$ > log K_{013}). A similar result was obtained for the analogous gallic acid complex[159].

Bis protonated species (viz. AlL(LH) and $Al(LH)_2$) were considered for protocatechuic acid; they were accepted in the least squares analysis but were rejected from the equilibrium model because the log K value derived for their carboxyl deprotonation was unacceptably high at c. 5.5. However it was necessary to include a monodentate carboxylate complex ($AlLH_2$) in the equilibrium model to obtain an adequate refinement at pH < 4.0. The log $'K_{112}$ value obtained for the formation of this complex is similar to that reported for formation of the Al(III) benzoate complex AlL (3.18)[167] and the monocarboxylate complex $AlLH_2$ formed with citric acid (2.62)[165].

The Al(III)-gallic acid system has recently been studied by Ohman and Sjoberg[159], working at L/M ratios ranging from 3 to 25. A proposed monomeric equilibrium model consisting of AlL, AlLH, AlL(LH) and AlL_2 explained the experimental data except in the pH region 4 - 7 where deviations between (TH) "observed" and "calculated" occurred. By varying the equilibrium constants individually it was found that the parameter for AlL(LH) depended on the L/M ratio; this was taken to imply the formation of polynuclear species. A search for ternary $Al_pL_qH_r$ complexes led to the formulation $Al_2L_2(LH)$. Further investigation yielded species Al_2L_3, $Al_2(OH)L_3$ and $Al_2(OH)_2L_3$ which when included in the model gave a minimum error square sum. The inclusion of all these complexes did not however lead to an improvement in σ(Zc), where (Zc) is the average number of OH reacted per mole of ligand.

In this work, the bad fit between pH 4 and 7 was removed when the simple species AlLOH was included in the equilibrium model for each of the three ligands investigated.

Titration of solutions with L/M ratios of 4.3 or greater for protocatechuic acid and 5.0 or greater for catechol and catechin resulted in negligible concentrations of Al(III) hydrolysis products. These titrations were reproducible and exhibited minimum drift in well defined buffer regions, and sharp end points. The catechol system had the largest concentration of Al(III) hydrolysis species, including the polymer $Al_{13}(OH)_{32}$ (see Figure 6.4), and the lowest value of -log $[Al(III)][OH]^3$. Catechin, then protocatechuic acid had progressively smaller contributions from hydrolysis products and the lowest value of the concentration quotient increased to 31.0 and 31.4 respectively. The existence of $Al_{13}(OH)_{32}$ in the aluminium-catechol system can be explained in terms of the higher pH at which catechol complexes. The increasing value of -log $'K_i$ for the proton displacement reactions (6.11) and (6.12) for protocatechuic acid, catechin and catechol (viz. 4.93, 5.58, 5.82 for i = 1 and 8.82, 8.85, 8.99 for i = 2), and of -log $'K_{11r-3}$, respectively means that the mono, bis and $Al(LH_{r-2})(OH)$ complexes form at lowest pH for protocatechuic acid and highest pH for catechol. This follows from the lower dianion basicity of protocatechuic acid. The equilibrium reaction for $Al_{13}(OH)_{32}$ formation has the term $[H]^{32}$ in the formation constant expression (6.7) and therefore the complexing of Al(III) by catechol at even

slightly higher pH values will markedly affect the resultant formation of this polymeric species.

The catechin complexes (mono, bis and tris) have larger stability constants than the respective catechol species despite the similar basicity of the 1,2-diphenolate groups in the two ligands. It is inferred that the benzopyran substituent in the C(4)-position of the coordinated 1,2-diphenolate anion in catechin will significantly disrupt the secondary hydration sphere about the aluminium ion; this desolvation would contribute to a more positive entropy change for catechin, and thus a higher stability.

d) Complexing reactions of B2.

The B2-Al(III) titration curve was similar to that for the catechin-Al(III) system for the first two buffer regions. This indicates that below a pH of 7 the dimer is probably complexing in a similar manner to catechin; e.g. the Al(III) bis species is formed from two B2 molecules each contributing only one B ring. This is exhibited diagrammatically in Figure 6.8. The similar values of the computed proton dependent constants for the respective mono and bis species support the above inference. Further, studies with molecular models of B2 indicate that strain-free tetradenate coordination to Al(III) is not possible although tridentate coordination would be feasible.

Further comparison of the titration curves for B2 and catechin indicates a distinct difference above pH 7; that is the third buffer regions were separated by c. 0.5 pH units. Part of this difference may be related to the fact that the

Figure 6.8 Possible coordination modes of B2

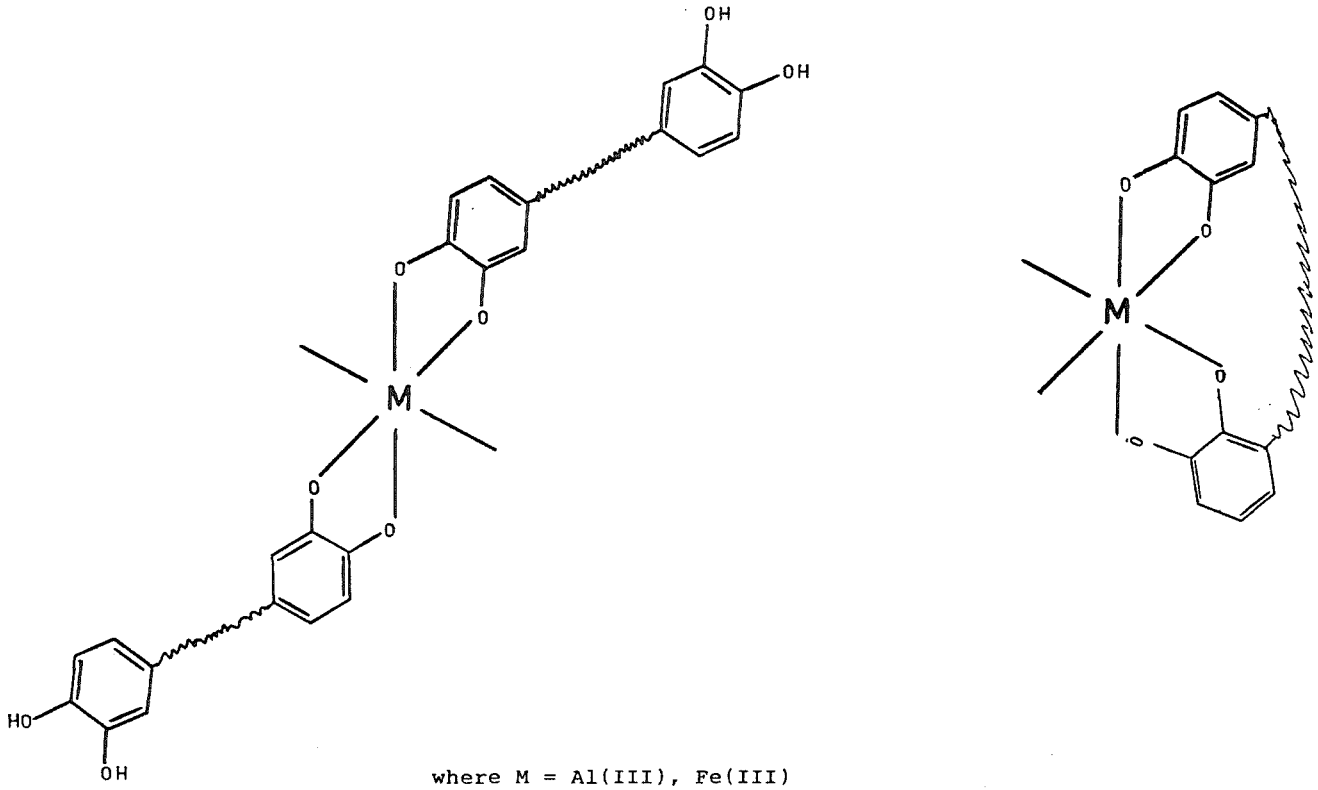

where M = Al(III), Fe(III)
~~~ implies two linked (C(4)-C(8)) benzopyran units
~~~

phenolic groups on the A ring of B2 are on average less acidic than those of catechin (both of which are in excess). However it is also predicted (from molecular model studies) that the steric effects of two coordinated B2 molecules may hinder the coordination of a third, resulting in a lower stability for the $Al(B2)_3$ complex. Hence the buffer region for this equilibrium would be located at higher pH.

CHAPTER 7

INTERACTIONS OF IRON(II) AND IRON(III) WITH POLYPHENOLS

The reactions of iron(III) with simple polyphenols (e.g. catechol) and large organic polymers containing catecholate and carboxylate functional groups (e.g. fulvic acid) have been studied.

Because the quinones of many polyphenols have reduction potentials that are similar in magnitude to the Fe^{3+}/Fe^{2+} couple (E^o = 0.749 V[168]) the phenols may participate in the redox reaction

$$2Fe(III) + LH_2 \rightleftharpoons 2Fe(II) + qno + 2H \qquad (7.1)$$

where qno is the o-quinone oxidation product of the polyphenol LH_2 (e.g. catechol E^o(qno) = 0.792 V[169]). This reaction is important because it can solubilize iron(III) by conversion to iron(II) in natural systems. However it will also destroy the strong complexing ability of 1,2-dihydroxybenzenes (e.g. tiron E^o(qno) = 0.955 V[169] a polyphenol which is not oxidized by Fe(III) at any pH forms very stable complexes with log K_{110} = 17.6 and log K_{120} = 14.9[170]).

Powell and Taylor[131] have investigated the extent of reaction (7.1) as a function of pH for protocatechuic acid (E^o = 0.885 V[169]), gallic acid (E^o = 0.799 V[171]), pyrogallol (E^o = 0.713 V[171]) and catechol. Sections 7.1 - 7.4 of this Chapter expand the study to other more complex polyphenols (e.g. catechin, fulvic acid and tannic acids) and investigate the effect of ligand and metal ratios and

absolute concentrations of ligand to metal on the redox process, as a function of pH and time.

Singer et al.[172] have investigated the redox process (7.1) by analysing for iron(II) (as the complex Fe(bathophenanthroline)$_3^{2+}$), but without an Fe(III) masking agent present. They observed apparently high concentrations of Fe(II) for many systems at pH 6.4 and inferred from their results that Fe(II) is stabilized against atmospheric oxidation by complex formation with polyphenols. Development of Fe(II) tests in the present study, in which a masking agent for Fe(III) was employed, indicted that the results obtained by Singer et al.[172] were interpreted incorrectly.

In quantitative titrations of iron(III)-ligand mixtures the pH dependent redox reaction (7.1) produces solutions of unknown stoichiometry when the system is weakly to strongly acidic. Avdeef et al.[138] in studies on iron(III)-catechol complexes and Migal et al.[153] in studies of iron(III)-protocatechuic acid complexes have ignored the effect of this process on solution stoichiometry; thus the accuracy of their stability constants for Fe(III)-ligand complexation reactions must be suspect.

Section 7.5 of this Chapter reports an investigation of the complexes formed between a selected series of ligands and Fe(III); where possible the stability constants for the complexation reactions have been investigated.

7.1 Spectrophotometric methods for the determination of iron concentrations

7.1.1 Iron(III)

The concentration of ferric ion in solution was measured by determining the absorbance of the $Fe(III)NCS(H_2O)_5$ complex[173] at 480 nm as described in Chapter 2.

At neutral pH polyphenols form stable complex species with Fe(III). However, when the pH is lowered reduction of iron and oxidation of the ligand occur ($6 > pH > 1$); at lower pH the complex is decomposed. To measure the extent of the redox process at any pH the oxidation states of iron were frozen by quickly decomposing any iron-ligand species with 5 M HCl. The use of 1 M HCl as outlined by Taylor[174] did not decompose the phenolate complexes quickly enough to prevent redox. The order of addition of the sample to acid or vice versa did not affect the results obtained, and once the sample was quenched (by acid) the oxidation states were stable with time (h).

7.1.2 Iron(II)

The concentration of ferrous iron in the presence of iron(III) and oxidizable organic matter was measured by determining the absorbance of the $Fe(II)(2,2'\text{-bipyridyl})_3$ complex at 525 nm (see Chapter 2). It was essential to mask iron(III) to prevent the redox reaction (7.2)

$$Fe(III)L_2 + 3bp \rightleftharpoons Fe(II)(bp)_3 + L + qno + 2H \quad (7.2)$$

which is promoted by the stability of the complex $Fe(2,2'\text{-bipyridyl})_3^{2+}$, ($\log \beta_{130} = 117.45$[175], E^o $Fe(III)(bp)_3$ /$Fe(II)(bp)_3$ = +1.06 V[176]).

Fadrus and Maly[177] have reported that iron(III) can be masked by NTA in the presence 1,10-phenanthroline and oxidizable organics whereas in the presence of 1,10-phenanthroline, O_2 and EDTA, iron(II) is oxidized to iron(III). To test the ability of NTA to quantitatively mask iron(III), a spectrophotometric titration of NTA into solutions containing Fe(III)-bis(phenalato) complexes was carried out in ammonium acetate buffer a pH 7 ($[Fe_T]$ 2 - 7×10^{-5} M; [ligand] 2 - 60×10^{-5} M; Fe(II)/Fe(III), 1/2 to 1/20. The results indicated a decrease in the FeL_2 absorption at 550 - 570 nm with increasing [NTA]. An NTA concentration of 0.02 M completely decomposed the phenolate complexes. Spectrophotometric analysis of solutions containing varying ratios of iron(II), iron(III) and polyphenols (catechol, catechin) confirmed the masking ability of NTA in the presence of 2,2'-bipyridyl, both in the dark and in direct light; the absorbance of the $Fe(II)(bp)_3$ complex was constant for at least one hour.

7.2 Polarographic determination of iron(III)

7.2.1 The polarographic technique

The technique of differential pulse polarography, DPP, was used for the determination of Fe(III) concentrations in dilute Fe(II)/Fe(III) solutions. Because DPP measures the change in current with the change in potential a current scale can be selected to full-scale deflection for the redox process of interest irrespective of what reduction has

occurred at a more positive potential. The rate of change of measured current with respect to potential approximates the derivative of a normal polarographic wave, yielding a peaked polarogram which provides increased resolution. DPP also provides enhanced sensitivity (cf. current sampled DC or pulse polarography) because the quantity measured is the rate of change of current, which arises almost entirely from the (Faradaic) reduction of the species of interest. In DPP the current is sampled (twice) late in the lifetime of the Hg drop where the rate of change of the electrode area is small; under conditions where $\underline{d}$(area)/$\underline{d}$(time) is small the capacitance current is small. Further when the total current is sampled the capacitance current has decayed almost to zero and the measured current is predominantly Faradaic. Figure 7.1 diagrammatically indicates the faster decay rate of the capacitance current.

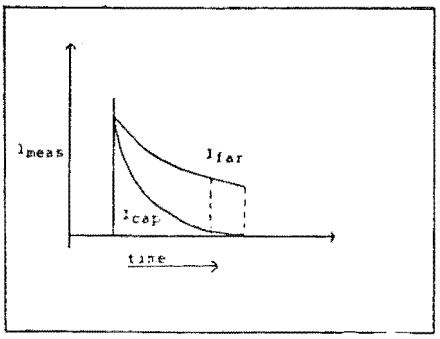

Figure 7.1 Current-time relationship during a pulse application to a psuedo stationary electrode

The additional sensitively gained in the differential pulse technique arises from the virtual elimination of the capacitance current, i.e. because the voltage pulse applied after the first current sampling is small (typically 25 mV) most of the resultant current which is then sampled is Faradaic.

7.2.2 Development of an analytical method

Iron(III) was determined polarographically using NTA to complex iron(III) and 2,2'-bipyridyl to mask iron(II) at pH 7.0 (ammonium acetate buffer). The Fe(III)-NTA reduction wave had $E_{1/2}$ c. -0.11 V. However, it was found that the reaction conditions developed for the spectrophotometric analysis of iron(II) (involving 0.2 M NTA and 0.004% bp buffered to pH 7 with ammonium acetate, 1 M) were not applicable to this polarographic analysis. Specifically the concentrations of NTA and bp were not high enough. This resulted in the peaks obtained from a DPP continuing to increase in height until a maximum value was reached c. 10 minutes after the first trace was recorded (8 min). From the spectrophotometric test for iron(II) it was known that all the ferrous iron was immediately complexed as the tris-bipyridyl complex. The drifting of the polarographic peak was therefore ascribed to i) the initial formation of $Fe_p(OH)_r$ species which then slowly complexed with NTA or ii) the initial formation of a ternary species consisting of iron, NTA and polyphenol[178] which slowly changed to a binary NTA complex. By increasing the concentrations of NTA and bipyridyl the rate of formation of complexes was increased and stable peak heights were obtained after 8 min, the time taken for deoxygenation of the test solution. Because each sample needed to be deoxygenated by nitrogen saturation a rapid analysis of redox-active samples was not possible. The ammonium acetate buffered system containing 0.25 M NTA and 0.1% bipyridyl gave the most constant peak heights with time; other buffers tested included glycine, pH 2.35, and

acetate/acetic acid, pH 4.8. After 45 minutes solutions exposed to the atmosphere in the dark and in diffuse light started to show a small decrease in peak height, indicating a conversion of the Fe(III)NTA complex to $Fe(II)(bp)_3$; this was confirmed spectrophotometrically. The peak height decreased by 9% after 2 h.

The method described here and in Chapter 2 for the polarographic determination of iron(III) was compared with the spectrophotometric tests for iron (Section 7.1) by analysing prepared solutions containing Fe(II), Fe(III) and catechol. In each case the concentrations of Fe(II) or Fe(III) were calculated from linear calibration curves generated from standard solutions (typical concentration ranges, Fe(III) $7x10^{-6}$ - $1x10^{-4}$ M; Fe(II) 1 - $10x10^{-5}$ M). In each case the spectrophotometrically determined [Fe(II)] when added to the [Fe(III)] determined by polarographic analysis totalled 100 $\pm$ 5% of the known total iron present. A typical DPP diagram is presented in Figure 7.2.

7.2.3 Reversibility of the Fe(III) reduction wave

The Ep value for the reduction of the Fe(III)NTA complex (see Figure 7.2) remained constant at c. -0.11 V throughout the Fe(III) and Fe(II) concentration range investigated; this suggested a reversible reduction process. It is important that the half-wave potential $E_{1/2}$ or peak potential Ep be independent of the concentrations of the reduced and oxidized forms of the electroactive substance. The anodic Hg wave preceding the Fe(III) reduction wave made the calculation of $E_{1/2}$ from a normal polarographic wave difficult in that a baseline could not be drawn for zero

Figure 7.2 Typical polarograms for the reduction of Fe(III)

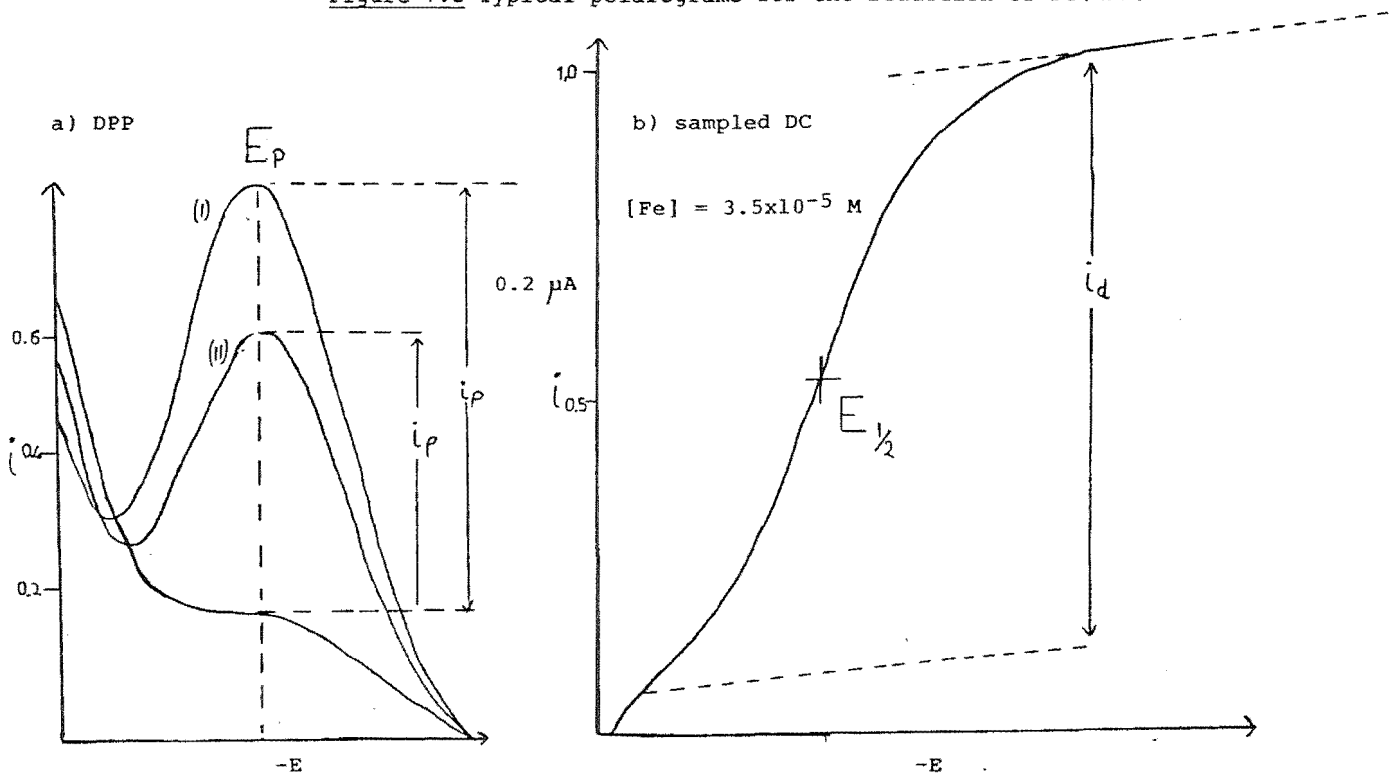

(I) [Fe] = 5.2x10^{-5} M

(II) [Fe] = 3.5x10^{-5} M

current (see Figure 7.2). The $E_{1/2}$ was calculated from the emf for maximum peak height using equation (7.3)[179]

$$Epeak = E_{1/2} - \Delta E/2 \qquad (7.3)$$

where ΔE, the pulse amplitude was -25 mV. Evaluation of $E_{1/2}$ permitted the baseline for zero current (curve (b) in Figure 7.2) to be drawn (parallel to the upper limiting current line).

The reversibility for this one-electron reduction was then assessed by an analysis of the current-voltage curve[180] using the relationship

$$(n/slope)\ (E_{1/2} - E) = \log\ (i/(id-i)) \qquad (7.4)$$

where n is the number of electrons in the reduction process and id is the limiting diffusion current.

For the reagent concentration used in this work the slope was 51 $\pm$ 2 mV compared with a slope of 59 mV required by theory for a reversible process.

7.2.4 Discussion

The polarographic method has the advantage that it may be used to analyse turbid solutions for iron(III) concentrations in the same range as the colourimetric thiocyanate test (c. 0.2 - 3 ppm).

The lower limit of detection for the polarographic method was c. 2×10^{-6} M Fe(III); the reagent purity was found to be the limiting factor. However, the time taken to analyse one sample is much longer than for the spectrophotometric methods because the test solution must initially be purged by nitrogen gas for a minimum of 8 minutes to be completely deoxygenated.

Compounds such as 2,2'-bipyridyl have been found to alter the sensitivity of this method (see Table 7.1). Therefore it was necessary to calibrate the instrument under conditions identical to those used for the sample.

Table 7.1 DPP peak height dependence on the concentration of 2,2'-bipyridyl

[Fe(III)] x10^6 M	[bp]	peak height μA
7.6	0.2%	0.11
7.6	0.1%	0.13
7.6	0.04%	0.15
7.6	0.02%	0.15

Solutions containing epicatechin were found to cause erratic and drifting baselines. A DPP polarogram for a solution containing the reagents and epicatechin only gave some small peaks in the region of Fe(III) reduction; these may arise from adsorption phenomena. The technique was not applicable to epicatechin solutions. Furthermore it was found that NTA was unable to sequester Fe(III) from the tannic acid molecule (confirmed spectrophotometrically).

It is envisaged that the polarographic method would only be employed if other techniques were unable to be used; this is because of the time required to analyse one sample, and the instability of the Fe(III) NTA complex as evidenced by the measurable decrease in the DPP peak 45 mins after the reagents are mixed with the sample.

7.3 Iron(III) polyphenol redox reactions

Reactions between iron(III) and phenolic soil organic matter, (e.g. catechol, tannins and fulvic acid), are of interest because of the possible role that they may play in the mobilization of iron in soils[181]. Recently a number of workers[138,182] have carried out studies on iron(III)-"catecholate" complexes, as models for microbial iron transport compounds (e.g. enterobactin).

As indicated earlier in this Chapter the reduction potential for the iron(III)/iron(II) couple is similar to the reduction potentials (o-quinone/polyphenol) for many naturally occurring polyphenols and there is a possibility of the redox process (7.1) occurring.

This section of work investigates the redox properties of simple polyphenols and more complex species such as fulvic acid.

7.3.1 Determination of iron

The analytical tests for iron outlined in Sections 7.1 and 7.2 were employed to analyse the redox state of Fe(II)-Fe(III) polyphenol solutions. The thiocyanate method was used most frequently because it was more rapid than the polarographic test and, provided greater sensitivity than the spectrophotometric method developed for iron(II).

7.3.2 Titration procedure

All redox titrations were performed in titration cells open to the atmosphere. The initial metal-ligand solution was prepared by slowly adding a known amount of standard Fe(III) solution to a well stirred ligand solution. During the addition of Fe(III) compensating amounts of KOH were

added to maintain the pH above 6.5; the slow addition of Fe(III) was necessary to prevent high local concentrations of acid which may facilitate reaction (7.1) between the polyphenol and metal.

To study redox processes the pH of the metal-ligand system was lowered to selected values by increments of HCl added from a micrometer syringe via a glass burette; use of a conventional syringe needle resulted in detectable dissolution of metal from the needle. When the desired pH value was attained a sample or samples were removed via a pipette (usually 5 ml) and transferred to volumetric flasks where either (i) the oxidation state of iron could be 'frozen' immediately by addition to 5 M HCl or (ii) the sample could be aged for a certain length of time. All samples were taken in duplicate.

7.3.3 Results

a) The redox properties of iron(III) with tiron, catechol, protocatechuic acid, epicatechin, B2 dimer, tannic acid and fulvic acid were investigated. For the simpler polyphenols solutions had catecholate and iron(III) concentrations of 2.2×10^{-3} M and 3.5×10^{-4} M respectively. The complex molecules tannic acid and fulvic acid were tested for redox activity at lower concentrations (20 and 60 mg/l) because of the insolubility of the parent ligands when solutions were quenched with acid. Figure 7.3 presents the results obtained (solutions aged 10 min between each sampling).

b) The ligand to metal ratio was varied for the catechol system (H_2L = 5 - 10×10^{-3} M) from a value of 3/1 to

Figure 7.3 Redox properties of iron-polyphenol systems

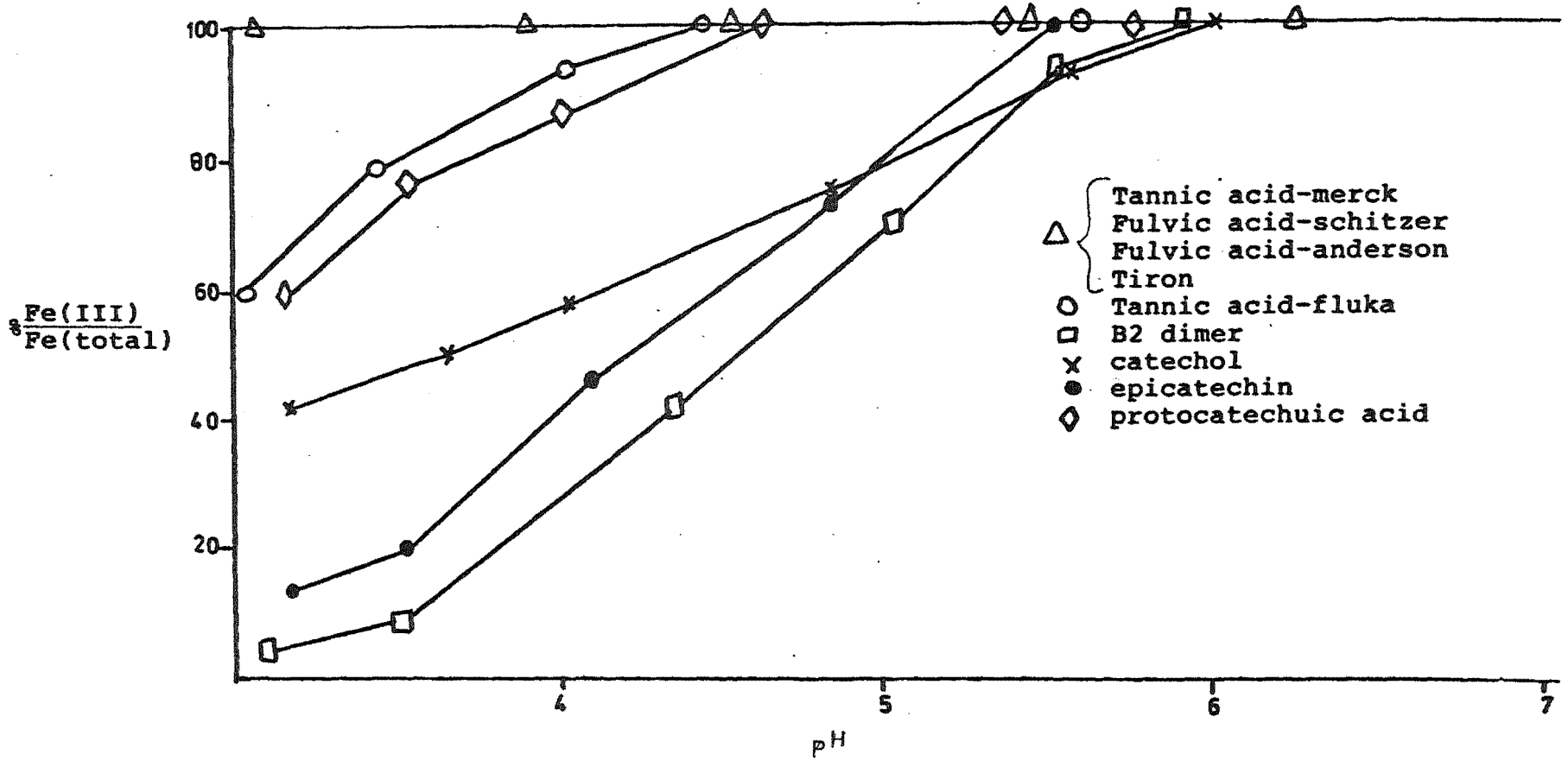

a value of 6/1. With the larger excess of ligand it was found that the pH at which the redox reaction initially occurred was lower (3/1, pH c. 4.4; 6/1, pH c. 3.6). The results of this study are presented in Figure 7.4.

c) Epicatechin-iron solutions of constant ligand to metal ratio (6.3/1) but with varying absolute concentrations (2 - 20x10^{-4} M) were sampled at a number of pHs. Although data were limited, it appeared that the most concentrated epicatechin solution was the most redox-stable in weakly acid solutions but underwent the most redox at the lowest pH sampled (see Figure 7.5).

d) The extent to which reaction (7.1) proceeds with time was investigated by sampling a catechol (2x10^{-3} M)-iron(III) (3.5x10^{-4} M) solution and quenching the samples at 5, 30, 60 and 720 minute intervals. The results are presented graphically in Figure 7.6. The redox process is fast in that most of the reduction of Fe(III) occurred in the first 5 minutes. Measurable reduction occurred for all solutions at pH $\leqslant$ 5.6.

7.3.4 Discussion

When iron(III) is reacted with a polyphenol such as catechol at low pH a transient green colour develops which quickly disappears leaving the solution with a pale yellow hue. The solution has an initial absorbance at 700 nm indicating the formation of FeL[183]; the yellow compound has an absorption maximum near 400 nm, which is consistent with quinone formation[132]. These observations provide evidence that the redox process is occurring rapidly (min), as displayed in Figure 7.6.

Figure 7.4 Effect of metal to ligand ratio on the composition of iron-catechol systems

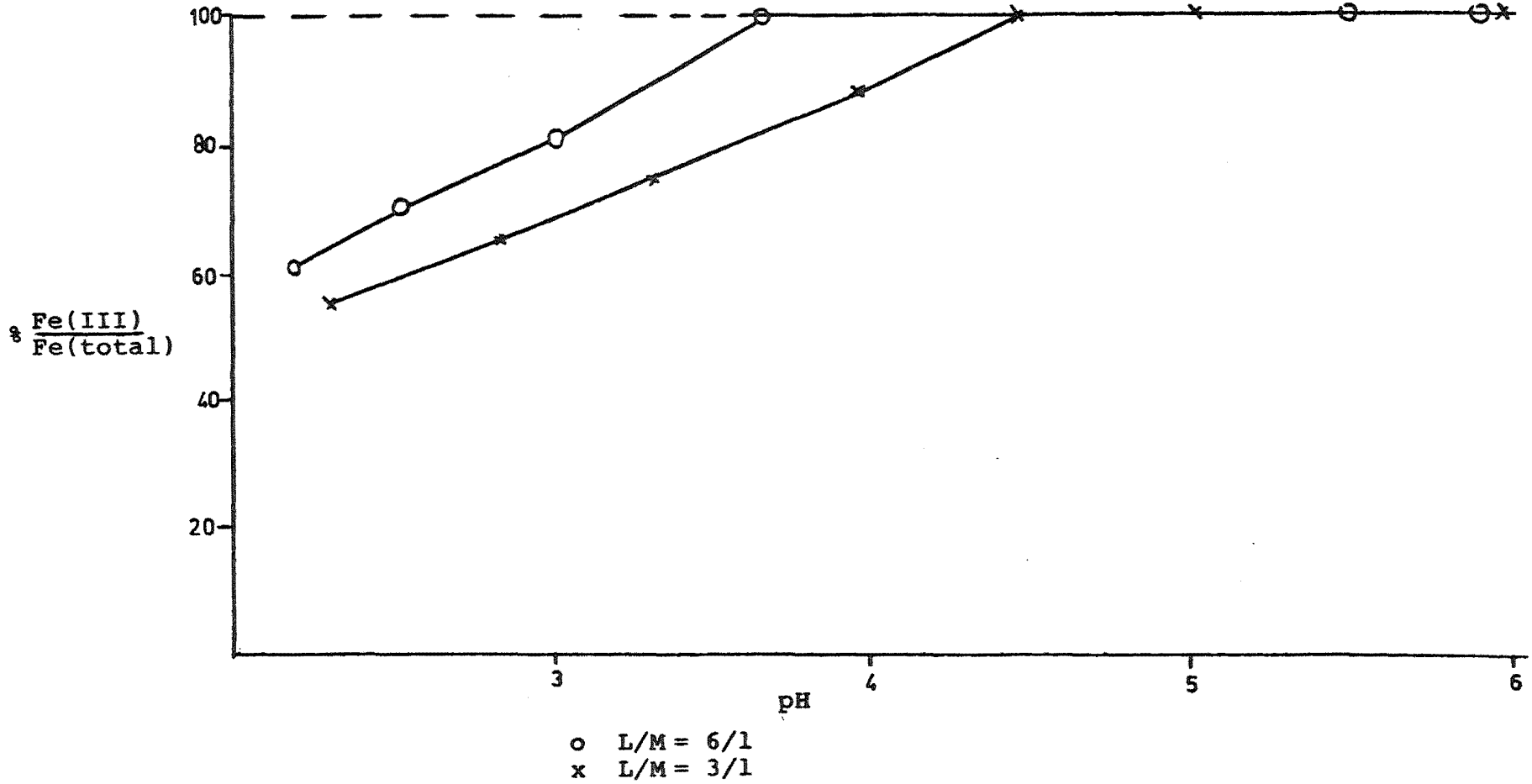

Figure 7.5 Effect of absolute concentration on the composition of iron-epicatechin systems

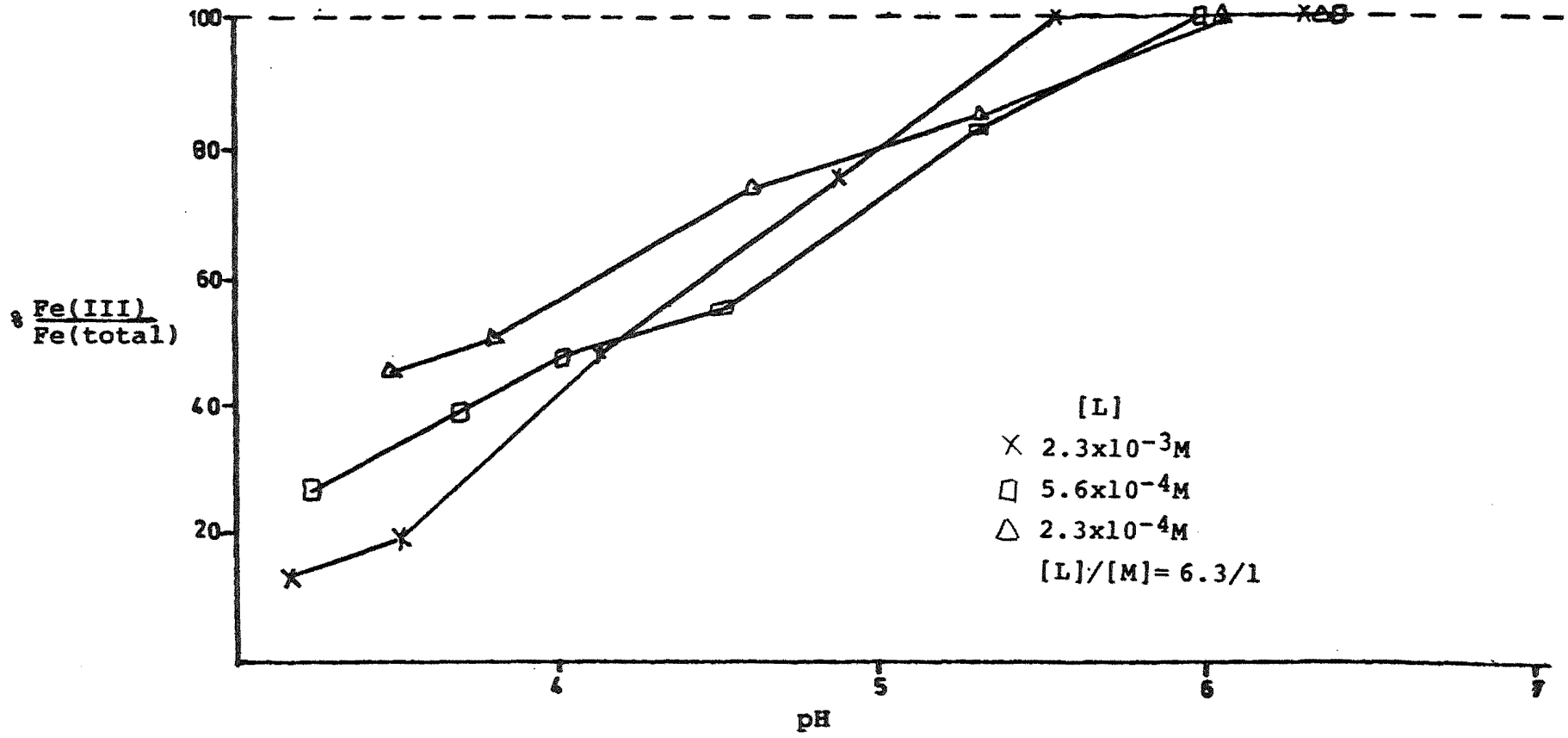

Figure 7.6 Effect of time on the composition of iron-catechol systems

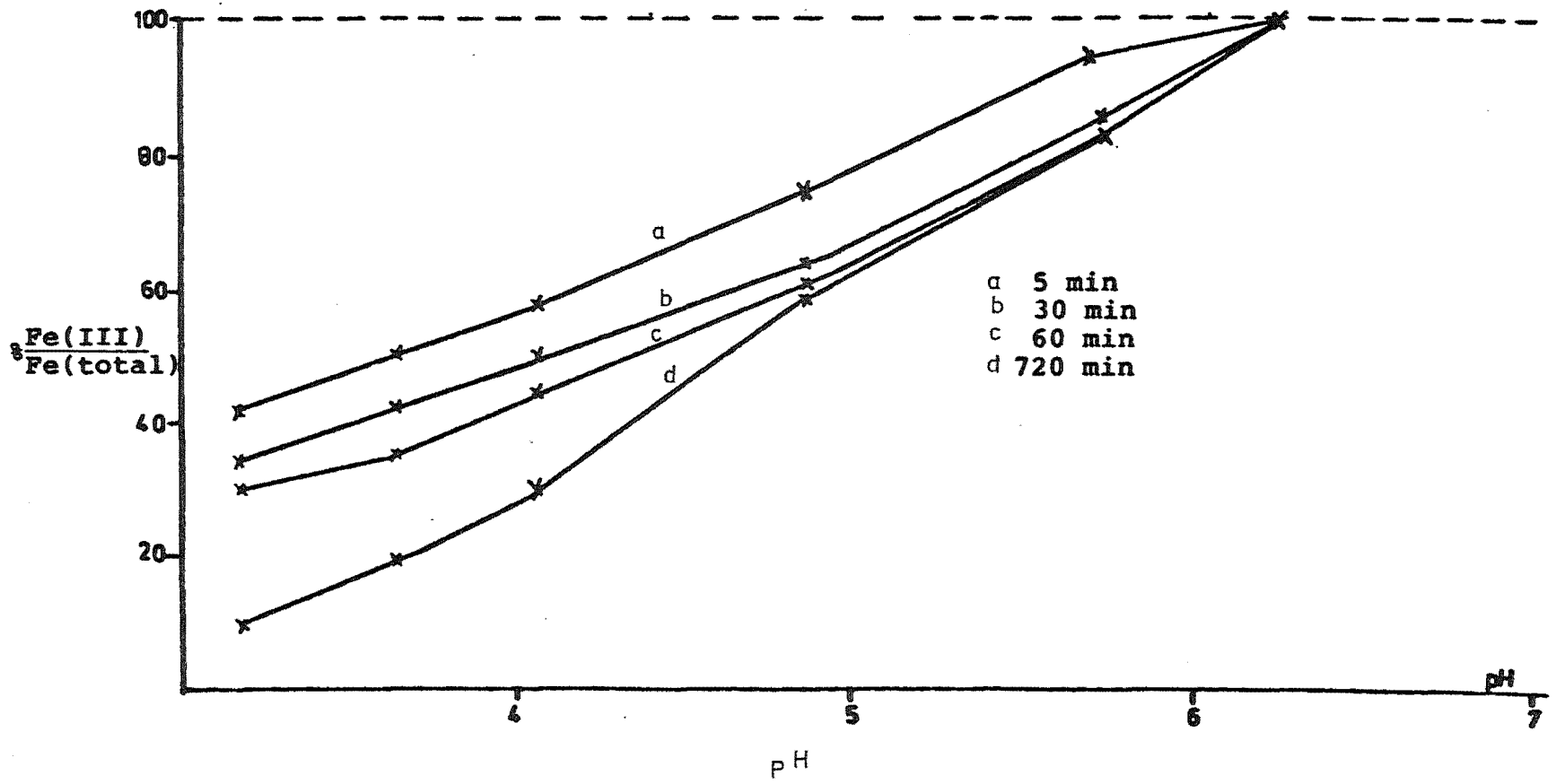

Investigating the kinetics of complex formation for a series of catechols with iron(III) Mentasti et al.[184] proposed a mechanism for the subsequent reduction of iron and oxidation of 1,2-dihydroxybenzenes which involves a semiquinone radical species:

$$Fe(III) + H_2L \rightleftharpoons FeL + 2H \rightleftharpoons Fe(II) + HCat\cdot + H$$

$$Fe(III) + Hcat\cdot \rightleftharpoons Fe(II) + quinone + H$$

$$2Fe(III) + H_2Cat \rightleftharpoons 2Fe(II) + quinone + 2H$$

However, it should be noted that subsequent work has shown that the overall redox reaction is not reversible[131] as stated by Mentasti. In an e.s.r. study Avdeef et al.[138] noted a peak which they ascribed to semiquinone formation although no semiquinone was observed for tiron; the present work supports the inference of no redox activity for tiron (Figure 7.3). An alternative mechanism was described by Hider et al.[185] who suggested that the redox-active species for catechol is a monoprotonated species Fe(III)LH which forms an Fe(II) monoprotonated semiquinone complex Fe(II)LH·. Although the monoprotonated species may well be the electron donor it has been established that Fe(II) does not complex with phenols below a pH of 7[131].

It was noted in this work that the species FeL_2, which is the dominant species in solution from pH 5.7 to 8 is not redox-active. By increasing the ligand to metal ratio the equilibrium $FeL + L \rightleftharpoons FeL_2$ is moved further to the right producing more redox inactive FeL_2 at any given pH. This is confirmed experimentally as indicated in Figure 7.4.

Increasing the absolute concentrations of the ligand and metal (at constant L/M ratio) resulted in a complex pattern of redox curves (Figure 7.5). This pattern may be explained as follows. As the absolute concentrations of reactants are increased the metal will complex at a lower pH: i.e. it will form the redox-active FeL at lower pH, but also this will change to redox inactive FeL_2 at lower pH than for less concentrated solutions. Therefore in the pH range where FeL is partially formed from $Fe(H_2O)_6^{3+}$ (pH < 3.5) there is more redox reaction, but in the pH range where FeL is partially converted to FeL_2 (pH > 5.5) there is less redox reaction in more concentrated solutions.

Although the metal-ligand ratio has been shown to be important in determining the critical pH below which reaction (7.1) occurs, dilute solutions of simple organic species found in the soil may be oxidized by iron(III) at pH values as high as 6; for example catechol Figure 7.3.

Figure 7.3 represents all the phenolic ligands investigated quantitatively. It is of interest that, excluding the tannin polymer Bl3 and tannic acid (Fluka), the large polymeric species do not enter into a redox reaction with Fe(III). Bl3 was shown to reduce iron in acid solution; precipitation of an Fe(III)-Bl3 complex prevented any quantitative interpretation but an analysis of the supernatant solution established the presence of ferrous ion. The small organic molecules which are not stabilized by electron withdrawing substituents (e.g. COOH, SO_3H) participate in a significant amount of redox at pH values commonly found in podzolized soils (c. 4.5). This suggests

that these molecules may be active in mobilizing iron(III) from its insoluble oxy-hydroxides by reducing it to the more soluble iron(II) rather than (or as well as) by complexation reactions.

7.4 The effect of organic matter on the oxidation of ferrous ion

7.4.1 Introduction

Singer & Theis[172,186] have investigated the interaction of Fe(II)-Fe(III) systems with certain naturally occurring organic compounds (e.g. citric acid, gallic acid). They concluded that molecules such as gallic acid can completely retard the oxidation of iron(II) in oxygen enriched solutions (P_{O_2} = 0.5 atm) by the formation of stable Fe(II)-organic complexes. They drew this conclusion from the (apparent) high ferrous ion concentrations (close to 100%) found in oxygenated solutions formed from iron(III) and these ligands at pH 6.3. The [Fe(II)] was determined by acidifying a sample from the test solution with acetate buffer (pH 4) and applying Lee and Stumm's[187] bathophenanthroline procedure. This method involved a solvent extraction procedure in which the iron(II) complexing agent bathophenanthroline was added to the iron-polyphenol solution, and shaken for 30 seconds with n-hexanol to extract the iron(II) complex. The aqueous layer was discarded and the absorbance of the coloured Fe(II) complex was measured at 533 nm. Interpolation from a calibration curve gave the concentration of iron(II) in the sample.

The interpretation in terms of stabilization of iron(II) by complex formation conflicts with results obtained in this work and by Taylor[131], which indicate that gallic acid (and other polyphenols) are unable to complex iron(II) in solutions at pH less than 7.

Two problems arise from the analytical method used by Singer and Theis[172,186]. Firstly, acidification to a pH of 4 for a ligand such as gallic acid would result in a significant fraction of the iron(III) being reduced (cf. catechol Figure 7.3). Secondly there was no masking agent for iron(III) to freeze its oxidation state in the presence of the iron(II) complexing agent and oxidizable organic matter; the result of adding bathophenanthroline would be an increased production of ferrous ions via reaction (7.2).

In view of the above problems the work of Singer et al.[172,186] was repeated. Lee and Stumm's[187] method of analysis was used to confirm their results and become familiar with the solvent extraction technique. Additional analyses were also undertaken using (i) 2,2'-bipyridyl as the iron(II) complexing agent and noting the absorbance at 525 nm as a function of time (ii) the method described by Lee et al.[187] but incorporating NTA to mask Fe(III), and (iii) the NTA-bipyridyl test described in Chapter 2.

7.4.2 Solution preparation and sample procedure

Solutions of citric or gallic acid ($1x10^{-4}$ M) were adjusted to pH 6.3 by addition of KOH prior to the slow addition of Fe(III) ($8x10^{-5}$ M) and compensating amounts of KOH; the ligand and metal concentrations were those used by Singer et al.[172,186]. When the pH had stabilized (min)

samples were removed for Fe(II) analysis by one of the methods described above.

7.4.3 Results

The method of Singer and Theis[172,186] when applied to iron(III)-gallic acid solutions (bathophenanthroline/ solvent extraction) indicated a significant amount of reduction; [Fe(III)] reduced: found 6.3×10^{-5} M, reported by Singer et al.[172,186] 3.4×10^{-5} M. For citric acid the results were [Fe(III)] reduced: found 4×10^{-6} M, reported 4.7×10^{-6} M.

If ammonium acetate buffered 2,2'-bipyridyl was added to gallic acid-iron(III) solutions initially at pH 6.3 then 53% of the total iron was reduced to iron(II) within 30 s. The amount of iron(II) produced increased with time (see Figure 7.7).

If NTA was present, that is added simultaneously with bathophenanthroline (pH 4.6) or bipyridyl (pH 7.0) then, using methods (ii) or (iii), no Fe(II) was detected in the citric acid or gallic acid systems; this indicated that Fe(III) was effectively masked by NTA and no redox reaction had occurred at pH 6.3 with either citric acid or gallic acid (Figure 7.7).

7.4.4 Discussion

The method of analysis used by Singer and Theis[172,186] for iron(II) has been shown to give misleading results; that is without a masking agent for iron(III) almost instantaneous reduction may occur, according to reaction (7.2). This result lead these workers to conclude that certain phenolics (e.g. gallic acid) can complex with

Figure 7.7 Effect of NTA as a masking agent for Fe(III)

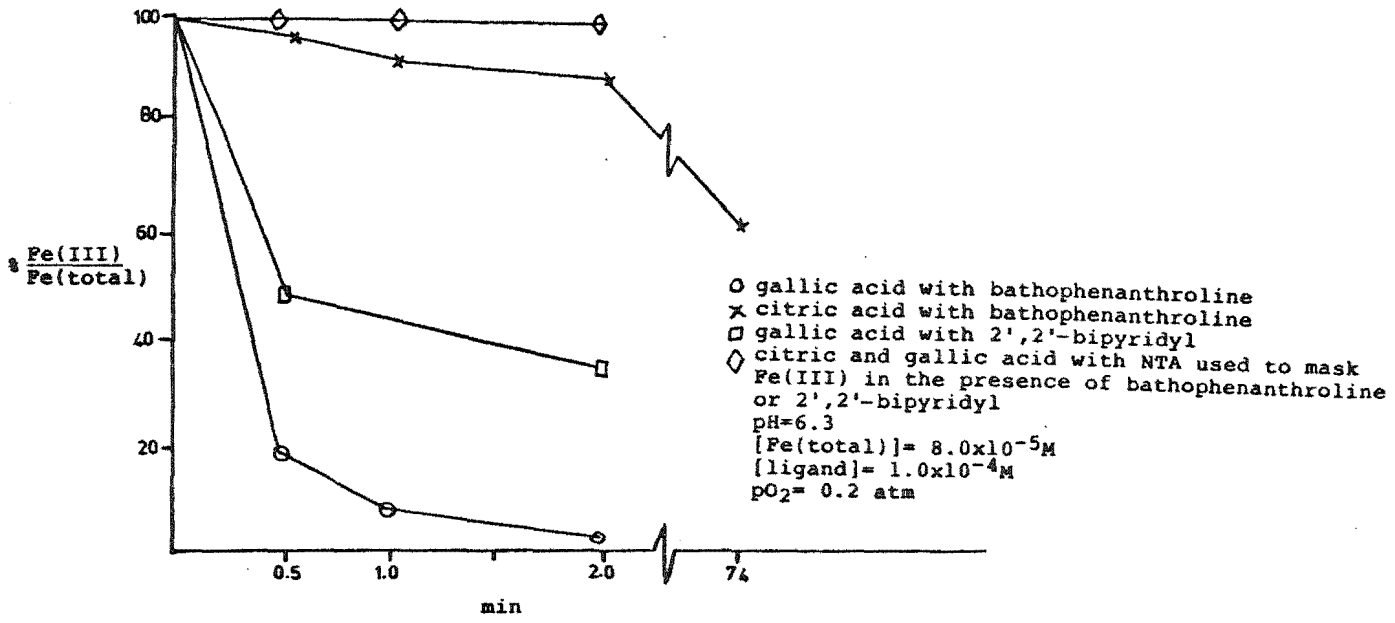

Fe(II) at pH < 7, stabilizing it against atmospheric oxidation for indefinite periods of time.

The results obtained in this work where the masking agent NTA was used for Fe(III), indicate that this interpretation is not correct e.g. at a pH of 6.1 100% of the iron is in the ferric state, rather than in the ferrous state as proposed by Singer et al.[172,186].

Scheme 1, which was reported by Singer and Theis[172] has mislead other workers in their study of Fe(II) oxidation processes[188].

An alternative scheme, Scheme 2, is proposed here on the basis of the results obtained in this work and the inability of 1,2-dihydroxybenzenes to complex Fe(II) below a pH of 7[131].

7.5 Protocatechuic acid

7.5.1 Potentiometric data

Protocatechuic acid was the only ligand for which quantitative equilibrium measurements could be made with Fe(III). This was possible because protocatechuic acid does not undergo the redox couple (7.1) until comparatively low pH values.

It was necessary to start these potentiometric titrations at pH values greater than six to prevent the redox reaction (7.1) occurring and hence destroying the solution stoichiometry. Potentiometric back titrations of standard HCl against alkaline Fe(III)-protocatechuic acid solutions were performed in 0.1 M KCl at 25°C.

The procedure used to prepare Fe(III)-ligand solutions at pH > 6 was (i) the ligand solution was thoroughly

Scheme 1

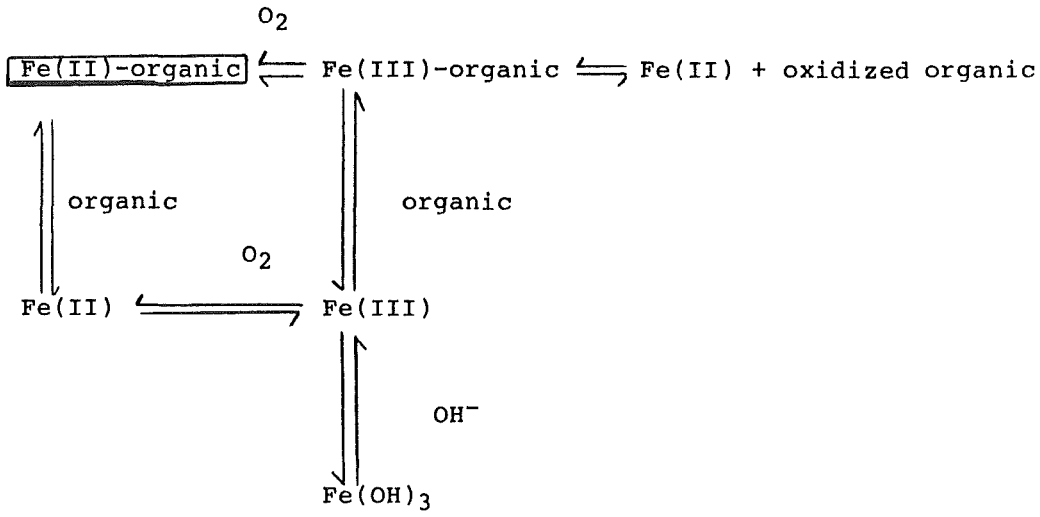

Scheme 2

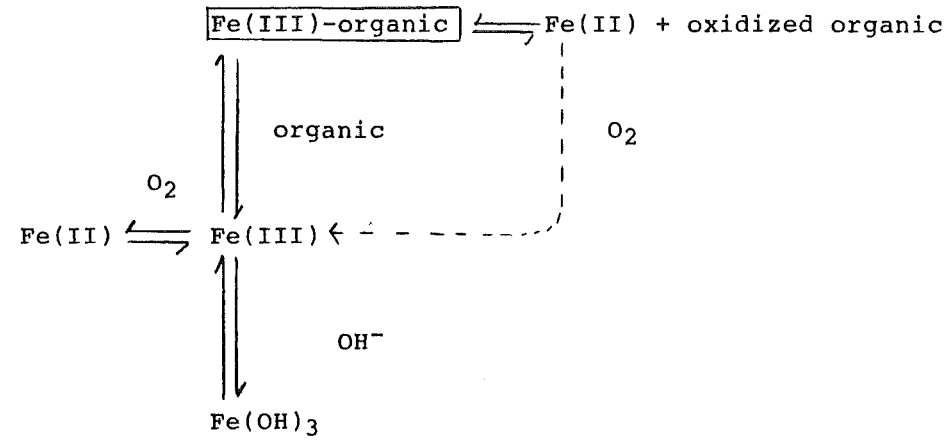

Designates dominant species

deoxygenated in the large titration cell by the method described in Chapter 2, (ii) a calculated amount of standard KOH was added from a micrometer syringe, (iii) standard Fe(III) was introduced slowly to this solution by use of a micrometer syringe until the required iron concentration was achieved.

Representative potentiometric data (pH-volume of titre) from two titrations of HCl against solutions of Fe(III) ($1.69 - 2.1 \times 10^{-4}$ M) and ligand ($1.0 - 1.3 \times 10^{-3}$ M) are listed in Table 7.2. Ligand/metal ratios of 6/1 were employed to ensure drift free buffer regions and to prevent redox occurring until the lowest possible pH (see Section 7.3.3). For consistency the reactions of Fe(III) with protocatechuic acid are discussed in terms of a KOH titration. The Fe(III)-protocatechuic acid titration curve shown in Figure 7.8 has one major end point at pH 6.8. The stoichiometry of this inflexion is consistent with the formation of FeL_2 and the deprotonation of the carboxyl group from all the ligand present i.e. reactions (7.5) and (7.6)

$$Fe(III) + 2LH_3 \rightleftharpoons Fe(III)L_2 + 6H \qquad (7.5)$$

and for excess ligand,

$$LH_3 \rightleftharpoons LH_2 + H. \qquad (7.6)$$

Two distinct buffer regions (pH c. 5 and 8) and three distinct changes of colour were observed. At pH values below 4 the solution was green/blue, changing to blue at pH c. 4.1 then to wine red at pH values greater than 7.2.

Titrations which proceeded to pH values below 4 were performed as rapidly as possible and at two minute intervals

Table 7.2 Representative data from back titrations of a protocatechuic acid-Ferric ion solution[a], 25°C

titre (ml)[b]	$_p$[H][c]	TH(obs)x10^2	TH(calc)x10^2
0.530	2.801	0.4346	0.4345
0.500	2.854	0.4149	0.4147
0.470	2.914	0.3951	0.3956
0.450	2.958	0.3819	0.3819
0.430	3.009	0.3687	0.3688
0.415	3.051	0.3587	0.3588
0.400	3.097	0.3488	0.3490
0.380	3.132	0.3422	0.3425
0.370	3.165	0.3356	0.3357
0.360	3.201	0.3290	0.3292
0.350	3.244	0.3224	0.3226
0.340	3.290	0.3155	0.3159
0.330	3.337	0.3092	0.3091
0.320	3.393	0.3026	0.3024
0.310	3.448	0.2960	0.2958
0.300	3.512	0.2894	0.2893
0.290	3.585	0.2827	0.2825
0.280	3.660	0.2761	0.2758
0.270	3.736	0.2695	0.2691
0.260	3.818	0.2629	0.2627
0.250	3.900	0.2563	0.2562
0.240	3.987	0.2497	0.2501
0.230	4.069	0.2430	0.2433
0.220	4.159	0.2364	0.2367
0.210	4.237	0.2298	0.2299
0.200	4.332	0.2232	0.2235
0.190	4.404	0.2166	0.2167
0.180	4.490	0.2099	0.2097
0.170	4.586	0.2033	0.2028
0.160	4.678	0.1967	0.1965
0.150	4.776	0.1901	0.1899
0.140	4.890	0.1834	0.1832
0.130	5.006	0.1768	0.1771
0.120	5.128	0.1702	0.1705
0.110	5.289	0.1636	0.1638
0.100	5.457	0.1569	0.1566
0.090	5.685	0.1503	0.1501
0.080	6.008	0.1436	0.1431
0.160[d]	7.241	0.1666	0.1668
0.150	7.468	0.1590	0.1592
0.140	7.629	0.1518	0.1510

Figure 7.2 (continued)

0.120	7.868	0.1392	0.1391
0.110	7.984	0.1334	0.1333
0.100	8.111	0.1267	0.1265

---

a Ionic strength = 0.1 M, T 25°C, moles OH^- added = 3.340×10^{-4}, [TL] = 1.021×10^{-3} M, [TM] = 1.693×10^{-4} M, Total vol = 150.610 ml

b Cumulative volume of 1.0009 M HCl added

c Hydrogen ion concentration obtained from calibration equation (see Chapter 3)

d Ionic strength = 0.1 M, T 25°C, moles OH^- added = 4.892×10^{-4}, [TL] = 1.286×10^{-3} M, [TM] = 2.122×10^{-4} M, Total vol = 150.810 ml

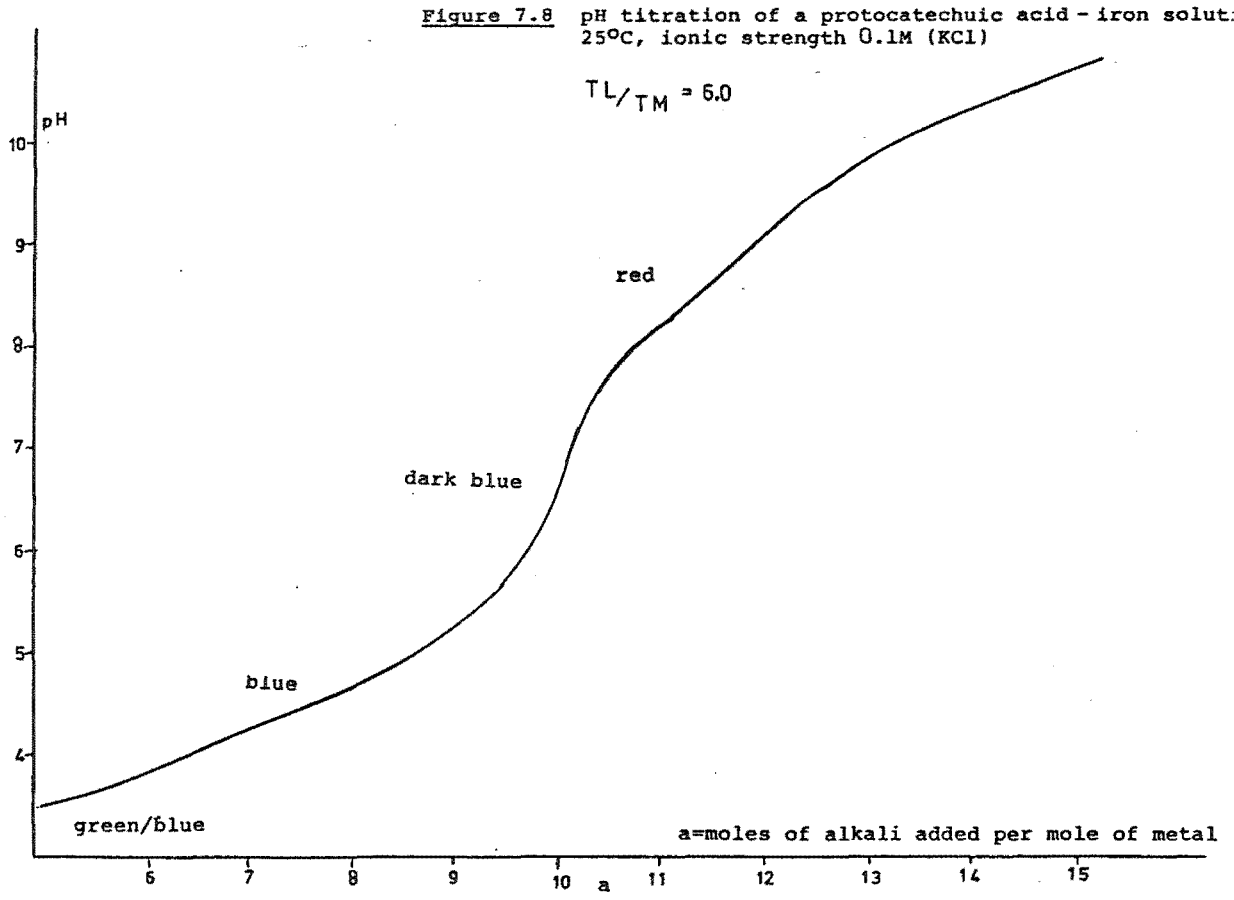

Figure 7.8 pH titration of a protocatechuic acid - iron solution, 25°C, ionic strength 0.1M (KCl)

$TL/_{TM} = 6.0$

aliquots were quenched so that the ferric ion concentration in solution could be measured quantitatively by the thiocyanate test. It was possible in one instance to reach a pH of c. 3 without measurable amounts of the redox reaction occurring, however, some precision in data collection was lost because of the rapid titration.

These data at low pH were collected for possible determination of the stability constant for the mono complex (viz. $Fe(III) + LH_3 \rightleftharpoons Fe(III)L + 3H^+$).

From the titration curve of tiron (a ligand which does not give a redox reaction with Fe(III)) it has been established, from the clearly defined buffer regions and the colour changes, that stable 1:1 (blue-green), 1:2 (blue-purple) and 1:3 (red) complexes form with iron(III)[170]. From the similar titration curves and colour changes shown by protocatechuic acid the existence of similar equilibria was assumed:

$$Fe(III) + L \rightleftharpoons FeL \qquad (7.7)$$

$$FeL + L \rightleftharpoons FeL_2 \qquad (7.8)$$

$$FeL_2 + L \rightleftharpoons FeL_3 \qquad (7.9)$$

These equilibria and the Fe(III) hydrolysis equilibria[189]

$$Fe + H_2O \rightleftharpoons FeOH \qquad (7.10)$$

$$Fe + 2H_2O \rightleftharpoons Fe(OH)_2 \qquad (7.11)$$

$$2Fe + H_2O \rightleftharpoons Fe_2OH \qquad (7.12)$$

$$2Fe + 2H_2O \rightleftharpoons Fe_2(OH)_2 \qquad (7.13)$$

were included in all Fe(III)-protocatechuic acid equilibrium models tested.

Below pH 6 a number of equilibrium species exist in solution, as indicated by the absence of a fixed isosbestic

point in the spectra collected in the pH range 6 - 2.5 (see Section 7.5.2); i.e. a simple equilibrium model including only FeL and FeL_2 is not adequate. The best least squares fit obtained for the potentiometric titration of protocatechuic acid ($1x10^{-3}$ M) and Fe(III) ($1.69x10^{-4}$ M) in the pH range 6 - 2.8 was for the metal-ligand equilibrium model described for Al(III)-protocatechuic acid (see Section 6.4 2). Therefore the equilibria considered were (7.7), (7.8) and

$$FeL + H \rightleftharpoons FeLH \qquad (7.14)$$

$$FeL + H_2O \rightleftharpoons FeLOH + H \qquad (7.15)$$

$$Fe + LH_2 \rightleftharpoons FeLH_2 \qquad (7.16)$$

Table 7.3 lists the refined constants obtained from a least squares analysis on 38 pH-volume of titre data points from one titration in the above pH range. The R-factor for this refinement was 0.18%. A second titration to low pH failed to refine for such an equilibrium model (or for a simplified model); that is, during the refinement process certain parameters were made negative. This lack of fit between experiment and model was ascribed to redox reaction (7.1) which, because the titration was not rapid enough, destroyed the known stoichiometry of the metal-ligand system.

The contribution of the Fe(III) hydrolysis species to the solution stoichiometry is graphically presented in Figure 7.9 as is the distribution of metal-ligand species as a function of pH. The term log $[Fe][OH]^3$ reached a maximum value of -36.8 at pH 5.3. This is slightly below the reported values for amorphous $Fe(OH)_3$ of c. -36[190].

Figure 7.9 Distribution of Fe(III) hydroxy and Fe(III)—ligand complexes for protocatechuic acid-Fe(III) solutions

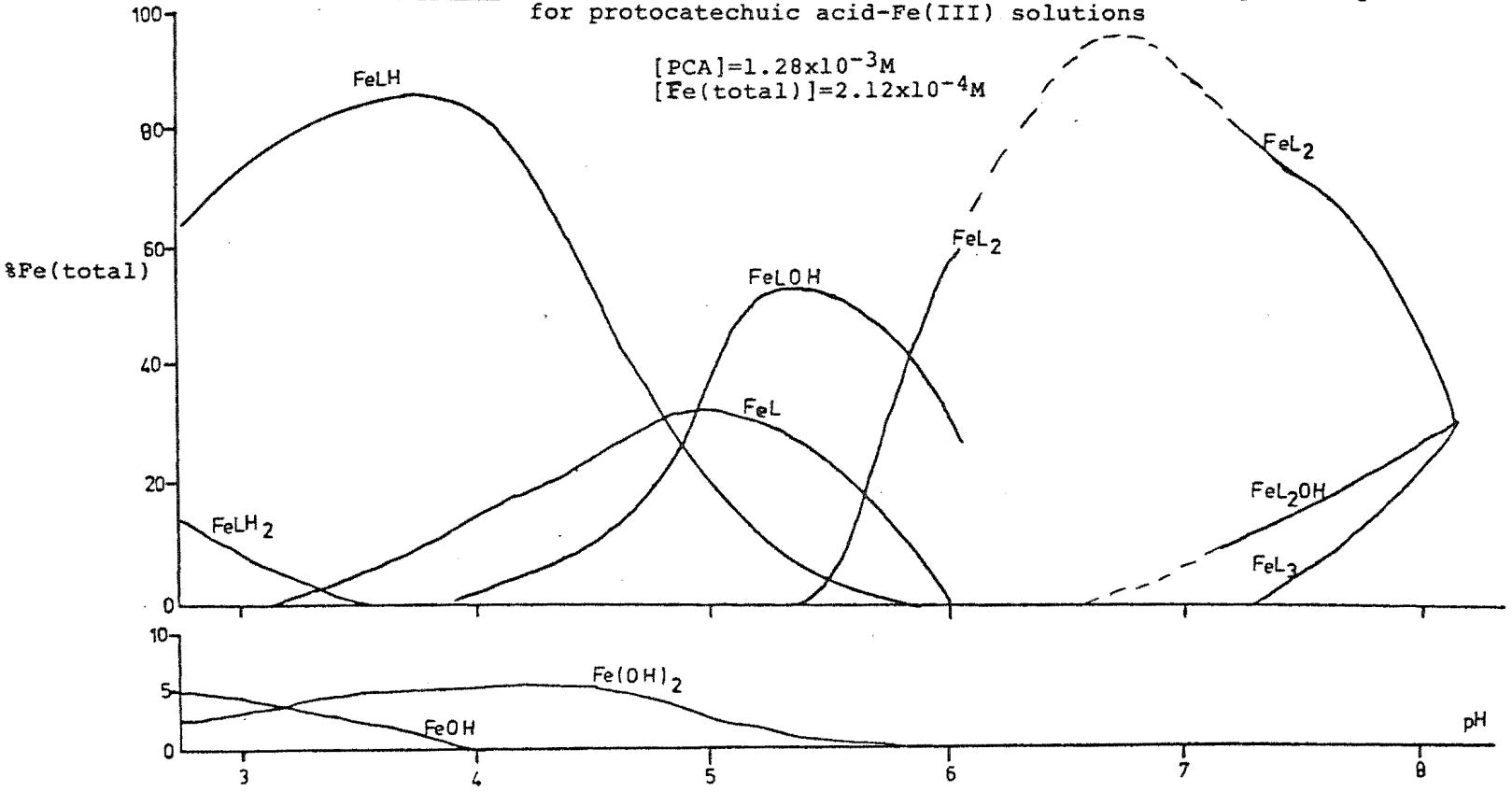

Table 7.3 Stability constants for the formation of Fe(III)-protocatechuic acid (LH_2^-) complexes

Reaction	constant	this work	Migal et al.[153]	Mentasti et al.[169]
$Fe(III) + LH_{r-2} \rightleftharpoons FeLH_{r-2}$	$\log K_{11r-2}$	19.50 ± 0.07[a]	18.99	20.41
$Fe(LH_{r-2}) + LH_{r-2} \rightleftharpoons Fe(LH_{r-2})_2$	$\log K_{12(2r-4)}$	14.32 ± 0.03	14.27	
$Fe(LH_{r-2})_2 + LH_{r-2} \rightleftharpoons Fe(LH_{r-2})_3$	$\log K_{12(3r-6)}$	8.70 ± 0.06 (9.5 ± 0.2)[b]	10.12	
$Fe(LH_{r-2}) + H_2O \rightleftharpoons Fe(LH_{r-2})OH + H$	$\log {}'K_{11r-3}$	-4.86 ± 0.03		
$Fe(LH_{r-2})_2 + H_2O \rightleftharpoons Fe(LH_{r-2})_2OH + H$	$\log {}'K_{12(2r-5)}$	-8.1 ± 0.2		
$Fe(III) + LH_r \rightleftharpoons FeLH_r$	$\log {}'K_{11r}$	4.5 ± 0.2		
$FeLH_{r-2} + H \rightleftharpoons FeLH_{r-1}$	$\log {}'K_{11r-1}$	4.70 ± 0.03		

a mean ± standard deviation calculated in non-linear least squares refinement.

b spectrophotometrically determined ± 1 standard deviation from 4 log k values calculated.

The reaction (7.9) was investigated in two back titrations of ligand ($1.69 - 1.84 \times 10^{-3}$ M)-Fe(III) ($1.5 - 2 \times 10^{-4}$ M) solutions (i.e. L/M = 6). The titrations each consisted of c. 12 data points in the pH range 7.3 - 8.4. Data collected at lower pH for these titrations were not used in the evaluation of other equilibrium processes because the iron(III) concentrations had not been checked spectrophotometrically in the acidic pH range. The stability constant was refined for reaction (7.9) by fixing the parameters for the acidic equilibrium species at their refined values. The poor fit obtained for this refinement was significantly improved on the inclusion of reaction (7.17) which had been characterized for the analogous aluminium(III) system.

$$FeL_2 + H_2O \rightleftharpoons FeL_2OH + H \qquad (7.17)$$

Results from a least squares analysis are listed in Table 7.2. Iron(III) hydrolysis products and iron(III) ligand species (other than FeL_2 and FeL_3) were less than 0.1% of the total iron concentration in the pH range investigated. The ion product expression log $[Fe(III)][OH]^3$ was less than -48.1 for this buffer zone. R-factors ranged from 0.5 - 1%.

The refined constants in Table 7.3 are only semi-quantitative because of the large errors inherent in a rapid titration and the small contribution from the redox reaction.

Computer subroutines used in the least squares analysis are listed in appendix D.

7.5.2 Spectrophotometric analysis

Using the back titration technique described in 7.5.1, oxygen free solutions of Fe(III) (9.3×10^{-5} M)-protocatechuic acid (5.6×10^{-4} M) were transferred from the airtight titration cell to the 1 cm spectrophotometer cell as described in Chapter 2. This cell required 3 ml of solution to be filled to a level at which a spectrum could be recorded. After a spectrum had been recorded the cell was removed from the spectrophotometer and rinsed thoroughly with DDW. It was then replaced in the spectrophotometer and flushed with N_2 before the next sample was taken.

Table 7.4 summarizes the spectrophotometric data obtained for solutions containing FeL_2 and FeL_3 i.e. in the pH range 6 - 11. Figure 7.10a presents the recorded spectra from pH 11.4 to 6 1.

Because an isosbestic point was observed in the pH range where FeL_2, FeL_2OH and FeL_3 are in equilibrium it was inferred that FeL_2 and FeL_2OH have very similar visible absorption spectra.

Below pH 6 no fixed isosbestic points were observed (Fig 10b). This may be because more than one equilibrium species was present (viz. FeL, FeL_2, FeLH) and/or the redox reaction (7.1) converted Fe(III) to Fe(II) and polyphenol to quinone, thus altering the stoichiometry of the system. (It is noted that the spectrophotometric titrations could not be performed rapidly). Only the apparent stability constant for the equilibrium

$$L + FeL_2 \rightleftharpoons FeL_3$$

Table 7.4 Spectrophotometric data for solutions of protocatechuic acid-Fe(III)[a], 25°C

equilibrium species	pH	absortion maxima		isosbestic point	
		λ_{max}[b]	ε_{max}	λ_{iso}	ε_{iso}
FeL_3	11.2	489	5600±100		
FeL_3 /FeL_2	8.3-7.6			545	4100±100
FeL_2	6.7-7.0	575	4300±150		

a [Fe] = 2.1×10^{-4} M
b values ± 1 nm

Figure 7.10(a) Spectrophotometric data for solutions of protocatechuic acid and Fe(III). 25°C, 1cm cell

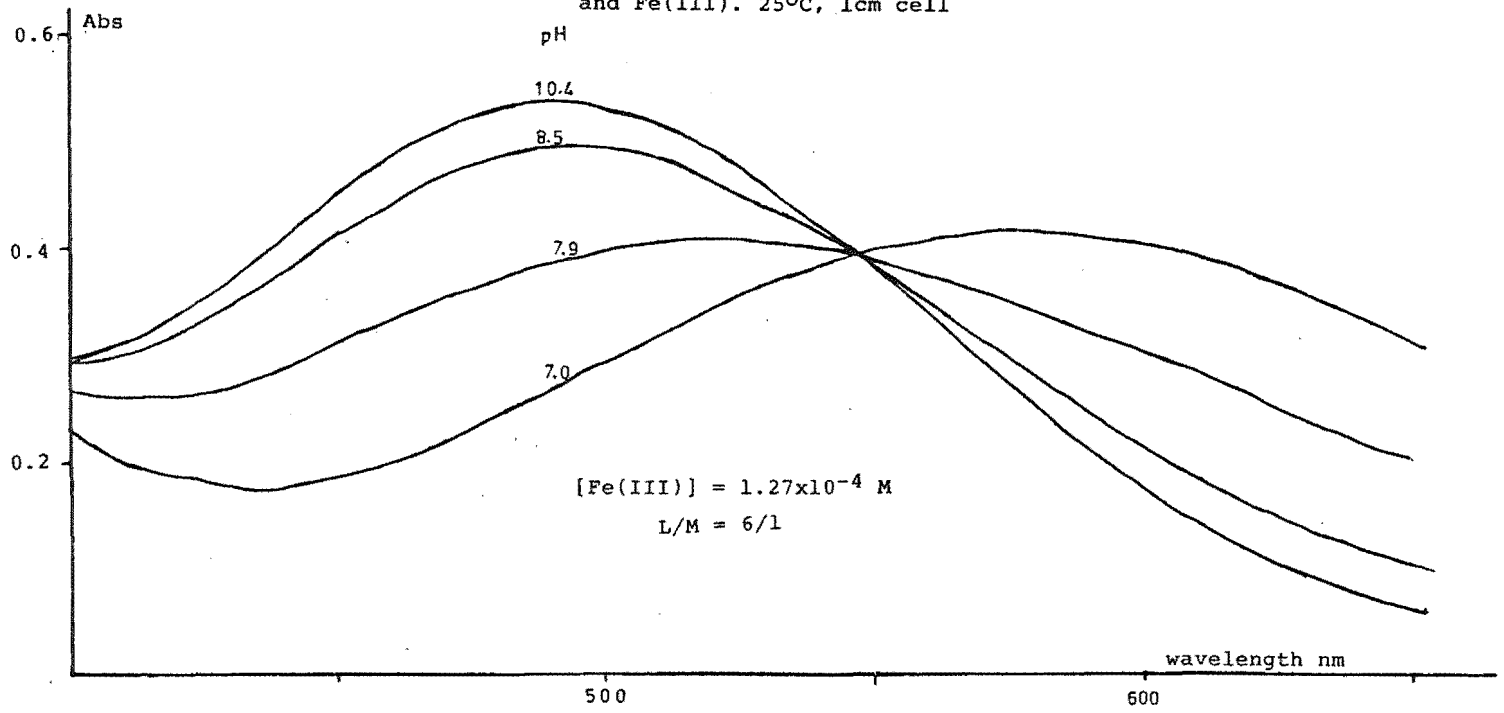

Figure 7.10(b) Spectrophotometric data for solutions of protocatechuic acid and Fe(III). 25°C, 1cm cell

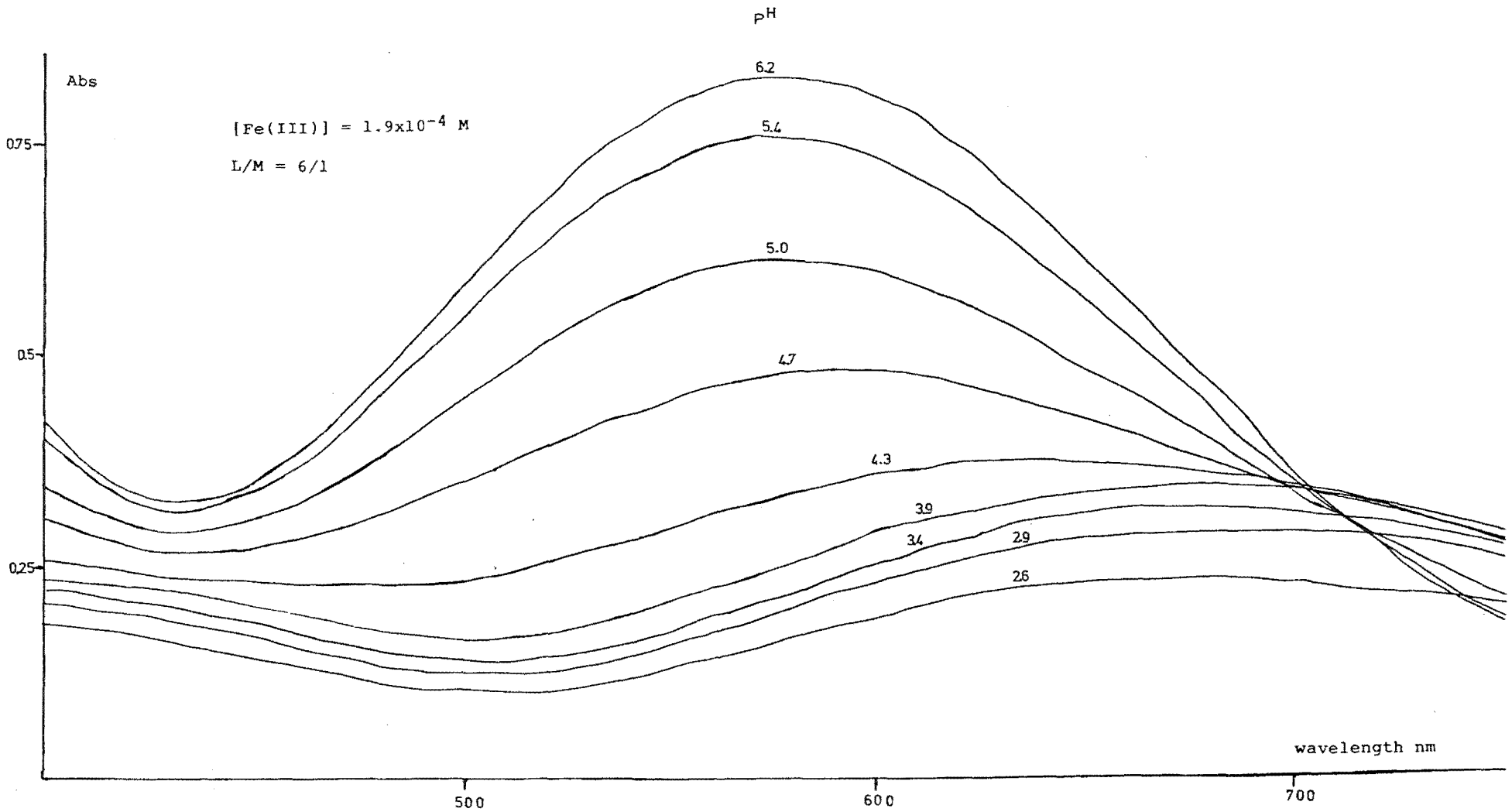

could be evaluated from spectrophotometric data; this calculation ignored the contribution from FeL_2OH.

The absorptions in the visible region of the spectrum at 575 and 489 nm, giving rise to dark blue and wine red colours respectively, reached maximum intensity at pH values consistent with the observed potentiometric titration end points for FeL_2 at pH 6 and the pH value corresponding to 100% FeL_3 formation (c. 9.1) respectively. Plots of Ab, the absorbance at a specified wavelength, against pH are called Vareille plots[191]. A Vareille plot confirmed the pH ranges at which the blue and red species remained at constant concentration (Figure 7.11).

Table 7.2 lists the value of K_{130} calculated from spectrophotometric data, using the general method described in Chapter 4 but modified for a metal-ligand system viz.

$$Ab = a_1.l.c_1 + a_2.l.c_2$$

$$c_1 + c_2 = Fe_T,$$

$$\text{and} \quad c_2 = Ab - a_1.Fe_T /(a_2 - a_1)$$

where the subscripts 1 and 2 refer to ML_2 and ML_3 respectively. The equilibrium reaction for the tris complex is (7.9). $[ML_3]$ and $[ML_2]$ were calculated from the above equations and $[L^{-3}]$ was calculated from the known protonation constants for protocatechuic acid and the measured hydrogen ion concentration. Table 7.5 summarizes the calculated quantities used in the determination of K_{130}.

7.6 Coordination mode for B2

The visible absorption spectra of Fe(III)-polyphenol complexes have been studied to elucidate the preferred mode

Figure 7.11 Vareille plots for protocatechuic acid-Fe(III), 1cm cell

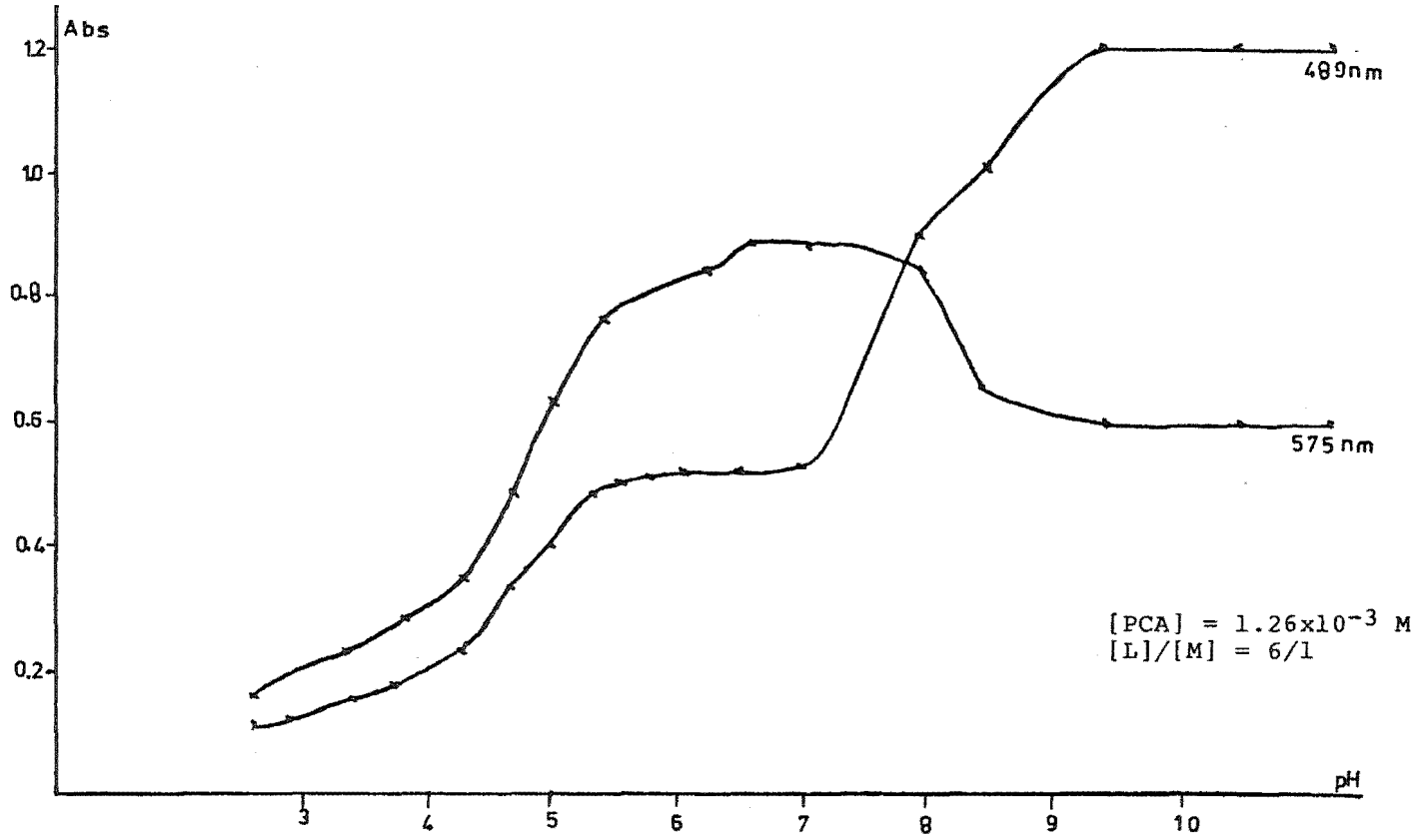

Table 7.5 Calculation of the apparent equilibrium constant for

$FeL_2 + L \rightleftharpoons FeL_3$ where L = protocatechuic acid

pH	absorbance	$[ML_2]x10^5$	$[ML_3]x10^5$	$[L^{3-}]x10^9$	log K
8.346	0.485[a]	1.602	7.846	1.609	9.48
7.761	0.361	5.286	4.193	0.149	9.72
8.346	0.290[b]	2.432	7.016	1.609	9.25
7.761	0.340	5.848	3.600	0.149	9.61

a wavelength 489 nm
b wavelength 575 nm

of coordination of B2 towards Fe(III); that is to determine whether B2 can act as a bi-, tri- or tetradentate ligand.

It is inferred that the epicatechin dimer B2 is unable to act as a tetradentate ligand supplying four B ring phenolate groups to the central metal atom (see Chapter 6 Figure 6.8). This inference is based on (i) the observed severe strain in molecular models when B2 supplies 2 B rings to Fe(III), and (ii) the similar pH range of the first two buffer zones in the titration of B2/Al(III) and catechin/Al(III) respectively.

In addition molar ratio plots were used to determine the complex stoichiometry at a known pH. These are plots of absorbance at a fixed wavelength against moles Fe(III) added. Data were compared for epicatechin and B2.

a) Epicatechin. Titration of Fe(III) into an epicatechin solution (7.4×10^{-4} M) maintained at pH 6.9 caused an absorbance maximum to develop in the visible spectrum at 565 nm. The pH value of 6.9 was chosen because it corresponded to the observed end point for bis complex formation in the catechol-iron system[154]. The absorbance maximum is similar to that reported[154] for the catechol bis species (573 $\pm$ 5 nm). The maximum intensity at 565 nm was reached at a L/M ratio of 2.0. Table 7.6 lists the data used to generate the molar ratio plot shown in Figure 7.12.

Table 7.6 Data used for the spectrophotometric analysis of epicatechin[a]-Fe(III) complexes at pH 6.9, 25°C

absorbance[b]	moles Fe(III) x10^5 added	[L]/[M]
0.554	0.618	6.0
1.036	1.236	3.0
1.263	1.502	2.5
1.328	1.870	2.0
1.320	2.070	1.8

a epicatechin = 3.71×10^{-5} moles
b wavelength 565 nm

The plot has an inflexion near L/M = 2.0, indicating that the stoichiometry of the complex is 2:1. Ratios significantly lower than 2.0 could not be studied because when this ratio was exceeded the excess Fe(III) may have precipitated as $Fe(OH)_3$, interfering with further spectrophotometric analysis.

The extinction coefficient calculated for $Fe(epicatechin)_2$ was 4200 $\pm$ 100 $mol^{-1}l\ cm^{-1}$ (cf. 3530 reported for the *bis* catecholate species[154]).

b) Epicatechin dimer, B2. The inferred stoichiometry of the B2-Fe(III) complex at a pH of 6.9 is two B2 molecules (or four B rings) per Fe(III) ion; i.e. only one B ring from each B2 molecule is involved in complexing.

However, as B2 has the capacity to act as a tetradentate ligand it was necessary to study this system with an excess of Fe(III) over B2 molecules. This was accomplished by having oxalic acid as an auxiliary complexing agent in the iron(III)-B2 solution, which

Figure 7.12 Molar ratios plot of a titration of Fe(III) against epicatechin at pH 6.9

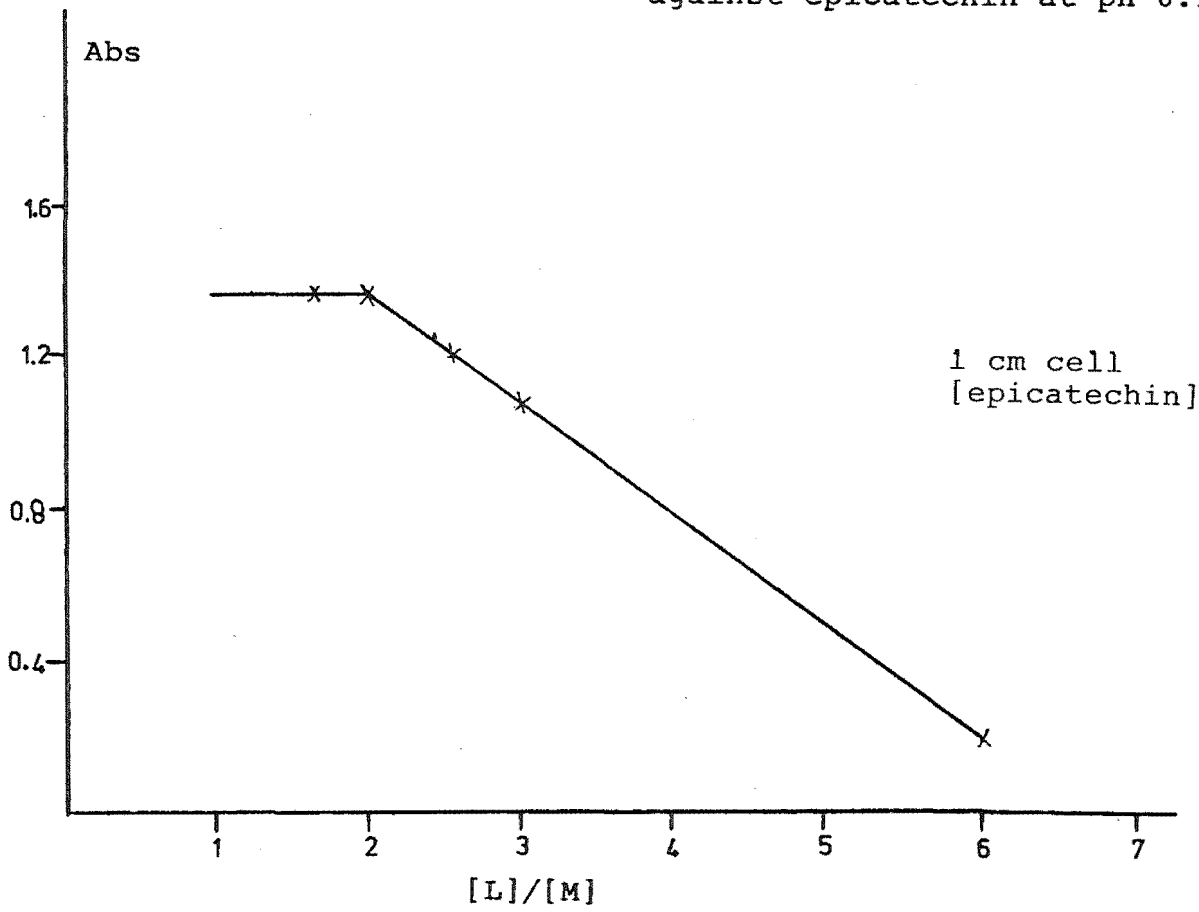

prevented any non-complexed Fe(III) from precipitating as $Fe(OH)_3$. Preliminary experiments with tiron and Fe(III) in the presence of oxalic acid indicated that the auxiliary complexing agent did not interfere with the bis complex formed by tiron.

Titration of Fe(III) into a B2 (1.0×10^{-4} M)-oxalic acid (1×10^{-3} M) solution held at pH 6.9 caused an initial absorbance maximum to form at c. 560 nm. The wavelength maximum remained constant at until the ligand/metal ratio was less than 2.0. At an L/M ratio of 1.75 the absorbance increased further and the maximum was shifted to 570 nm. This shift implied a change in coordination mode for the B2 complex. Table 7.7 lists the data used to generate the plot shown in Figure 7.13.

Table 7.7 Data used for the spectrophotometric analysis of B2[a]-Fe(III) complexes at pH 6.9, 25°C

absorbance[b]	moles Fe(III) $\times 10^5$ added	[L]/[M]
0.122	0.515	3.0
0.156	0.618	2.5
0.190	0.772	2.0
0.207	0.882	1.75
0.243	1.029	1.5
0.284	1.235	1.25
0.331	1.544	1.0
0.374	2.059	0.75
0.386	2.470	0.625

a B2 = 1.545×10^{-5} moles
b wavelength 560 nm

Figure 7.13 Molar ratios plot for solutions containing Fe(III) and B2 at pH 6.9

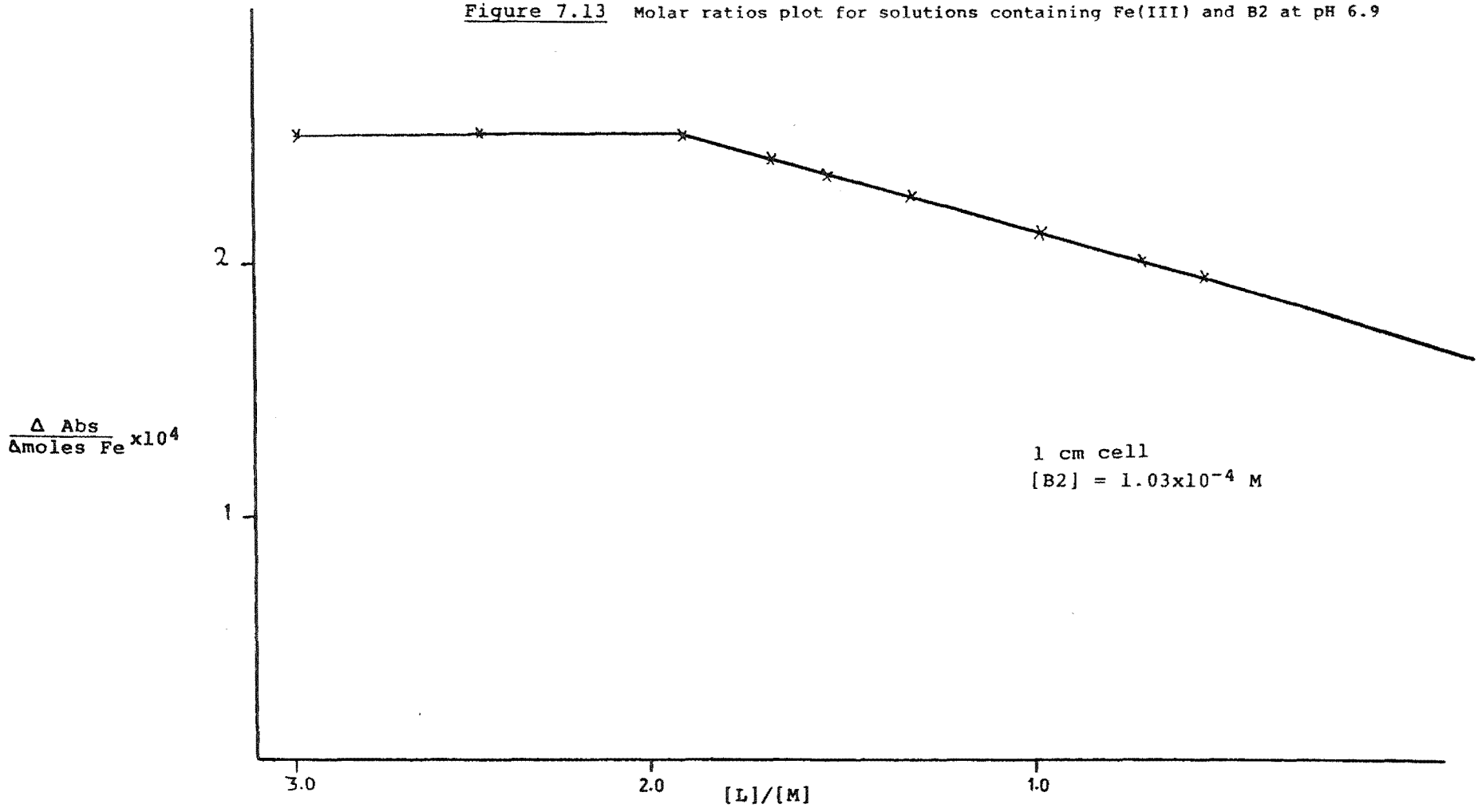

(Δabsorbance)/ Δ(moles of Fe(III) added) is plotted against the L/M ratio; the plot has an inflexion near [L]/[M] = 2.0 indicating that the stoichiometry of the complex is 2:1. The λ max at 560 nm indicates that 4 phenolate groups are coordinated to the central Fe(III) ion. Therefore when [B2] is greater than 2x[Fe(III)] the preferred mode of coordination is bidentate.
Further incremental addition of Fe(III) resulted in a smaller increase in absorbance than would be observed if a bis complex was continuing to form; that is the ratio (Δabsorbance)/ Δ(moles of Fe(III) added) decreased when the [L]/[M] ratio was less the 2.0 (see Figure 7.13). Thus Fe(III) added beyond a [L]/[M] ratio of 2/1 was coordinated by B2 but the shift in λmax and change in (Δabsorbance)/ Δ(moles of Fe(III) added) indicate that the mode of coordination was different.

It was found that the presence of oxalate lowered the extinction coefficient of the $Fe(B2)_2$ complex (cf. 3800 in the presence of oxalate, 4500 mol l^{-1} cm^{-1} for B2/Fe(III) only).

The extinction coefficient and the wavelength of maximum absorbance are similar for bis epicatechin and bis B2-iron(III) complexes; viz. 4200 mol l^{-1} cm^{-1}, 565 nm and 4500 mol l^{-1} cm^{-1}, 560 nm respectively. Hence it is inferred that the bis complexes for the monomer (epicatechin) and dimer (B2) have similar modes of coordination (see Chapter 6 Figure 6.8).

c) Epicatechin polymer, B13.

Solutions of ferric ion and B13 were prepared at pH 6.3 by slow addition of standard Fe(III) to a solution of B13, with compensating addition of alkali to keep the pH constant. Because of the uncertain composition of B13 only qualitative measurements were carried out.

At pH 6.8 a solution of Fe(III) (1.85×10^{-4} M) and B13 (c. 8.5x10-5 M) had an absorbance maximum at 570 nm with an absorbance of 0.722. The same absorbance was recorded after filtering the solution through a 0.45μm millipore membrane filter. No visible precipitate was observed on the membrane filter. The extinction coefficient at 570 nm was 3900 mol l^{-1} cm^{-1}. The wavelength and extinction coefficient are consistent with an Fe(III)-bis catecholate complex.

In Chapter 9 the preparation and analysis of solid B13 salts of Cu(II), Ca(II), Al(III) and Fe(III) are discussed.

7.7 Discussion

Stability constants obtained in this work are compared with those reported by other workers in Table 7.3. Migal et al.[153] used a spectrophotometric method to study the complex formation between Fe(III) and protocatechuic acid. They proposed the existence of three complexes (FeL, FeL_2 and FeL_3) but reported no precautions taken against the atmospheric oxidation of the ligand at pH > 7 and made no reference to the redox reaction (7.1). Their spectrophotometric curves did not show an isosbestic point below pH 4 but had a slight absorbance maximum at c. 400 nm

which possibly represents quinone formation. Hence their reported stability constants must be considered qualitative.

Mentasti et al.[184] investigated the complex formation between Fe(III) and a series of polyphenols including protocatechuic acid. These workers noted that complex formation is followed by redox decomposition, and therefore used a stopped-flow spectrophotometer to measure complex formation. Their value for log K_{110} (20.4) compares favourably with that reported here, 19.5.

Inclusion of the ternary complexes FeLOH and FeL_2OH in the equilibrium model removed the large residuals observed in the least squares analysis of pH-volume of titre data in the pH ranges 4.7 - 6 and 7.5 - 8.4. The refined constant for the hydrolysis of the FeL species has a sensible value, viz. log $'K_{11-1}$ (-4.8) < log β_{10-1} (-3.05); cf. AlOH and AlLOH cited in Chapter 6. The complex FeLOH has a concentration maxima at pH 5.4, at 55% of total metal.

The assignment of stoichiometry for FeL_2 was consistent with a sharp end point corresponding to the completion of the complexing reactions (7.7), (7.8) and deprotonation of the carboxyl group from all the protocatechuic acid. Other workers[170] have shown that analogous ligands (e.g. tiron) form complexes FeL, FeL_2 and FeL_3 in pH ranges consistent with those observed for protocatechuic acid.

As outlined in Chapter 6, FeLH was also included in the equilibrium model because the complex FeL formed in the pH range where the carboxyl group is only partially deprotonated. The log $'K_{111}$ value of 4.69 for the

protonation of FeL is greater than that for the carboxylate protonation of the free ligand, log K_{013} = 4.26 (cf. log 'K_{111} for AlLH was found to be 4.65). This difference has been explained for Al(III) in Chapter 6.

The carboxyl coordinated species $FeLH_2$ was included in the equilibrium model because it had improved the fit obtained in the Al-protocatechuic acid system. It was found to have only a small effect in the Fe(III) system because the minimum pH was not low enough for this species to contribute significantly to the solution stoichiometry. The maximum concentration of $FeLH_2$, 13% of total metal, was observed at pH c. 2.8. Hence the reported value of log 'K_{112} has a large error, but the refined value c. 4.5 is similar to that reported for formation of the Fe(III) benzoate complex (log K 5.34[192]).

For each datum point in a least squares analysis the concentrations of the Fe(III) hydrolysis species were calculated and expressed as a % of the total [Fe(III)]. The concentration of these species totalled < 0.1% of total metal at pH values greater than 7, but at pH values less than 6 significant concentrations of FeOH and $Fe(OH)_2$ were computed. FeOH was 7.0% of total metal at pH 2.8 but decreased to less than 0.1% at pH 5.3 $Fe(OH)_2$ had a maximum concentration of 5.9% at pH 4.5. The overall distribution of these hydrolysis species can be seen in Figure 7.9.

Also calculated at each datum point was the product $[Fe(III)][OH]^3$. This value was then compared to a literature value for the concentration solubility product of

ferric hydroxide, which was not exceeded at any point in the titration.

The collection of spectra over the pH range in which FeL_3 was forming permitted the equilibrium constant $'K_{130}$ to be evaluated. The average value obtained does not compare favourably with the value obtained from least squares analysis of potentiometric data. This is ascribed to the presence of the FeL_2OH species.

Because of redox reaction (7.1) it was not possible to collect meaningful potentiometric data below pH 5.5 for epicatechin or its dimer or polymer. However, from spectrophotometric analysis it was determined that epicatechin, its dimer B2 and its polymer B13 form bis complexes with similar spectrophotometric characteristics; viz. wavelength maxima and corresponding extinction coefficients were 565, 4200; 560, 4500; 567 nm, 3900 mol l^{-1} cm^{-1} respectively.

From a plot of $(\Delta$absorbance$)/\Delta$(moles of Fe(III) added) versus the ratio Fe(III)/B2 it was established that B2 acts as a bidentate ligand towards Fe(III), i.e. it is not able to coordinate both its B rings via their phenolate oxygens. Hence it is inferred that the $Fe(B2)_2$ complex will form at a similar pH to $Fe(epicatechin)_2$ (cf. $Al(B2)_2$ and $Al(epicatechin)_2$ discussed in Chapter 6.).

CHAPTER 8

SOIL TESTS

Information on the concentrations of readily exchangeable aluminium and iron in soils help to classify horizon types. This information is normally derived from laboratory analyses, but it would be of value at the time of field sampling. Further, if the oxidation state of iron is known, this can indicate whether the soil conditions are reducing or oxidizing.

Thus simple tests that could be applied in the field to obtain semi-quantitative information on the concentration and oxidation state of iron and the concentration of aluminium may be of value. They would allow comparison of the concentrations of these metals down a soil profile and aid in the choice of samples to be taken back to the laboratory for further analysis.

This chapter describes the development of field tests for semi-quantitative determination of iron and aluminium in soil.

The ferrous ion test is a modification of the quantitative iron(II) test developed in Chapter 7. Use is made of the masking effect of NTA to prevent Fe(III) interference.

The aluminium test was developed using buffered chrome azurol-S, CAS, as the colourimetric reagent for Al(III). The Al(III) hydrolysis products that react with this aluminium indicator were investigated. The major

interfering species Fe(III) was masked by reduction to Fe(II) with ascorbic acid. In the development stage, this test was used in the laboratory to semi-quantitatively measure exchangeable Al(III)[193] for several horizons form a number of different soil profiles. Methods for the use of this test in the field are discussed.

8.1 Ferrous ion soil test

8.1.1 Introduction

The presence of ferrous ion in soils may imply that the soil conditions are reducing. The movement of iron down a soil profile is a key indicator used to identify podzolized soils; hence reduction of Fe(III) to the more soluble and therefore mobile Fe(II) is important in consideration of the mode of transport for iron.

Ferrous ion is known to rapidly oxidize to ferric ion in weakly acidic solutions when it is exposed to the atmosphere. Therefore a simple test that permits the identification of ferrous ion in the field would be of value because transport of a soil back to the laboratory for analysis may result in iron(II) oxidation.

Two field tests for ferrous ion have been reported. Richardson and Hole[194] employed the iron(II) indicator 1,10-phenanthroline, whereas Childs[195] used 2,2'-bipyridyl because the colour of its deep red iron(II) complex is further removed from natural soil colours (cf. 1,10-phenanthroline which forms a reddy-brown complex with iron(II)). However, neither of these workers employed a masking agent for iron(III) to prevent its reduction. It has been shown (see Chapter 7) that many ligands found in

soils, including polyphenols, can reduce Fe(III) to Fe(II) especially when in the presence of an iron(II) complexing agent such as 2,2'-bipyridyl. Hence positive ferrous ion tests may result from ferric ion bound to oxidizable organic matter.

It was found in this work that nitrilotriacetic acid will complex with iron(III) and prevent its reduction in the presence of 2,2'-bipyridyl. Thus the quantitative method for the spectrophotometric determination of Fe(II) described in Chapter 7 was adapted for field work.

A second field analysis could be simply executed by omitting the NTA from the test solution. The development of a more intense colour in the sample than when NTA was included implied that redox-active ferric organic complexes were initially present.

8.1.2 Ferrous test

The development of an analytical test for ferrous ion is described in Chapter 7. The Fe(II) was complexed with 2,2'-bipyridyl (0.01%) and the Fe(III) masking agent NTA was added (0.025 M). Ammonium acetate (1 M, pH 7) was used as a buffer. The masking of iron(III) by NTA in the presence of 2,2'-bipyridyl and phenolic ligands has been confirmed for samples exposed to direct light for up to 60 min (see Chapter 7, Section 7.1.2).

Two buffered reagent solutions were prepared, one containing 2,2'-bipyridyl and NTA (reagent A) and the other 2,2'-bipyridyl only (reagent B).

In a typical field test small samples of soil (c. 1 g) were placed in vials containing reagents A and B

respectively (5 ml). The solution colours were observed and compared after 5 min in the light (or dark).

8.1.3 Results

The soil test outlined in Section 8.1.2 has been applied to a series of gley podzol soils (see Table 8.1). It should be noted that the results from these tests, and therefore the conclusions are valid only for the time and place of sampling.

The development of colour for a test solution containing reagent A indicated that ferrous ion was present in the soil solution. The development of a more intense colour for a test sample in reagent B than in reagent A (where both samples are in the dark) implied that redox active ferric organic complexes also were initially present in the soil solution. Further, if a test sample in reagent B developed a more intense colour in the light than in the dark then the presence of light sensitive redox active ferric organic complexes was inferred (e.g. citrate, oxalate).

If a semi-quantitative estimate of the Fe(II) concentration was required, then the sample colours could be compared with those for standard Fe(II) solutions.

8.1.4 Discussion

Any field test is limited by how reproducibly and representatively a particular soil can be sampled. For even qualitative interpretation it must be emphasized that the high variability of soil composition may be a limiting factor. For example, in these tests distinctly different

Table 8.1 Field test results for ferrous iron and ferric-organic complexes in gley soils[a]

Horizon	reagent	result	conclusion
Alg (0-16 cm)	A[b]	.weak test (5 min)	some Fe(II) present
	B[c] (dark)	.weak test (5 min)	" " "
	B (light)	.strong test (5 min)	light sensitive Fe(III)-organic complexes
A2g (16-30 cm)	A	.weak test (5 min)	some Fe(II) presnt
	B (dark)	immediate colour stronger than for Alg	readily reduced Fe(III)-organic complexes
	B (light)	similar intensity to dark test	
A1 (0-20 cm)	A	weak test (10 min)	some Fe(II) present.
	B (dark)	weak test (10 min)	no reducible Fe(III)-organic complexes
	B (light)	weak test (10 min)	
A21g (30-37 cm)	A	no colour	no Fe(II) present
	B (light)	no colour	

a "v. weak" < 0.5 ppm Fe(II) in solution; "weak" 0.5 -1.0 ppm; "strong" > 2 ppm
b NTA-2',2-bipyridyl see Section 8.1.2
c 2',2-bipyridyl see Section 8.1.2

colour responses have been observed for samples taken in close proximity in a profile.

The results given in Table 8.1 indicate the importance of a masking agent for Fe(III). When NTA was omitted from the reagent solution (i.e. solution B) an intense positive test was obtained for Fe(II) in three of the soils tested, whereas in the presence of NTA (reagent A) only a slight positive test was obtained. From the former result an incorrect assumption could be made concerning the oxidation state of iron in the soil.

Two field tests have been reported which employ colourimetric reagents for ferrous iron; neither used a masking agent for ferric iron. Richardson and Hole[194] reported the use of unbuffered 1,10-phenanthroline. This test when used on soils containing redox active iron(III) complexes would give a positive ferrous colour, even if no Fe(II) was initially present. Further, the use of KCl electrolyte which is known to lower the the pH of soil solution[196], may promote the instantaneous reduction of certain iron(III) complexes even in the absence of 1,10-phenanthroline. This would be pertinent if the pH was around 4, a value often encountered in podzolized soils.

Childs[195] reported two field tests for ferrous iron, both using 2,2'-bipyridyl in ammonium acetate buffer (pH 7). The tests exploit the photoreduction of ferric-organic complexes (e.g. citrate[197], oxalate[198]) to ferrous iron. If a more intense colour results for a sample in the light than in the dark it is inferred that photoreduction of Fe(III) has occurred. The second test, involving colour

development in the dark, is used to determine if ferrous ion was initially present. Childs stated that buffering solutions to pH 7 reduces the rate at which redox active Fe(III)-organic complexes are decomposed to produce ferrous iron. However it has been shown in Chapter 7 that when an Fe(II) complexing agent such as 2,2'-bipyridyl is present Fe(III) reduction can occur rapidly (min) at pH 7; i.e. the bipyridyl increases the reduction potential of the Fe(III)/Fe(II) couple. Hence at pH 7 Childs' field test may give a positive colour even in the dark if ferrous ions are absent but redox active Fe(III)-organic species are present.

8.2 Al(III) soil test

8.2.1 Selection of a colourimetric reagent

A literature survey revealed that many methods exist for the spectrophotometric determination of aluminium[199]. Although most of these tests have adequate sensitivity for measurements on soil solutions (< 1 ppm Al(III)) they are limited to laboratory use because of the special conditions required for colour development. For example, many reagents form a coloured "lake" with aluminium for which heating is required, and experimental variables must be carefully controlled to ensure reproducible results. Furthermore, once formed, the lakes are not stable with time.

For a field method to be of use it must be rapid and specific for aluminium and the reagents should require minimal manipulation to produce a colour. The eye must also be able to clearly detect a colour change for different concentrations of Al(III).

Two colourimetric reagents with suitable characteristics were selected, pyrocatechol violet (3,3',4'-trihydroxyfuchsone-2''-sulfonic acid), PCV (8.1) and chrome azurol S (3''-sulpho-2'',6''-dichloro-3,3'-dimethyl-4'-hydroxyfuchson-5,5'-dicarboxylic acid), CAS (8.2).

For PCV it was found that the pH for colour development (metal complexing) was c. 6. However, Al(III) solutions at this pH were found to quickly polymerize (s) to a form or forms that were unreactive with PCV. Therefore with this reagent it was necessary to first add acidic PCV to the aluminium sample, or vice versa; this step was followed by a buffer to provide pH control and hence to develop the colour. The acidic conditions could labilize inorganic or organic forms of aluminium. Further, once the buffer was added no more sample or reagent could be added to improve colour development because of partial polymerization of the aluminium. These factors represent disadvantages for field work. With this reagent uncertain knowledge of Al(III) levels may necessitate preparation of a series of test solutions if insufficient (or excess) Al(III) was present to cause a distinct colour change.

For this reason, it was decided to employ CAS which complexes with Al(III) at a lower pH by virtue of the more acidic protons on the donor oxygens. At this pH (4.9) aluminium does not polymerize to an unreactive form on the time scale of the experiment. It was possible to add sample, reagent or buffer in any order and still obtain the same immediate colour change for a given Al(III)

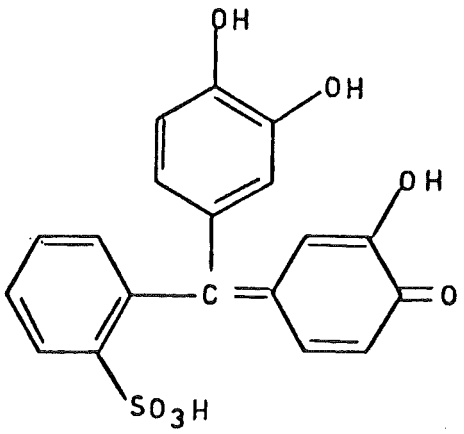

PCV(8.1)

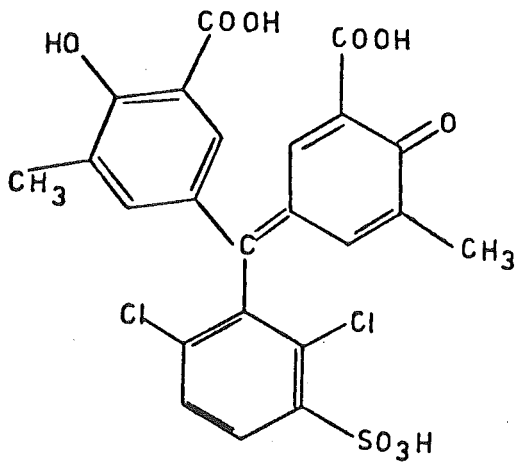

CAS(8.2)

concentration; viz. the same change in absorbance and λ max on coordination (see Figure 8.1).

8.2.2 Selection of solution conditions for CAS-aluminium complexing

This section outlines the preliminary tests that gave information on the properties of CAS and the solution conditions necessary for colour development.

a) Purity of CAS reagent. The tetra-acidic form of CAS was prepared by acid precipitation from a concentrated solution (20% w/v) as described by Langmyhr[200]. A quantitative potentiometric titration of standard KOH against a solution of CAS (8.2×10^{-4} M) resulted in an end point at pH 7.0, which corresponded to the removal of three protons and confirmed the purity of the reagent (see Figure 8.2). Colour changes were observed at pH c. 4.2 (red to orange) and c. 6 (orange to yellow), indicating a changing electronic environment for the CAS entity, i.e. deprotonation. Data from a titration of standard KOH against a solution of CAS (8.2×10^{-4} M) and Al(III) (3.7×10^{-4} M) are presented as curve b in Figure 8.2. The Al-ligand titration curve was depressed relative to the ligand only curve and the solution exhibited a colour change from red to violet at pH c. 4.1 which indicated the start of complex formation. A stoichiometric end point was observed at pH 6; it corresponded to the formation of an Al(III)-CAS complex for which one weakly acidic proton had been forced from the ligand by metal coordination. Above pH 7.5 further buffering was exhibited but no additional end points were observed.

Figure 8.1 Spectrophotometric curves for CAS and for CAS-Al(III), pH 4.9 , [Al(III)]=2×10^{-5}M, [CAS]=1.68×10^{-4}M

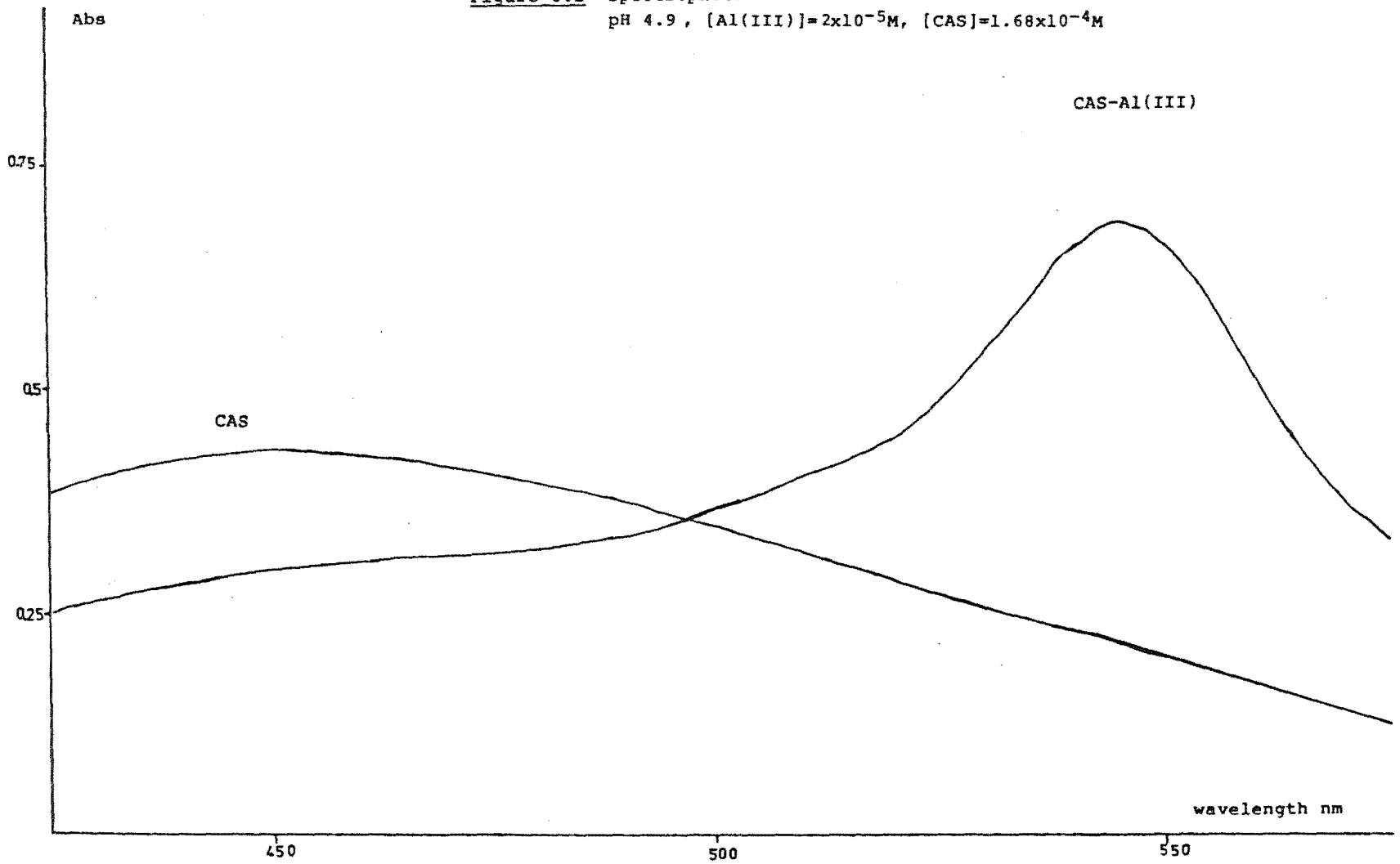

Figure 8.2 Potentiometric titration of (a) CAS only; (b) CAS-Al(III)

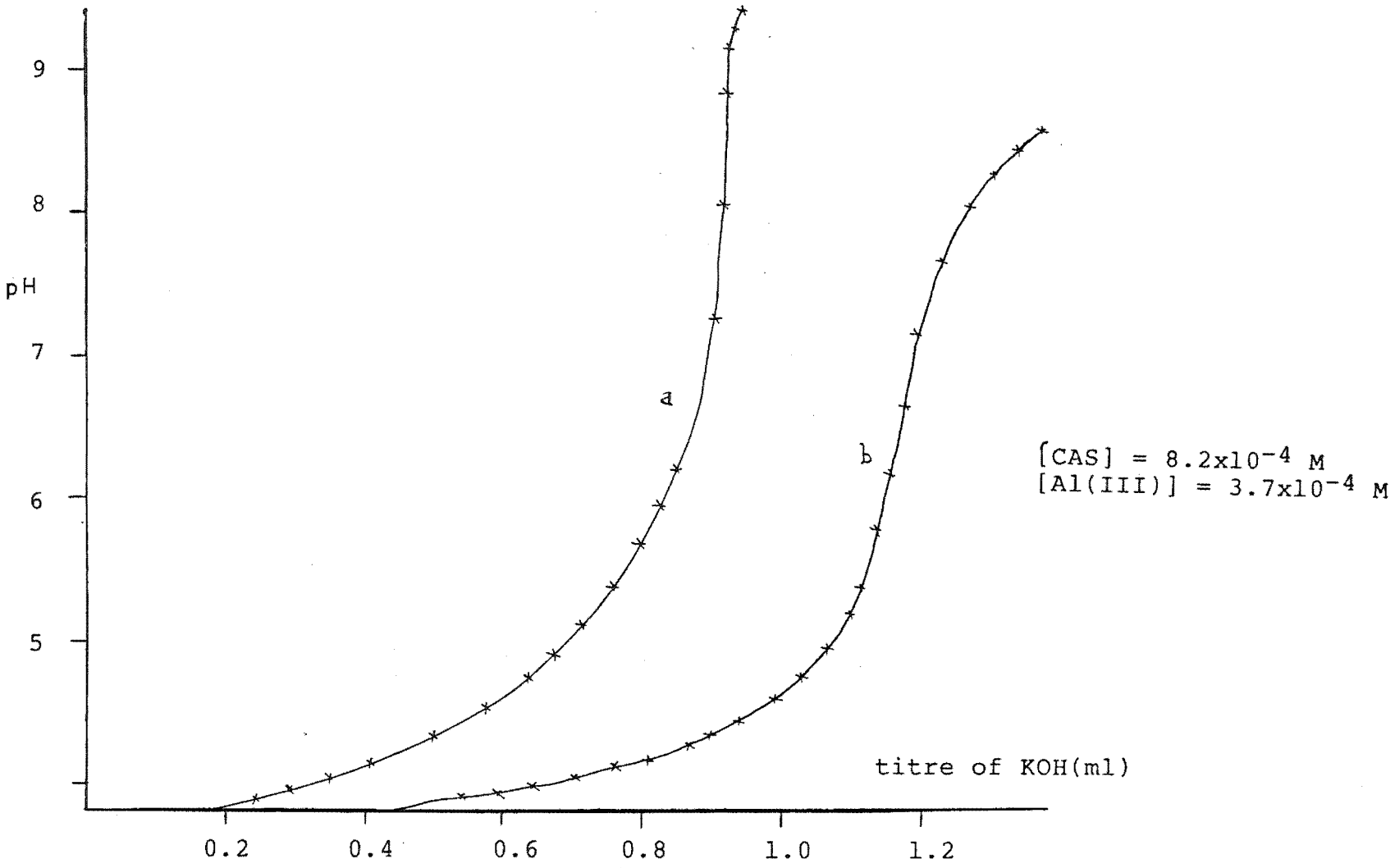

At selected pH values visible absorption spectra were recorded for CAS and CAS-Al(III) solutions. Figure 8.3 plots the absorbance at 544 nm against pH. At pH > 8.2 the spectra for CAS and CAS-Al(III) solutions were identical; this indicated that the Al(III)-CAS complex formed at lower pH had probably dissociated. Therefore the additional buffering observed in the potentiometric titration of an Al(III)-CAS solution at this pH could be ascribed to the formation of Al(III) hydroxo species.

The data represented in Figure 8.3 are similar to absorbance-pH data reported by Pakalns[201].

b) Effect of buffer type and concentration on colour development.

The absorbances for Al(III)-CAS solutions containing different buffers at varying concentrations are summarized in Table 8.2. It was found that the acetic acid/acetate buffer at high concentrations severely interfered with colour development. Pakalns reported a similar effect[201]. A similar but much less pronounced effect was noted for hexamine, and this buffer (0.2 M, pH 4.9) was chosen for all further work.

A small but measurable difference was noted when the ionic strength was varied. Hence for quantitative measurements of [Al(III)] ionic strength was maintained at 0.2 M.

c) Rate of colour development, and colour stability.

Figure 8.4 is a graphical representation of CAS-Al(III) colour development versus time. Curve x represents an addition of 0.2 ml of CAS reagent (2.8×10^{-3} M)

Figure 8.3 Absorbance-pH curves at 544nm

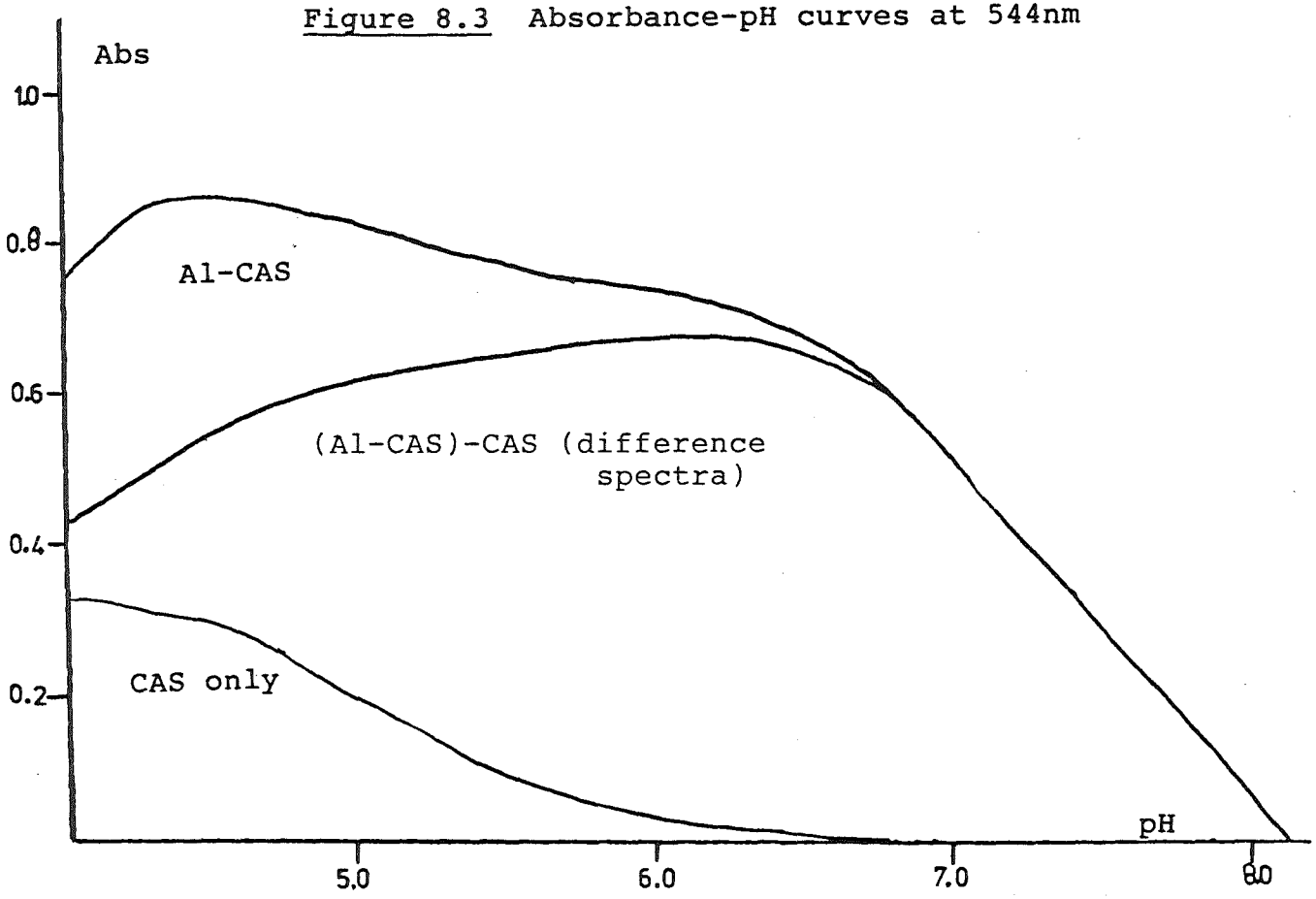

Table 8.2 Effect of solution conditions on CAS colour development[a]

buffer	ionic strength	absorbance[b]
acetic acid/acetate[c]	0.1	0.705
acetic acid/acetate	0.2	0.505
acetic acid/acetate	0.5	0.284
hexamine[d]	0.1	0.696
hexamine	0.2	0.644
hexamine (0.5 M)	0.5	0.576
hexamine (0.2 M)	0.3[e]	0.670
hexamine (0.2 M)	0.7	0.658

a [CAS] = 2.8×10^{-3} M, Al(III) = 0.27ppm

b λ max = 544 nm

c pH = 4.7

d pH = 4.9

e Ionic strength = buffer + KCl

Figure 8.4 Colour development for Al(III)-CAS complex with time. λ=544nm, pH 4.9

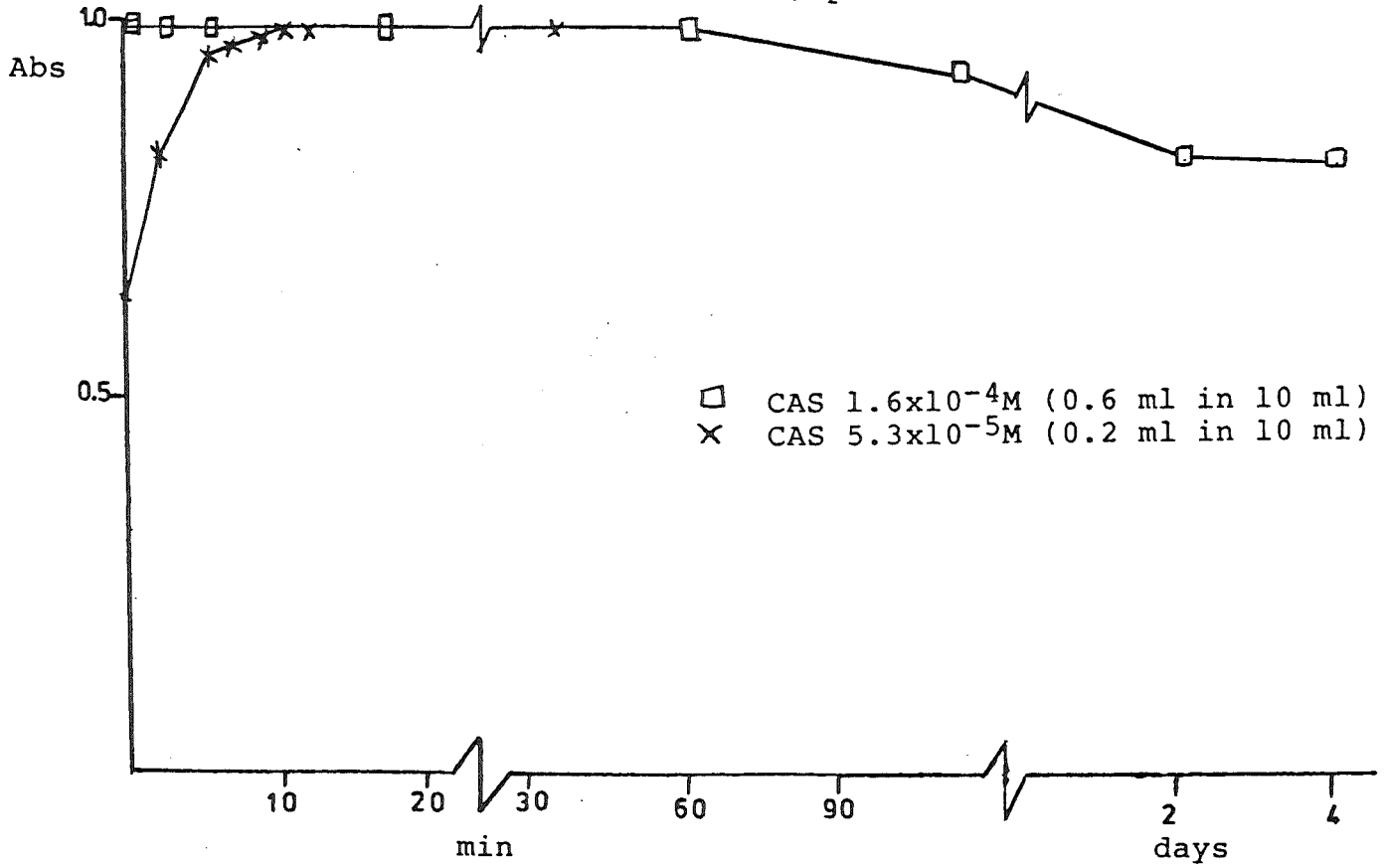

to a final sample volume of 10 ml; this concentration of CAS required c. 10 min for complete colour development. It was found that by increasing the final concentration of CAS by a factor of three (0.6 ml, 2.8×10^{-3} M) the time taken for full colour development was c. 1 min (curve □ Figure 8.4). Therefore this reagent composition was used.

The absorbance of the CAS reagent solution when buffered at pH 4.9 was invariant with time. It was also found that the CAS-Al(III) complex was stable with time (days) after an initial period of one day in which a 10% loss of absorbance was established for a series of standard solutions (0, 0.14, 0.27, and 0.4 ppm); this change was not apparent to the eye.

d) Absorbance versus concentration.

At 544 nm the absorbance was linearly related to Al(III) concentration in the range 0.03 - 0.8 ppm (1 cm cell). However at this wavelength the calibration curve did not pass through the origin (see Figure 8.5). The absorbances at 544 nm were corrected for a small contribution from uncomplexed CAS, based on changes in the absorbance maximum at 442 nm for uncoordinated ligand.

It has been reported that surfactants may enhance the bathochromic shift observed upon metal complexing by colourimetric reagents; i.e. there will be an enhancement of the spectral colour change. This shift which results from further deprotonation of the hydroxyl groups on the CAS molecule[202] is often accompanied by an increase in the extinction coefficient for the metal complex.

Figure 8.5 Typical Al(III)-CAS calibration curve, 1 cm cell

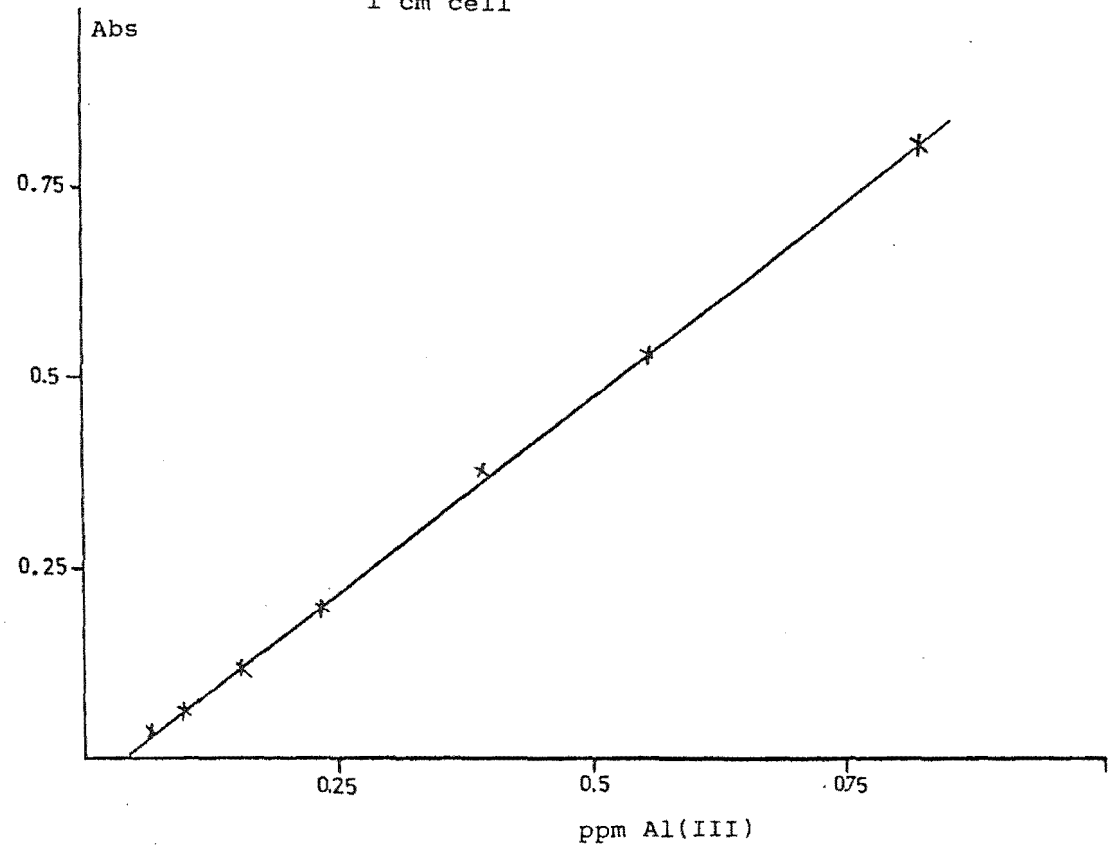

The surfactant cetyltrimethylammonium bromide, CTAB (0.5 ml, $5x10^{-3}$ M) was added to CAS-Al(III) solutions ([Al(III)]: 0, 0.27, 0.54 ppm). The result was a shift in the ligand absorption maximum to c. 500 nm (with a corresponding colour change from yellow to red for solutions containing ligand only), and a shift in the absorption maximum for the Al(III)-CAS complex to a wavelength > 600 nm. This shift did not provide an enhanced visual colour recognition. Further, it was found that the CTAB-Al(III)-CAS colour was not stable with time (h) (cf. days for Al(III)-CAS) and the coloured surfactant adduct was adsorbed onto the sample bottle. A similar behaviour for this surfactant was reported by West et al.[202]. This adsorbed complex could only be removed by soaking the sample bottle in concentrated acid. The surfactant was not used in the laboratory or field test for Al(III).

e) Examination of interferences.

It has been reported that CAS forms stable intensely coloured complexes with many metal ions[202], for example Be^{2+}, Cu^{2+}, Fe^{3+}, Th^{4+}, Ti^{4+} and Zr^{4+}. Of these only Fe(III) may be expected in significant concentrations in soil solutions. Table 8.3 lists the compounds and ions tested for interference in the colourimetric determination of Al(III) by CAS.

f) Masking of interferants.

The interference of iron(III) can be masked by ascorbic acid. Ascorbic acid reduces iron(III) to iron(II) which does not form a complex with CAS. One millilitre of 1% (w/v) ascorbic acid was sufficient to mask 20 ppm of

Table 8.3 Interferences in the determination of Al with CAS

Test species	conc (ppm)	Al(III) taken (ppm)	Al(III) found (ppm)	%error	colour
PO_4	80	0	0	0	nc
PO_4	80	0.54	0.32	-41	slight
F	1.9	0	0	0	nc
F	1.9	0.54	0.03	-94	no colour
Ca	80	0	0.02		nc
Ca	80	0.54	0.489	-9	nc
Mg	8	0	0	0	nc
Mg	8	0.54	0.48	-10	nc
Cu	71	0	0	0	nc
Cu	71	0.54	0.51	-5	nc
H_4SiO_4	200	0	0	0	nc
H_4SiO_4	200	0.54	0.08	-85	no colour
H_4SiO_4	20	0.54	0.52	-4	nc
Fulvic acid	6mg l^{-1}	0.54	0.54	0	nc
Fe(III)	0.8	0.54	>1.4	>100	

KEY nc = no change

Fe(III). The reduction of Fe(III) was rapid and > 99% complete in c. 3 min even if the iron(III) was complexed with CAS prior to the addition of the ascorbic acid.

g) Chromophore stability.

Solutions of CAS (c. $3x10^{-3}$ M) were found to be stable for at least 2 months when stored in opaque plastic bottles.

8.3 Reactivity of aluminium hydroxo species with CAS

To test the reactivity of CAS towards solutions containing monomeric and polymeric aluminium hydroxo species a series of Al(III) solutions in the pH range 4.5 - 6.5 were prepared.

8.3.1 Preparation of hydrolyzed aluminium solutions

Acidic solutions of Al(III) ($1x10^{-4}$ M) were prepared by adding a known amount of standard Al(III) to 50 ml of CO_2 free DDW contained in polypropylene bottles (25°C, 1 M KCl). The high ionic strength was employed because (i) the field test for Al(III) used 1 M KCl as the Al(III) exchanging reagent, and (ii) the aluminium(III) hydrolysis constants used it the computer evaluation of solution stoichiometry (appendix M) were those published by Mesmer et al.[147] for 1.0 M (KCl) solution.

The acidic Al(III) solutions were adjusted to pH values in the range 4.5 - 6.5 by the addition of KOH from a micrometer syringe. Care was taken to keep the solutions free of carbon dioxide by bubbling nitrogen (CO_2 scrubbed) through the aluminium solutions when the screw top was removed from the bottle for pH measurements.

After the addition of KOH significant pH drift was detected; thus the initial pH measurements were only

approximate. After one day, and before any analytical measurements were made on the solutions, the pH was remeasured; Table 8.4 lists the variation of pH with time for each sample.

8.3.2 Analysis of Al(III) solutions

To determine which fraction of Al(III) reacted with CAS three different methods of analysis were employed:

i) A sample was removed from the polypropylene bottle and centrifuged at 2500 rpm for 30 min. An aliquot was then removed from the top 1 cm of the supernatant solution and analysed by the CAS method. The spectrum was periodically checked for changes in absorbance, for up to 60 min.

ii) Part of the sample obtained in (i) was acidified to pH 2 with HCl and allowed to digest for 30 min on a steam bath. After cooling to room temperature an aliquot was analysed by the CAS method; the result represented the total aluminium concentration in solution.

iii) A sample of uncentrifuged aluminium solution was added to the CAS reagent solution and then centrifuged for 10 min at 2500 rpm. A sample was removed from the top 1 cm of the supernatant and the spectrum recorded (400 - 600 nm). The spectrum was checked periodically for changes in absorbance, up to 60 min.

8.3.3 Results

The hydrolyzed aluminium solutions had pH values ranging from 4.6 to 6.5. The analytical results for reactive Al(III) (methods (i) and (iii)) and total Al(III) in solution (method (ii)) are listed in Table 8.5.

Table 8.4 Variation of pH with time for hydrolyzed Al(III) solutions

solution	initial	1 day	2 day	3 day
1	4.62	4.62		
2	4.62	4.81	4.77	4.78
3	5.17		5.10	5.08
4	5.79	5.19		
5	5.54	5.53	5.22	5.22
6	5.54	5.50		
7	5.68	5.67		
8	6.35	6.41	6.52	6.51

Table 8.5 Analysis of hydrolyzed Al(III) solutions[a]

pH	total Al(III) in solution[b] ($x10^4$)	reactive Al(III) in supernatant[c] ($x10^4$)	calculated $Al_{13}(OH)_{32}$ ($x10^4$)[d]	reactive Al(III) in solution[e] ($x10^4$)
4.62	0.99	1.0	0	
4.78	1.0	0.97	0	0.87
5.08	1.0	0.67	0.56	0.59
5.19	0.89	0.63	0.63	
5.22	0.96	0.42	0.72	0.34
5.50	0.52	0.13	0.43	
5.67	0.31	0.1	0.24	
6.51	0.65	0.0	0.56	0[f]

a Initial total Al(III) $1x10^{-4}$ M
b Acid digestion method (ii) Section 8.3.2
c determined by method (i) Section 8.3.2
d calculated from computer program listed in Appendix M
e determined by method (iii) Section 8.3.2
f a coloured precipitate was noted in the centrifuge tube

For the Al(III) solution at pH 6.5 precipitation was noted when buffered CAS was added prior to centrifuging. For solutions analysed by methods (i) and (iii) no absorbance increases with time were noted.

For analysis of exchangeable aluminium in soils samples (2 g) were mixed with 1 M KCl (20 ml) and shaken for ten minutes. The decanted solution was centrifuged at 2500 rpm for 30 min and filtered through a 0.45μm Millipore membrane filter to remove organic matter suspended in solution (e.g. small roots). The supernatant solution was then treated as described in i) and ii) Section 8.4.2. The results are listed in Table 8.6.

8.3.4 Reactivity of CAS towards hydrous aluminosilicates

Allophane and imogolite are hydrous aluminosilicate clays that are often found in soils[203]. They often occur as cementing or coating materials in association with the fine clay fraction. They have insufficient long range order to be identified by X-ray powder diffraction. Imogolite is a semi-crystalline aluminosilicate which has a tubular structure; electron micrographs show it as a fibrous lattice between clay particles. Allophane is an aluminosilicate with spherical structure. Both compounds have hydroxo-aluminium surface layers. Farmer et al.[75] have reported that it is possible to detect the presence of these clays in soils by the unique infrared absorption band near 348 cm^{-1}. Synthetic imogolites, and the more poorly ordered precursor proto-imogolite, are reported[204] to exhibit infrared absorption spectra which are nearly identical to those of natural samples. In view of the possible role of

Table 8.6 Reactive and total Al(III) extracted from selected soils

soil	pH(H_2O)	reactive Al(III)[a] in supernatant (meq)	total Al(III)[b] in solution (meq)
SB 9567 F	5.0	0.94	1.57
SB 9738 C	5.7	0.43	0.51
SB 9749 B	5.4	0.13	0.16
SB 9749	5.5	0.60	0.70

a as determined by method (i) Section 8.3.2

b as determined by method (ii) Section 8.3.2

proto-imogolite in the transport of aluminium[42] (and iron[46]) in acidic soil solution it was decided to prepare and characterize synthetic imogolite and test the reactivity of CAS towards both this product and a natural sample of allophane.

a) Preparation. Imogolite was prepared by the method of Farmer et al.[44]. It was prepared in polypropylene bottles from a perchloric acid hydrolyzed solution of aluminium-t-butoxide (5.0×10^{-3} M) and silicon tetraethoxide (2.7×10^{-3} M); total solution volume 100 ml. The initial pH was adjusted to c. 4.4 and the solution was heated in a boiling water bath for 4 days. The pH was remeasured and found to be c. 3.3. The hydrous aluminosilicate was recovered by freeze drying.

b) Characterization of synthetic imogolite and natural allophane.

The observed drop in solution pH from 4.4 to 3.3 was consistent with imogolite formation[45] but was not definitive proof. The presence of a distinctive infrared absorption band at 348 cm^{-1} confirmed the formation of imogolite (see Figure 8.6). As indicated by Farmer[75], it was necessary to heat the imogolite sample at 150°C for 16 hours to obtain a spectrum showing the required absortion. Not all preparations for which the distinctive drop in solution pH was noted gave the 348 cm^{-1} band in their infrared spectra. The infrared spectrum obtained for a sample of Silica Springs allophane, curve c in Figure 8.6, was similar to that reported[203]; it had a band at 348 cm^{-1}.

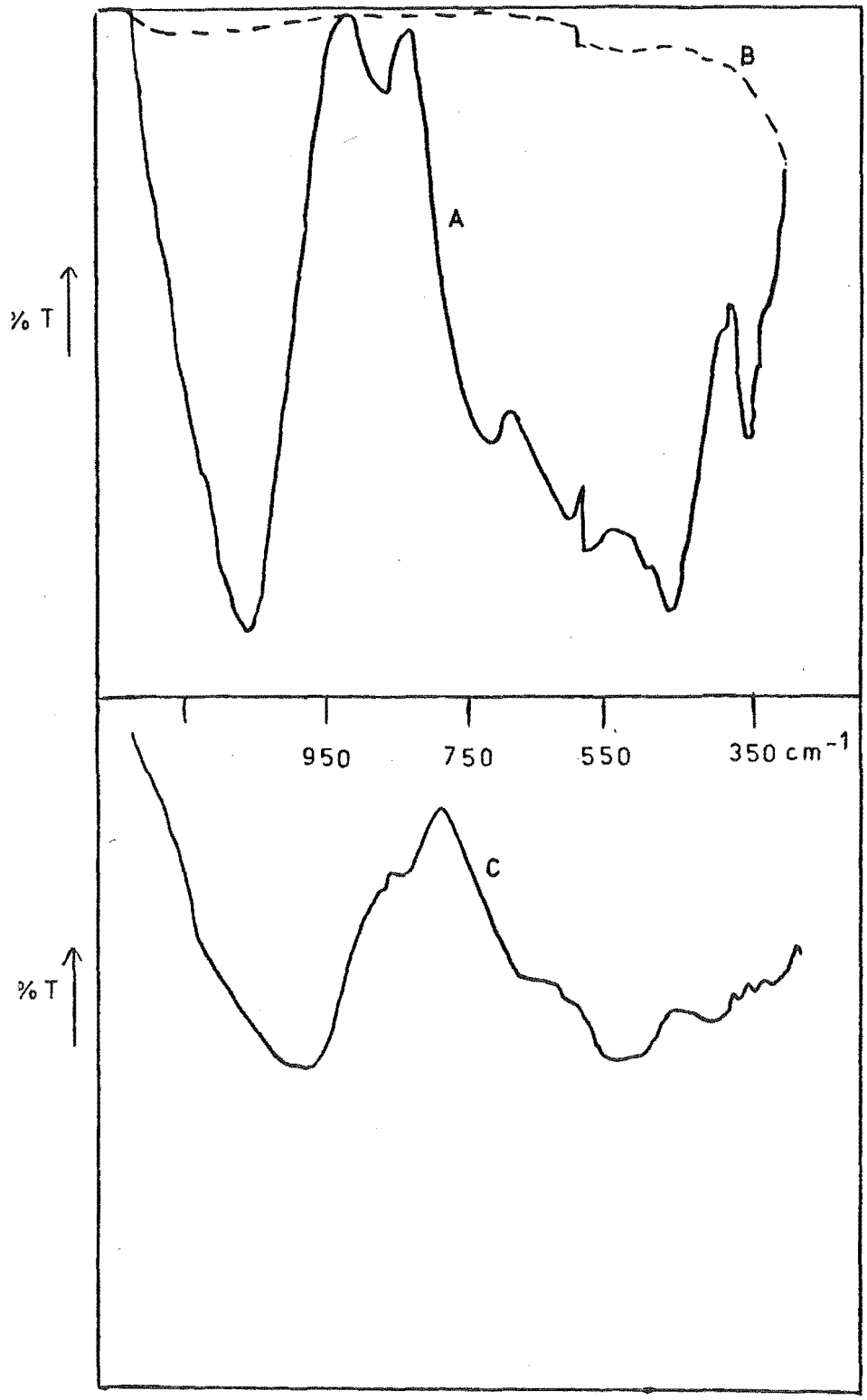

Figure 8.6 IR absorption spectra

A-imogolite 3 mg/500 mg KBr, heated at 150°C for 16h
B-KBr disc heated at 150°C for 16h
C-Silica Springs allophane 8 mg/500 mg KBr,
heated at 150°C for 16h

The reactivity of allophane and imogolite toward CAS was determined as follows: Silica Springs allophane (7 mg) and imogolite (3 mg) were placed in separate flasks with 5 ml DDW, and left overnight. A calculated excess of CAS reagent was then added.

For the allophane sample no visual colour change was observed in the CAS solution, although the surface of the solid adopted a purple colour. Neither was any visible change observed for the imogolite suspension although the 3 mg sample, if decomposed, contained enough Al(III) to change the CAS reagent from yellow to faint red. After centrifuging the imogolite suspension then decanting the supernatant liquid a blue coloured precipitated was observed. This precipitate was freeze dried. The infrared spectrum of a heated sample indicated that imogolite was still present.

8.3.5 Discussion

The results given in Table 8.5 are summarized graphically in Figure 8.7. The computed concentration of $Al_{13}(OH)_{32}$ was derived from the data of Mesmer and Baes[147]. The curve o represents soluble unreactive aluminium and is obtained from the difference between the total and reactive aluminium values. The similarity of this curve to that for $Al_{13}(OH)_{32}$ implies that "unreactive aluminium" may be approximated to the polymer $Al_{13}(OH)_{32}$.

The results obtained after extracting soils with 1 M KCl (Table 8.6) indicate that in general a greater percentage of Al(III) in the soil extract is in a reactive form, at a given pH, than in the synthetic solution. In

Figure 8.7 Reactivity of hydrolyzed Al(III) solutions

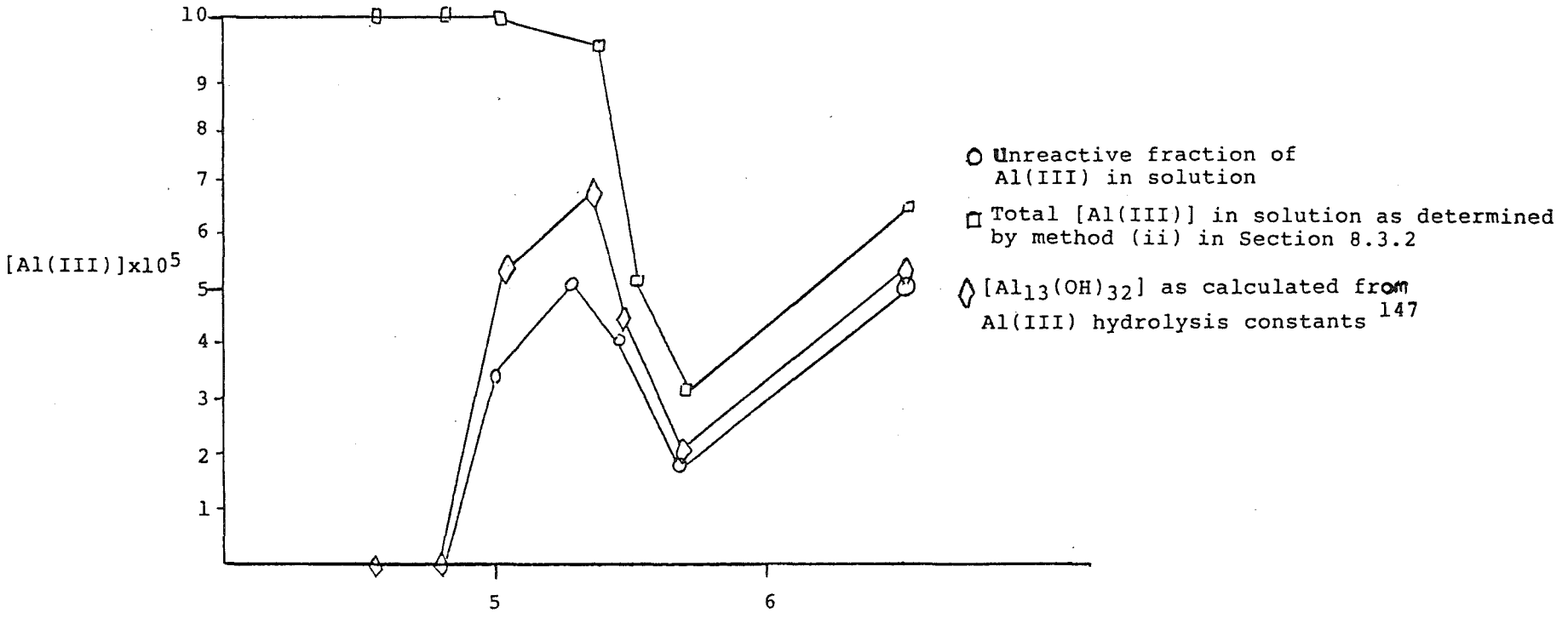

soils, and in the soil extracts, organic acids (e.g. fulvic acid) may complex Al(III) thus preventing it from hydrolyzing extensively and becoming non-reactive towards CAS.

It has been shown that neither Silica Springs allophane nor imogolite reacts with CAS, but the colourimetric reagent does adsorb on to the hydrous alumino silicates making them coloured.

8.4 Semi-quantitative soil testing

8.4.1 Extraction of exchangeable Al(III) in soils

The electrolyte used to extract the exchangeable Al(III) from soil samples was 1.0 M KCl. This reagent was used because it has been reported to remove exchangeable Al from soils with a minimum extraction of non-exchangeable forms of aluminium[205]. Further, for the soils tested in this work KCl-extractable aluminium values were available from measurements made by Soil Bureau or Lincoln College. This afforded a comparison for the results obtained in this work.

To determine a suitable extraction time for soils two samples of gley soils (5 g) were extracted with 1 M KCl in leaching columns at a flow rate of 1.5 ml/min. Samples were supported in sand (10 g) over a plug of macerated filter paper. In separate experiments the sand (which had been washed with acid and 2,2'-bipyridyl) was leached with 1 M KCl and the leachate analysed for Fe(III) and Al(III). No iron was found, but Al(III) concentrations of c. 0.1 ppm were found repeatedly. Thus 0.1 ppm Al(III) was subtracted from results for all subsequent leaching experiments.

The total volume of KCl passed through the two soils, Bu45 (a Maimai fine sandy loam[206], pH(H_2O) 4.4) and Du76-2 (a Maimai fine sandy loam, pH(H_2O) 5.7), was 100 ml. It was collected in fractions of 10, 10, 40 and 40 ml and analysed for aluminium by the colourimetric method employing PCV, described by Dougan and Wilson[207]. The results for cumulative extraction of aluminium are presented graphically in Figure 8.8.

Sivasubramaniam and Talibudeen[208] have suggested that the linear part of a cumulative extraction curve (X-Y, Figure 8.8) corresponds to the non-exchangeable Al. The exchangeable Al is then obtained by extrapolating the linear part of the curve (X-Y-Z, Figure 8.8) to zero eluent volume. This is indicated graphically in Figure 8.8 with a representation of the curves reported by these workers.

For the more acidic soil, Bu45, it was found that 15% of total Al(III) was extracted in the first 10 ml of leachate, and 36% in the next 10 ml fraction. A further 39% was removed in the next 40 ml, while the last fraction contained c. 10% of the total Al(III) extracted. For the less acidic soil, Du76-2, the rate of extraction of aluminium was reasonably constant (i.e. a linear curve was obtained).

Thus from the form of the cumulative extraction curves Bu45 contains larger quantities of both exchangeable and non exchangeable Al(III) than does Du76-2.

As it was not practical to leach soils for semi-quantitative measurements in the field an extraction technique which involved shaking a small sample of soil with

Figure 8.8 Soil extraction data; Aluminium concentration in 1 M KCl leachate

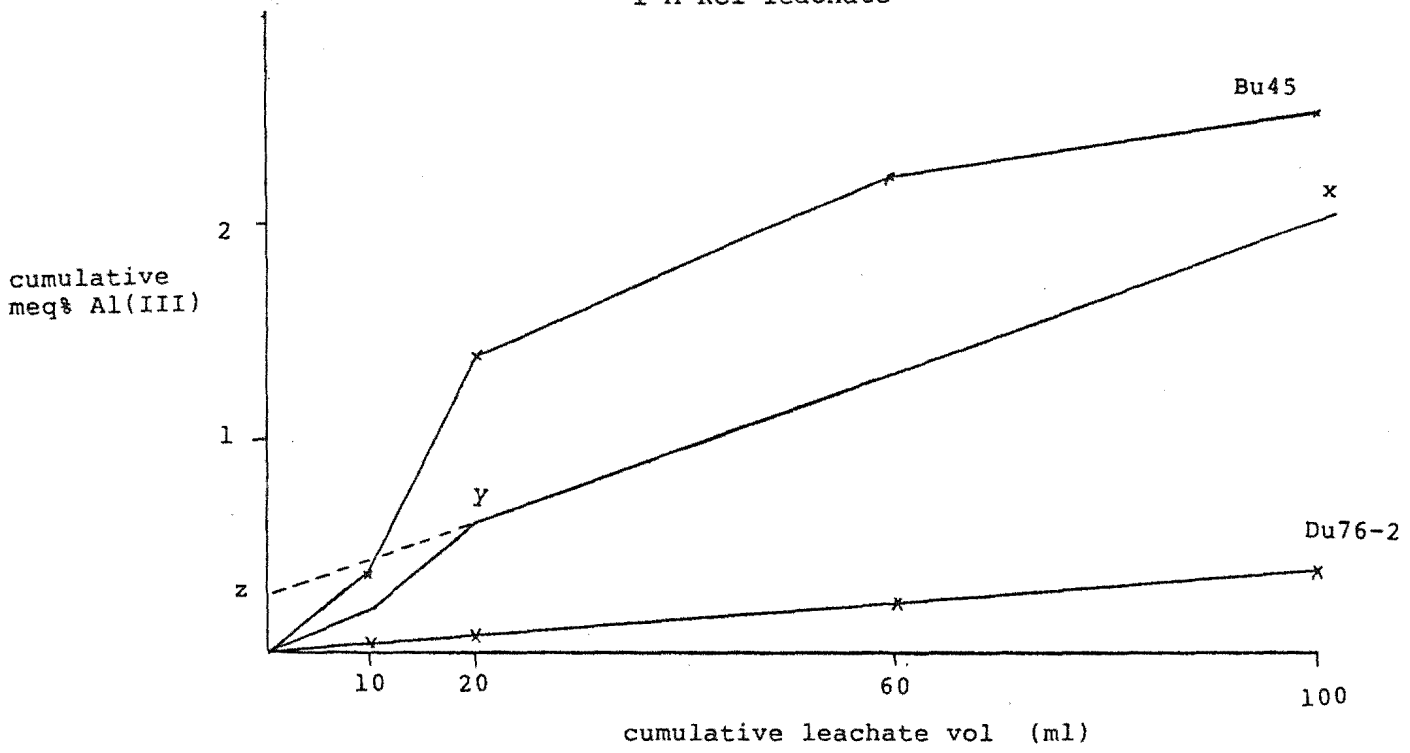

1 M KCl was investigated. In the development stage in the laboratory soil samples were weighed (1 g) and various shaking times were considered. It was found that the most efficient extraction was achieved when the soil was initially shaken with 10 ml of 1 M KCl, for 30 s and again for 30 s after 3 - 4 min, then left to settle for 5 min.

Longer shaking and settling times and larger volumes of extractant did not significantly increase the quantity of Al(III) extracted. Identical colours were obtained for aliquots taken from the top, middle and bottom of the supernatant in the sample vial. This procedure established that there was no Al(III) concentration gradient in the KCl extractant solution. Thus this method was employed for all semi-quantitative extractions performed on soils in the laboratory.

8.4.2 Results

A number of air dried soils representing different New Zealand soil types were selected for this study. Many of these soils were supplied by the New Zealand Soil Bureau. The soils were extracted with KCl as described in Section 8.4.1. From the supernatant solution an aliquot was taken and added dropwise to a reagent solution consisting of CAS (0.6 ml; 3×10^{-3} M), ascorbic acid (1 ml, 1%) and hexamine reagent (2 ml) in a small clear glass vial, until a colour change was observed. The sample volume was added from a calibrated pipette so that the volume could be recorded and a calculated amount of DDW added to make a total volume of 10 ml. The colour developed by a sample was then compared visually against a series of colours developed for solutions

containing known concentrations of Al(III). The Al(III) standards used in this work were 0 ppm (yellow), 0.4 ppm (light red), 0.8 ppm (red) and 1.6 ppm (purple). The colours obtained for 0, 0.8 and 1.6 ppm solutions are shown in Figure 8.9.

Table 8.7 lists the levels of extractable Al (in meq%) for the soils studied. The term meq%, commonly used by soil scientists, represents milliequivalents per 100 grams. The term equivalent is defined as 1 gram atomic weight of hydrogen or the amount of any other ion that will combine with or displace this amount of hydrogen. For example a trivalent cation such as Al(III) can take the place of three H^+ ions. Consequently, its atomic weight must be divided by 3 to obtain the equivalent weight. The "reported" values for extractable aluminium given in Table 8.7 result from 16 h leaching with 1 M KCl. They are included for comparison and were determined either by flame atomic absorption or by titration.

It was found that soils with a pH(H_2O) value > 5.5 generally gave an extractable aluminium value, by the rapid extraction-CAS method, which was significantly lower than that determined by atomic absoprtion spectroscopy or titration following a 16 h extraction. Figure 8.10 presents graphically the relationship between soil pH and CAS measured extractable aluminium expressed as a percentage of the 16 h value. No correlation was evident between the rapid extraction CAS values and soil statistics such as percent C in soil, aluminium extracted by P_2O_7, and pH(KCl).

Figure 8.9 Aluminium test colours

(1) standard Al(III) colours (a) 0ppm; (b) 0.8 ppm; (c) 1.6 ppm

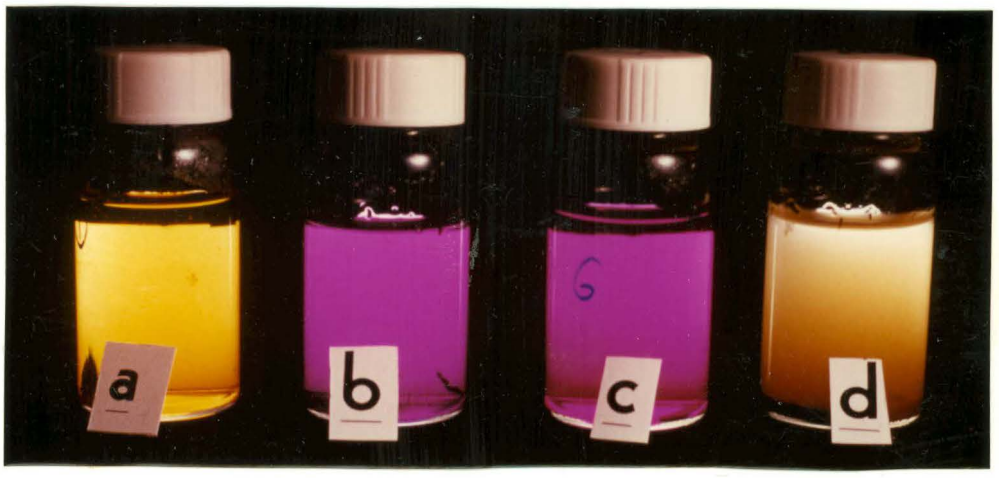

(2) typical colours obtained in an Al(III) test. (a) 0ppm, (b) test solution > 1.6 ppm (c) 1.6 ppm (d) KCl/soil solution.

Table 8.7 KCl extractable Al

Soil number	location	type	horizon	meq% reported	meq% CAS measured	pH(H_2O)
1	WINGATUI	rs	Ap	0.1	0.0	5.9
2	WINGATUI	rs	Bwg1	0.2	0.0	5.9
3	WINGATUI	rs	Bwg2	0.3	0.05	5.8
4	WINGATUI	rs	Cg	0.1	0.0	5.9
5	WINGATUI	rs	2Cg	1.5	0.9	5.0
6	WINGATUI	rs	3Cg	1.1	0.66	5.4
7	EYRE	fsl	Ap1	0.08	0.33	5.8
8	EYRE	fsl	Ap2	0.55	0.38	5.6
9	EYRE	fsl	Bw1	1.9	0.88	5.4
10	EYRE	fsl	Bw2	0.96	0.44	5.5
11	EYRE	fsl	Bw3	0.35	0.22	5.8
12	EYRE	fsl	C1	0.3	0.0	6.0
13	EYRE	fsl	C	0.37	0.06	6.1
14	MANGATEPOPO	pybe	A	0.6	0.44	5.5
15	MANGATEPOPO	pybe	A1	0.9	0.66	5.6
16	MANGATEPOPO	pybe	Bhs	0.7	0.44	5.7
17	MANGATEPOPO	pybe	Bs	0.2	0.06	6.0
18	MANGATEPOPO	pybe	Bw	0.1	0.0	6.2
19	TAHORA	slybe	Bw1	9.4	6.6	5.3
20	KUMARA	sl	AHg	3.7	2.6	4.4
21	FLAGSTAFF	sl	Ah	2.4	2.2	3.6
22	CHARLESTON	s	Au1	1.2	0.72	4.3
23	ADDISON	ls	Ah1	0.48	0.22	5.4
24	HOPE	fslp	Bc	3.6	1.76	5.0
25	CASS	sl	Bw	4.7	1.76	5.3
26	CASS	sl	Bs	2.1	0.66	5.3
27	KATRINE	sl	Bw	0.4	0.0	5.6
29	KATRINE	sl	Bs	2.9	0.66	5.6
30	KATRINE	sl	Bw	1.3	0.28	6.0
31	CAVE STR	sl	Ab	0.5	0.39	6.1
32	CAVE ST	sl	Bw	0.7	0.55	5.9
33	OLD MAN RANGE	fsl	Ah	9.7	4.4	4.05
34	OLD MAN RANGE	fsl	Bw	7.7	5.5	4.55
35	OLD MAN RANGE	sl	Bw	4.1	2.2	4.7
36	OLD MAN RANGE	sl	C	2.0	0.88	4.9

KEY :
rs = recent soil
fsl = fine sandy loam
pybe = podzolized yellow brown earth
slybe = silt loam yellow brown earth
sl = silt loam
s = sand
ls = loamy sand

Detection limit c. 0.1 ppm/ml sample added

Figure 8.10 Soil extraction correlation

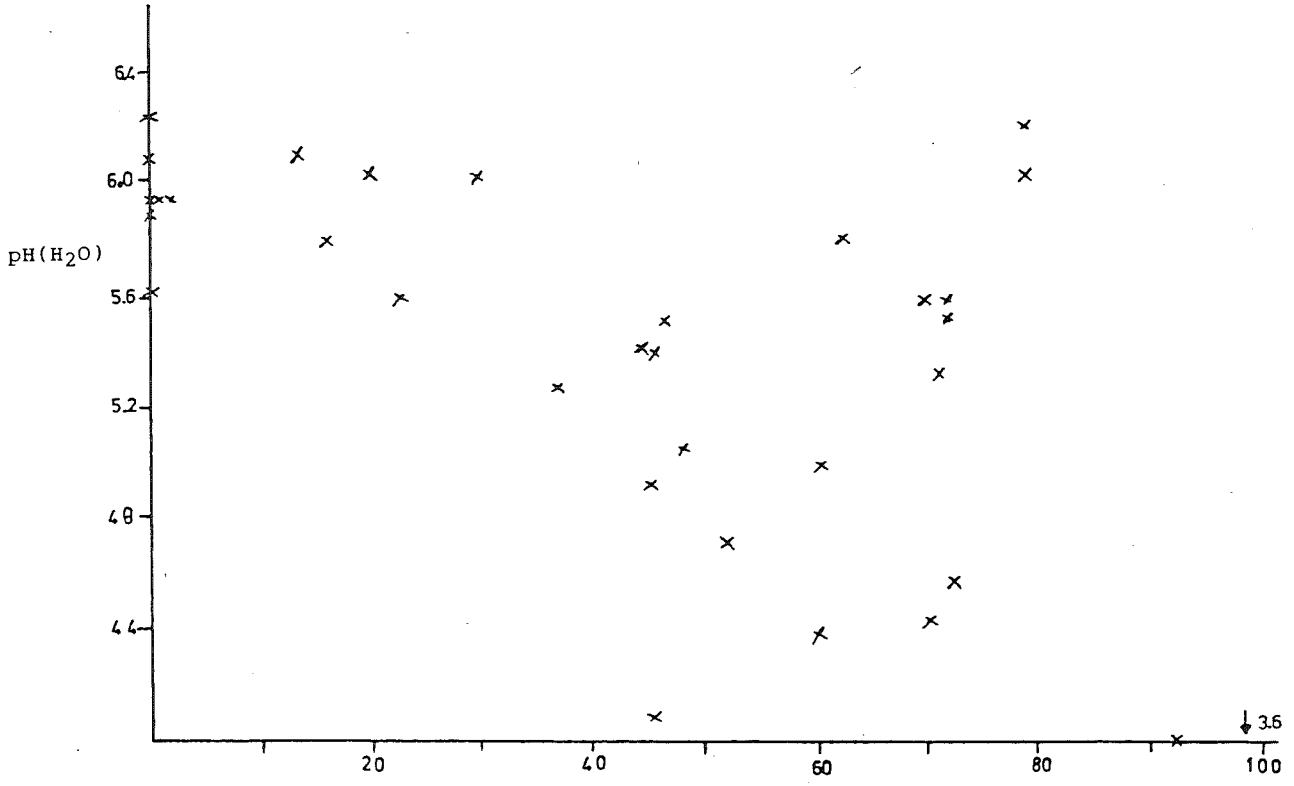

8.4.3 Discussion

In the laboratory analysis of these soils each sample was weighed to ensure reproducibility. In most instances duplicate soil samples yielded extractable Al values with a maximum variability of 20%, as determined by the eye against standard colours. Hence it was concluded that this CAS-Al test was able to semi-quantitatively measure the level of KCl extractable Al(III) in soil, using the eye to detect colour change.

It was anticipated that this would also be the case in the field situation, but it was noted that the limitations in this case would be (i) the reproducibility of the amount of soil sampled, and (ii) the soil variability, resulting in different colours for the same soil and sample size.

Soils with high values of pH(H_2O) (c. > 5.5) gave low concentrations of CAS-reactive aluminium on extraction with KCl. This can not be ascribed to the polymerization of Al(III) in solution because total Al analysis on selected soils had indicated that most of the Al(III) extracted by KCl was in the reactive form (see Section 8.3.3). It was therefore implied that soils with a high pH have little exchangeable Al(III) that can be extracted by the rapid method described here. This may indicate that the normal extraction method used in the laboratory, which involves leaching soils for 16 hours and which indicates measurable levels of extractable aluminium for some of these soils, may be extracting significant amounts of non-exchangeable Al(III) from the soil; (see Figure 8.8). For soils with high pH the non-exchangeable aluminium represents a high

proportion of aluminium extracted in 16 h, hence the rapid extraction method yields low to very low values for these soils.

It is worth noting that pH is not the only variable controlling the activity of aluminium in the soil solution. For example the clay mineral kaolinite contains both aluminium and silicon. Under conditions that favour the formation of kaolinite, (rather than amorphous aluminium oxides), the concentration of silicates in the soil solution will also determine the activity of aluminium.

8.5 Field application of the CAS test

8.5.1 Method

The ability of the CAS method to determine the presence of exchangeable Al(III) and rank soils within a profile was assessed under field conditions. Because high concentrations of Al(III) were encountered in the strongly weathered soils studied a concentrated solution of CAS was used ($1x10^{-2}$ M). This also enabled a large range of Al(III) concentrations to be catered for; e.g. Table 8.8 indicates that there is a 10-fold range of aluminium concentrations (representing 0.1 - 9 ppm in the leaching solution) that may be relevant to pedologists or agronomists.

Table 8.8 Levels of Al(III) in soil

Ranking	Pedology (meq%)	Agronomy (meq%)
Low	0-1	0-0.5
Medium	1-5	0.5-1
High	5-10	>1
v.High	>10	

It is recognised that soil variability and soil sampling are major limitations in field work. To minimize the latter problem, a standard volume of "1 teaspoon of soil" was the quantity taken.

A number of methods for applying this field test were explored.

i) A sample of soil was extracted with 1 M KCl and an aliquot of the supernatant extractant was then added to buffered CAS reagent. The colour developed could then be compared with (a) colours for other soil samples within a profile or b) colours for standard aluminium solutions.

ii) A sample was placed in a spot dish and covered with a thin layer of white barium sulphate to enhance any colour change. The buffered CAS reagent was then added dropwise. The rate of development of colour was used as the criterion for ranking different soils. Alternatively the soil sample was extracted in the spot dish with 1 M KCl for 2 min before addition of CAS reagent (1 drop). Colour development was immediate.

iii) A buffered CAS reagent was sprayed as a fine mist onto an exposed soil profile by use of a simple garden sprayer. If desired a thin layer of barium sulphate could be applied to the profile from a squeeze bottle to aid colour detection.

8.5.2 Results and discussion

Listed in Table 8.9 are the results obtained from the application of the above methods to a soil profile examined on the Bealy Spur c. 15 km south of Arthur's Pass. This

Table 8.9 Analysis of a Bealy Spur soil; a summit profile

horizon	depth (cm)	pH H_2O	Al(III)[210] (KCl extractable)	Al(III) ranking KCl extractable	spot dish	spray
O	6-0	3.7	6.5	least	least	+
E	0-5	3.7	8.4	medium	medium	+
Bhs	9-17	4.5	7.5	most	most	+

soil is classified as a podzolized yellow-brown earth and had been studied extensively by other workers[210].

Both methods i) and ii) ranked the soils in the profile quite distinctly; i.e. definitive colour differences were observed (see Figure 8.11). No attempt was made to quantify the amounts of Al(III) present because of uncertainty in sample weight. The spot dish method required the least manipulation of sample and reagents but retained the ability to rank the soil. The spray test (method (iii)) gave a positive result for the whole profile, indicating the presence of readily exchangeable Al(III), but did not provide clear differentiation between soil horizons.

It is envisaged that the spot dish method, because of its simplicity, would be most readily accepted by field workers (e.g. pedologists.).

Figure 8.11 Results for analysis of a Bealy Spur soil; a summit profile

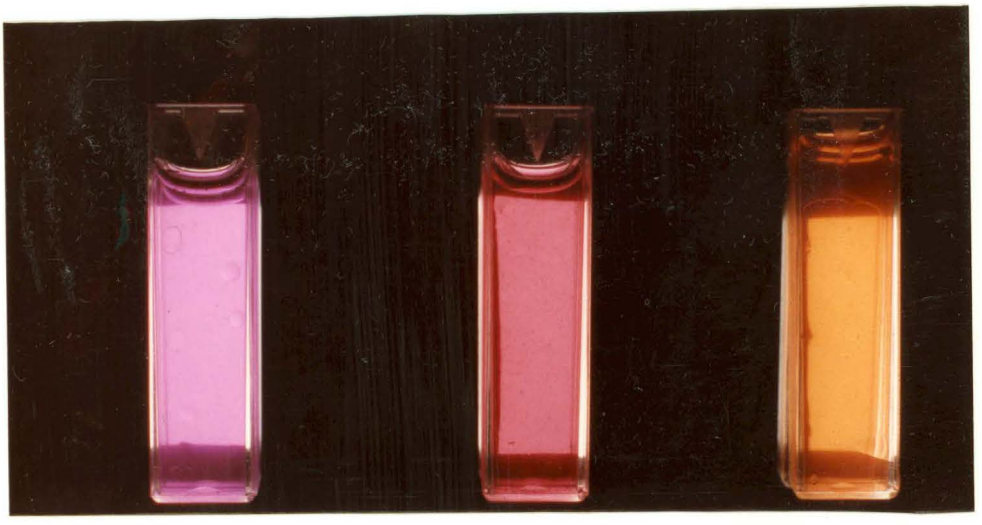

From left to right. Bhs, E, O, horizon

CHAPTER 9

THE COMPLEXING ABILITY OF POLYPHENOLS

It has been established from this work that Al(III) and Fe(III) form stable complexes with 1,2-dihydroxybenzenes. However other naturally occurring oxygen donor ligands such as carboxylic acids also form stable complexes with these metals[33]. Ligands such as these are often considered responsible for solubilizing Fe(III) and Al(III) by attacking minerals[32], clays[211] and amorphous metal hydroxides[212] in the zone of weathering in soils, and hence mobilizing these metal ions from normally insoluble compounds. The profile of a podzolized soil exhibits the end result of a downward movement of solubilized iron and aluminium (and organic matter).

Part A of this chapter describes a computer simulation used to assess the effect that organic ligands may have in complexing Al(III) when both are at low concentration as found in soil solution. Calculations used the stability constants for Al(III)-polyphenol complexes determined in this work and the "best" literature values for the stability constants of a representative selection of other aluminium complexes. The results were used to indicate which organic acids could complex Al(III) most effectively at soil pH. The acids most effective in complexing Al(III) in a competitive situation were also determined by computer simulation. The solubility of crystalline aluminium

hydroxide (gibbsite) in solutions of individual and competing ligands was also considered as a function of pH.

Part B of this chapter describes a semi-quantitative investigation of the reactions of some polyphenols, particularly Bl3, with metal ions such as Fe(III), Al(III), Cu(II) and Ca(II).

The ability of selected ligands to dissolve $Fe(OH)_3$ either by complex formation or oxidation reduction has been determined.

By use of a copper ion selective electrode a comparison between the stability of catechol-copper complexes and Bl3-copper complexes was attempted.

PART A

COMPUTER SIMULATION OF THE FORMATION OF METAL-LIGAND COMPLEXES

9.1 Introduction

Many ligands with potential metal complexing sites have been isolated from, or identified in, soil extracts and plant extracts[213]. For example, large organic polymers such as fulvic and humic acids are readily isolated from podzolized soils and have been shown to contain keto, hydroxy, phenolic and carboxylic donar groups[36]. However it is not possible to obtain accurate metal-ligand equilibrium data for these molecules because of their complexity and heterogeneity.

Simple low molecular weight aliphatic and aromatic carboxylic acids and polyphenols have also been identified in the soil environment[33]. The protonation and metal complexing reactions of these simple organic molecules are well documented so these ligands have been used to model the mobilization of Al(III) in the soil. The following representative selection of ligands was used (where references indicate the source of stability constant data), tiron[214], protocatechuic acid and catechin (1,2-dihydroxybenzenes), malic acid[215] and citric acid[216] (aliphatic hydroxy carboxylic acids), malonic acid[217] and oxalic acid[218] (dicarboxylic acids), kojic acid[219] representing the hetero ring of flavanols) and salicylic[162] and phthalic acids[167] (aryl carboxylic acids).

The computer program has been described elsewhere[220]. By use of an iterative process and the ligand-proton and ligand-metal equilibrium constants it calculates the percentage distribution of metal among complex species ($Al_pL_qH_r$) and hydroxo species (Al_pH_{-r}); this calculation is performed as a function of pH and for any given metal concentration or ligand concentration. The program is able to consider a maximum of 25 ligands competing for the metal ion. The equilibrium metal ion concentration may be governed by the total metal in solution or may be governed by the solubility of a solid phase (e.g. gibbsite) in equilibrium with the solution.

The pH range investigated was 4.0 - 8.0 which encompasses that generally found in soils. Likewise the selected concentrations of Al(III) (0.05 - 0.15 ppm) and of

organic matter (OM) (1 - 20 ppm) were considered representative of the [Al(III)] and [OM] in soil solutions[221,222]. A log Ksp value of -33 was selected for gibbsite[223] and used in calculations on the solubility of gibbsite in various ligand solutions. The Al(III) hydrolysis constants used were those described in Chapter 6, except for $Al(OH)_4$; for this species the value recently reported by Ohman[161] was used after being adjusted for ionic strength.

9.2 Results

Appreciable dissolution of gibbsite in the pH range 4 - 8 requires the presence of complexing ligands. The relative potential of a ligand to mobilize metal ions may be described by the total concentration of soluble complexed metal species (Al_T) formed by equilibration of this ligand (at a given concentration) with gibbsite. The term Al_T is given by $\sum Al_pL_qH_r + \sum Al_pH_{-r}$. Figure 9.1 plots pAl_T against pH for individual solutions of various ligands at $5x10^{-6}$ M. The curves are shown in relation to that for the solubility of gibbsite in water (solid curve) which is seen to increase at pH > 6.5 due to the formation of $Al(OH)_4$.

Amongst the ligands chosen, citric acid and tiron are the only ones which at low concentration can complex appreciable amounts of Al(III). However at pH values > 6.5, citric acid at $5x10^{-6}$ M is unable to compete effectively against OH^- for the aluminium. Oxalic acid complexes with Al(III) in the pH range 4.5 - 6 but has a much smaller "mobilizing capacity" than has citric acid. It is noted that oxalic acid has a log K_{011} value of 3.55[223]; therefore

Figure 9.1 Solubility of gibbsite in water and in ligand solutions (5×10^{-6} M)

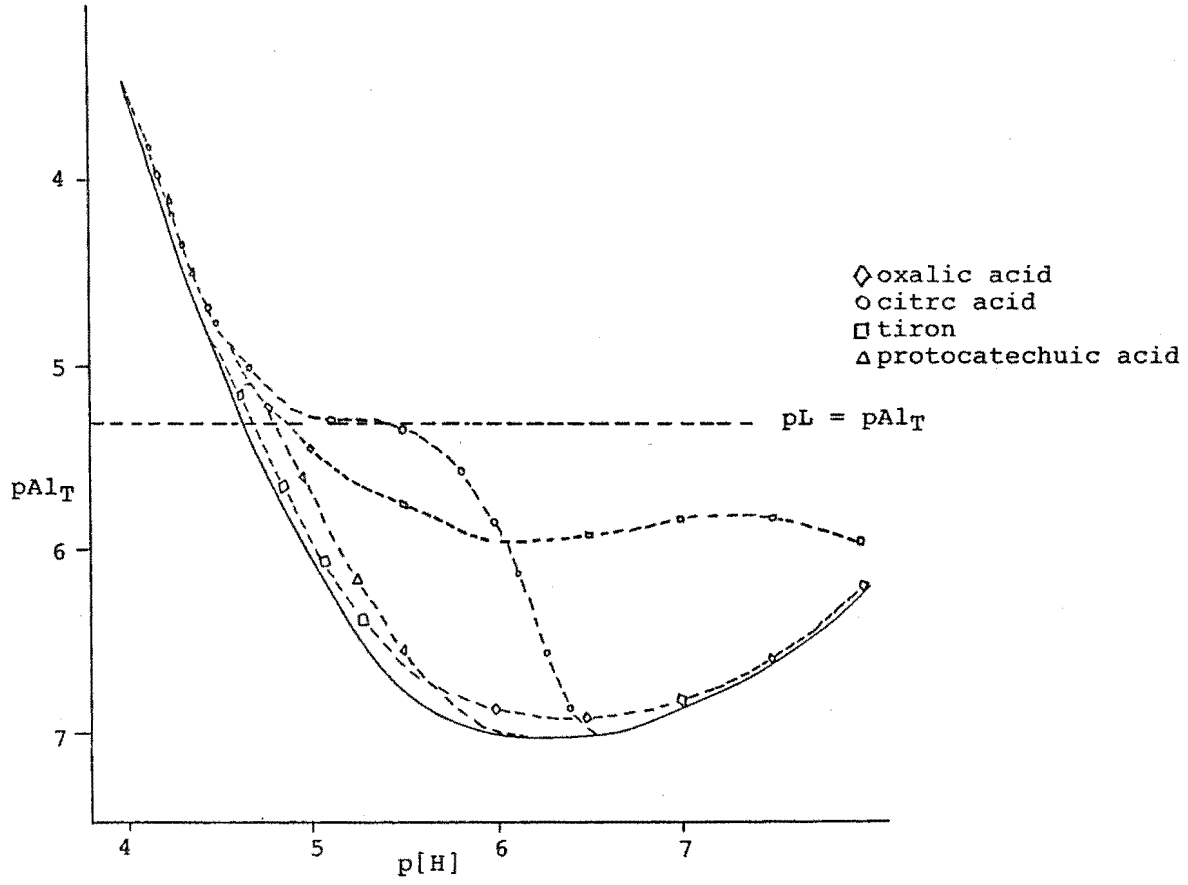

the free ligand concentration [Ox^{2-}] would not increase significantly above pH 4.6. In contrast citric acid has log K_{011} 5.8 such that the concentration of free ligand increases significantly up to pH c. 7.0, while tiron has log K_{011} and log K_{012} > 7 so that the free ligand concentration continues to increase throughout the pH range shown. These differences, as well as the magnitude of the metal-ligand constants and the stoichiometry of metal-ligand complexes, contribute to the relative shapes and positions of the curves shown. Other polyphenols investigated (protocatechuic acid and catechin) were not effective complexing agents at this concentration. The enhanced mobilizing capacity of tiron over the other polyphenols can be ascribed to the lower basicity of its dianion (in which respect tiron is atypical of the polyphenols found in soil).

For other ligands the order of "mobilizing capacity" at pH 6 was calculated as protocatechuic acid > catechin > oxalic acid and (not shown because of their minimal "mobilizing capacity") > kojic, salicylic > malonic, malic > phthalic.

Another way of ranking the ligands is to compare the concentrations of various ligands required to increase the solubility of gibbsite (say) tenfold at a given pH. The required quantity of ligand (pL_T) was calculated from the stability constant data for the ligands and the free metal concentrations as calculated from the Ksp for gibbsite. Figure 9.2 presents the results for each of the ligands at pH 4.5 and pH 6.0. The ligands required at lowest

Figure 9.2 Concentration of ligand required to increase the solubility of gibbsite ten fold

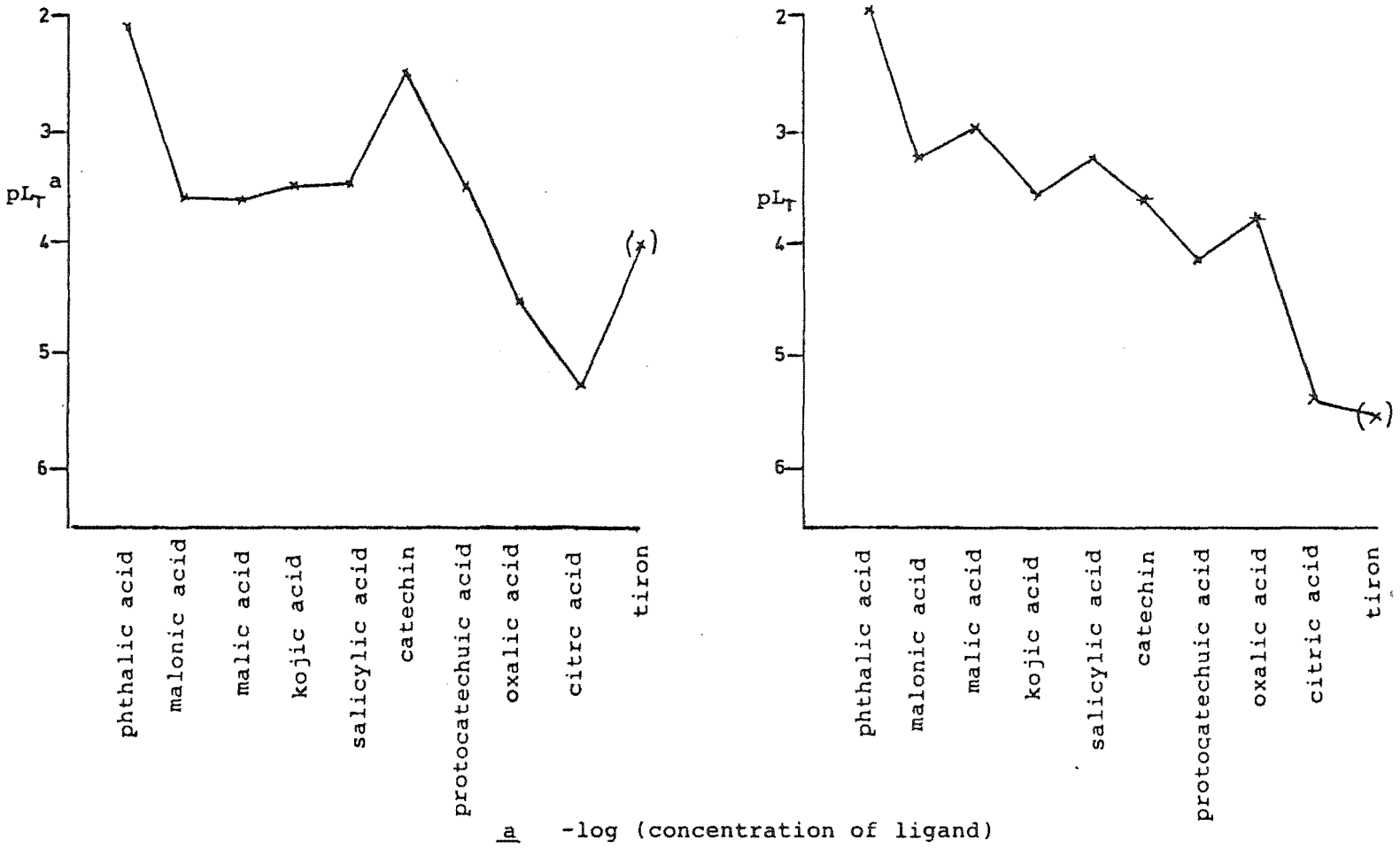

a -log (concentration of ligand)

concentration (highest pAl_T) will be the most effective mobilizing agents.

By comparison of Figures 9.2(a) and (b) (excluding the atypical polyphenol tiron) it is seen that citric acid is a more effective mobilizing ligand than catechin or protocatechuic acid by factors of 80 and 16 at pH 4.5 and 6 respectively. It is noted that citric acid and fulvic acid, the high molecular weight water-soluble organic fraction in soil, have similar affinities for Cu(II)[224] in aqueous solution. It should also be noted that the polyphenols catechin and protocatechuic acid are required at significantly higher concentration at pH 4.5 (Figure 9.2(a)) than at pH 6 to increase the solubility of gibbsite tenfold. This is because their "free ligand" concentration increases significantly (c. 10^3) in the pH range 4.5 to 6 (i.e. both ligands have log K_{011} and log K_{012} values > 6.

In the soil system many ligands will compete simultaneously for the available metal ions. Figure 9.3 plots as a function of pH the % composition calculated for the reaction between Al(III) (total concentration $1x10^{-6}$ M) and a solution containing all the ligands considered in this work (each at $5x10^{-6}$ M). At pH values below 6 the carboxylate ligands oxalate and citrate are determined as the dominant complexing species. At pH > 6.5 tiron alone complexes the Al(III) until pH 7.25 when $Al(OH)_4$ begins to form. All the other ligands included in the equilibrium calculation did not contribute significantly (> 1%) to solution stoichiometry at any pH.

Figure 9.3 Distribution of Al(III) in a system of competing ligands (5×10^{-6} M) with a total metal concentration of 10^{-6} M

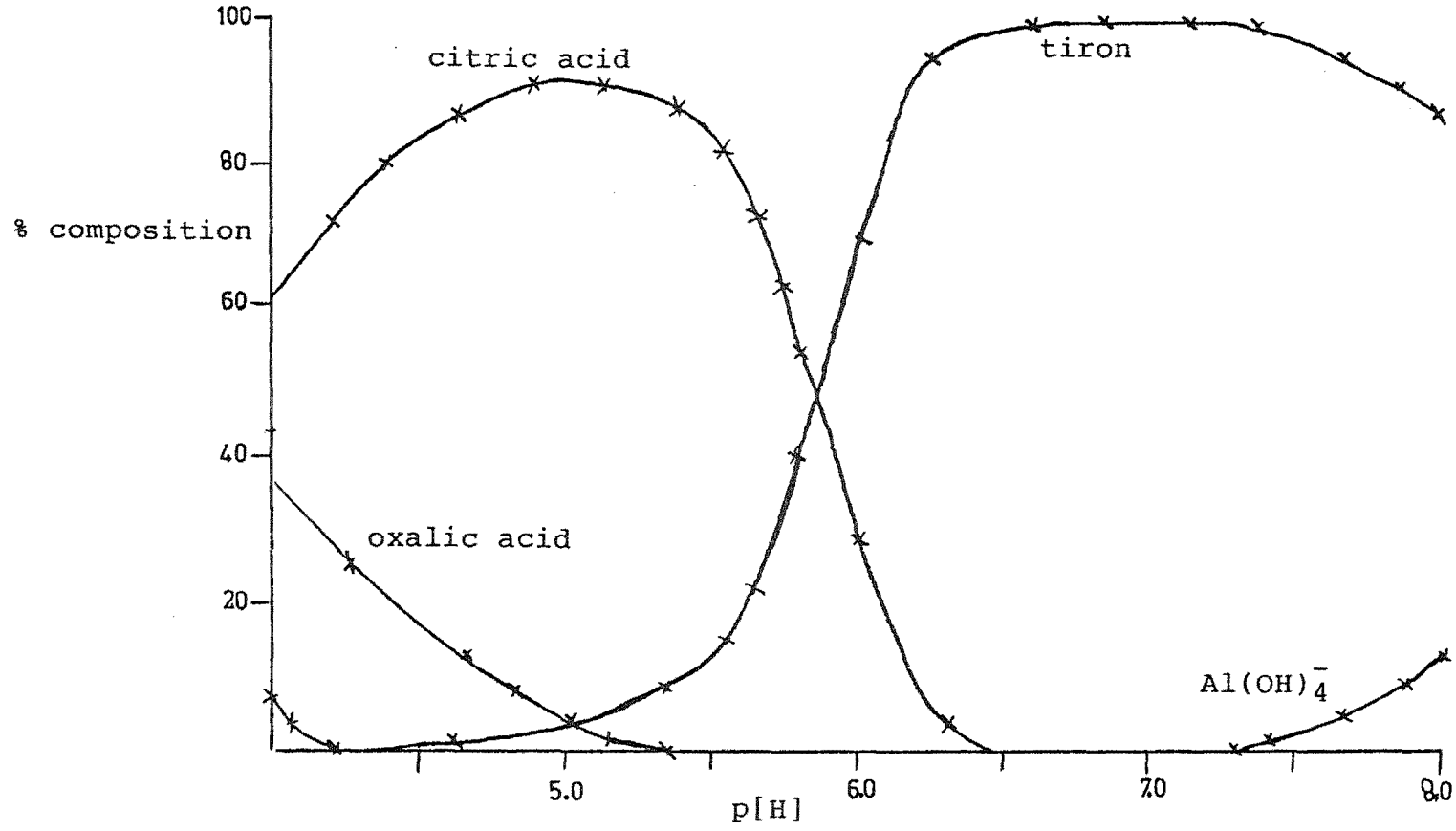

9.3 Conclusions

The computer simulation studies have established that certain organic acids isolated from or identified in soils are able (by complex formation) to dissolve aluminium from minerals and maintain it in solution throughout the pH range 4 - 8.0, even when the ligand concentration is as low as 5×10^{-6} M.

In acid soils ligands containing carboxylate functional groups will be most effective at complexing aluminium. These organic acids range from simple species such as oxalic and citric acids to the large polymeric soil molecules such as fulvic acid.

At higher pH values (pH > 6) polyphenols were found to be relatively more effective as complexing species.

The results of these calculations support the concept of chemical weathering of minerals and clays by organic acids. Such weathering results in dissolution of generally sparingly soluble elements Fe, Al (and Si) and their transport in solution as metal-ligand complexes.

It is noted however that the reduction potential of the soil system will influence the ability of organic species to complex with metal ions. In part this is because some organic acids are vulnerable to oxidation and give oxidized forms that are generally not as effective as complexing agents; e.g. it has been reported that quinones, the oxidation products of polyphenols, do not complex with aluminium[161].

If the soil conditions are reducing it is likely that some organically complexed Fe(III) will be reduced to the

Fe(II) state. The Fe(II) will not be complexed by polyphenols below pH 7[131] but will still be mobile because of the increased solubility of iron(II) in weakly acidic solution.

PART B

REACTIONS OF FE(III) WITH POLYPHENOLS (INCLUDING A CONDENSED TANNIN)

9.4 Dissolution of Fe(III) hydroxide by polyphenols

This section of work outlines the methods that were used to rank the polyphenols tiron, catechol and B13 in their ability to dissolve iron hydroxides in freshly hydrolized solutions of Fe(III).

9.4.1 Method

A standard acidic iron(III) solution was added to CO_2 free DDW (25 ml) to give a final concentration of 4.4×10^{-5} M. The pH of this solution was then adjusted to 4.25 or 5.25 with standard KOH. No iron hydroxide precipitate was visible at this concentration at either pH. Stock solutions of ligands (1×10^{-3} M) were also adjusted to pH 4.25 and 5.25 in the manner described. The ligands employed were tiron, catechol and B13. A volume of the ligand solution was then added to the iron solution of the same pH such that the final concentration of ligand was 3×10^{-4} M. The pH values of the resultant solutions were remeasured; no change in pH was observed. The iron-ligand mixtures were left to stand at room temperature and were

stirred periodically for 1 day; any changes in colour or precipitate formation were noted.

9.4.2 Results

a) Tiron. This ligand is not oxidized by iron(III) in acidic solutions; therefore iron(III) complexing alone will dissolve ferric hydroxide in tiron solutions. It has been reported that tiron forms a 1:1 complex FeL in the pH range 1 - 4, and a 1:2 complex FeL_2 in the pH range 3 - 6.

Ten minutes after the addition of ligand to the ferric hydroxide solutions a faint blue colour was apparent. The colour intensified with time (h). No precipitate was observed in solution or collected on a 0.45μm membrane filter.

Spectrophotometric analysis of the solution at pH 5.25 indicated that within two hours most of the colloidal $Fe(OH)_3$ was dissolved and the iron complexed as the $Fe(tiron)_2$ species. This was inferred from the measured wavelength maximum at 560 nm and extinction coefficient of 4100 (per mole of iron) calculated on the basis of complete dissolution and complex formation (cf. reported for $Fe(tiron)_2$: wavelength max 561 nm, extinction coefficient 4550^{170}).

For the sample at pH 4.25 the measured wavelength maximum was 575 nm and the calculated extinction coefficient at this wavelength 2840. The difference in these two parameters with respect to the sample at pH 5.25 was ascribed to the presence of both mono and bis tiron iron(III) species in solution.

b) Catechol. On addition of catechol to the iron(III)-hydroxide solutions no colour change was observed until 24 h. The colour resulted from a precipitate which was subsequently collected on a 0.45 μm membrane filter. Spectrophotometric analysis of the filtrate indicated that no soluble ferric-ligand complexes had formed at pH 4.25 or pH 5.25.

Addition of acidic thiocyanate to the precipitate indicated that it contained Fe(III).

c) Bl3. Addition of Bl3 to the iron(III) solutions produced a dark coloured precipitate after 24 h. The solutions were filtered through a 0.45 μm membrane filter; spectrophotometric analysis on the filtrates confirmed that no soluble ferric-ligand complexes had formed in either solution. Addition of acidic thiocyanate to the collected precipitates indicated that Fe(III) was present.

9.4.3 Discussion

These results indicate that tiron is more effective at complexing Fe(III) and dissolving colloidal iron-hydroxy polymers than is catechol or Bl3. This enhanced mobilizing capacity of tiron is ascribed to its redox stability in the presence of ferric ion and the formation of slightly more stable complexes with Fe(III)[170]. This result supports the findings from a computer simulation on the ability of a range of ligands to dissolve ferric hydroxide; for the same series of ligands discussed in Section 9.4 tiron was the most effective iron-mobilizing polyphenol[220].

Tiron is an atypical polyphenol in that it is not oxidized by Fe(III). Its redox stability arises from the

electron withdrawing sulphonate groups. In contrast both B13 and catechol undergo oxidation in the presence of Fe(III) in acid solutions (see Chapter 7). At pH values of 5.25 and (especially) 4.25 any iron(III) complex formed with catechol or B13 will be partly decomposed according to the following redox reaction:

$$2Fe(III) + \text{polyphenol} \rightleftharpoons \text{quinone} + 2H^+ + 2Fe(II).$$

The dark precipitates observed when these two ligands are reacted with the $Fe(OH)_3$ colloid may be quinone products. Any Fe(II) produced would be slowly oxidized to Fe(III) which would form insoluble $Fe(OH)_3$ or form further complexes with the ligand. $Fe(OH)_3$ associated with a quinone precipitate would give a positive ferric ion test with acidic thiocyanate. The net effect of this redox process would be to convert all the polyphenol to quinone.

9.5 Complex formation by B13

The stoichiometries of soluble complexes and precipitates formed by reaction of B13 with metal ions have been investigated.

9.5.1 The reaction of iron(III) with B13

It had been observed that in solutions of B13 and iron(III) soluble complexes formed at high L/M ratios while at low L/M ratios dark coloured precipitates formed. Experiments were performed to determine the critical L/M ratio at which complete precipitation occurred.

Solutions with a range of stoichiometries were prepared by slow addition of a standard iron(III) solution to stirred solutions of B13 (c. 3.7×10^{-4} M) held at pH 6.8. The solution stoichiometries expressed as moles of Fe(III)

per mole of B rings in the Bl3 solution were 1/10, 1/6, 1/5, 1/4, 1/3 and 1/2. All solutions immediately developed a dark blue colour that remained constant in intensity (by visual comparison) for a period of at least 4 h. With the 1/3 and 1/2 systems a definite turbidity was observed in the solutions after c. 10 min. After standing for 4 h all solutions were centrifuged (2500 rpm, 10 min). Precipitates were isolated from the 1/3 and 1/2 solutions and collected on a 0.45 μm membrane filter. Visible absorption spectra were measured to determine how much Fe(III)-Bl3 complex remained in solution; this assessment was based on the assumption that the bis complex would have a similar absorption spectrum to that for Fe(epicatechin)$_2$.

9.5.2 Results and discussion

At pH 6.8 Fe(III) forms bis complexes with catecholate ligands; these have λmax c. 565 nm and λmax c. 4000 (per mole of Fe(III)). The spectra for solutions of Fe(III)-Bl3 complexes with metal ligand ratios 1/10 to 1/5 had λmax at 570 nm and λmax (per mole of Fe(III)) in the range 4100 - 3800. Spectrophotometric data obtained for solutions of different stoichiometry are summarized in Table 9.1. As the M/L ratio was further increased the λmax value decreased until a ratio of 1/2 was reached; at this point all the Fe(III)-Bl3 complex had precipitated from solution. No precipitation was noted for the 1/4 system; however the observed change in the magnitude of the extinction coefficient may imply some precipitation and/or change in the Fe(III)/ligand coordination mode.

Table 9.1 Spectrophotometric data for B13-Fe(III) systems

Fe/B ring ratio	ε ($\pm$200) at 570 nm[a]	λ_{max} ($\pm$3) nm
1/10	4100	570
1/6	3900	570
1/5	3810	570
1/4	3470	570
1/3	3056	575
1/2	0	---

a expressed per mole of Fe(III)

Thus this study has shown that a metal B ring ratio between 1/3 and 1/2 (i.e. a metal/B13 ligand ratio between 4.3/1 and 6.5/1) is critical for complete precipitation of the B13-iron(III) complex.

9.5.3 B13 salt preparation

The solubility and stoichiometry of a small series of B13-metal salts was investigated.

To a series of standard solutions of B13 (7.28×10^{-5} M; pH 6) calculated amounts of Fe(III), Al(III), Cu(II) and Ca(II) solutions were added to produce metal-ligand solutions with a ratio of metal/B rings of 1/1 ([M] = 9.4×10^{-4} M) and 1/7 ([M] = 1.35×10^{-4} M). During this incremental addition of metal ions compensating volumes of KOH were added as required to maintain pH at 6. The resultant solutions were left to equilibrate for 6 h with periodic readjustment to pH 6 if necessary. Precipitates when formed were isolated by centrifuging at 2500 rpm for 10 min then collected on 0.45 μm membrane filters and dried over P_2O_5 in a desiccator.

Ultraviolet spectrophotometric analysis was used to measure the concentration of B13 remaining in the supernatant solution. Unionized polyphenols have an intense absorbance at c. 285 nm; for B13 this maximum was at 279 nm and had an extinction coefficient of 4000 (per mole of B rings). For ultraviolet spectrophotometric analysis solutions were first acidified to pH 1 to decompose any metal complexes present. For the iron system visible absorption spectra afforded an estimate of the concentration of Fe(III) complexed to B13 as a bis catecholate species (ε= 4100).

Atomic absorption spectroscopy was used to analyse for metal ion concentrations in filtrates or in solutions containing digested precipitates. In the latter case a weighed sample of organic precipitate was first washed with 0.1 M HCl to remove any adsorbed metal ions or metal hydroxides. The organic content of the precipitate was then decomposed by digestion with H_2O_2 for 24 h and then heated for 1 h; unreacted H_2O_2 was boiled off before the solutions were made up to a standard volume for analysis.

9.5.4 Results

a) Fe(III). Addition of Fe(III) to a solution of B13 resulted in a dark precipitate forming from a solution containing 1 mole of Fe per mole of B rings. An ultraviolet spectrum of the acidified filtrate indicated that no B13 was left in solution (i.e. no measurable absorbance was recorded in the wavelength range 400 - 250 nm). Atomic absorption analysis on the filtrate confirmed that there was no iron left in solution.

For the system having a 1/7 ratio of iron to B rings the solution colour immediately changed from colourless to dark blue upon the addition of Fe(III); no precipitate was observed in the solution, nor after centrifuging and filtering. Ultraviolet and visible absorption spectra confirmed that all the B13 (ε4000 at 279 nm) and all the iron (present as a bis catecholate complex with ε = 4100 at 570 nm) was in solution. Atomic absorption analysis of the filtrate also confirmed that 100% of the added iron(III) was in solution.

A weighed amount of the iron-B13 precipitate obtained from the 1:1 reaction mixture was equilibrated for 8 h with an accurately known volume of 0.1 M HCl. A sample of the supernatant solution was analysed for iron content and was found to contain 5% of the total iron in the original solution. Subsequent H_2O_2 digestion of the precipitate and iron analysis indicated that it contained 1 mole of Fe per 1.3 moles of B rings.

b) Al(III). For aluminium solutions with metal/B ring ratios of 1/1 and 1/7 precipitates were observed to form immediately. The 1/1 solution contained visibly more precipitate than the 1/7 solution. Insufficient precipitate was formed in the 1/7 system to allow an aluminium analysis by atomic absorption spectroscopy. Centrifuged filtered solutions of the 1/1 and 1/7 systems were acidified and analysed by ultraviolet absorption. The results for the 1:1 system indicated that no B13 was left in solution whereas for the 1/7 system c. 70% of the B13 remained in solution.

Atomic absorption analysis of a weighed digested (H_2O_2) sample of the precipitate obtained from the 1:1 system indicated that the precipitated salt contained 1 mole of Al per 1.9 moles of B rings.

c) Cu(II). Calculations using the Cu(II)-catechol[225] system as a model indicated that at pH 6 approximately 50% of the added copper should be complexed with Bl3. Addition of Cu(II) to solutions of Bl3 to give metal/B ring ratios of 1/1 and 1/7 resulted in precipitates. More precipitate was observed for the 1:1 system. Insufficient precipitate was formed in the 1/7 system to permit analyses. Ultraviolet spectrophotometric analysis of the filtrates obtained after centrifuging and filtering these solutions indicated that for the 1/7 system approximately 100% of the Bl3 remained in solution, whereas for the 1:1 system 0% of the Bl3 remained in solution.

Atomic absorption analysis of a weighed digested (H_2O_2) sample of precipitate from the 1/1 system indicated that the precipitated salt contained 1 mole of Cu per 2.4 moles of B rings.

d) Ca(II). For calcium no precipitate formed for either the 1/7 or 1/1 systems. Analysis by ultraviolet absorption indicated that for both systems 100% of the Bl3 was in solution. Metal analysis indicated that 100% of the total metal was also in solution.

9.5.5 Copper ion selective electrode studies

A copper ion selective electrode (I.S.E.) was employed to gain quantitative information on the complexing of Bl3 with copper.

Standard solutions of copper at 0.01 and 0.0001 M (I = 0.1 M KNO_3) were prepared and used to calibrate the I.S.E. before and after each titration.

A more thorough calibration involved use of solutions of citric acid ($1.1x10^{-3}$ M) and copper ($7.5x10^{-4}$ M) which were titrated with standard KOH. From the measured pH and the known stability constants for the citric acid-copper complexes, the free metal concentrations were computed as a function of pH. A linear calibration of emf versus pCu was obtained down to a metal concentration of $3x10^{-7}$ M.

Titrations of Cu(II) ($1.49x10^{-4}$ M)-catechol ($1.04x10^{-3}$ M) solutions repeatedly resulted in pH-pM(Cu) data that were not consistent with the pH-volume of titre curves; that is, the measured free metal concentration was at least 1 order of magnitude too low at pH values (c. 4) where catechol was not complexing significantly with copper. This discrepancy was related to the effect of catechol on the I.S.E. Although emf readings were stable and the Nernstian slope of 29 mV was maintained, the copper(II) standards gave markedly different emf readings before and after immersion in the catechol solution (Δ(emf) 33 - 51 mV). If the "after-titration" calibration was taken as the valid one, then results consistent with pH-volume of titre curves were obtained. However because of the large shift in calibration the results are at best semi-quantitative.

Titrations of KOH against a Cu(II) ($1x10^{-3}$ M)-Bl3 ($7.6x10^{-5}$ M) solution produced a distinct brown precipitate

above pH 6. Hence reliable results were not obtained for this system either.

Figure 9.4 presents the results obtained for these two systems; they indicate that for solutions with the same catecholate to metal ratio the free metal concentrations show a similar variation with pH.

9.5.6 Discussion

From the analysis of Bl3-metal salts prepared at pH 6 it was found that the molar ratio of metal to ligand was greater for iron than for Al and Cu. This may imply that at pH 6 Bl3 forms more stable complexes with Fe(III) than with Al(III) or Cu(II) or that the iron complexes have the greater tendency to polymerize.

For Ca(II) no precipitate was formed at a Ca/B ring ratio of 1/1. This may indicate that a soluble complex is formed or, because the Ksp for $Ca(OH)_2$ was not exceeded, that uncomplexed calcium remains in solution. No other conclusions could be drawn for this system.

The semi-quantitative results obtained from I.S.E. studies indicate that they have similar affinities for Cu(II) in the pH range 5 - 6. Thus it may be inferred that Bl3 and catechol form copper complexes of similar stability i.e. there is no significant "chelate effect" to be derived from the Bl3 structure.

9.6 Conclusions

Studies to assess the ability of polyphenols to dissolve $Fe(OH)_3$ have shown that only tiron, a polyphenol that is not oxidized by ferric ion, is able to complex iron and solubilize $Fe(OH)_3$ over the pH range 4.25 - 5.25.

Figure 9.4 Free metal concentration versus pH for catechol-Cu(II) and for Bl3-Cu(II) solutions

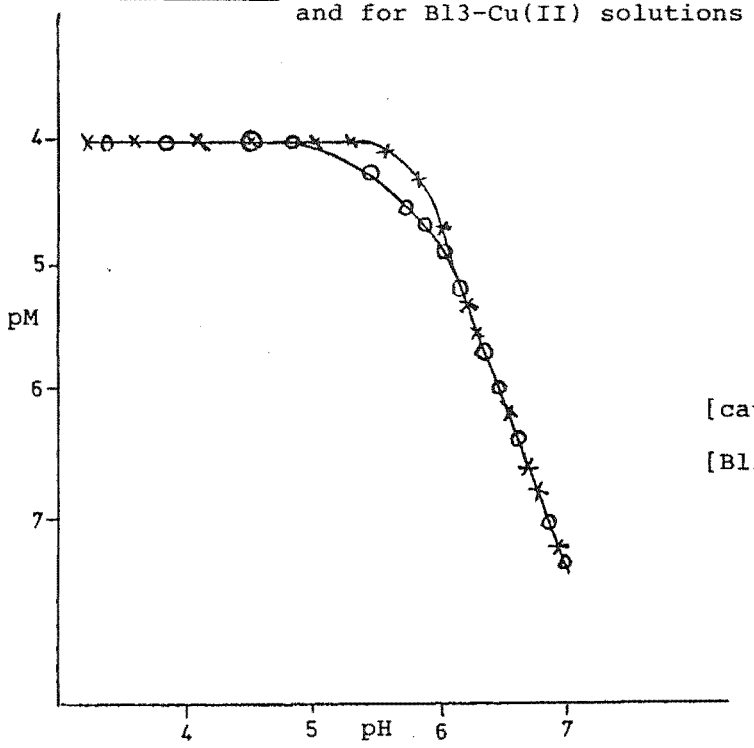

[catechol] = $1x10^{-3}$ M

[Bl3] = $7.6x10^{-5}$ M

Catechol and Bl3, polyphenols which are oxidized by ferric ion and which form weaker complexes with iron(III), did not dissolve measurable amounts of $Fe(OH)_3$ over a 24 h period. In these solutions dark precipitates formed which gave a positive test for iron(III); it was not certain whether the Fe(III) was complexed or precipitated as $Fe(OH)_3$, with the dark colour arising from quinone (oxidized polyphenol).

When metal ion solutions were added to solutions of Bl3 at pH 6 metal complexes precipitated for Fe(III), Al(III) and Cu(II). Precipitation occurred for M/B ring ratios as small as 1/7 for Al(III) and Cu(II), and at 1/1 for Fe(III).

The insolubility of Bl3 complexes has important implications for soil processes such as podzolization; that is, these large polyphenol polymers may be less effective than low molecular weight acids in mobilizing metals such as iron and aluminium if precipitation occurs on complexing. Further, the inability of catechol to dissolve $Fe(OH)_3$ and form soluble complexes suggests that polyphenols may mobilize iron in the podzolization process only by reduction of Fe(III) to Fe(II), a process which will be favoured by acidic conditions.

CHAPTER 10

CONCLUSIONS

Listed in the introduction of this thesis are a number of theories that have been proposed to explain the mechanism of podzolization. In recent years the most widely documented mechanism for podzolization is one which involves soil organic matter in a number of steps which can be summarized as (i) geochemical dissolution of minerals in the A horizon, enhanced by organic acids, (ii) chelation of Al(III) and Fe(III) by soil organic matter (containing phenolic, hydroxy and carboxylic acid functional groups) to form soluble complexes, and depending on conditions some subsequent reduction of Fe(III) to Fe(II) by the ligands, (iii) transport of these metal organic complexes down the soil profile, and (iv) precipitation of complexes as the metal/organic ratio increases.

Much of the work described here has involved the study of polyphenols and their interaction with aluminium and iron. The study involved molecules ranging from low molecular weight species such as catechol to a high molecular weight condensed tannin (a polymer having 13 epicatechin units linked together).

From this work a number of observations have allowed inferences about the role that polyphenols may play in the podzolization process.

(i) In acidic conditions (pH 4 - 6), as might be found in a podzolized soil, polyphenols (e.g. protocatechuic

acid and catechin) are unable to compete successfully for Al(III) against citric acid.

Recently it was reported that fulvic acid, a major component of soil humus[226], coordinates metal ions in a polycarboxylate mode at soil pH[224]. Further, coordination of metal ions by fulvic acid was closely modelled by citric acid. This suggests that fulvic acid may also compete with polyphenols for metal ions at pH values commonly found in podzolized soils.

(ii) Investigations into the mode of coordination of B2, an epicatechin dimer, and B13, an epicatechin polymer, suggest that the complexes formed between these organics and metal ions such as Al(III) are not significantly more stable than the complexes formed by their simple monomeric units. Thus it is proposed that these polymeric polyphenols will be no more dominant in the mechanism of podzolization than will simple polyphenols.

(iii) It has been found that the Fe(III), Al(III) and Cu(II) complexes of B13 have limited solubility. For example, B13-Fe(III) complexes precipitate when a ratio exceeding 2 moles of Fe(III) to one mole of B rings is reached. This result also implies that low molecular weight organic species may be as important in the solubilization and transport of iron and aluminium as are larger organic polymers. This view is supported in a recent publication by Buurman et al.[33].

(iv) For the polyphenols studied in this work (except tiron) the redox stability of complexes with Fe(III) is dependent on pH. For solutions whose pH is less than six

there is a possibility that, in addition to iron(III) complex formation, ferric ion may be reduced to ferrous ion with the corresponding oxidation of the polyphenol to a quinone. This redox process may be important in the mobilization of iron because (i) $Fe(OH)_2$ has a higher solubility than has $Fe(OH)_3$, and (ii) the complexing ability of the polyphenol is lost in this process because the redox couple is irreversible under soil conditions. For solutions with pH < 5 this redox process will become increasingly important.

It is significant that two fulvic acid samples did not undergo redox reactions with iron, even at pH 3. Thus it may be inferred that iron(III) fulvic acid complexes once formed are redox stable and may move iron down a soil profile until excess metal leaching causes precipitation.

The results and conclusions of this work generally support the podzolization mechanism involving complexing or redox action by organic acids (fulvate theory).

Recently Farmer and co-workers[41-46] have proposed a "silicate" theory of podzolization which involves the transport of iron and aluminium as colloidal sols incorporating silicate. This theory does not require the assistance of organic acids in the transport of these elements, although Farmer acknowledges that organic acids may be involved in the initial dissolution of sesquioxides. This theory has been criticized by Buurman et al.[33], who state "there is ample evidence to attribute the mobilization, transportation and precipitation of sesquioxides to complexing organic compounds" (see Chapter

1). It is also noted that sol formation is inhibited by complexing organic acids.

It is possible however that the "fulvate" and "silicate" podzolization mechanisms operate together; i.e. both metal-organic and metal-silicate complexes may coexist in the soil. If these species coexist it is likely that the soil environment will determine which process dominates.

APPENDIX A

FORTRAN PROGRAM TO CALCULATE $\bar{n}_H$ FOR SOLUTIONS OF CATECHOL

```
      SUBROUTINE PRELIM(YO,X,NO)
      DIMENSION YO(200),X(1,200),HYDR(200),XKCL(200),TTL(200)
      READ(5,43)AKOH,VOL,TLI,CORR,ACIDXS
      READ(5,499)SLOPE,YINT,DRA,DRB,DRC
      READ(5,500)DCA,DCB,DCC,XSTR
      WRITE(6,42)
      ATC=0.625
      BIST=0.0
      DO 2 I=1,NO
      TR=YO(I)
C     EXPTAL ELECTRODE DRIFT CORRECTIONS
      IF(X(1,I)-DRA)45,45,46
   46 IF(X(1,I)-DRB)47,47,48
   48 IF(X(1,I)-DRC)402,402,403
   47 X(1,I)=X(1,I)-DCA
      GO TO 45
  402 X(1,I)=X(1,I)-DCB
      GO TO 45
  403 X(1,I)=X(1,I)-DCC
   45 CONTINUE
C     CORR IS EQUAL TO 0.800 TO CONVERT pH RAW TO pH MEAS
      X(1,I)=X(1,I)+CORR
      WRITE(6,50)X(1,I)
C   SLOPE CORRECTION TO PRIMARY BUFFER SLOPE
      X(1,I)=X(1,I)*SLOPE-YINT
      WRITE(6,51)X(1,I)
C     TO CHANGE pHm TO pH+
      X(1,I)=1.0002*X(1,I)-0.109132
      WRITE(6,52)X(1,I)
      H=10.**(-X(1,I))
      TL=TLI*VOL/(VOL+YO(I))
      TTL(I)=TL
      ALK=(YO(I)*AKOH/1000.)-ACIDXS
      ALL=ALK*1000./(VOL+YO(I))
C IONIC STRENGTH OF KCL & KOH
      XKCL(I)=(XSTR*VOL/(VOL+YO(I))+AKOH*YO(I)/(VOL+YO(I)))
      ACID=2.0*TTL(I)-ALL
  419 ATC1=ATC
      YO(I)=TR
      AWK=1.008E-14/ATC
      HYDR(I)=AWK/H
      TH=ACID+HYDR(I)-H
      WRITE(6,44)ACID,HYDR(I),YO(I),X(1,I),TTL(I),XKCL(I),BIST,ATC
      YO(I)=TH/TTL(I)
```

```
C     IONIC STRENGTH CALCULATION
      CL=0.0
      CLH=0.0
      IF(YO(I)-1.0)410,410,411
  411 IF(YO(I)-2.0)412,412,416
  410 CL=(1.0-YO(I))*TTL(I)
      CLH=(YO(I)-0.0)*TTL(I)
      GO TO 416
  412 CLH=(2.0-YO(I))*TTL(I)
      CL=0.0
      GO TO 416
C      IONIC STRENGTH EQUATION XKCL=KOH AS WELL
  416 BIST=XKCL(I)+HYDR(I)+CLH+3.0*CL
  417 CONTINUE
C     DETERMINATION OF KWC IN ATC OF WATER
      ATC=10.**((-1.0124*SQRT(BIST))/(1.0+1.1833*SQRT(BIST))+0.279*BIST
     1-0.0472*((BIST)**1.50))
      IF((ATC1-ATC)-0.001)2,2,419
    2 CONTINUE
   43 FORMAT(F10.4,F10.2,E10.4,F10.3,E10.4)
   44 FORMAT(E10.4,5X,E10.4,2X,2(F10.4,2X),E10.4,1X,3(E10.4,2X))
   42 FORMAT('  ACID        HYDR(I)          YO(I)       X(1,I)     TTL(I)
     1  XKCL      BIST         ATC ')
   50 FORMAT(2X,'pHm='F8.3)
   51 FORMAT(5X,'pHm1='F8.3)
   52 FORMAT(8X,'pH+='F8.3)
  499 FORMAT(F10.4,2X,F10.4,1X,F6.3,1X,2(F5.3,1X))
  500 FORMAT(3(F8.3,2X),F10.4)
      RETURN
      END
      SUBROUTINE CALC(X,P,I,Y)
      DIMENSION X(1,200),P(4)
      H=10.**(-X(1,I))
      ABP=P(1)*H*(1.0+2.0*P(2)*H+3.0*P(2)*P(3)*H**2)
      ABB=1.0+P(1)*H*(1.0+P(2)*H+P(2)*P(3)*H**2)
      Y=ABP/ABB
      RETURN
```

To calculate $\bar{n}_H$ for protocatechuic acid the above program was indentical to the that for catechol except for the following changes;

```
    ACID = 3.0*TTL(I) - ALL

416 BIST = XKCL(I) + HYDR(I) + 3.08CLH + 6.0*CL
```

APPENDIX B

FORTRAN PROGRAM TO CALCULATE $\bar{n}_H$ FOR SOLUTIONS OF CATECHIN OR EPICATECHIN

```
      SUBROUTINE PRELIM(YO,X,NO)
      DIMENSION YO(200),X(1,200),HYDR(200),XKCL(200),TTL(200)
      READ(5,43)AKOH,VOL,TLI,CORR,ACIDXS
      WRITE(6,42)
      ATC=0.625
      BIST=0.0
      DO 2 I=1,NO
      TR=YO(I)
      IF(X(1,1)-7.7)45,45,46
   46 IF(X(1,I)-8.3)47,47,48
   47 X(1,I)=X(1,1)-0.002
      GO TO 45
   48 IF(X(1,1)-8.8)402,402,403
  402 X(1,I)=X(1,I)-0.006
      GO TO 45
  403 X(1,I)=X(1,I)-0.010
   45 CONTINUE
      X(1,I)=X(1,1)+CORR
      X(1,I)=X(1,I)*1.0147-0.0701
      X(1,1)=1.0002*X(1,1)-0.109132
      H=10.**(-X(1,I))
      TL=TLI*VOL/(VOL+YO(1))
      TTL(I)=TL
      ALK=(YO(I)*AKOH/1000.)-ACIDXS
      ALL=ALK*1000./(VOL+YO(I))
      XKCL(I)=(0.095*VOL/(VOL+YO(I)))+(AKOH*YO(I)/(VOL+YO(I)))
      ACID=4.0*TTL(I)-ALL
  419 ATC1=ATC
      YO(I)=TR
      AWK=1.008E-14/ATC
      HYDR(I)=AWK/H
      TH=ACID+HYDR(I)-H
      WRITE(6,44)ACID,HYDR(I),YO(I),X(1,1),TTL(I),XKCL(I),BIST,ATC
      YO(I)=TH/TTL(I)
```

```
C      IONIC STRENGTH CALCULATION
       IF(YO(I)-2.)410,411,411
  410  IF(YO(I)-1.)412,413,413
  411  IF(YO(I)-3.)414,415,415
  415  CLH3=(4.0-YO(I))*TTL(I)
       CLH2=0.0
       CLH=0.0
       CL=0.0
       GO TO 416
  414  CLH3=(YO(I)-2.0)*TTL(I)
       CLH2=(3.0-YO(I))*TTL(I)
       CLH=0.0
       CL=0.0
       GO TO 416
  413  CLH3=0.0
       CLH2=(YO(I)-1.0)*TTL(I)
       CLH=(2.0-YO(I))*TTL(I)
       CL=0.0
       GO TO 416

  412  CLH3=0.0
       CLH2=0.0
       CLH=(YO(I)-0.0)*TTL(I)
       CL=(1.0-YO(I))*TTL(I)
C       IONIC STRENGTH EQUATION XKCL=KOH AS WELL
  416  BIST=XKCL(I)+CLH3+3.0*CLH2+6.0*CLH+10.0*CL+HYDR(I)
  417  CONTINUE
C      DETERMINATION OF KWC IN ATC OF WATER
       ATC=10.**((-1.0124*SQRT(BIST))/(1.0+1.1833*SQRT(BIST))+0.279*BIST
      1-0.0472*((BIST)**1.50))
       IF((ATC1-ATC)-0.001)2,2,419
    2  CONTINUE
   43  FORMAT(F10.4,F10.2,E10.4,F10.3,E10.4)
   44  FORMAT(E10.4,5X,E10.4,2X,2(F10.4,2X),E10.4,1X,3(E10.4,2X))
   42  FORMAT('  ACID         HYDR(I)     YO(I)       X(1,1)      TTL(I)
      1     XKCL      BIST          ATC ')
       RETURN
       END
       SUBROUTINE CALC(X,P,I,Y)
       DIMENSION X(1,200),P(4)
       H=10.**(-X(1,I))
       ABP1P=P(1)*H
       ABP2P=P(1)*P(2)*2.0*H**2
       ABP3P=ALOG10(P(1))+ALOG10(P(2))+ALOG10(P(3))+(3.0*ALOG10(H))
       ABP4P=ALOG10(P(1))+ALOG10(P(2))+ALOG10(P(3))+ALOG10(P(4))
      1+(ALOG10(H)*4.0)
       ABP4P=ALOG10(3.0)+ABP2P
       ABP5P=ALOG10(4.0)+ABP3P
       ABP6P=ABP1P+ABP2P+10.**(ABP4P)+10.**(ABP5P )
       ABP7P=ABP1P+(ABP2P/2.0)+10.**(ABP2P)+10.**(ABP3P)
       Y=ABP6P/ABP7P
       RETURN
       END
```

APPENDIX C

ORTRAN PROGRAM TO CALCULATE $\bar{n}_H$ FOR SOLUTIONS OF B2

```
      SUBROUTINE PRELIM(YO,X,NO)
      DIMENSION YO(200),X(1,200),HYDR(200),XKCL(200),TTL(200)
      READ(5,43)AKOH,VOL,TLI,CORR,ACIDXS
      READ(5,499)SLOPE,YINT,DRA,DRB,DRC
      READ(5,500)DCA,DCB,DCC,XSTR
      WRITE(6,42)
      ATC=0.625
      BIST=0.0
      DO 2 I=1,NO
C          SYRINGE CORRECTION IS 0.998 * VOL DELIVERED
      YO(I)=YO(I)*0.998
      TR=YO(I)
C   EXPTAL ELECTRODE DRIFT CORRECTIONS
      IF(X(1,I)-DRA)45,45,46
   46 IF(X(1,I)-DRB)47,47,48
   48 IF(X(1,I)-DRC)402,402,403
   47 X(1,I)=X(1,I)-DCA
      GO TO 45
  402 X(1,I)=X(1 I)-DCB
      GO TO 45
  403 X(1,I)=X(1,I)-DCC
   45 CONTINUE
C   CORR IS EQUAL TO 0.800 TO CONVERT pH RAW TO pH MEAS
      X(1,I)=X(1,I)+CORR
      WRITE(6,50)X(1,I)
C  SLOPE CORRECTION TO PRIMARY BUFFER SLOPE
      X(1,I)=X(1,I)*SLOPE-YINT
      WRITE(6,51)X(1,I)
C   TO CHANGE pHm TO pH+
      X(1,I)=1.0002*X(1,I)-0.109132
      WRITE(6,52)X(1,I)
      H=10.**(-X(1,I))
      TL=TLI*VOL/(VOL+YO(I))
      TTL(I)=TL
      ALK=(YO(I)*AKOH/1000.)-ACIDXS
      ALL=ALK*1000./(VOL+YO(I))
```

```
C IONIC STRENGTH OF KCL & KOH
      XKCL(I)=(XSTR*VOL/(VOL+YO(I))+AKOH*YO(I)/(VOL+YO(I)))
      ACID=8.0*TTL(I)-ALL
  439 ATC1=ATC
      YO(I)=TR
      AWK=1.008E-14/ATC
      HYDR(I)=AWK/H
      TH=ACID+HYDR(I)-H
      WRITE(6,44)ACID,HYDR(I),YO(I),X(1,I),TTL(I),XKCL(I),BIST,ATC
      YO(I)=TH/TTL(I)
C     IONIC STRENGTH CALCULATION
      IF(YO(I)-7.0)410,414,414
  410 IF(YO(I)-6.0)411,415,415
  411 IF(YO(I)-5.0)412,416,416
  412 IF(YO(I)-4.0)413,417,417
  413 IF(YO(I)-3.0)419,418,418
  414 CLH7=(8.0-YO(I))*TTL(I)
      CLH6=0.0
      CLH5=0.0
      CLH4=0.0
      CLH3=0.0
      CLH2=0.0
      GO TO 420
  415 CLH7=(YO(I)-6.0)*TTL(I)
      CLH6=(7.0-YO(I))*TTL(I)
      CLH5=0.0
      CLH4=0.0
      CLH3=0.0
      CLH2=0.0
      GO TO 420
  416 CLH7=0.0
      CLH6=(YO(I)-5.0)*TTL(I)
      CLH5=(6.0-YO(I))*TTL(I)
      CLH4=0.0
      CLH3=0.0
      CLH2=0.0
      GO TO 420
  417 CLH7=0.0
      CLH6=0.0
      CLH5=(YO(I)-4.0)*TTL(I)
      CLH4=(5.0-YO(I))*TTL(I)
      CLH3=0.0
      CLH2=0.0
      GO TO 420
  418 CLH7=0.0
      CLH6=0.0
      CLH5=0.0
      CLH4=(YO(I)-3.0)*TTL(I)
      CLH3=(4.0-YO(I))*TTL(I)
      CLH2=0.0
```

```
  419 CLH7=0.0
      CLH6=0.0
      CLH5=0.0
      CLH4=0.0
      CLH3=(YO(I)-2.0)*TTL(I)
      CLH2=(3.0-YO(I))*TTL(I)
      GO TO 420
C       IONIC STRENGTH EQUATION XKCL=KOH AS WELL
  420 BIST=XKCL(I)+CLH7+3.0*CLH6+6.0*CLH5+10.0*CLH4+15.0*CLH3+HYDR(I)
     1+21.0*CLH2
C      DETERMINATION OF KWC IN ATC OF WATER
      ATC=10.**((-1.0124*SQRT(BIST))/(1.0+1.1833*SQRT(BIST))+0.279*BIST
     1-0.0472*((BIST)**1.50))
      IF((ATC1-ATC)-0.001)2,2,439
    2 CONTINUE
   43 FORMAT(F10.4,F10.2,E10.4,F10.3,E10.4)
   44 FORMAT(E10.4,5X,E10.4,2X,2(F10.4,2X),E10.4,1X,3(E10.4,2X))
   42 FORMAT('  ACID          HYDR(I)          YO(I)       X(1,I)     TTL(I)
     1  XKCL       BIST          ATC ')
   50 FORMAT(2X,'pHm='F8.3)
   51 FORMAT(5X,'pHm1='F8.3)
   52 FORMAT(8X,'pH+='F8.3)
  499 FORMAT(F10.4,2X,F10.4,1X,F6.3,1X,2(F5.3,1X))
  500 FORMAT(3(F8.3,2X),F10.4)
      RETURN
      END
      SUBROUTINE CALC(X,P,I,Y)
      DIMENSION X(1,200),P(10)
      H=10.**(-X(1,I))
      P1=ALOG10(P(1))
      P2=ALOG10(P(1))
      P3=ALOG10(P(2))
      P4=ALOG10(P(3))
      P5=ALOG10(P(4))
      P6=ALOG10(P(5))
      P7=ALOG10(P(6))
      P8=ALOG10(P(7))
      PH=ALOG10(H)
      AB1=P1+PH
      AB2=AB1+PH+P2
      AB3=AB2+PH+P3
      AB4=AB3+PH+P4
      AB5=AB4+PH+P5
      AB6=AB5+PH+P6
      AB7=AB6+PH+P7
      AB8=AB7+PH+P8
      AA1=10.**(AB1)
      AA2=10.**(AB2)
      AA3=10.**(AB3)
      AA4=10.**(AB4)
      AA5=10.**(AB5)
      AA6=10.**(AB6)
      AA7=10.**(AB7)
      AA8=10.**(AB8)
      ZXA=AA1+2.0*AA2+3.0*AA3+4.0*AA4+5.0*AA5+6.0*AA6+7.0*AA7+8.0*AA8
      ZXB=1.0+AA1+AA2+AA3+AA4+AA5+AA6+AA7+AA8
      Y=ZXA/ZXB
      RETURN
      END
```

APPENDIX D

FORTRAN PROGRAM TO CALCULATE TH FOR SOLUTIONS OF ALUMINIUM ION AND CATECHOL OR PROTOCATECHUIC ACID

```
      SUBROUTINE PRELIM(YO,X,NO,AB,ATL,ATM)
      DIMENSION YO(200),X(1,200),AB(6),ATM(200),ATL(200),ATH(200)
C     READ INITIAL CONCENTRATIONS OF LIGAND, METAL, EXCESS ACID
C              ******* DATED 061082 **************
C       THIS PROGRAM NOW CONTAINS A1OH3,A1LH2,A1LOH ***JK009**** SOURCE
C     READ TOTAL VOL, TITRANT CONCN.
      READ(5,60)ANAOH,VOL,TLI,TMI,ACID,CORR,DELTA
C     B1,B2,B3 ARE CUMULAT&VE PROTONATION CONSTANTS
      READ(5,61)B1,B2,B3,ACIDK
C         BUFFER CORRECTIONS  AND CALIBRATION CONSTANTS
      READ(5,62)SLOPE,SINT,CALS,CINNT
      AB(1)=10.**(B1)
      AB(2)=10.**(B2)
      AB(3)=10.**(B3)
      WRITE(6,74)
C     CONVERT HYDROGEN ION ACTIVITY TO CONCENTRATION
       DO 1 I=1,NO
      X(1,I)=X(1,I)+0.800-DELTA
      XT=X(1,I)-3.500
      IF(XT)9,10,10
    9 X(1,I)=0.063-X(1,I)*0.018+X(1,I)
   10 CONTINUE
C        BUFFER SLOPE CORR FOR LATEST TITRATION
      X(1,I)=X(1,I)*SLOPE+SINT
       X(1,I)=(X(1,I)*CALS-CINNT)
      H=10.**(-X(1,I))
C     CALC DILUTION FACTORS FOR TITRANT VOLUMES YO(I)
      YO(I)=YO(I)*CORR
      AQ=VOL/(VOL+YO(I))
      ALKK=((YO(I)*ANAOH)/1000.)-ACID
      ALKA=(ALKK*1000.)/(VOL+YO(I))
      ATM(I)=TMI*AQ
      ATL(I)=TLI*AQ
C      CALC TOTAL ACID (NOW YO(I)) FOR LEAST SQUARES REFINEMENT
      ATH(I)=ACIDK*ATL(I)+1.611E-14/H-ALKA
      WRITE(6,70)YO(I),X(1,I),ATL(I),ATM(I),ATH(I)
    1 YO(I)=ATH(I)
```

```
      WRITE(6,74)
      WRITE(6,76)ANAOH,VOL,ACID,SLOPE,SINT,CALS,CINNT
      WRITE(6,77)CORR,DELTA,ACIDK
      WRITE(6,75)
      WRITE(6,78)
   60 FORMAT(2F10.4,3E10.3,2F5.3)
   61 FORMAT(3F10.3,F6.4)
   62 FORMAT(4F10.4)
   70 FORMAT(2(F6.3,2X),3(E10.4,2X))
   74 FORMAT(' YO(I)    X(1,I)     ATL          ATM           ATH   ')
   75 FORMAT(' A1 A1L A1L2 A1L3  A1H A1LH2 A1LOH 061082')
   76 FORMAT(' KOH= ',F9.3/' VOL= ',F9.3/' ACID= ',E10.4/' SLOPE= ',
     1F8.4,' SINT= ',F8.4/' CALS=',F8.4,'CINNT=',F10.4)
   77 FORMAT('  CORR= ',F9.3,/' DELTA= ',F5.3,'  SEE PAGE61B LB3 FOR
     1 SYRINGE CORR ',F5.3,'=ACIDK ')
   78 FORMAT(/' BETA7 IS A1OH3 ',/'ALSO A1LOH A1LH2 CAN BE INCLUDED')

      RETURN
      END
      SUBROUTINE CALC(I,P,X,ATM,ATL,AB,H2L,Y,D,FM,ZF,A1L,A1L2,A1L3,HYDR,
     1A1LH,A1OH,A1OH2,A1OH4,A12OH2,A13OH4,A113OH32,A1LH2,A1LOH,A1OH3,ZKS
     2P,A1L2OH,A133)
      DIMENSION P(10),X(1,200),ATM(200),ATL(200),AB(200),AL(200)
      DIMENSION SH2L(200),ATH(200)
      H=10.**(-X(1,I))
      IF(I-1)1,1,2
    1 H2L=3.*ATL(I)/(2.+3.*H*AB(3)/AB(2))
      FM=ATM(I)/2.0
      GO TO 3
    2 H2L=SH2L(I-1)
    3 CONTINUE
C     ALUMINIUM HYDROLYSIS CONSTANTS
      BETA1=10.**(-5.461)
      BETA2=10.**(-10.036)
      BETA3=10.**(-7.7)
      BETA4=10.**(-23.491)
      BETA5=(-103.149)
      BETA6=10.**(-13.694)
      BETA7=10.**(-15.737)
      A=2.*BETA3/H**2
      AZ=3.*BETA6/H**4
C     USE TRIAL VALUE OF H2L TO SOLVE FOR FM.
      B=1.0+P(1)*H2L/(H**2)*(1.0+P(4)*H2L/(H**2)*(1.0+P(6)*H2L/(H**2)))
     1+BETA1/H+BETA2/H**2+P(1)*P(7)*H2L/H
     2+BETA4/(H**4)+BETA7/H**3
     3+P(5)*H2L+P(1)*H2L/H**3*(P(3)+P(4)*P(2)*H2L/H**2)
     4+P(8)*(P(1)*H2L/H**2)/H
C     SOLVE CUBIC FOR H2L BY NEWTON RAPHSON
      NX=0
      NY=0
```

```
   27 FN=ALOG10(13. )+BETA5+13. *ALOG10(FM)-32. *ALOG10(H)
      IF(X(1,I)-6.0)54,55,55
   55 FN=0.0
      AA=0.0
      GO TO 56
   54 AA=10. **(FN)
   56 CONTINUE
      FX=AA+AZ*FM**3+A*FM**2+B*FM-ATM(I)
      FXP=13. *AA/FM+3. *AZ*FM**2+2. *A*FM+B
      XM=FM-FX/FXP
      PFM=-ALOG10(FM)
      PXM=-ALOG10(XM)
      G=PFM-PXM
      FM=XM
      IF(ABS(G)-0.001)25,25,26
   26 NX=NX+1
      IF(NX-20)27,25,25
C     USE FM TO OBTAIN IMPROVED VALUE FOR FREE LIGAND
C     SOLVE CUBIC FOR H2L BY NEWTON RAPHSON
   25 DZXA=(3.0*P(6)*P(4)*P(1))
      DZXB=ALOG10(DZXA)
      DZZ=6. *ALOG10(H)
      DAZ=DZXB-DZZ
      DZ=ALOG10(FM)
      DAZA=DAZ+DZ
      DA=10. **(DAZA)
      DB=2.0*P(4)*P(1)*FM/H**4*(1.0+P(2)/H)
C     fully deprotonated form is always neglible so it is not icluded
      DC=1. +H*AB(3)/AB(2)+AB(1)/(AB(2)*H)+P(1)*FM/H**2+P(1)*P(7)*FM/H
     1+P(5)*FM+P(1)*P(3)*FM/H**3+P(8)*(P(1)*FM/H**2)/H
      N=0
   30 FX=DA*H2L**3+DB*H2L**2+DC*H2L-ATL(I)
      FXP=3. *DA*H2L**2+2. *DB*H2L+DC
      Z=H2L-FX/FXP
      PZ=-ALOG10(Z)
      PFL=-ALOG10(H2L)
      G=PZ-PFL
      H2L=Z
      IF(ABS(G)-0.001)20,20,21
   21 N=N+1
      IF(N-40)30,20,20
   20 IF(NY-21)7,22,22
   22 TFM=FM*(1.0+BETA1/H+BETA2/H**2+FM*A)+13. *FN+FM*BETA4/(H**4)
     1+FM**3*AAZ
C     TEST IF NON-COMPLEXED M LESS THAN HALF A %
      XD=100. *TFM-ATM(I)
      IF(XD) 7,6,7
    6 ZF=1.0+P(4)*H2L/H**2*(1.0+P(6)*H2L/H**2)+P(7)*H
      ZA1LH=ATM(I)/ZF
      TFMP=99.
      GO TO 8
```

```
    7 CONTINUE
C       USE IMPROVED VALUE OF H2L TO RECALCULATE FM
        NM=0
        B=1.0+P(1)*H2L/(H**2)*(1.0+P(4)*H2L/(H**2)*(1.0+P(6)*H2L/(H**2)))
       1+BETA1/H+BETA2/H**2+P(1)*P(7)*H2L/H
       2+BETA4/(H**4)+BETA7/H**3
       3+P(5)*H2L+P(1)*H2L/H**3*(P(3)+P(4)*P(2)*H2L/H**2)
       4+P(8)*(H2L*P(1)/H**2)/H
   28 FN=ALOG10(13.)+BETA5+13.*ALOG10(FM)-32.*ALOG10(H)
       IF(X(1,I)-6.0)46,47,47
   47 FN=0.0
       AA=0.0
       GO TO 48
   46 AA=10.**(FN)
   48 CONTINUE
       FX=AA+AZ*FM**3+A*FM**2+B*FM-ATM(I)
       FXP=13.*AA/FM+3.*AZ*FM**2+2.*A*FM+B
       AM=FM-FX/FXP
C       TEST FM FOR CONVERGENCE
       PFM=-ALOG10(FM)
       PAM=-ALOG10(AM)
       G=PAM-PFM
       FM=AM
       IF(ABS(G)-0.001)42,42,41
   41 NM=NM+1
       IF(NM-20)28,42,42
   42 G=PXM-PAM
       PXM=PAM
       NY=NY+1
       IF(NY-20)29,40,40
   29 IF(ABS(G)-0.001)40,40,25
    8 CONTINUE
   40 CONTINUE
       SH2L(I)=H2L
       ZF=100./ATM(I)
       A1LH=P(1)*P(7)*H2L*FM*ZF/H
       A1L=P(1)*FM*H2L*ZF/(H**2)
       A1L2=A1L*H2L*P(4)/(H**2)
       A1L3=H2L*P(6)*A1L2/(H**2)
       A1LH2=P(5)*ZF*H2L*FM
       A1L2OH=A1L2*P(2)/H
       A1LOH=P(1)*P(3)*FM*H2L*ZF/H**3
       A133=P(8)*ZF*(P(1)*H2L*FM/H**2)/H
       FN=BETA5+13.*ALOG10(FM)-32.*ALOG10(H)
       IF(X(1,I)-6.0)50,51,51
   51 FN=0.0
       FNN=0.0
       GO TO 52
   50 FNN=10.**(FN)
   52 CONTINUE
```

```
      TFM=FM*(1. +BETA1/H+BETA2/H**2+BETA4/H**4+FM*A)+13. *FNN
     1+3. *BETA6*FM**3/H**4+BETA7*FM/H**3
      HYDR=TFM*ZF
      A1OH=BETA1*FM*ZF/H
      A1OH2=ZF*BETA2*FM/H**2
      A1OH4=ZF*BETA4*FM/H**4
      A12OH2=ZF*FM**2*A
      A113OH32=ZF*13. *FNN
      A1OH3=ZF*BETA7*FM/H**3
      A13OH4=ZF*AAZ*FM**3
C       KSP for al-hydroxide
      ZOH=1. 611E-14/H
      ZKS=FM*ZOH**3
      ZKSP=ALOG10(ZKS)
C     CALCULATE TOTAL ACID (YCALC) FROM FM,H2L AND TRIAL PARAMETERS
      Y=H+H2L*(2. +AB(1)/(AB(2)*H)+3. *H*AB(3)/AB(2))
     1-BETA1*FM/H-BETA2*2. *FM/H**2-2. *BETA3*FM**2/H**2
     2-4. *BETA4*FM/(H**4)-32. *FNN+P(1)*P(7)*H2L*FM/H
     3-4. *BETA6*FM**3/H**4-3. *BETA7*FM/H**3
     4+P(5)*FM*H2L*2. -P(1)*FM*H2L/H**3*(P(3)+P(4)*P(2)*H2L/H**2)
     5-P(8)*(P(1)*H2L*FM/H**2)/H
      RETURN
```

To calculate TH for ferric ion and protocatechuic acid solutions the program was idenetical except for the Al(III) hydrolysis constant expressions

APPENDIX E

FORTRAN PROGRAM TO CALCULATE TH FOR SOLUTIONS OF ALUMINIUM ION AND CATECHIN

```
      SUBROUTINE PRELIM(YO,X,NO,AB,ATL,ATM)
      DIMENSION YO(200),X(1,200),AB(6),ATM(200),ATL(200),ATH(200)
C     READ INITIAL CONCENTRATIONS OF LIGAND, METAL, EXCESS ACID
C           ******* DATED 061082 **************
C       THIS PROGRAM NOW CONTAINS A1OH3,A1LH2,A1LOH ***JK002**** SOURCE
C     READ TOTAL VOL, TITRANT CONCN.
      READ(5,60)ANAOH,VOL,TLI,TMI,ACID,CORR,DELTA
C     B1,B2,B3 B4 ARE CUMULAT&VE PROTONATION CONSTANTS
      READ(5,61)B1,B2,B3,B4,ACIDK
C         BUFFER CORRECTIONS  AND CALIBRATION CONSTANTS
      READ(5,62)SLOPE,SINT,CALS,CINNT
      AB(1)=B1
      AB(2)=B2
      AB(3)=B3
      AB(4)=B4
      WRITE(6,74)
C     CONVERT HYDROGEN ION ACTIVITY TO CONCENTRATION
       DO 1 I=1,NO
      X(1,I)=X(1,I)+0.800-DELTA
      XT=X(1,I)-3.500
      IF(XT)9,10,10
    9 X(1,I)=0.063-X(1.I)*0.018+X(1,I)
   10 CONTINUE
C        BUFFER SLOPE CORR FOR LATEST TITRATION
      X(1,I)=X(1,I)*SLOPE+SINT
       X(1,I)=(X(1,I)*CALS-CINNT)
      H=10.**(-X(1,I))
C     CALC DILUTION FACTORS FOR TITRANT VOLUMES YO(I)
      YO(I)=YO(I)*CORR
      AQ=VOL/(VOL+YO(I))
      ALKK=((YO(I)*ANAOH)/1000.)-ACID
      ALKA=(ALKK*1000.)/(VOL+YO(I))
      ATM(I)=TMI*AQ
      ATL(I)=TLI*AQ
C      CALC TOTAL ACID (NOW YO(I)) FOR LEAST SQUARES REFINEMENT
      ATH(I)=ACIDK*ATL(I)+1.611E-14/H-ALKA
      WRITE(6,70)YO(I),X(1,I),ATL(I),ATM(I),ATH(I)
    1 YO(I)=ATH(I)
      WRITE(6,74)
      WRITE(6,76)ANAOH,VOL,ACID,SLOPE,SINT,CALS,CINNT
      WRITE(6,77)CORR,DELTA,ACIDK
      WRITE(6,75)
      WRITE(6,78)
      WRITE(6,79)AB(1),AB(2),AB(3),AB(4)
```

```
   60 FORMAT(2F10.4,3E10.3,2F5.3)
   61 FORMAT(4F10.3,F6.4)
   62 FORMAT(4F10.4)
   70 FORMAT(2(F6.3,2X),3(E10.4,2X))
   74 FORMAT(' YO(I)   X(1,I)    ATL          ATM          ATH  ')
   75 FORMAT(' A1 A1L A1L2 A1L3  A1H A1LH2 A1LOH 061082')
   76 FORMAT(' KOH= ',F9.3/' VOL= ',F9.3/' ACID= ',E10.4/' SLOPE= ',
     1F8.4,' SINT= ',F8.4/' CALS=',F8.4,'CINNT=',F10.4)
   77 FORMAT('  CORR= ',F9.3,/' DELTA= ',F5.3,'  SEE PAGE61B LB3 FOR
     1 SYRINGE CORR ',F5.3,'=ACIDK ')
  78 FORMAT(/' BETA7 IS A1OH3 ',/'ALSO A1LOH A1LH2 CAN BE INCLUDED')
  79 FORMAT(/' AB(1)= ',F10.4,/'AB(2)=',F10.4,/'AB(3)=',F10.4,
     1/'AB(4)=',F10.4)
      RETURN
      END
      SUBROUTINE CALC(I,P,X,ATM,ATL,AB,H4L,Y,D,FM,ZF,A1L,A1L2,A1L3,HYDR,
     1A1LH,A1OH,A1OH2,A1OH4,A12OH2,A13OH4,A113OH32,A1LH2,A1LOH,A1OH3,ZKS
     2P,A1L2OH,A133,A1L22,A1L32)
      DIMENSION P(10),X(1,200),ATM(200),ATL(200),AB(200),AL(200)
      DIMENSION SH4L(200),ATH(200)
      H=10.**(-X(1,I))
C       ABK is the dissociation of the complexes above pH 6.5
      ABA=AB(3)-AB(4)
      ABC=AB(2)-AB(4)
      ABD=AB(1)-AB(4)
      ABE=10.**(ABC)
      ABF=10.**(ABD)
      ABB=10.**(ABA)
      PPP2=ABB**2
      PPP5=ABB**3
      IF(I-1)1,1,2

    1 FM=ATM(I)/2.0
      GO TO 3
    2 H4L=SH4L(I-1)
    3 CONTINUE
C     ALUMINIUM HYDROLYSIS CONSTANTS
      BETA1=10.**(-5.461)
      BETA2=10.**(-10.036)
      BETA3=10.**(-7.7)
      BETA4=10.**(-23.491)
      BETA5=(-103.149)
      BETA6=10.**(-13.694)
      BETA7=10.**(-15.737)
      A=2.*BETA3/H**2
      AZ=3.*BETA6/H**4
C     USE TRIAL VALUE OF H4L TO SOLVE FOR FM.
      B=1.0+P(1)*H4L/(H**2)*(1.0+P(4)*H4L/(H**2)*(1.0+P(6)*H4L/(H**2)))
     1+BETA1/H+BETA2/H**2+P(1)*P(7)*H4L/H+(P(1)*H4L**2*P(4)/H**4)*(
     2PPP2/H**2+(1./H)*(P(6)*PPP5*H4L/H**4))+BETA4/(H**4)+BETA7/H**3
     3+P(5)*H4L+P(1)*H4L/H**3*(P(3)+P(4)*P(2)*H4L/H**2)
     4+P(8)*(P(1)*H4L/H**2)/H
```

```
C       SOLVE CUBIC FOR H4L BY NEWTON RAPHSON
        NX=0
        NY=0
   27   FN=ALOG10(13.)+BETA5+13.*ALOG10(FM)-32.*ALOG10(H)
        IF(X(1,I)-6.0)54,55,55
   55   FN=0.0
        AA=0.0
        GO TO 56
   54   AA=10.**(FN)
   56   CONTINUE
        FX=AA+AZ*FM**3+A*FM**2+B*FM-ATM(I)
        FXP=13.*AA/FM+3.*AZ*FM**2+2.*A*FM+B
        XM=FM-FX/FXP
        PFM=-ALOG10(FM)
        PXM=-ALOG10(XM)
        G=PFM-PXM
        FM=XM
        IF(ABS(G)-0.001)25,25,26
   26   NX=NX+1
        IF(NX-20)27,25,25
C       USE FM TO OBTAIN IMPROVED VALUE FOR FREE LIGAND
C       SOLVE CUBIC FOR H4L BY NEWTON RAPHSON
   25   DZXA=(3.0*P(6)*P(4)*P(1))
        DZXB=ALOG10(DZXA)
        DZZ=6.*ALOG10(H)
        DAZ=DZXB-DZZ
        DZ=ALOG10(FM)
        DAZA=DAZ+DZ
        DDA=10.**(DAZA)
        DA=DDA*(1.0+PPP5/H**3)
        DB=2.0*P(4)*P(1)*FM/H**4*(1.0+P(2)/H+PPP2/H**2)
C       fully deprotonated form is always neglible so it is not icluded
        DC=1.+ABB/H+ABE/H**2+ABF/H**3+P(1)*FM/H**2+P(1)*P(7)*FM/H
      1+P(5)*FM+P(1)*P(3)*FM/H**3+P(8)*(P(1)*FM/H**2)/H
        N=0
   30   FX=DA*H4L**3+DB*H4L**2+DC*H4L-ATL(I)
        FXP=3.*DA*H4L**2+2.*DB*H4L+DC
        Z=H4L-FX/FXP
        PZ=-ALOG10(Z)
        PFL=-ALOG10(H4L)
        G=PZ-PFL
        H4L=Z
        IF(ABS(G)-0.001)20,20,21
   21   N=N+1
        IF(N-40)30,20,20
   20   IF(NY-21)7,22,22
   22   TFM=FM*(1.0+BETA1/H+BETA2/H**2+FM*A)+13.*FN+FM*BETA4/(H**4)
      1+FM**3*AAZ
C       TEST IF NON-COMPLEXED M LESS THAN HALF A %
        XD=100.*TFM-ATM(I)
        IF(XD) 7,6,7
    6   ZF=1.0+P(4)*H4L/H**2*(1.0+P(6)*H4L/H**2)+P(7)*H
        ZAILH=ATM(I)/ZF
        TFMP=99.
        GO TO 8
```

```
    7 CONTINUE
C     USE IMPROVED VALUE OF H4L TO RECALCULATE FM
      NM=0
      B=1.0+P(1)*H4L/(H**2)*(1.0+P(4)*H4L/(H**2)*(1.0+P(6)*H4L/(H**2)))
     1+BETA1/H+BETA2/H**2+P(1)*P(7)*H4L/H+(P(1)*H4L**2*P(4)/H**4)*(PPP2
     2/H**2+(1.0/H)*(P(6)*PPP5*H4L/H**4))+BETA4/(H**4)+BETA7/H**3
     3+P(5)*H4L+P(1)*H4L/H**3*(P(3)+P(4)*P(2)*H4L/H**2)
     4+P(8)*(H4L*P(1)/H**2)/H
   28 FN=ALOG10(13.)+BETA5+13.*ALOG10(FM)-32.*ALOG10(H)
      IF(X(1,I)-6.0)46,47,47
   47 FN=0.0
      AA=0.0
      GO TO 48
   46 AA=10.**(FN)
   48 CONTINUE
      FX=AA+AZ*FM**3+A*FM**2+B*FM-ATM(I)
      FXP=13.*AA/FM+3.*AZ*FM**2+2.*A*FM+B
      AM=FM-FX/FXP
C     TEST FM FOR CONVERGENCE
      PFM=-ALOG10(FM)
      PAM=-ALOG10(AM)
      G=PAM-PFM
      FM=AM
      IF(ABS(G)-0.001)42,42,41
   41 NM=NM+1
      IF(NM-20)28,42,42
   42 G=PXM-PAM
      PXM=PAM
      NY=NY+1
      IF(NY-20)29,40,40
   29 IF(ABS(G)-0.001)40,40,25
    8 CONTINUE
   40 CONTINUE
      SH4L(I)=H4L
      ZF=100./ATM(I)
      A1LH=P(1)*P(7)*H4L*FM*ZF/H
      A1L=P(1)*FM*H4L*ZF/(H**2)
      A1L2=A1L*H4L*P(4)/(H**2)
      A1L3=H4L*P(6)*A1L2/(H**2)
      A1LH2=P(5)*ZF*H4L*FM
      A1L2OH=A1L2*P(2)/H
      A1LOH=P(1)*P(3)*FM*H4L*ZF/H**3
      A133=P(8)*ZF*(P(1)*H4L*FM/H**2)/H
      A1L22=PPP2*A1L2/H**2
      A1L32=PPP5*A1L3/H**3
      FN=BETA5+13.*ALOG10(FM)-32.*ALOG10(H)
      IF(X(1,I)-6.0)50,51,51
   51 FN=0.0
      FNN=0.0
      GO TO 52
   50 FNN=10.**(FN)
   52 CONTINUE
```

```
      TFM=FM*(1.+BETA1/H+BETA2/H**2+BETA4/H**4+FM*A)+13.*FNN
     1+3.*BETA6*FM**3/H**4+BETA7*FM/H**3
      HYDR=TFM*ZF
      A1OH=BETA1*FM*ZF/H
      A1OH2=ZF*BETA2*FM/H**2
      A1OH4=ZF*BETA4*FM/H**4
      A12OH2=ZF*FM**2*A
      A113OH32=ZF*13.*FNN
      A1OH3=ZF*BETA7*FM/H**3
      A13OH4=ZF*AAZ*FM**3
C       KSP for al-hydroxide
      ZOH=1.611E-14/H
      ZKS=FM*ZOH**3
      ZKSP=ALOG10(ZKS)
C     CALCULATE TOTAL ACID (YCALC) FROM FM,H4L AND TRIAL PARAMETERS
      Y=H+H4L*(4.+3.*ABB/H+2.0*ABE/H**2+ABF/H**3)
     1-BETA1*FM/H-BETA2*2.*FM/H**2-2.*BETA3*FM**2/H**2
     2-4.*BETA4*FM/(H**4)-32.*FNN+P(1)*P(7)*H4L*FM/H
     3-4.*BETA6*FM**3/H**4-3.*BETA7*FM/H**3+A1L2OH*3.0/ZF
     4+P(5)*FM*H4L*2.0+2.0*A1L/ZF+4.0*A1L2/ZF+6.0*A1L3/ZF+3.0*A1L32/ZF
     5+2.0*A1L22/ZF+P(8)*(P(1)*H4L*FM/H**2)/H
C   NB because of extra protons A1L2OH has a positive proton count of 3
      RETURN
```

APPENDIX F

CALCULATION OF HYDROGEN ION CONCENTRATIONS FROM HYDROXIDE ION CONCENTRATIONS

Knowledge of the hydroxide ion concentration and the ionic strength of a test solution allows the concentration of hydrogen ions in solution to be calculated.

The hydrogen ion concentrations were calculated from the ionic activity product of water,

viz. $K_{wc} = a_H\, a_{OH} / aH_2O = m_H\ m_{OH}\ (f_H\, f_{OH} / a_{H_2O})$.

The term in parentheses, the "activity coefficient function" must be estimated by an empirical relationship. Such a relationship has been described by Harned and Owen[100].

viz. $\log (f_H\, f_{OH} / a_{H_2O}) = -2SI^{0.5}/(1+A'I^{0.5}) + I + CI^{1.5}$

where

$$S = 1.814 \times 10^6/(DT)^{1.5}$$

$$A' = 50.3a^o\ (DT)^{-0.5}$$

$$= b^o + b_1 t$$

$$c = c^o + c_1 t$$

In this work the data of Harned and Owen for KCl at 25°C was used.

DT^a	2.341×10^4 at 25°C
a^o	3.6
b^o	0.266
c^o	-0.035

b_1	5.2×10^{-4}
c_1	-4.88×10^{-4}
t^b	25

---

a D = dielectric constant, T = temperature ^{o}K

b t=temperature ^{o}C.

APPENDIX G

DATA FROM A TITRATION OF 4-METHYLBENZENE-1,2,-DIOL WITH KOH[a]

Titre(ml)[b]	pH[c]
0.130	8.994
0.160	9.176
0.190	9.337
0.210	9.443
0.230	9.545
0.250	9.647
0.260	9.704
0.270	9.760
0.280	9.817
0.290	9.879
0.300	9.947
0.305	9.981
0.310	10.014
0.315	10.050
0.320	10.086
0.325	10.123
0.330	10.159
0.335	10.210
0.340	10.241
0.345	10.284
0.350	10.328
0.355	10.374
0.360	10.420
0.365	10.468
0.370	10.514
0.375	10.558
0.380	10.602

a Ionic strength 0.1 M KCl; T 25°C; [4-methylbenzene-1,2,-diol] = 6.77×10^{-3} M; total volume = 150.00 ml

b Cumulative volume of 1.224 M KOH added

c Hydrogen ion concentration obtained from calibration equation (see Chapter 3)

APPENDIX H

DATA FROM A TITRATION OF PROTCATECHUIC ACID WITH KOH[a]

Titre (ml)[b]	pH[c]
0.100	3.669
0.170	3.884
0.240	4.078
0.320	4.285
0.400	4.504
0.450	4.656
0.490	4.795
0.515	4.895
0.535	4.988
0.540	5.014
0.560	5.126
0.580	5.269
5.590	5.356
0.600	5.458
0.610	5.589
0.620	5.764
0.630	6.021
0.640	6.431
0.660	7.162
0.680	7.507
0.700	7.711
0.720	7.861
0.750	8.028
0.790	8.202
0.830	8.344
0.900	8.553
1.000	8.822
1.100	9.105
1.200	9.470
1.300	10.087
1.400	10.663

a Ionic strength 0.1 M KCl; T 25°C; [protocatechuic acid] = 4.53×10^{-3} M; total volume = 60.00 ml

b Cumulative volume of 1.064 M KOH added

c Hydrogen ion concentration obtained from calibration equation (see Chapter 3)

APPENDIX I

DATA FROM A TITRATION OF 3',4',-DI-O-METHYLCATECHIN WITH HCL[a]

Titre (ml)[b]	pH[c]
2.170	8.488
2.150	8.434
2.130	8.578
2.110	8.635
2.090	8.690
2.070	8.729
2.030	8.821
2.010	8.873
1.990	8.930
1.970	8.972
1.950	9.021
1.930	9.062
1.910	9.105
1.890	9.159
1.870	9.210
1.860	9.230
1.840	9.286
1.830	9.312
1.820	9.334
1.810	9.363
1.800	9.387
1.790	9.415
1.780	9.438
1.770	9.467
1.760	9.495
1.750	9.521
1.740	9.547
1.730	9.571
1.720	9.600
1.710	9.629
1.690	9.682
1.650	9.778
1.625	9.830
1.600	9.906
1.575	9.961
1.550	10.002
1.525	10.050
1.500	10.110
1.485	10.139
1.450	10.194
1.420	10.235
1.380	10.292
1.340	10.350
1.300	10.396
1.250	10.447
1.200	10.500
1.150	10.547

1.100	10.589
1.050	10.622
1.000	10.666
0.900	10.733
0.800	10.794

---

a Ionic strength 0.1 M KCl; T 25°C;

[3',4',-di-O-methylcatechin] = 1.1×10^{-3} M;

total volume = 50.00 ml

b Cumulative volume of 0.079 M HCl added

c Hydrogen ion concentration obtained from calibration equation (see Chapter 3)

APPENDIX J

DATA FROM A TITRATION OF B2 WITH KOH[a]

Titre(ml)[b]	pH[c]
0.030	7.635
0.035	7.748
0.040	7.839
0.045	7.926
0.050	7.997
0.055	8.066
0.060	8.119
0.065	8.177
0.070	8.226
0.075	8.271
0.080	8.313
0.085	8.350
0.090	8.386
0.095	8.423
0.100	8.456
0.105	8.486
0.110	8.518
0.115	8.549
0.120	8.576
0.125	8.602
0.130	8.625
0.135	8.648
0.140	8.674
0.145	8.696
0.150	8.719
0.155	8.741
0.160	8.764
0.165	8.785
0.170	8.807
0.180	8.847
0.185	8.866
0.190	8.885
0.200	8.923
0.210	8.961
0.220	8.994
0.230	9.027
0.240	9.061
0.250	9.093
0.260	9.126
0.270	9.156
0.280	9.187
0.290	9.216

0.300	9.246
0.310	9.276
0.320	9.306
0.330	9.333
0.340	9.358
0.350	9.387
0.360	9.413
0.370	9.440
0.380	9.467
0.390	9.493
0.400	9.520
0.415	9.560
0.430	9.596
0.440	9.620
0.450	9.647
0.465	9.684
0.480	9.722
0.500	9.770
0.515	9.810
0.530	9.844
0.540	9.868
0.550	9.892
0.560	9.916
0.570	9.940
0.580	9.964
0.600	10.011
0.610	10.037
0.620	10.061
0.630	10.084
0.640	10.105
0.650	10.129
0.660	10.154
0.680	10.199
0.700	10.243
0.720	10.287
0.740	10.328
0.760	10.370
0.780	10.411
0.800	10.450
0.820	10.486
0.840	10.521
0.870	10.573
0.900	10.623

---

a Ionic strength 0.1 M KCl; T 25^{o}C; [B2] = 5.54x10^{-4} M; total volume = 60.00 ml

b Cumulative volume of 0.138 M KOH added

c Hydrogen ion concentration obtained from calibration equation (see Chapter 3)

APPENDIX K

REPRESENTATIVE SPECTROPHOTOMETRIC DATA USED FOR LOG K EVALUATION FOR 4-METHYLBENZENE-1,2-DIOL

absorbance	p[H]	ionic strength	$I^{0.5}/(1+I^{0.5})$	log K
0.862[a]	14.410	2.712	0.622	12.056
0.839	14.172	1.959	0.583	12.920
0.809	13.999	1.503	0.551	13.119
0.774	13.867	1.203	0.523	13.238
0.829[b]	14.410	2.712	0.622	13.151
0.801	14.172	1.959	0.583	13.213
0.761	13.999	1.503	0.551	13.297
0.722	13.867	1.203	0.523	13.344

a wavelength 257.0 nm, ε_L 5655, ε_{LH} 2566

b wavelength 307.0 nm ε_L 5630, ε_{LH} 1710

APPENDIX L

REPRESENTATIVE SPECTROPHOTOMETRIC DATA USED FOR LOG K EVALUATION FOR PROTOCATECHUIC ACID

absorbance	p[H]	ionic strength	$I^{0.5}/(1+I^{0.5})$	log K
0.733[a]	13.587	0.705	0.456	12.701
0.712	13.494	0.579	0.432	12.739
0.685	13.409	0.479	0.409	12.790
0.657	13.331	0.399	0.387	12.830
0.628	13.258	0.335	0.367	12.864
0.593	13.190	0.283	0.347	12.912
0.499[b]	13.587	0.705	0.456	12.754
0.510	13.494	0.579	0.432	12.788
0.520	13.409	0.479	0.409	12.824
0.541	13.331	0.399	0.387	12.849
0.560	12.258	0.335	0.367	12.880
0.582	13.190	0.285	0.347	12.927

a wavelength 320.0 nm, ε_L 1028, ε_{LH} 249

b wavelength 298.0 nm ε_L 601, ε_{LH} 1120

APPENDIX M

FORTRAN PROGRAM TO CALCULATE ALUMINIUM HYDROXO SPECIES DISTRIBUTION

```
C        PROGRAM TO CALCULATE Al HYDROXY DISTRIBUTION
C
C        BETA VALUES CALCULATED FROM MESMER & BAES FOR IONIC STRENGTH 1.0
C
   10 FORMAT(' Al(H2O)6=',E10.4,2X,F9.3,2X,E10.4,1X,I2)
   11 FORMAT('      Al       AlOH    Al(OH)2    Al(OH)3    Al(OH)4 Al2(O
     1OH)2 Al3(OH)4  Al13(OH)32   KSP ')
   12 FORMAT(9(1X,F9.2))
   14 FORMAT(E10.4,E10.4)
   15 FORMAT(I2)
   18 FORMAT('AL(H2O)6= ',E10.4,F9.3,F9.3,2X,E10.4)
      READ(5,14)TAL,H
C FOR IONIC STRENGTH OF 1.0
      BETA1=10.**(-5.992)
      BETA2=10.**(-10.833)
      BETA3=10.**(-16.533)
      BETA4=10.**(-24.022)
      BETA5=10.**(-7.7)
      BETA6=10.**(-13.429)
      BETA7=-107.930
C        TRIAL VALUE OF Al IN MASS BALANCE FOR TOTAL METAL
      J=1
      AL=TAL/100.
      TPH=-ALOG10(H)
      WRITE(6,10)AL,TPH,TAL,J
      AB1=1.0+BETA1/H+BETA2/H**2+BETA3/H**3+BETA4/H**4
      AB2=2.0*BETA5/H**2
      AB3=BETA6*3.0/H**4
    3 Z=ALOG10(13.0)+BETA7+13.*ALOG10(AL)-32.*ALOG10(H)
      AB13=10.**(Z)
      C=AB13+AB3*AL**3+AB2*AL**2+AB1*AL-TAL
      CD=13.*AB13/AL+3.0*AB3*AL**2+2.0*AB2*AL+AB1
      XAL=AL-C/CD
      PAL=-ALOG10(AL)
      PXAL=-ALOG10(XAL)
      D=PAL-PXAL
      AL=XAL
      WRITE(6,18)AL,PAL,PXAL,H
      WRITE(6,15)J
      IF(ABS(D)-0.001)1,1,2
    2 J=J+1
      IF(J-200)3,1,1
    1 CONTINUE
```

```
      ZZ=ALOG10(13.0)+BETA7+13.*ALOG10(AL)-32.*ALOG10(H)
      Z13=10.**(ZZ)
      SF=100./TAL
      ALOH=BETA1*AL*SF/H
      ALOH2=BETA2*AL*SF/H**2
      ALOH3=BETA3*AL*SF/H**3
      ALOH4=BETA4*AL*SF/H**4
      AL2OH2=AL**2*AB2*SF
      AL3OH4=AL**3*AB3*SF
      AL13OH32=Z13*SF

      BAL=AL*SF
      ZOH=1.611E-14/H
      ZKS=AL*ZOH**3*0.702**3*0.042
C  DAVIES EQN USED FOR ACT COEF AT IONIC STR 1.0
      ZKSP=ALOG10(ZKS)
      WRITE(6,11)
      WRITE(6,12)BAL,ALOH,ALOH2,ALOH3,ALOH4,AL2OH2,AL3OH4,AL13OH32,ZKSP
      CLOSE(5,STATUS='KEEP')
      CLOSE(6,STATUS='KEEP')
      STOP
      END
```

REFERENCES

1. Jenny, H., Factors of Soil Formation, New York, McGraw-Hill, 1941.
2. Glinka, K. D., Treatise on Soil Sci., Gosudarstvennce Selskokhoz Yaistvennce Izdatelsho, Moscow, 1931., Israel Program for Scientific Translations, Jerusalem, 1963.
3. Ponomareva, V. V., Theory of Podzolization.'Nauka'., Moskva-Leningrad, 1964., Israel Program for Scientific Translations, Jerusalem, 1969.
4. Muir, A., Adv. Agron., 1961, 13, 1.
5. Bridges, E. M., World Soils, London, Cambridge, University Press, 1978.
6. Taylor, N. H., Pohlen, I. J., Soil Survey Method, N.Z. Soil Bur. Bull., 25, 1970.
7. Stevenson, F. J., Humus Chemistry, New York, J. Wiley & Sons, 1982.
8. MacKney, D., J. Soil Sci., 1961, 12, 23.
9. Giddens, K. M., Soil Survey Sheets., unpublished data, N. Z. Soil Bureau, 1981-1982.
10. Coulson, C. B., Davies, R. I., Lewis, D. A., J. Soil Sci., 1960, 11, 20.
11. Petersen, L., Podzols and Podzolization, Copenhagen, DSR FORLAG, 1976, p121.
12. Stobbe, P. C., Wright, J. R., Soil Science Society of America Proceedings, 1959, 23, 161.
13. Mattson, S., Nilsson, I., Ann. Agric. Coll. Sweden, 1934, 2, 115.

14. Mattson, S., Koutler-Andersson, E., Ann. Agric. Coll. Sweden, 1942, 10, 240.

15. Deb, B. C., J. Soil Sci., 1949, 1, 112.

16. Ref. 11, p134.

17. Davies, R. I., Soil Sci., 1971, 111, 80.

18. Atkinson, H. J., Wright, J. R., Soil Sci., 1957, 84, 1.

19. Bloomfield, C., Nature, 1952, 170, 540.

20. Bloomfield, C., J. Soil Sci., 1953, 4, 5.

21. Bloomfield, C., J. Soil Sci., 1954, 5, 39.

22. Bloomfield, C., J. Soil Sci., 1954, 5, 46.

23. Bloomfield, C., J. Soil Sci., 1954, 5, 50.

24. Bloomfield, C., J. Sci. Food Agric., 1957, 8, 389.

25. Bloomfield, C., Rothamsted Experimental Station, Hapenden, Herts., Report. 1963, p226.

26. Muir, J. W., Logan, J., Brown, C. J., J. Soil Sci., 1964, 15, 220.

27. Muir, J. W., Logan, J., Brown, C. J., J. Soil Sci., 1964, 15, 226.

28. Coulson, C. B., Davies, R. I., Lewis, D. A., J. Soil Sci., 1960, 11, 30.

29. Haslam, E., The Flavonoids: Advances in Research, (Eds. Harborne, J. B., Marby, T. J., London, Chapman & Hall, 1982.

30. Hingston, F. J., Aust. J. Soil Res., 1963, 1, 67.

31. Shindo, H., Onta, S., Kuwatsuka, S., Soil Sci. Plant Nutr., 1978, 24, 233.

32. Huang, W. H., Keller, W. D., American Mineralogist, 1971, 56, 1082.

33. Buurman, P., Van Reeuwijk, L. P., J. Soil Sci., 1983, in press.

34. Schnitzer, M., Skinner, S. I. M., Soil Sci., 1963, 96, 86.

35. Schnitzer, M., Skinner, S. I. M., Soil Sci., 1963, 96, 181.

36. Schnitzer, M., Skinner, S. I. M., Soil Sci., 1965, 99, 278.

37. Ref. 11, p120.

38. Crawford, D. V., Soils and Fertilizers, 1956, 19, 197.

39. Alexander, M., Aleem, M. I., J. Agr. Food Chem., 1961, 9, 44.

40. Ref. 11, p145.

41. Farmer, V. C., Russell, J. D., J. Soil Sci., 1980, 31, 673.

42. Farmer, V. C., Colloques Internationaux du C.N.R.S Nancy, 1981, 303, 275.

43. Farmer, V. C., Anderson, H. A., J. Soil Sci., 1982, 125.

44. Farmer, V. C., Fraser, A. R., Tait, J. M., J. Chem. Soc., Chem. Comm., 1979, 462.

45. Farmer, V. C., Fraser, A. R., Tait, J. M., Geochim. Cosmochim. Acta, 1979, 43, 1417.

46. Farmer, V. G., Fraser. A. R., J. Soil Sci., 1982, 33, 737.

47. Inoue, K., Huang, P. M., Agronomy Abstracts, 1983, 219.

48. Shindo, H., Kurwatsuka, H., Soil Sci. Plant Nutr., 1977, 23, 185.

49. Davies, R. I., Coulson, C. B., Lewis, D. A., Royal Dublin Soc. Scientific Proc., 1960, 1, 183.

50. Czochanska, Z., Yeap Foo, L., Newman, R. H., Porter, L. J., J. Chem. Soc., Perkin Trans. I, 1980, 9, 1668.

51. PHM64., Research pH meter, Operating Instructions, 7612C, Radiometer, Copenhagen.

52. Research pH meter, Operating Instructions, 1226-B, Beckman Instruments Inc., California, 1963.

53. Glass Electrodes, Beckman Instruments Inc., 678 D, California, 1966.

54. Brezinski, D. P., Analyst, 1983, 108, 1285.

55. Taylor, M. C., Ph. D. Thesis, University of Canterbury, 1980, p34.

56. Kee, T. S., M. Sc. Thesis, University of Canterbury, 1975, p8.

57. Ref. 55, p36.

58. Russell, J. M. R., Ph. D. Thesis, University of Canterbury, 1977, p78.

59. C.R.C. Handbook Chem. & Phys., 60th Ed., 1979, F11.

60. Vogel, A. I., A Textbook of Quantitative Inorganic Analysis, 3rd Ed., London, Longmans Green & Co., 1961, p196.

61. Hedwig, R. G., Ph. D. Thesis, University of Canterbury, 1972, p24.

62. Bates, R. G., Determination of pH Theory & Practice, 2nd Ed, New York, J. Wiley & Sons, 1973, p97.

63. Ref. 55, p28.

64. Gran, A., Anal. Chim. Scand., 1950, 4, 599.

65. Rodd's Chemistry of Carbon Compounds, 2nd Ed., Ed. by Coffey, S., Amsterdam, Elsevier Scientific Publishing Company, 1973, 3, part D.

66. Private communication Drs. L. Porter & Yeap Foo.

67. Kennedy, J. A., Munroe, M. H. G., Powell, H. K. J., Porter, L. J., Yeap Foo, L., Aust. J. Chem., 1984, 37, 885.

68. Sweeney, J. G., Iacobucci, G. A., J Org. Chem., 1979, 44, 2298.

69. Private communication Dr. L. Porter.

70. Porter, L. J., Yeap Foo, L., J. Chem. Soc., Perkin Trans. I, 1983, 1535.

71. Flecther, A. C., Porter, L. J., Haslam, E., Gupta, R. K., J. Chem. Soc., Perkin Trans. 1, 1977, 1628.

72. Ref. 60, p516.

73. Ref. 60, p468.

74. Ref. 55, p39.

75. Farmer, V. C., Fraser, A. R., Clay Minerals, 1977, 12, 55.

76. Model 174 A, Polarographic Analyzer, Operating & Service Manual., E.G.& G. Princeton Applied Research, U.S.A., 1979.

77. Model 303 Static Mercury Drop Electrode, Operating & Service Manual., E.G.& G. Princeton Applied Research, U.S.A., 1979.

78. Eisenman, G., Glass Electrodes for Hydrogen and other Cations, New York, Marcel Dekker Inc., 1976.

79. Ref. 62., p342.

80 Bates. R. G., C.R.C. Critical Reviews in Analytical Chemistry, 1981, 10, 247.

81. Harned, H. S., Treatise on Physical Chemistry, U. S. A., D. Van Nostrand Comp., 1924.

82. Ref. 62., p36.

83. Ref. 62., p55.

84. ASTM., Standard Test Method for pH of Aqueous Solutions With the Glass Electrode., ANSI/ASTM, Philadelphia, 1978, E70.

85. IUPAC., Manual of Symbols and Terminology for Physiochemical Quantities, Oxford, Pergamon Press, 1979, 30.

86. Bates, R. G. J. Res. Natl. Bur. Stand., 1962, 66A, 179.

87. Ref. 62., p73.

88. Ref. 62., p72.

89. Ref. 61., p59.

90. Bates, R. G., Bower, V. E., Miller, R. G., Smith, E. R., J. Res. Natl. Bur. Stand., 1951, 47, 433.

91. Stables, B. R., Bates, R. G., J. Res. Natl. Bur. Stand., 1969, 73A, 37.

92. Hamer, W. J., Acree, S.F., J. Res. Natl. Bur. Stand., 1944, 32, 215.

93. Hamer, W. J., Pinching, E., Acree, S. F., J. Res. Natl. Bur. Stand., 1945, 35, 539.

94. Bates, R. G., Acree, S. F., J. Res. Natl. Bur. Stand., 1945, 34, 373.

95. Bower, V. E., Paabo, M., Bates, R. G. J. Res. Natl. Bur. Stand., 1961, 65A, 267.

96. McBryde, W. A. E., Analyst, 1969, 94, 337.

97. Powell, H. K. J., Curtis, N. F., J. Chem. Soc (B)., 1966, 1205.

98. Powell, H. K. J., Hedwig, G. R., Anal. Chem., 1971, 43, 1206.

99. Powell, H. K. J., Kennedy, J. A., Taylor, M. C., Anal. Chim. Acta, 1683, 147, 351.

100. Harned, H. S., Owen, B., The Physical Chemistry of Electrolyte Solutions, 2nd Ed. New York, Reinhold, 1950.

101. Ref. 55, Appendix 10.

102. Ref. 55, Appendix 4.

103. Ref. 55, p62.

104. Ref. 55,, p92.

105. Avdeef, A., Bucher, J. J., Anal. Chem., 1978, 50, 2137.

106. May, P. M., Williams, D. R., Linder, P. W., Torrington, R. G., Talanta, 1983, 29, 249.

107. Powell, H. K. J., Taylor, M. C., Talanta, 1983, 30, 885.

108. Rossotti, F. J. C., Modern Coordination Chemistry, New York, Interscience, 1970.

109. Rossotti, H., The Study of Ionic Equilibrium, London, Longman, 1978.

110. Rossotti, H., Chemical Applications of Potentiometry, London, D. Van Nostrand, 1969.

111. Rossotti, F. J. C., Rossotti, H., The Determination of Stability Constants, U.S.A., McGraw-Hill Book Company, 1961.

112. Ref. 61, Appendices C, D.

113. Ref. 61, p63.

114. Sabatini, A., Vacca, A., J. Chem. Soc., Dalton Trans., 1972, 1693.

115. Vilenkin, N. Y., Successive Approximation, London, Pergamon Press, 1964.

116. Forbes, W. F., Interpretive Spectroscopy, Ed. Freeman, S. K., New York, Reinhold, 1965.

117. Beer, A., Ann. Physik. Chem., 1852, 2, 78.

118. Argen, A., Acta Chem. Scand., 1955, 49, 56.

119. Ref. 55, p112.

120. Ref. 55, p100.

121. Robinson, R. A., Stokes, R. H., Electrolyte Solutions, 2nd Ed. London, Butterworths, 1959, p231.

122. Sears, K. D., Casebier, R. L., Herget, H. L., Stout, G. H., McConollish, L. E., J. Org. Chem., 1974, 39, 3244.

123. Kiatgrajai, P., Wellans, J. D., Gollob, L., White, J., J. Org. Chem., 1982, 47, 2910.

124. Sillen, L. G., Martell, A. E., Stability Constants Spec. Publ. Nos. 17 & 25 (The Chemical Society), London, 1964, 1971.

125. Haslam, E., Opie, C. T., Begley, M. J., unpublished data.

126. Engel, D. W., Halling, M., Hundt, H. K. L., Roux, D. G., J. Chem. Soc., Chem. Comm. 1978, 695.

127. Calculations courtesy of Dr. V. McKee.

128. Slabbert, N. P., Tetrahedron, 1977, 33, 821.

129. Kortum, G., Vogel, W., Andrussow, K., Dissociation Constants of Organic Acids in Aqueous Solutions, London, Butterworths, 1961.

130. Mehta, P. P., Whalley, W. E., J. Chem. Soc., 1963, 5327.

131. Powell, H. K. J., Taylor, M. C., Aust. J. Chem., 1982, 35, 739.

132. Mason, H. S., J. Biol. Chem., 1949, 181, 803.

133. Hewgill, F. R., MTP. Int. Rev. Sci. Org. Chem., Ser. One, 1973, 10, 167.

134. Kuhnle, J. A., Windle, J. J., Wais, A. C., J. Chem. Soc. (B)., 1961, 613.

135. Jenson, O. N., Pedersen, J. A., Tetrahedron, 1983, 39, 1609.

136. Bolton, P. D., Hepler, L. G., Chem. Soc., Quarterly Reviews, 1971, 25, 521.

137. Martell, A. E., Tyson, C. A., J. Amer. Chem. Soc., 1968, 90, 3379.

138. Avdeef, A., Sofen, S. R., Bregnante, T. L., Raymond, K. N., J. Amer. Chem. Soc., 1978, 100, 5362.

139. Havelkova, L., Bartusek, L., Coll. Czech. Chem. Comm., 1969, 34, 3722.

140. Dubey, S. N., Mehrota, R. C., J. Inorg. Nucl. Chem., 1964, 6, 1543.

141. Ref. 55, p10.

142. Ohman, L., Sjoberg, S., Polyhedron, 1982, 2, 1329.

143. Harada, H., Nippon Kagaku Zasshi, 1969, 90, 267.

144. Sunkel, J., Deutsche Bunsenges Phys. Chem., 1968, 567.

145. Migal, I. K., Ivanov, V. A., Zh. Obshch. Khim., 1967, 37, 380.

146. Aveston, J., J. Chem. Soc., 1965,4438.

147. Mesmer, R. E., Baes, C. F., The Hydrolysis of Cations, Wiley, New York, 1976.

148. Ohman, L., Forsling, W., Acta Chem. Scand., 1981, A35, 795.

149. Chen. D. T. Y., Can. J. Chem., 1973, 51, 3528.

150. Singh, S. S., Can. J. Chem., 1967, 47, 663.

151. Frink, C. R., Sawhney, B. L., Soil Sci., 1967, 103, 144.

152. Davies, C. W., J. Chem. Soc., 1973, 51, 3528.

153. Migal, P. K., Ivanov, V. A., Russ, J. Inorg. Chem., 1973, 18, 536.

154. Ref. 55, p163.

155. Job, P., Ann. Chim., 1928, 10, 9.

156. Ref. 111, pg 52.

157. Stout, G. H., Jensen, L. H., X-ray Structure Determination A Practical Guide, London, Collier-MacMillan, 1968.

158. Sabatini, A., Vacca, A., Gans, P., Talanta, 1975, 21, 53.

159. Ohman, L., Sjoberg, S., Acta Chem. Scand., 1982, A35, 201.

160. Ohman, L., Sjoberg, S., Acta Chem, Scand., 1982, A36, 47.

161. Ohman, L., Sjoberg, S., Ingri, N., Acta Chem. Scand., 1983, A37, 561.

162. Ohman, L., Sjoberg, S., Acta Chem. Scand., 1983, A37, 875.

163. Goina, T., Olariu, M., Bocaniciu, L., Rev. Roumaine de Chimie, 1970, 15, 1049.

164. Jejurkar, C. R., Mavani, I. P., Bhattacharya, P. K., Ind. J. Chem., 1972, 10, 1190.

165. Knoche, W., Lopez-Quinela M, Thermochim. Acta, 1983, 62, 295.

166. Markham, K. R., Porter, L. J., J. Chem. Soc. (C), 1970, 344.

167. Napoli, A., Liberti, A., Gazz. Chim. Ital., 1970, 100, 906.

168. Ref. 59, D-155.

169. Mentasti, E., Pelizzetti, E., Saini, G., J. Inorg. Nucl. Chem., 1976, 38, 785.

170. McBryde, W. A. E., Can. J. Chem., 1964, 43, 1917.

171. Ball, E. G., Chen, T. T., J. Biol. Chem., 1933, 102, 691.

172. Singer, P. C., Theis, T. L., Environmental Sci. & Tech., 1974, 8, 569.

173. Sultan, S. M., Bishop, E., Analyst, 1982, 107, 1060.

174. Ref. 55, p38.

175. Irving, H., Mellor, D. H., J. Chem. Soc., 1962, 5222.

176. Kennedy, J. A., Powell, H. K. J., White, J. M., Aust. J. Soil. Res., 1982, 20, 261.

177. Fadrus, H., Maly, J., Analyst, 1975, 100, 549.

178. Heller, J., Schwarzenbach, G., Helv. Chim. Acta, 1951, 34, 1876.

179. Bond, A. M., Modern Polarographic Methods in Analytical Chemistry, New York, Marcel Dekker, 1980.

180. Heyrovsky, J., Kuta, J., Principles of Polarography, New York, Academic Press, 1966.

181. Ref. 11, p135.

182. Hider, R. C., Mohd-Nor A. R., Silver, J. C., Morrison I. E., Rees, L. V. C., J. Chem. Soc., Dalton Trans., 1981, 609.

183. Ref. 55, p158.

184. Mentasti, E., Pelizzetti, E., Saini, G., J. Chem. Soc., Dalton Trans.,1973, 2609.

185. Hider, R. C., Hawlin, B., Miller, J. R. Mohd-nor, A. R., Silver, J. Inorg. Chim. Acta, 1983, 80, 51.

186. Singer, P. C., Theis, T. L., Trace Metals and Metal-Organic Interactions in Natural Waters, Ed. Singer P. C., U.S.A., Ann Arbor, 1973.

187. Lee, G. F., Stumm, W., J. Amer. Water Works Assoc., 1962, 52, 1567.

188. Pankan, J. F., Morgan, J. J., Environmental Sci. & Tech., 1981, 15, 1155.

189. Ropars, S., Rougee, M., Momentau, M., Lexa, D., J. Chem. Phys., 1968, 65, 816.

190. Whittemore, D. O., Langmuir, D., Ground Water, 1975, 13, 360.

191. Vareille, L., Bull. Soc. Chim. France, 1955, 870.

192. Desai, A. G., Milburn, R. M., J. Amer. Chem. Soc., 1969, 91, 1958

193. Coleman, N. T., Weed, S. B., Soil Science Society of America Proceedings, 1959, 23, 146.

194. Richardson, J. L., Hole, F. D., Soil Sci. Soc. Am. J., 1979, 43, 552.

195. Childs, C. W., Aust. J. Soil. Res., 1981, 19, 175.

196. Pratt, P. F., Blair, F. L., Soil Sci., 1961, 91, 357.

197. Frahn, J. L., Aust. J. Chem., 1958, 11, 399

198. Baker, A. D., Casadavell, A., Gofney, H. D. Gellender, M., J. Chem. Ed., 1980, 4, 314.

199. Fishman, M. J., Endmann, D. E., Steinheimer, T. R., Anal. Chem, 1981, 53, 184R.

200. Langmyhr, F., Anal. Chim. Acta, 1963, 29, 149.

201. Pakalns, P., Anal. Chim. Acta, 1965, 32, 57.

202. Chester, J. E., Dagnall, R. M., West, T. S., Talanta, 1970, 17, 13.

203. Parfitt, R. L., Furker, R. J., Henmi, T., Clays and Clay Minerals, 1980, 28, 5.

204. Farmer, V. C., Fraser, A. R., Int. Clay. Conference, 1978, 547.

205. Bache, B. W., Sharp, G. S., Geoderma 1976, 15, 91.

206. Ref. 55, p184.

207. Dougan, W. K., Wilson, A. L., Analyst, 1974, 99, 413.

208. Sivasubramaniam, S., Talibudeen, O., J. Soil Sci., 1972, 23, 163.

209. Mew, G., Lee, R., N. Z. J. Sci., 1981, 24, 1.

210. Conference, Soil with Variable Charge, Guide Book 2, Soil Bureau, D. S. I. R., 1981.

211. Ismail, F. T., Soil Sci., 1970, 109, 257.

212. Schnitzer, M., Wright, J. R., Soil Science Society of America Proceedings, 1963, 171.

213. Ref. 11, p137.

214. Havelkova, L., Bartusek, L., Coll. Czech. Chem. Comm., 1969, 34, 2722.

215. Pavlinova, A. V., Vysotskaya, T. D., Ukrain. Khim. Zhur., 1969, 35, 1.

216. Ohman, L., Sjoberg, S., J. Chem. Soc., Dalton Trans., 1983, 2513.

217. Athavole, V., Mahadevan, N., Mathur, P. K., Sathe, R. M., J. Inorg. Nucl. Chem., 1967, 29, 1947.

218. Battari, E. Ciavatta, L. Gazzetta, 1968, 98, 1004.

219. Okac, A., Kolarik, Z., Coll. Czech. Chem. Comm., 1952, 24, 266.

220. Powell, H. K. J., Taylor, M. C., N.Z. Soc. Soil Sci., 1980, Part 5, 88.

221. Juo. A.S.R. Commun. Soil Sci. & Plant Analysis, 1977, 8, 17.

222. Bruckert, S., Jacquin, F., Soil Biol. Biochem., 1966, 1, 275.

223. Stability Constants of Metal Ion Complexes, Part A, IUPAC; Pergamon Press, 1982.

224. Cressy, P. J., Monk. G. R., Powell. H. K. J., Tennet, D. T., J. Soil. Sci., 1983, 34, 783.

225. Migal, I. K., Ivanov, V. A., Russ. J. Inorg. Chem., 1972, 17, 543.

226. Mak, M. K. S., Langford, C. H., Can. J. Chem., 1982, 60, 2023.